UNIVERSITY OF SOUTHAMPTON

Endothelin-1 induced focal ischaemia:

A novel model of spinal cord injury

Dominic John Corkill BSc (Hons)

Doctor of Philosophy

School of Biological Sciences

August 2003

Declaration

The work presented in this thesis was carried out by the author in full time registered postgraduate candidature at the University of Southampton, and is entirely the author's own work except for the collaborations indicated in the acknowledgements.

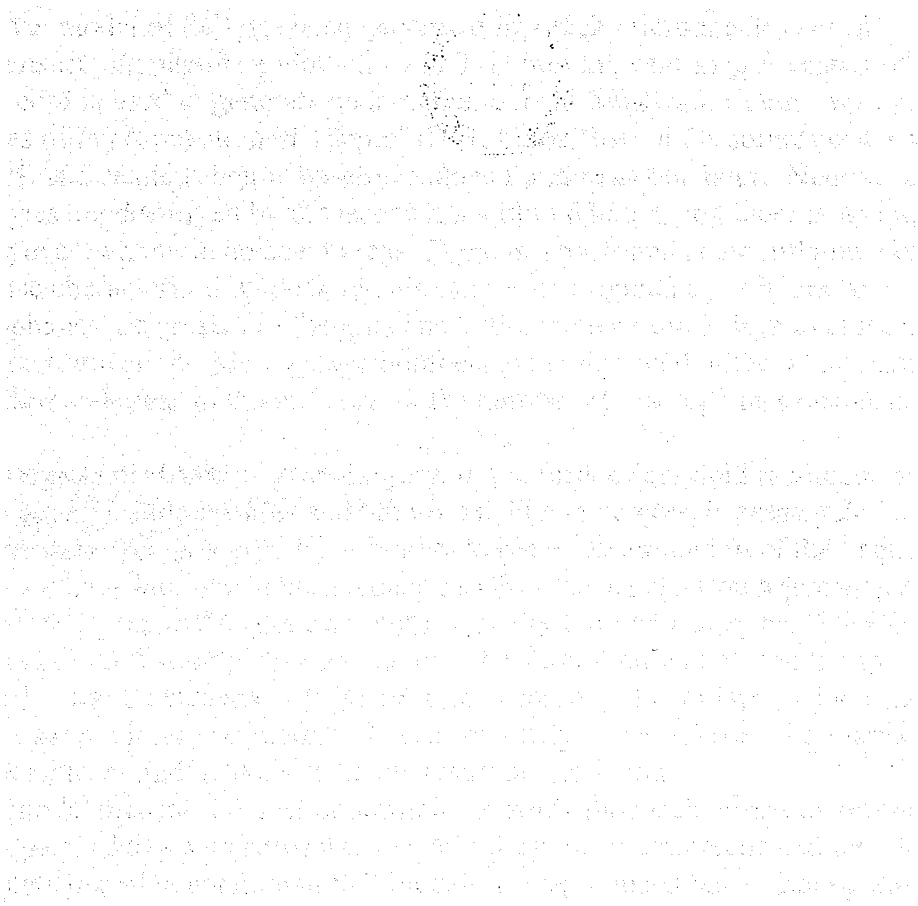

UNIVERSITY OF SOUTHAMPTON

ABSTRACT

FACULTY OF SCIENCE
SCHOOL OF BIOLOGICAL SCIENCES
Doctor of Philosophy

ENDOTHELIN-1 INDUCED FOCAL ISCHAEMIA: A NOVEL MODEL OF SPINAL CORD INJURY

By Dominic John Corkill

Injury to the human spinal cord results in the destruction of grey matter, which contains neurons, and white matter, which contains axons. Injury to the white matter causes much of the paralysis and sensory loss seen after spinal cord injury (SCI). Direct mechanical injury and secondary mechanisms such as ischaemia and inflammation contribute to the tissue loss. Existing animal models of SCI generate complex lesions consisting of both primary and secondary injury, which makes it difficult to study the mechanisms that contribute to secondary injury

A novel model of SCI has been generated in which microinjection of the vasoconstricting peptide endothelin-1 (ET-1) into the ventral grey matter of the rat spinal cord is used to generate an atraumatic focal ischaemic lesion. Within 15 minutes of microinjection of 15pmol ET-1, blood flow in the spinal cord is reduced by 90%, and remains below baseline values for at least one hour. Neurons and astrocytes are destroyed by the ischaemia within 6 hours, and there is widespread astrocyte activation in adjacent areas. There is a profound acute inflammatory response characterised by peak recruitment of neutrophils at 24 hours, and macrophages are present in the grey and white matter from 3 days to at least 21 days after microinjection. Macrophage numbers are maintained in the white matter from 7 to 21 days, whereas in the grey matter the number of macrophages decreases at this time.

Histological evidence of axonal injury, in the form of amyloid precursor protein (APP) positive axon profiles and 'end-bulb'-like structures, is present 24 hours and 3 days after microinjection of ET-1 but not vehicle. Examination of the ventral white matter axons 3 days after microinjection of ET-1 using electron microscopy revealed substantial injury to the axoplasm but less injury to myelin sheaths. Microinjection of the excitotoxin *N*-methyl-D-aspartate into the ventral grey matter of the spinal cord resulted in more extensive myelin injury and sparing of axoplasm, which suggests that the axonal injury seen after ET-1 is not solely due to release of glutamate from injured neurons and is likely to be the result of ischaemia.

This model presents a novel opportunity to study the mechanisms of secondary injury, particularly with respect to axonal injury, in an atraumatic setting. All the characteristics of conventional SCI models are reproduced but without paralysis of the animals or the involvement of direct mechanical injury. It is hoped that this will provide a platform for future studies examining the contribution of inflammation and excitotoxicity to axonal loss in the white matter, and the development of therapeutic strategies to limit axon injury in acute spinal cord injury.

Table of contents:

List of Figures and Tables

Acknowledgements

There are a number of individuals who require specific acknowledgement for their technical and scientific contribution to this thesis:
Dr. Walace Gomes-Leal, who collaborated on the excitotoxicity studies, and generated the electron microscopic images for Chapter 5.
Dr. Matthew Cuttle, who provided valuable guidance and advice on the use of the confocal microscope in Chapter 6.
Dr. Jeff Bagust who collaborated on the preliminary electrophysiology studies described in Chapter 7.

In addition my thanks are extended to Mrs. Sara Waters and Dr. Daniel Anthony who both equipped me with techniques essential for the performance of this research. Along the way I have been helped and assisted by all the members of the CNS Inflammation Group, our neighbours the Molecular Neuropathology Group and the technical staff in the BRF. Particular mention is deserved by many, including Michelle Botham, Dr. Paula Hughes, Emma Rankine, Dr. Martine Bernades-Silva, Dr. Delphine Boche and Dr. Colm Cunningham.

Special thanks are due to Dr. Tracey Newman, who has maintained my sanity with liberal amounts of discussion, caffeine, and carbohydrate.

I am indebted to Prof. Hugh Perry, who gave me both the opportunity and the support to generate this thesis, and whose clarity and guidance has been essential. My gratitude is also extended to the International Spinal Research Trust, which funded my studentship.

Ultimately, there is one person who made this thesis possible, my wife Amanda-Jane, and without her unstinting support I could not have seized this opportunity, or enjoyed it as fully.

Dominic John Corkill
August 2003

Abbreviations used

AA	Arachidonic acid
AMPA	Alpha-amino-3-hydroxy-5-methyl-4-isoxazole propionic acid
AP	Action potential
BBB	Blood-brain barrier
BP	Blood pressure
BSCB	Blood-spinal cord barrier
CAP	Compound action potential
CMBC	Concentration of moving blood cells
CNS	Central nervous system
CSF	Cerebrospinal fluid
ECM	Extracellular matrix
ELISA	Enzyme linked immunosorbant assay
ET-1	Endothelin-1
Glu	Glutamate
HIF-1	Hypoxia inducible factor-1
i.a.	Intra-arterial
i.v.	Intravenous
IU	International Units
KA	Kainic acid
IL-1β	Interleukin-1β
LD	Laser Doppler
LDF	Laser Doppler flowmetry
MCAO	Mid-cerebral artery occlusion
MCP-1	Macrophage chemoattractant protein-1
MP	Methyl-prednisolone
NMDA	*N*-methyl-D-aspartate
NO	Nitric oxide
NOS	Nitric oxide synthase
NSAIDs	Non-steroidal anti-inflammatory drugs
PBS	Phosphate buffered saline
PLP	Periodate lysine paraformaldehyde
PMN	Polymorphonuclear cells (neutrophils)

S6b	Sarafotoxin 6b
s.c.	Subcutaneous
SCI	Spinal cord injury
TNFα	Tumour necrosis factor-α
VWF	Von Willebrand factor
WPB	Weibel-Palade body

Chapter 1 – General Introduction

1.0 Background to spinal cord injury

The fundamental issue in human spinal cord injury (SCI) is that injury to and loss of axons in the white matter leads to paralysis and sensory loss, which cannot currently be reversed. Acute spinal cord injury is estimated to affect between 20 and 40 people per million per year (Tator and Fehlings 1991; Taoka and Okajima 1998) in the developed world. In the U.S.A. alone there are up to 10,000 spinal cord injuries (SCI) each year (NSCIC 2001), the majority of which are the result of motor vehicle accidents (44%). The median age at time of injury is 26 years, and the resulting lifetime of disability is at a high cost to the individual affected in terms of quality of life, and to society at large with respect to the financial costs of support.

Spinal cord injury has proved highly resistant to therapy. High doses of the steroid methylprednisolone used within the first few hours of injury have been shown to be of some benefit (Bracken *et al.* 1990), but this effect may only be marginal and there is a clear need for new, more effective, treatments. The significant reductions in mortality resulting from SCI have been brought about by the introduction of antibiotics. Spinal injury often results in loss of normal bladder control and during the First World War, 80% of British soldiers who became paraplegic through injury died from urinary tract infections (Oliver *et al.* 1988). The development of antibiotics in the inter-war years and the establishment of specialist spinal injury centres to provide rehabilitative care have greatly improved the quality of life for individuals with SCI.

The causes of spinal cord injury have changed over time, with the adoption of safer working practices resulting in fewer industrial injuries. Spinal cord injuries from motor vehicle accidents and sporting activities represent an increasing proportion of new cases. In addition quadriplegia, resulting from cervical spine injury, has become more prevalent as through prompt medical intervention many more people survive the initial injury.

Research into SCI has for many years focussed on the neuronal loss that occurs in the secondary phase, but attention has now returned to the white matter. Functional loss may occur as a direct result of mechanical trauma to axons in the white matter, or

through secondary injury. Haemorrhage and ischaemia of the spinal cord can initiate coagulation and necrosis, and provoke an acute inflammatory response. New therapeutic strategies to protect axons following acute SCI may result in the salvaging of axons which would otherwise have been destroyed. This preservation of axons is likely to be of great benefit for individuals with SCI.

1.1 Aims and Objectives of the Research Project

The aim of this project was to establish an *in vivo* model of SCI that uses focal ischaemia to generate a lesion in the rat spinal cord with minimal mechanical trauma. Conventional models of SCI often rely on a contusion injury or mechanical trauma to injure the spinal cord, which results in a complicated lesion involving direct mechanical injury and secondary pathology. SCI develops as a result of complex interdependent mechanisms including haemorrhage and inflammation, and it is not possible to use *in vitro* systems to model the lesion, although much valuable work has been done *in vitro* to investigate specific mechanisms contributing to spinal cord dysfunction.

It has been known for many years that spinal cord ischaemia alone is sufficient to generate a haemorrhagic lesion with behavioural and pathological changes consistent with spinal cord injury (Woodward and Freeman 1956). It is also widely understood that the lesion that develops after a spinal cord injury has two components (Tator and Fehlings 1991), the primary mechanical injury and the secondary injury that arises as a result of the activation of numerous pathological cascades (see Figure 1.1.1). By using focal ischaemia to generate the lesion the primary injury will be separated from secondary pathological events, and enable us to examine the contribution of secondary processes to spinal cord injury.

The first objective was to develop a methodology that can deliver a reproducible focal ischaemia of the spinal cord with a minimum amount of mechanical trauma. The potent vasoconstricting peptide endothelin-1 (ET-1) has been used previously to generate ischaemic lesions in the rat striatum by microinjection into the parenchyma (Kurosawa *et al.* 1991; Fuxe *et al.* 1992) or by direct application onto the mid-cerebral artery (Sharkey and Butcher 1995). This suggested that microinjection of ET-1 into the spinal cord could be used to generate a focal ischaemic lesion, and preliminary

Figure 1.1.1 ***Primary and secondary injury***

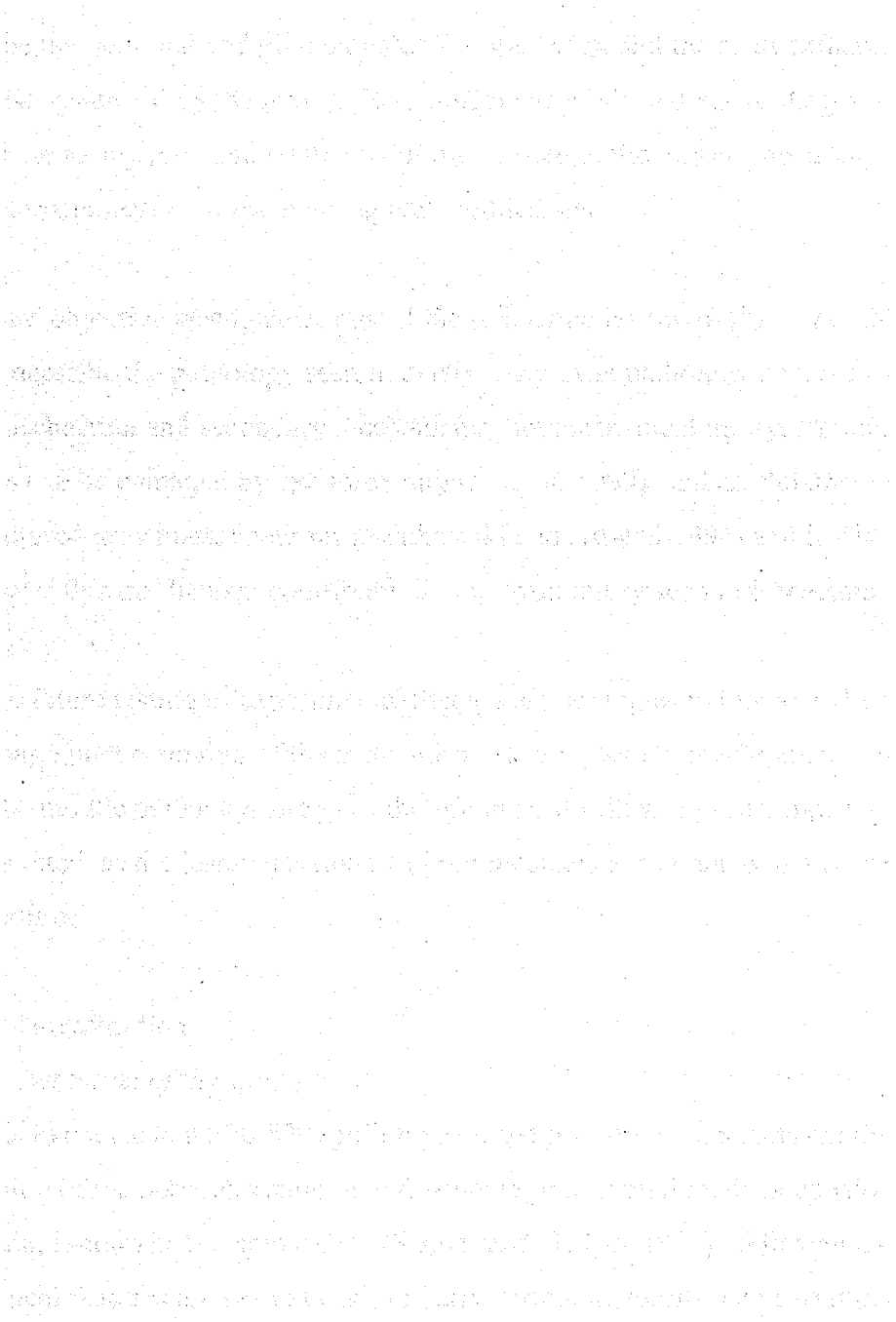

experiments showed this to be the case (Perry V.H. and Anthony D.C., unpublished observations). Development of this technique into a usable model required that it was fully characterised with respect to the optimum dose of ET-1, the onset and duration of ischaemia, functional changes arising in white matter axons, and the pharmacological specificity of the vasoconstricting effect. The next objective was to describe the neuronal and glial pathology in the lesion and the acute inflammatory response generated by the injury. Recruited neutrophils and macrophages may contribute to any grey and white matter injury seen in the lesion, and are a characteristic feature of traumatic spinal cord lesions.

The third objective was to determine if the ischaemic lesion results in axonal injury, and to describe the pathology seen in detail. Any axon pathology observed should be due to ischaemia and secondary mechanisms, not mechanical injury. Axonal myelin sheaths can be damaged by excitotoxicity (Li *et al.* 1999), and as glutamate is released from injured grey matter neurons (Szatkowski and Attwell 1994) and it will be useful to know if this mechanism contributes to any axon injury seen in ischaemia.

Finally, future testing of experimental therapeutic strategies in this model will require a thorough understanding of the mechanisms driving lesion development. Novel insights into the pathophysiology of the spinal cord following acute injury may be also be generated, as the lesion develops without mechanical trauma to axons or the vasculature.

1.2 Introduction

1.2.1 Evolution of the spinal cord

There is evidence that 500-550 million years ago primitive organisms exhibited patterning of the nervous system into distinct regions including diencephalon, midbrain, hindbrain and spinal cord (Kumar and Hedges 1998). Allowances for these anatomical features are seen in casts of early vertebrate fossils, and surviving relatives of pre-vertebral chordates, such as *amphioxus,* have the basic pattern of the vertebrate central nervous system (Holland and Holland 1999). Clearly the vertebrate, or more specifically the mammalian, spinal cord is a structure of extremely ancient origin, and having undergone half a billion years of evolution has developed into a highly specialised part of the CNS.

1.2.2 Anatomy

The spinal cord extends from the medulla at the base of the brain to its most caudal extremity, the filum terminale. Along its length arise thirty-one pairs of nerves in the rat (Zeman and Innes 1963), formed from the afferent fibres entering the spinal cord at the dorsal surface and the efferent nerve fibres leaving on the ventral. The spinal cord is a flexible tissue that must bend and twist as an animal moves. To achieve this the spinal cord is held suspended in a column of cerebrospinal fluid (CSF), which acts as a hydraulic cushion. The fluid is formed in the choroid plexus and flows rostro-caudally through the central canal of the cord in addition to around the outer surface. Immediately around the spinal cord is the pial membrane, which is vascularised and is in contact with the cerebrospinal fluid filled subarachnoid space (see Figure 1.2.2.1). Along the length of the pia are fine folds of membrane, the ligamentum denticulatum, which hold the cord in the middle of the space and are attached to the arachnoid mater. Immediately adjacent to this arachnoid barrier is the dura mater, the tough fibrous membrane, which holds the CSF at a pressure of 100-150mmH_2O and helps to protect the cord from injury.

The grey matter of the cord is a highly vascularised region. It contains neurons along with their supportive glial cells, and is surrounded by the white matter, which consists of axons and glia (Feldman *et al.* 1997). Astrocytes supply neurons with nutrients absorbed from blood vessels and maintain the extracellular environment by taking up K^+ and Cl^- ions, and also neurotransmitters, such as glutamate. Morphologically these cells can be divided into fibrous astrocytes, which are found in white matter areas, and protoplasmic astrocytes, which are present in all other areas (Feldman *et al.* 1997). Oligodendrocytes, which myelinate certain axons and thereby increase their conduction speed, form linear arrays where axons are grouped together into bundles. Microglia, the resident macrophages of the central nervous system, are also present and may play an important role in the acute inflammatory process.

In all the work discussed below, it is to be assumed that the rat is the species used, unless otherwise stated.

Figure 1.2.2.1 Anatomy of the spinal cord

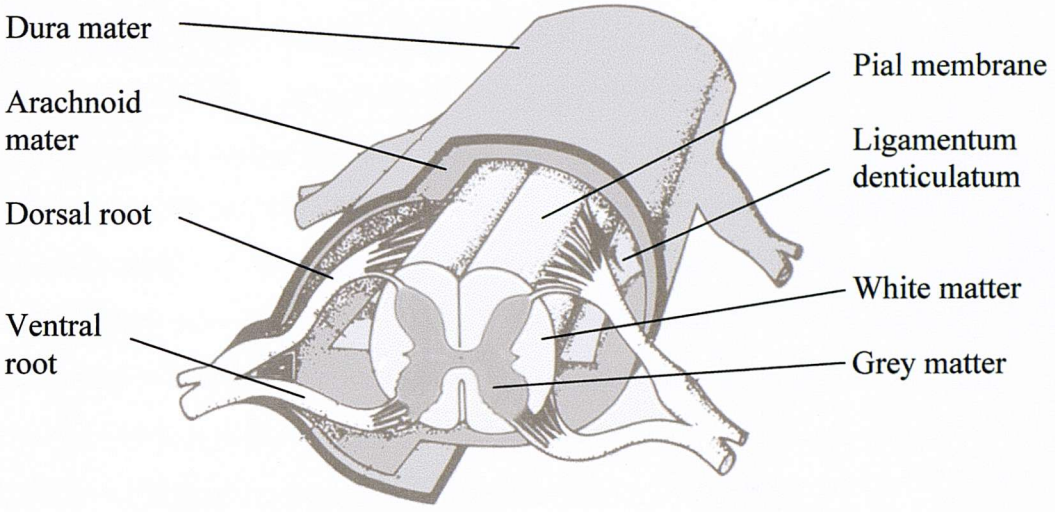

Diagram of the spinal cord showing the relative positions of the protective membranes which surround the white and grey matter. (Adapted from Snell, R.S. (1992), Clinical Neuroanatomy for Medical Students, Little Brown & Co., USA)

1.3 Experimental spinal cord injury

1.3.1 Historical perspective

The study of the spinal cord can be traced back as far as Hippocrates (460-370 B.C.) (Marketos and Skiadas 1999a) and Galen of Pergamun (129-200 A.D.), who showed experimentally that severing the spinal cord resulted in paralysis and loss of sensation below the lesion (Marketos and Skiadas 1999b). The first significant attempts to understand the nature of spinal injuries occurred in the early twentieth century. It was known at this time that spinal injury could result from a fracture dislocation of the vertebrae, and a model to simulate the resulting compression of the spinal cord was developed in the dog by Allen (Allen 1911). He dropped a captive weight onto the surface of the cord to deliver a reproducible impact, and found a correlation between the force of impact and the neurological outcome of the animals. Following impact he noted that a traumatic lesion developed, with a haemorrhagic necrosis of the grey matter. He made an incision into the cord to drain the haemorrhagic material, and animals that received this drainage showed a improved neurological outcome. This observation led Allen to propose the concept of a 'biochemical factor', present in the haemorrhagic and necrotic material, which was exacerbating the spinal cord damage.

1.3.2 Experimental models of SCI

Animal models of SCI have since been developed in many species including rabbits (Cassada *et al.* 2001), rodents (Faden *et al.* 1981), cats (Faden *et al.* 1981) and primates (Bingham *et al.* 1975). Lasting paraplegia can be produced in dogs with a weight drop of 450g-cm (g-cm is a product of weight in grams and height in cm) onto the dura at the surface of the spinal cord (Allen 1911). The rat and rabbit are particularly sensitive to this sort of injury, showing significant damage with much less force, for example 25gm-cm or 50g-cm in the rat (Carlson *et al.* 1998; Rosenberg *et al.* 1999).

More detailed study of the evolution of the lesion has shown that the dorsal part of the grey matter is relatively free of damage immediately after the impact, whilst a haemorrhagic lesion develops in the central grey matter within two hours. Following a severe impact (500gm-cm) in the dog the area of necrosis as a percentage of the total cross sectional area of the cord is already 40% at 4 hours and by 24 hours there is

only a thin rim of white matter left, surrounding a mass of necrotic tissue and blood (Osterholm 1974).

In human spinal cord injury the ventral parts of the cord are displaced following a dorsal compression, which results in the stretching of axons. Axons do have some capacity to stretch slowly, but at the relatively high velocities experienced in a traumatic impact (0.5 – 1m.s^{-1}) axonal transection can occur (Honmou and Young 1995). Compression and stretching can both disrupt the vascular supply to the tissue and lead to ischaemia, which may result in additional axonal and vascular damage. Experimental models have been developed which mimic these contusive and ischaemic components of spinal cord injury (see Table 1.3.2.1).

1.4 Pathological mechanisms in SCI

1.4.1 Primary and secondary damage

The initial physical injury of the cord, for example fracture dislocation of the spine, produces primary damage to the cord through the direct physical disruption of the grey and white matter of the cord. The concept of secondary damage, i.e. that following the physical trauma of the injury there is a secondary phase of damage as a result of activation of biological processes, has become generally accepted. The ischaemia, haemorrhage and oedema characteristic of SCI are all considered to be part of this secondary injury (Osterholm 1974). The area of the spinal cord affected by the mechanical impact is analogous to the core of an ischaemic stroke, in that the injury sustained in this area may be irreversible. The tissue surrounding this area may be amenable to intervention to salvage the neurons, glial cells and axons at risk, and in this way resembles the penumbral area around a stroke.

1.4.2 Pathological mechanisms

Spinal cord injuries are complex traumatic events that lead to the initiation of many potentially harmful biological mechanisms. In addition to damage to neurons, axons and glia there is injury to the vascular system, which can result in blood-spinal cord barrier disruption and ischaemia. The most relevant mechanisms are discussed below, although further elaboration is provided where appropriate in the experimental chapters which follow.

1.4.2.1 Vascular injury and ischaemia

In the dog, ligation of the radicular arteries produces a spinal cord lesion characterised by a haemorrhagic, necrotic central area, resulting in the loss of the grey matter and surrounding areas of white matter (Woodward and Freeman 1956). This pattern of injury is identical to that seen following a weight drop injury, which suggests that much of the non-mechanical damage may be due to ischaemia. Normal blood flow in the dog spinal cord is only 30-45% of that in the brain on a weight for weight basis (Ducker and Perot 1971) and it has been suggested that this difference in perfusion may leave the cord more vulnerable than the brain to hypoxic insult. A lack of 'reserve capacity' may result in a reduced ability to cope with a drop in perfusion, such as may occur following trauma (Ducker and Perot 1971). It is also possible that the difference simply reflects that the proportions of white and grey matter in the spinal cord and brain are different, and hence the metabolic demand of the two tissues.

Morphological changes in the vascular system in response to injury have been studied using corrosion casts of the normal (Koyanagi *et al.* 1993a) and injured (Koyanagi *et al.* 1993b) rat spinal cord. From 15 minutes after the injury induced by clip compression at C8-T1, the vasculature of the grey matter at the injury site was inaccessible to the polyester resin. The authors show that there was extravasation of the resin at the injury site at 15 minutes, suggesting that active haemorrhage is present at this time. The sulcal arteries, which emerge from the ventral spinal artery and pass through the ventral median fissure to supply the ventral grey matter, were constricted, leaving fine ridges on the casts where the endothelial cell nuclei had been compressed by the underlying smooth muscle.

Haemorrhage in the grey matter is one of the early consequences of SCI. Electron microscopy has been used to demonstrate that erythrocytes are present in the perivascular spaces surrounding post-capillary venules 15 minutes after a T10 contusion injury in Rhesus monkeys (Dohrmann *et al.* 1971). Axonal disruption and ischaemic damage to the endothelium were not observed until 4 hours later. The accumulation of blood-borne cells in the perivascular spaces can lead to the narrowing of vessels and the subsequent ischaemia of the surrounding tissue. Thus haemorrhage in the grey matter may lead to ischaemic insult to the adjacent white matter.

Table 1.3.2.1 Experimental SCI methodologies

Electrolytic lesion	Mathers and Falconer 1991
Clip compression	Koyanagi, Tator et al. 1993; Baffour, Achanta et al. 1995
Weight drop	O'Brien, Lenke et al. 1994; Taoka, Okajima et al. 1997
Blocking weight	Fujimoto, Nakamura et al. 2000
L-NAME ischaemia	Yezierski, Liu et al. 1996
Systemic hypotension	Kobrine, Evans et al. 1979
Excitotoxicity	Pisharodi and Nauta 1985
Excitotoxicity quisqualate	Brewer, Bethea et al. 1999
Balloon catheter in aorta	Hirose, Okajima et al. 2000
Contusion	Carlson, Parrish et al. 1998; Yu, Jimenez et al. 2000
Aortic occlusion	Francel, Long et al. 1993
Endothelin (intrathecal)	Hokfelt, Post et al. 1989
Photochemical ischaemia	Hao, Herregodts et al. 1994
Radicular artery ligation	Woodward and Freeman 1956

1.4.2.2 Lipid peroxidation and antioxidants

Oxidative stress and the presence of free iron in areas of haemorrhage results in lipid peroxidation, which damages cell membranes and may result in cell death. Methylprednisolone (MP), a glucocorticoid with potent anti-inflammatory effects, has been tested in the clinic (Bracken *et al.* 1990), and although there is some criticism of the study (Hurlbert 2000), high dose methylprednisolone has been adopted as first line therapy in acute spinal cord injury. At the high doses required to show efficacy in the human clinical trials, the activity of methylprednisolone is believed to be due to inhibition of lipid peroxidation rather than glucocorticoid receptor activation. Animal studies have reported that high dose steroids are effective in SCI, although improved behavioural outcomes have not always been observed (Faden and Salzman 1992).

Tirilizad (U-74006F) is a synthetic aminosteroid which has little mineralocorticoid or glucocorticoid effects, but does potently inhibit lipid peroxidation, is effective in rat SCI (Behrmann *et al.* 1994). This study produced a small, but significant, improvement in behavioural scores (open field walking test) in animals receiving tirilazad. More evidence of efficacy has come from a rabbit model of SCI induced by aortic occlusion (Francel *et al.* 1993), where the authors showed that 36% of the animals receiving tirilizad were paraplegic 96 hours after occlusion compared to 79% of the vehicle dosed animals.

1.4.2.3 Arachidonic acid metabolites

Calcium entering an injured cell can activate phospholipases A_2 and C, and these can catalyse the production of arachidonic acid (AA) from phospholipids released from the membrane of an injured cell. This AA is a substrate for lipoxygenases and cyclo-oxygenases (Moncada *et al.* 1985), which are enzymes responsible for the downstream synthesis of leukotrienes (Salmon and Higgs 1994).

Leukotriene B_4 is a neutrophil and monocyte chemoattractant and has been observed to increase following experimental SCI (Xu *et al.* 1990). Another leukotriene, LTC_4, is reported to have an effect on vascular permeability and may contribute to the breakdown of the blood-brain barrier (BBB) seen after injury (Mitsuhashi *et al.* 1994).

Thromboxane A_2 (TXA_2), a platelet aggregating and vasoconstrictive derivative of the cyclo-oxygenase pathway, and 5-hydroxyeicosatetraenoic acid (5-HETE), a precursor of leukotrienes, are both increased in the spinal cord of rabbits following a period of ischaemia (Shohami *et al.* 1987). An additional property of 5-HETE is that it can reduce the production of prostacyclin (prostaglandin-I_2 (PGI_2)), which is a vasodilator and inhibits platelet aggregation. It has been proposed that the disturbance of the TXA_2/PGI_2 ratio towards a more vasoconstrictive, platelet aggregation promoting position, contributes to the vascular disturbances seen in SCI. Inhibition of the TXA_2 synthetic pathway resulted in an 80% reduction in TXA_2 but only a 40% reduction in vascular damage as measured by fluorescein uptake in a rat model of SCI (Mitsuhashi *et al.* 1994). This probably reflects both the high potency of the remaining TXA_2 and the multitude of other factors contributing to the vascular damage. Another approach to manipulating the TXA_2/PGI_2 ratio has been to use the PGI_2 analogue Iloprost, which also inhibits TNFα production *ex vivo* (Taoka and Okajima 2000). Unfortunately the systemic side effects seen in patients, resulting from the vasodilatation, which included headache and flushing, have precluded any further development of this agent in SCI.

1.4.2.4 Excitotoxic damage

Excitotoxicity has been suggested as another possible mechanism by which the secondary injury is produced in SCI. The extracellular concentration of glutamate is elevated after brain injury, and *N*-methyl-D-aspartate (NMDA)-sensitive glutamate receptor blockade has been shown to decrease the amount of neuronal damage observed in experimental models of stroke (Simon *et al.* 1984), and SCI (Faden and Simon 1988).

In ischaemia, mitochondria are deprived of glucose and oxygen and are unable to continue the synthesis of adenosine triphosphate (ATP). This ATP is essential for maintaining the membrane resting potential of neurons, via Na^+/K^+-ATPase, which normally consists of a higher $[Na^+]_{EC}$ and a higher $[K^+]_{IC}$. In the absence of ATP, this enzymic antiporter fails, and Na^+ flows into the cell and K^+ flows out, resulting in a net depolarisation (Szatkowski and Attwell 1994).

The excitatory amino acid glutamate (Glu) is normally retrieved from the synaptic cleft by a Na^+ and voltage dependent co-transporter (Nicholls and Attwell 1990). When the Na^+ gradient has been compromised by the lack of ATP, the result is an efflux of Glu (Rossi *et al.* 2000). There are three types of ligand gated ion channels sensitive to Glu, the alpha-amino-3-hydroxy-5-methyl-4-isoxazole propionic acid (AMPA), kainate- and NMDA-receptors. In addition to these ion channels, there are also a family of G-protein coupled receptors for which Glu is an endogenous ligand. Among this group of metabotropic glutamate receptors there are a number (mGluR4, mGluR6 and mGlur7), which have been proposed to be involved in the presynaptic release of Glu, and probably do not participate in the ischaemic events.

Under ischaemic conditions the presence of extracellular Glu and the reversal of normal transmembrane ionic gradients leads to the opening of the NMDA-receptor ion channel, and the influx of Ca^{2+} into neurons. In addition, Glu interacts with AMPA/kainate sensitive channels to allow additional depolarising Na^+ into the cell, which contributes to the opening of voltage-gated Ca^{2+} channels. Blockade of the NMDA-receptor with the specific antagonist MK801 has been shown to have a neuroprotective effect in SCI (Faden and Simon 1988), improving the neurological outcome for rats following a traumatic injury.

The distribution of glutamate receptors is not limited to neurons. AMPA and kainate type glutamate receptors are present on oligodendrocyte myelin and astrocytes. It has been shown that the selective AMPA antagonist GYKI52466 prevents glutamate mediated axonal damage during white matter trauma or anoxia *in vitro* (Li *et al.* 1999). This group also showed that blocking the Na^+-dependent glutamate transporter, which is located on the axonal membrane, protected the white matter during anoxia or trauma. In contrast to the reports that MK801 has a protective effect in SCI, *in vitro* studies have shown that white matter from the dorsal columns is not protected from glutamate toxicity by MK801 (Li and Stys 2000). Microinjection of the AMPA/kainate antagonist NBQX (2,3-dihydroxy-6-nitro-7-sulfamoyl-benzyo(*f*)quinoxaline) into spinal cord impact lesions in the rat (Rosenberg *et al.* 1999) reduced the axonal damage and myelin disruption, and prevented the loss of some astrocytes.

1.4.2.5 Calcium

The influx of calcium is believed to be the key step in ischaemia-induced neuronal cell death, although it is likely that some cells can survive mild excitotoxicity, and only those that surpass some threshold are ultimately destroyed. The increase in intracellular Ca^{2+} observed in ischaemic tissue is believed to be a key factor in the activation of the apoptotic pathway. An increase in total tissue calcium content has been observed in the rat spinal cord after a mechanical injury (Happel *et al.* 1981), and calcium entry into astrocytes (Du *et al.* 1999), axons (LoPachin and Lehning 1997) and neurons (Szatkowski and Attwell 1994) has been reported following injury or ischaemia. Increased intracellular calcium activates neutral proteases, phospholipase-A2 and other proteases, and leads to the release of mitochondrial contents such as cytochrome-c and caspase-9, resulting in cell death (see section on apoptosis below). Calcium has also been shown *in vitro* to exert a toxic effect on anoxic white matter (Waxman *et al.* 1991), and more recently it was demonstrated that a Na^{+}/Ca^{2+} exchanger is present on myelinated axons (Steffensen *et al.* 1997), which could potentially be reversed under anoxic conditions and lead to axonal disruption. Use of calcium channel blocking agents, such as nimodipine, showed some utility in experimental cord injury, but only when the resulting systemic hypotension was controlled (Tator and Fehlings 1991).

1.4.2.6 Apoptosis

Not all cells that are destroyed as a result of spinal cord ischaemia die through the excitotoxic, and potentially necrotic, mechanism just described. Apoptosis, which is a form of programmed cell death, is an active process requiring energy and the synthesis of new proteins. This type of cell death is also reported to contribute to neuronal and glial death in SCI. It has been shown using specific staining methods (e.g. terminal deoxynucleotidyl transferase (TdT)-mediated deoxyuridine triphosphate (dUTP)-biotin nick end labelling (TUNEL)) that apoptotic neurons are present in the grey matter 4 hours after a T9-10 weight drop injury (Liu *et al.* 1997). The number of apoptotic neurons peaked at 8 hours, but the number of apoptotic glial cells in the grey matter continued to rise until 24 hours after injury. A second wave of glial apoptosis was identified in the white matter adjacent to the lesion 7 days after the injury. These results have been confirmed in the monkey (*Macaca mulatta*), where glial cells distal to the lesion are still undergoing apoptosis in fibre tracts 3 weeks after contusion

(Crowe *et al.* 1997). These glial cells have been identified as apoptotic oligodendrocytes, which die as the axons which they ensheathe undergo Wallerian degeneration. As oligodendrocytes ensheathe a number of axons this could lead to the demyelination of non-injured axons.

Activation of caspases is one of the key elements of apoptosis, and can ultimately lead to the formation of death-receptor complexes (Matsushita *et al.* 2000). Using a mouse model of spinal cord ischaemia induced by aortic occlusion, this group demonstrated that caspase-8 mRNA was upregulated from 3 hours to 1 day post injury in the grey matter of the cord. Caspase-8 activates caspase-3, which is a key step in activating neuronal cell death in the brain (Nagata 1997). The caspases ultimately activate nuclear enzymes with DNase activity, which destroy the chromosomal DNA (for review see (Chalmers-Redman *et al.* 1997)).

Transient global ischaemia in the dog can lead to the collapse of oxidative metabolism within neuronal mitochondria, which results in disruption of mitochondrial membranes and the release of the organelle contents into the cytosol (Krajewski *et al.* 1999). Once released, cytochrome-c in the cytosol binds to Apaf-1, and this complex can lead to the activation of pro-caspase-9, which can also be released by the mitochondria.

1.4.3 Immune activation and inflammation in SCI

The role of the immune system is to defend an organism from pathogens and injury, and to assist in the restoration of function. Within the CNS, the inflammatory response following tissue trauma is desirable in that it clears away cellular debris that would otherwise persist, with the potential to trigger autoimmunity. As the CNS has a limited ability to regenerate in mammals, the additional damage caused by the normal inflammatory processes results in pathology.

1.4.3.1 Complement

The rupture of cells as a result of the physical trauma of SCI can lead to the exposure of cellular organelles such as mitochondria, which can activate the classical complement cascade (Sim 1994). This would constitute a normal, non-pathological reaction, which has evolved to clear away cell debris. There is some evidence that up-

regulation of the complement system does occur following transient forebrain global ischaemia (Schafer *et al.* 2000). In this study, microglia were shown to up-regulate C1q mRNA as early as 1 hour after insult. C1q is the starting point of the classical complement cascade. Monocytes and macrophages have receptors for C1q, which may stimulate them to become phagocytotic, and C1q has also been shown to induce chemotaxis in human neutrophils (Leigh *et al.* 1998).

1.4.3.2 Cytokines

Traumatic injury of the cord leads to the production of pro-inflammatory cytokines in the lesion, such as interleukin-1β (IL-1β), from endothelial cells and vascular smooth muscle cells (Tonai *et al.* 1999), microglia, astrocytes and macrophages (Wang *et al.* 1997). Other inflammatory cytokines, such as tumour necrosis factor-α (TNFα) and interleukin-6 (IL-6), are also increased locally after a spinal cord lesion (Leskovar *et al.* 2000). The effects of TNFα and IL-1β in the early lesion appear to be critical, as injection of these cytokines alone can produce the characteristic early neutrophil recruitment and delayed macrophage recruitment observed after SCI (Schnell *et al.* 1999b).

The involvement of these inflammatory cytokines in CNS inflammation has been well documented (Rothwell 1997). Following an impact trauma to the spinal cord IL-1β mRNA is upregulated within 1 hour and remains above normal levels for at least 7 days (Wang *et al.* 1997). IL-1β increases vascular permeability by opening the blood-spinal cord barrier (Schnell *et al.* 1999b), activates glia and promotes indirect neurotoxicity via the induction of nitric oxide (NO) (Hu *et al.* 1997; Rothwell 1997).

The response of endothelial cells to the presence of TNFα and IL-1β is to increase expression of the adhesion molecules ICAM-1 and VCAM-1 which allow neutrophils and monocytes to move through the blood-brain barrier into the tissue parenchyma. Following spinal cord contusion in the rat, neutrophils move into the tissue parenchyma within 4 hours and peak in density at 24 hours (Carlson *et al.* 1998). A similar pattern is seen in a murine model (Schnell *et al.* 1999a), where following a mechanical lesion in the dorsal cord maximum numbers of neutrophils are present at 48 hours.

Another consequence of IL-1β activation of endothelial cells is the upregulation of the chemokine cytokine-induced neutrophil chemoattractant (CINC), which has been observed in a rat model of permanent MCAO (Liu *et al.* 1993). The CINCs have been proposed as a potential target for therapeutic intervention because of their potent neutrophil chemoattractant properties (Yamasaki *et al.* 1997). Following SCI, up-regulation of other chemokines (MCP-1, MCP-5 and IP-10) is seen before leukocyte influx (Mennicken *et al.* 1999).

TNFα can induce endothelial cells to produce endothelin-1 (ET-1), which as well as having potent vasoconstrictive properties (Yanagisawa *et al.* 1988c), has many other properties, including the ability to induce endothelial cell proliferation, and a role as a signalling molecule in certain areas of the brain and spinal cord (Hosli and Hosli 1991). ET-1 also induces IL-8, a neutrophil chemoattractant, in murine (Hoffman *et al.* 1998), and human (Zidovetzki *et al.* 1999) brain derived endothelial cells *in vitro*.

The production of anti-inflammatory cytokines is normally upregulated as a consequence of inflammation in order to aid the resolution of the inflammatory process. One such cytokine, interleukin-10 (IL-10), has been investigated in an excitotoxic model of SCI (Brewer *et al.* 1999). In this study quisqualate, an AMPA-receptor agonist that can induce excitotoxicity was microinjected into the grey matter of the spinal cord at the lower thoracic and lumbar segments (T12-L12). Systemic IL-10 administration (5μg.rat^{-1} i.p. 30 minutes post quisqualate) resulted in a statistically significant reduction in the amount of grey matter damage seen after 72 hours. Co-injection of IL-10 (5ng.rat^{-1}) with quisqualate significantly exacerbated the lesion, suggesting that within the developing lesion itself the inflammatory response may be beneficial.

1.4.3.3 Macrophages

Microglia are the resident macrophages of the CNS, and can be stimulated by a variety of noxious or inflammatory stimuli into losing their stellate morphology and adopting a mobile, phagocytic phenotype (Kreutzberg 1996). These cells are phenotypically indistinguishable from macrophages derived from blood-borne

monocytes, which are recruited to the site of injury by many factors produced in the lesion, including the chemokine MCP-1 (Le *et al.* 2000).

One of the characteristics of severe SCI in both humans and rats is progressive cavitation, resulting in the rostro-caudal destruction of grey matter and surrounding white matter (Tator and Fehlings 1991). The contribution of macrophages and microglia to cavitation has been investigated by microinjection of zymosan particles into the corpus callosum (Fitch *et al.* 1999) and spinal cord (Popovich *et al.* 2002). Zymosan has α-mannan and β-glucan residues, which can bind to macrophage mannose receptors and the β-glucan binding site of the CR3 β2-integrin to induce phagocytosis. It was found that activation of macrophages with zymosan *in vitro* could lead to rapid morphological changes in astrocytes when these cells were added to astrocyte cell cultures. There was hypertrophy of the astrocytes, and cellular damage occurred due to the physical contraction of some processes. The use of the peroxisome-proliferator activated receptor-γ (PPAR-γ) agonist ciglitazone, which is a potent negative regulator of macrophage activation, resulted in a reduction in the *in vitro* 'cavitation' induced by zymosan conditioned macrophages (Fitch *et al.* 1999). The activation of microglia following direct microinjection of zymosan into the spinal cord was sufficient to induce axonal transection, demyelination and behavioural deficits (Popovich *et al.* 2002).

Monocytes are also recruited to the lesion from the circulation, where they undergo a change in phenotype to become macrophages. Depletion of peripheral macrophages using clodronate loaded liposomes have provided behavioural and histological evidence that macrophages enter the lesion from the periphery after the injury and contribute to the loss of function seen after SCI (Popovich *et al.* 1999).

1.4.3.4 Neutrophils

The recruitment of neutrophils into the lesion is seen as being one of the key deleterious events in SCI, and has been the subject of much speculation with regards to novel therapeutics. An increase in the number of activated neutrophils has been observed in the systemic circulation following acute stroke in man (Bednar *et al.* 1997). The current clinical therapy, high dose methylprednisolone (MP) within 8 hours of injury (Bracken *et al.* 1990), does not affect neutrophil recruitment in rat

models of SCI, and therefore there is a good case for supplementing the MP regime with other agents which can reduce the damaging effects of neutrophils or prevent their recriutment (Taoka and Okajima 1998).

Gabexate mesilate (GM), a protease inhibitor with anti-cytokine effects, has been shown to have a positive effect in experimental SCI through the inhibition of leukocyte activation rather than through its anti-coagulant properties (Taoka *et al.* 1997). The authors demonstrated that post-SCI neutrophil myeloperoxidase (MPO) activity in the injured segment was reduced after GM treatment, and this corresponded with a better functional recovery than animals receiving equivalent anticoagulant treatment. GM was also reported to have a potent inhibitory effect on TNFα production *ex vivo*. Reduced TNFα production *in vivo* with correspondingly reduced up-regulation of adhesion molecules which would account for the decrease in neutrophil infiltration seen.

One of the ways in which neutrophils contribute to the developing lesion is by the production of elastase, which can degrade the extracellular matrix, increase vascular permeability and reduce the structural integrity of the tissue. Synthetic inhibitors of this enzyme, such as Eglin C and L658758, have been tested in experimental SCI with some success (Taoka *et al.* 1998; Taoka and Okajima 2000). Another action of neutrophils is to secrete free radicals, which can damage nearby cells and enhance the inflammation by stimulating the release of AA metabolites. The hormone melatonin has recently been shown to be neuroprotective in SCI models, and this activity is believed to be mediated through hydroxyl and peroxyl radical scavenging (Fujimoto *et al.* 2000).

1.4.4 Secondary injury to the white matter

Both grey and white matter can be destroyed following spinal cord injury. This can be seen by the increase in the area of necrosis following a mechanical injury, which expands into the adjacent grey and white matter from the impact site (Liu *et al.* 1997). Destruction of neurons in the grey matter results in abnormal reflex and autonomic function specific to the level of spinal cord injury. Injury to the axons in adjacent white matter tracts results in loss of function in many systems above and below the

level of the lesion, and for this reason preservation and restoration of these axons is likely to lead to dramatic improvements in quality of life for individuals with SCI.

In addition to the direct transection of axons resulting from physical trauma, axons can be injured through secondary events following injury. Macrophages recruited into a traumatic spinal cord lesion have been implicated in generating 'bystander' damage to axons (Blight 1992). Microglia, the resident macrophages of the CNS, can be activated in an otherwise intact spinal cord by microinjection of zymosan, and this has been shown to cause irreversible damage to axons (Popovich *et al.* 2002). Ischaemia also injures axons, as metabolic failure results in calcium entry into the axoplasm (Stys 1998), and the subsequent activation of degradative enzymes, such as the calpains (George *et al.* 1995). If the ischaemia is not reversed and the axon undergoes sufficient injury, the process becomes irreversible and this generates permanent axonal loss. Traumatic axonal injury can result in the release of cytochrome-c and caspase-3 from mitochondria into the axoplasm, both of which can also contribute to degeneration (Buki *et al.* 2000). Axons that have been stretched but not transected physically may also degenerate as a result of calcium entry (Wolf *et al.* 2001). Sodium channels can be opened by the mechanical trauma allowing depolarising sodium into the axon, which in turn reverses the Na^{+}/Ca^{2+}-exchanger.

1.4.5 Mechanisms of axonal degeneration

Whatever the initial cause of injury, axonal degeneration has a distinctive pathology, characterised by anterograde Wallerian degeneration of the distal portion of the axon and retrograde degeneration of the proximal portion. Wallerian degeneration can proceed rapidly in the spinal cord, at a rate of approximately $3mm.h^{-1}$ (George and Griffin 1994), with the axon breaking up into many small degenerate fragments. The existence of a mutant mouse strain that exhibits slow Wallerian degeneration in response to injury has established that this degeneration is an active, not passive, process (Coleman and Perry 2002). Following transection of an axon in a normal C57 mouse, the distal segment degenerates and is unable to conduct action potentials after 1 day. Axonal transection in the C57/*Wld(S)*-mutant mouse results in the delay of this degenerative mechanism, and the axon is capable of conducting action potentials for at least 2 weeks.

Axonal injury is an important therapeutic target in acute injuries such as SCI (Stys 1998) and stroke (Dewar *et al.* 1999), and in chronic immune mediated degenerative conditions such as multiple sclerosis (Coleman and Perry 2002). Identification of novel treatments for spinal cord injury that interfere with or inhibit the mechanisms of axonal destruction may result in the preservation of axons that would otherwise have been lost.

Clearly there are many mechanisms that contribute to the pathology seen in the spinal cord following injury. Ischaemia caused by coagulation and vascular injury appears to be one the major contributors, as it leads to energy failure and subsequent injury to axons, neurons and glial cells. In addition to strategies aimed at overcoming these pathological cascades, there is much interest in the exploitation of existing mechanisms that permit regeneration in non-CNS tissues or are involved in the early development of the CNS.

1.5 Regeneration in the CNS

1.5.1 Scar formation

It has been known for some time that lower vertebrates, such as amphibians and fish, can regenerate the spinal cord after injury (Guth *et al.* 1983). In these organisms transection of the cord induces the proliferation of cells adjacent to the injury, resulting in restoration of the tissue. By contrast, a similar lesion in the mammalian cord results in the proliferation of fibroblasts, which proliferate to form a dense collagenous plug. In lower vertebrates the ependymal cells of the central canal form a bridge spanning the lesion site, which acts as a scaffold for the tissue to regenerate around, and this ultimately permits the elongation of axons across the wound. In mammals, the collagenous environment is not conducive to the repair of the spinal cord and axons do not enter. Additionally a glial scar is formed by the proliferation and activation of astrocytes, in the areas adjacent to the transection, which also prevents neurite outgrowth. Strategies that could lead to regeneration of the injured human spinal cord would bring great benefits to individuals with existing spinal injuries, as reconnection of the CNS to the periphery may permit sensation, movement and autonomic function. However, inappropriate regeneration could result in pain and further autonomic dysfunction. A full review of regeneration in SCI is beyond the

scope of this introduction; a broader account of the field can be obtained from a recent review by Ramer *et al* (Ramer *et al.* 2000).

1.5.2 Extracellular matrix

Experiments using peripheral nervous system tissue grafted into the CNS (David and Aguayo 1981) demonstrated that something present in the mammalian CNS environment prevented axons traversing the lesion scar area, rather than the lack of growth being due to some intrinsic property of the axon. Hibernating squirrels, which do not generate a glial scar or collagenous plug in response to spinal cord transection, still fail to send axons across the lesion (Guth *et al.* 1981).

The extracellular matrix (ECM) has been identified as a key element in defining the permissive or non-permissive properties of the CNS with respect to axonal regeneration. It has been demonstrated that normal white matter in the corpus callosum can support the growth of axons from implanted embryonic or adult dorsal root ganglion cells (Davies *et al.* 1997). However, not all the axons regenerated in this study, and it was observed that those that failed had done so in areas rich in proteoglycan. Removal of proteoglycan by treatment with a chondroitinase can restore the ability of peripheral nerve neurites, from embryonic chick dorsal root ganglia, to enter spinal cord tissue *in vitro* (Zuo *et al.* 1998). This has also been demonstrated *in vivo* in a dorsal column hemisection model, using peripheral nerve grafts as a substrate for regrowth of axons from Clark's nucleus (Yick *et al.* 2000). Recently chondroitinase ABC has been shown to promote functional recovery after a dorsal column lesion in the rat (Bradbury *et al.* 2002). The authors infused the enzyme (6μl of $10U.ml^{-1}$) into the lesion area every other day for 10-days after dorsal column transection and saw an improvement in grid and beam walking performance.

The role of collagen-IV and laminin, two main constituents of the basal lamina, in axonal growth following SCI has been studied (Weidner *et al.* 1999b). The deposition of basal lamina and fibrillar collagen has been suggested to be a physical barrier to axonal growth following injury, and the authors used 2,2'-bipyridine, an iron chelating inhibitor of prolyl 4-hydroxylase, to inhibit deposition of these ECM constituents following dorsal column transection. They showed that laminin and collagen-IV were

co-localised in the matrix of the lesion and axons had either turned away from this matrix upon contact or had undergone degeneration. Administration of 2,2'-bipyridine did prevent local formation of basal lamina in the lesion area but did not prevent axons from degenerating or turning back upon entering the lesion, which suggests that other signals may be involved.

1.5.3 Neurotrophins

Neurotrophic factors have been shown to have a positive effect on axon recovery after injury when administered locally. Fibroblasts genetically engineered to express neurotrophin-3 (NT-3) can increase corticospinal axon growth following a dorsal hemisection lesion (Grill *et al.* 1997) when implanted into the lesion cavity. Further experiments have been carried out using fibroblasts expressing a variety of neurotrophins including NT-3, brain-derived neurotrophic factor (BDNF), nerve growth factor (NGF) and basic fibroblast growth factor (bFGF) (McTigue *et al.* 1998). This study showed that NT-3 and BDNF expressing fibroblasts both promoted the regrowth of axons through a contusion lesion, and significantly increased the number of oligodendrocytes in the lesion, suggesting that they may have a role in myelination of regenerating axons. Although these results are encouraging, the growth of axons across a lesion is not useful unless they can reconnect to the correct target cells or structures.

Other factors in the lesion environment can play a positive role in axon guidance. Schwann cells transfected to over-express nerve growth factor (NGF) have been shown to permit the growth of axons through a collagenous matrix implanted into transected dorsal columns (Weidner *et al.* 1999a). Closer examination of the Schwann cell-axon interactions showed that the adhesion molecule L1 was present on the surface of the non-myelinating Schwann cells and the regenerating non-myelinated axons, whereas L1 was absent from myelinating Schwann cells and their axons. The authors suggest that this L1 specificity could be a means to ensure correct myelination status of regenerating axons.

1.5.4 Inhibition by myelin

CNS myelin itself is an inhibitor of axonal growth, and specific components, such as Nogo-A (Chen *et al.* 2000) have been identified as being responsible for the non-

permissive status of the CNS environment (Horner and Gage 2000). The existence of a family of inhibitory proteins was first demonstrated by the use of a monoclonal antibody, IN-1, which was raised against a fragment of a myelin protein known to be an inhibitor of neurite outgrowth. The gene encoding this antigen has now been identified (Chen *et al.* 2000), and it is known to encode at least 3 proteins Nogo-A, -B and –C. Nogo-A appears to be the gene product responsible for the inhibition of neurite outgrowth as an anti-Nogo-A antibody allows dorsal root ganglion cells to grow on CNS myelin *in vitro*. The interaction between Nogo-A, which is located on the surface of oligodendrocytes and myelin, and the growth cone of a regenerating axon is mediated by a specific receptor. Nogo-66, a 66-amino acid portion of Nogo-A, which is present at the extracellular surface, is sufficient to generate a non-permissive environment for axonal regeneration. NgR, the receptor that interacts with Nogo-66 has been identified (Fournier *et al.* 2001), and expression of this receptor in retinal ganglion cells, which are normally insensitive Nogo-66, results in growth cone collapse on exposure to Nogo-66.

The IN-1 antibody has also been used to promote regeneration *in vivo*. Rats which have had their corticospinal tracts severed at the cervical level lose the fine control of the forepaw digits. Treatment with the IN-1 antibody for 2 weeks resulted in an improvement in the control of these digits which was not seen in control animals (Raineteau *et al.* 2001). The corticospinal tracts did regenerate, but there was a dramatic increase in fibres sprouting in the rubrospinal tracts, which demonstrates that compensatory regeneration can occur when inhibitory molecules are masked or inactivated.

Recently another ligand for the NgR receptor, oligodendrocyte myelin glycoprotein (OMgp), has been identified (Wang *et al.* 2002). OMgp is a myelin protein that can inhibit neurite outgrowth *in vitro*, and screening against a library of possible receptors showed that it binds to the NgR with a high affinity. This suggests that there may be a family of inhibitory ligands which all mediate their effect through a common nogo receptor.

1.6 Endothelin-1

One of the major physiological events which occurs in the spinal cord following traumatic injury is ischaemia. This is mediated by a number of vascular events including haemorrhage, oedema and vasoconstriction (Tator and Fehlings 1991). Ischaemia alone can produce a spinal cord lesion equivalent to one induced by a contusion injury (Woodward and Freeman 1956), and vasoconstricting substances such as endothelin-1 (ET-1) are found in the lesion following a mechanical injury (McKenzie *et al.* 1995). Microinjection of ET-1 into the rat striatum (caudate putamen) has been used to produce focal ischaemic lesions (Fuxe *et al.* 1992), and so it may be useful to pursue the use of ET-1 as a tool to induce focal ischaemic injury in the spinal cord. This purely ischaemic and non-mechanical injury could provide insight into some of the pathological processes occurring in spinal cord injury.

1.6.1 Physiology of Endothelin-1

The endothelins are a family of vasoconstricting peptides first identified by Yanagisawa and co-workers in the supernatant of cultured porcine aortic endothelial cells (Yanagisawa *et al.* 1988a; Yanagisawa *et al.* 1988b; Yanagisawa *et al.* 1988c). The potent vasoconstriction produced by these peptides makes them useful tools to model pathological situations where blood flow is interrupted or reduced.

Three distinct forms of endothelin have been characterised, endothelin-1 (ET-1), ET-2 and ET-3. These have different receptor binding properties at the two known types of endothelin receptors, ET_A and ET_B. Although originally defined in terms of their cardiovascular effects it is now widely appreciated that the endothelins may also play a wider role in the CNS as a neurohormone or modulator of neurotransmission (Mosqueda-Garcia *et al.* 1993; Damon 1998; Webber *et al.* 1998; Sluck *et al.* 1999).

The mature, 21 amino acid, ET-1 peptide is generated from a precursor molecule, big endothelin-1, by an endothelin converting enzyme. Inhibition of this enzyme by phosphoramidon abolishes the pressor response seen after administration of exogenous big ET-1 but not ET-1 (Fukuroda *et al.* 1990). Under normal physiological conditions there is very little free ET-1 in the circulation as it is rapidly bound to ET_B receptors in the lungs and metabolised (Kurtel and Ghandour 1999).

Figure 1.6.1.1 Mechanisms of action of ET-1

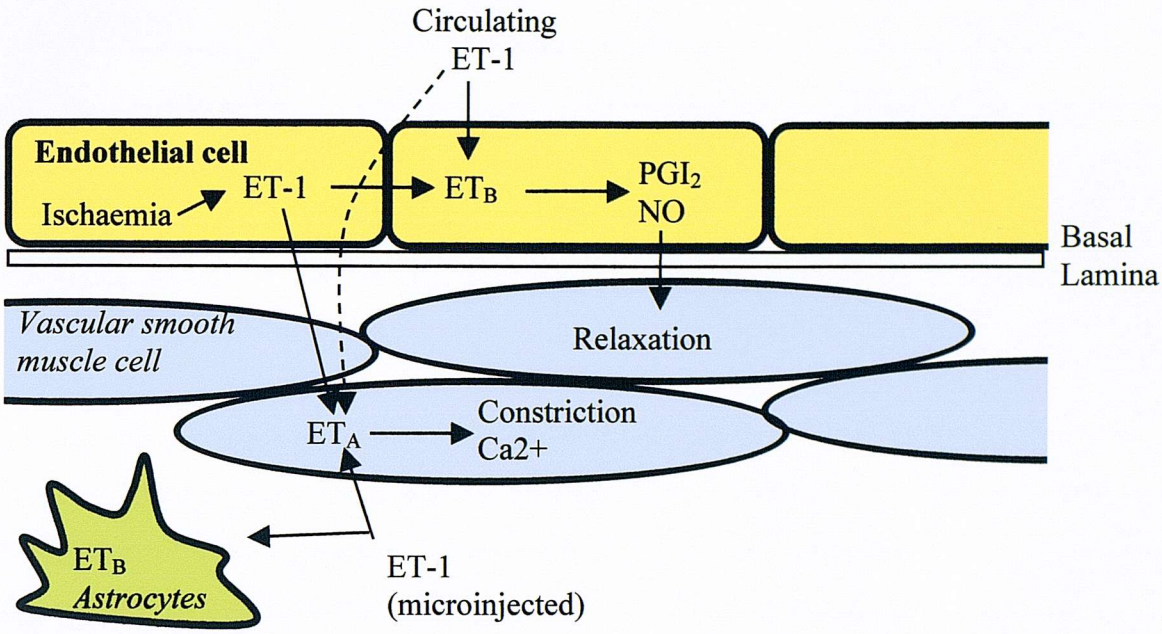

Diagram of proposed ET-1 mechanisms of action in the CNS vasculature and surrounding tissue. Systemic administration of ET-1 produces a transient ET_B receptor mediated depressor response in blood vessels which have an intact endothelium, followed by a ET_A receptor mediated pressor response. In denuded vessels only the pressor response is seen. Ischaemic endothelial cells increase their production of ET-1 and secrete it across the basal lamina to elicit an ET_A receptor mediated constriction of the smooth muscle. ET-1 in the tissue parenchyma, for example following microinjection, can access the vasoconstricting ET_A receptors and the ET_B receptors found on astrocytes.

ET-1 is involved in maintaining the basal tone of the vasculature, and in the periphery constitutive expression of ET-1 also regulates microvascular permeability (Victorino *et al.* 2000). ET-1 is released at the abluminal surface of the endothelial cell where it diffuses to the smooth muscle layer, causing a calcium-dependent constriction (Masaki *et al.* 1999) via the activation of ET_A receptors (Fernandez *et al.* 1998). A feedback mechanism exists whereby ET-1 can stimulate vasodilation via an ET_B receptor mediated increase in endothelial cell NO release (Karaki *et al.* 1993). This is summarised in Figure 1.6.1.1.

Hypoxia causes endothelial cells to increase synthesis of ET-1 (Yamashita *et al.* 2001) via the hypoxia-inducible factor-1 (HIF-1) and activator protein-1 (AP-1) binding sites of the ET-1 promoter. Increased secretion of ET-1 in this situation promotes endothelial cell proliferation and angiogenesis.

1.6.2 Non-vascular Endothelin receptors

It has been noted that endothelin receptors are present in non-vascular locations within the CNS (Nambi *et al.* 1990; Kohzuki *et al.* 1991), and that all the components required for an endothelin based communication system, the precursor proteins, converting enzymes and functional receptors, are present in certain areas of the brain (Sluck *et al.* 1999). For example dopaminergic neurons in the striatum with functioning ET_B receptors have been identified (Webber *et al.* 1998). Astrocytes (Venance *et al.* 1998) and microglia (McLarnon *et al.* 1999) expressing ET_B receptors have been reported, but not oligodendrocytes (Rogers *et al.* 1997).

1.6.3 Experimental ischaemia

Exogenous ET-1 can be used to generate an ischaemic lesion either via the vasoconstriction of the blood vessels entering a tissue, for example closure of the mid-cerebral artery using abluminal application of ET-1 (Sharkey and Butcher 1995) or by shutting down the microcirculation, for example microinjection into the striatum (Fuxe *et al.* 1992). Used in this way ET-1 is believed to mediate its effects purely via its actions on ET_A receptors.

1.8 Summary

Mechanical injury to the spinal cord results in haemorrhage, ischaemia, necrosis and the formation of a fibrotic and glial scar. This lesion can spread acutely within the grey and white matter, resulting in the loss of tissue not directly affected by the mechanical injury. Evidence from the literature suggests that ischaemia is a key factor in the activation of many of the pathological mechanisms seen in SCI, and induction of ischaemia alone can generate a lesion with all the features of a mechanical SCI. Many mechanisms contribute to the neuronal and axonal degeneration observed, and calcium entry and the activation of proteases is the common finale to these events, resulting in permanent loss of function. Although progress is being made with regenerative techniques for restoring spinal cord function to individuals with existing injuries, there is as yet no treatment to repair the spinal cord. In this context the prevention of axonal loss, and hence functional loss, is essential.

The induction of focal ischaemia in the ventral grey matter represents a new opportunity to investigate the role of secondary mechanisms, which have the potential to be inhibited or modulated by novel therapeutic strategies, in the evolution of spinal cord injury. In the following chapters, a new rodent model of SCI is described in which ischaemia is used to generate both grey and white matter pathology, without any direct mechanical injury to the spinal cord.

Chapter 2 - Methodology

2.1 Introduction

There are a number of ways to study the effects of ischaemia on the spinal cord, including the use of *ex vivo* models of tissue ischaemia (Li and Stys 2000) and *in vitro* cell culture techniques (Yu *et al.* 2001). The model described below represents a novel technique to induce focal ischaemia, resulting in spinal cord injury without significant mechanical trauma.

This chapter presents the techniques that are used in the experimental chapters. Specific details, for example concentrations, dilutions and doses, are provided in these chapters. All of the animal procedures described below were performed under a UK Home Office licence (PPL 30/1462) in accordance with the Animals (Scientific Procedures) Act 1986.

2.2 Methodology I – **Spinal cord microinjection: histology**

2.2.1 Anaesthesia

Male Wistar rats (Harlan, Bicester, Oxon.), weighing 180-260g, were anaesthetised with Hypnorm (Janssen-Cilag, UK) /Hypnovel(Roche, UK). Hypnorm and Hypnovel were diluted separately 1:1 with sterile water for injection and injected separately subcutaneously (s.c.) in the scruff with a dose volume of 1.35ml.kg^{-1} (dose administered: midazolam 3.38mg.kg^{-1}, fentanyl citrate 0.21mg.kg^{-1}, fluanisone 6.75mg.kg^{-1}). This dose of anaesthetic produces approximately 45 minutes of surgical anaesthesia followed by a prolonged period of sleep. A top-up dose of anaesthesia was occasionally required, and in these instances 0.1ml of each diluted component was administered s.c. on the flank of the animal.

2.2.2 Preparation of micro-pipettes

Finely drawn glass micro-pipettes were prepared by pulling a calibrated borosilicate glass 5µl capillary (Sigma, UK) in a vertical pipette puller (Model 700C, David Kopf Instruments) set with the following parameters: heater 66%, solenoid 76%. Micro-pipettes made using this method have a tip diameter in the region of 30-50µm. The pipettes were filled by drawing the solutions up through the pipette tip using a vacuum

generated by a 10ml disposable syringe connected via length of flexible cannula. Positive pressure was applied to deliver the pipette contents.

2.2.3 Microinjection into the spinal cord

Each animal was shaved along the midline from the base of the skull to a point approximately two-thirds down the spine, and the skin cleaned with a dilute (>1:10) solution of chlorhexidine (Hibiscrub (4% chlorhexidine gluconate) Zeneca). A homeothermic blanket unit (Harvard Apparatus, UK) consisting of a thermostatically controlled blanket and a rectal temperature probe was used to maintain body temperature at ~37°C during the procedure. A longitudinal dorsal midline incision was made to expose the connective tissue and the nuchal adipose body overlying the thoracic muscles, and these were blunt dissected and retracted rostrally. The blood supply to the nuchal adipose body emerges between the fourth and fifth thoracic vertebrae, which allows identification of the seventh thoracic vertebra (T7). A partial laminectomy was performed at T7 to expose the spinal cord; the dura was left intact at this stage. The muscle was dissected away from T6 and T8 to enable the immobilisation of the spine in a modified stereotaxic frame (David Kopf, USA) using clamps that attach to the spinal processes. Once the spine was clamped securely, and thus isolated from respiratory movement, a 27 gauge sterile needle was used to pierce and cut the dura dorsal to the required injection site. A finely drawn pre-filled glass micro-pipette was positioned over the spinal cord and lowered so that the tip was located in the ventral grey matter at T7 (0.4-0.5mm lateral, 1.5-1.6mm ventral).

Solutions were administered over at least 2 minutes, and the capillary left for a further 2 minutes before being withdrawn slowly. The muscle layers overlying the spine were re-apposed using 4/0 Vicryl sutures (Johnson & Johnson), and the nuchal adipose body and associated connective tissue were repositioned before closing the skin incision with 12mm Michel clips (IMS, UK). Post-operatively the animals were placed in a thermostatically controlled recovery chamber and monitored until the righting reflex had returned, at which time the animal was returned to a clean cage containing additional shredded-paper bedding, and with water and rodent diet pellets *ad libitum*.

2.2.4 Microinjection of substances into the caudate putamen

Each animal was shaved along the midline from the top of the head rostrally, and the skin cleaned as described above. Once the animal had been positioned in the stereotaxic frame, a longitudinal midline scalp incision was made to expose the skull, and the intersection of the sagittal and coronal sutures (bregma) located. A burr hole was made in the skull overlying the caudate putamen (striatum), and a finely drawn pre-filled glass micropipette was lowered such that the tip was located in the striatum (+1.0mm rostral, 3.0mm lateral, 4.5mm ventral to bregma). Microinjections were usually performed on the left hemisphere, unless vessels on the pial surface precluded lowering the capillary, in which case another burr hole was made and the right hemisphere injected.

Solutions were administered over at least 2 minutes, and the capillary left for a further 2 minutes before being withdrawn slowly. The skin overlying the skull was reapposed using 4/0 Mersilk sutures (Johnson & Johnson).

2.2.5 Endothelin lesions

Endothelin-1 (human/porcine sequence (E7764), Sigma, UK) was dissolved in sterile saline to give a 100pmol.μl^{-1} stock solution, which was stored at -20°C until use. Prior to administration this was diluted to 60pmol.μl^{-1} with sterile saline (containing the inert blue dye monastral blue or colonyl blue) and used to fill a finely drawn glass micro-pipette. 0.25µl of endothelin-1 (equivalent to 15pmol) solution or vehicle alone was then administered as described above.

2.2.6 Perfusion

At the appropriate time after micro-injection animals were deeply anaesthetised with Sagatal (Rhône-Mérieux) (sodium pentobarbitone 60mg.rat^{-1} i.p.), and pinned out in a supine pose. An abdominal incision was made to gain access to the peritoneal cavity, and parallel incisions were made along either side of the abdomen up to the thorax. At this point the diaphragm was pierced, the ribcage cut back to reveal the thoracic cavity and the dissected abdominal/thoracic tissue pinned back to allow access to the heart. A peristaltic pump (Gilson, UK) was used to perform transcardiac perfusion with 100ml of heparinised saline (5 IU.ml^{-1}). Saline or fixative were delivered using a

23G butterfly needle (Abbot) positioned in the left ventricle and held in place with a pair of artery forceps. The right atrium was pierced to allow efflux of solutions. Once the perfusate leaving the atrium was clear, one of the fixatives described below was administered until fixation was complete. Fixation was assessed by observing the stiffening of the tissues, the extent of which varies between the fixatives. PLP produces light fixation and the tissues are not completely rigid, whereas Bouin's fixative results in a pronounced rigidity in the muscles and skin.

2.2.7 Fixation

The fixatives described below were chosen with respect to the anticipated immunohistochemistry to be carried out on the tissue (see section 2.7).

2.2.7.1 Periodate Lysine Paraformaldehyde (PLP)

PLP was prepared and used immediately at the time of fixation. 200mM lysine HCl (BDH) was adjusted to pH 7.4 using 132mM potassium dihydrogen phosphate (Sorenson's potassium phosphate, BDH). To make 1 litre of fixative, 375ml of lysine HCl (volume before pH adjustment) was added to 200ml of 10% w/v paraformaldehyde solution (dissolved by heating to 60°C and the addition of a small amount of 1M NaOH, cooled before use). To this was added 2.14g of sodium periodate, and the volume made up to 1000ml with 0.1M phosphate buffer (1:2 dilution of standard 0.2M phosphate buffer – see immunohistochemistry section below). After adjusting this to pH 7.2 using 1M NaOH, 2ml of glutaraldehyde (25% solution) was added to yield a final concentration of 0.05% glutaraldehyde.
Following dissection, PLP fixed tissue was post-fixed for 6 hours at 4°C before being transferred to sucrose solution (30% w/v in 0.2M phosphate buffer) for cryoprotection also at 4°C. The tissue was then removed, dried gently with a tissue to remove any surface sucrose solution, and coated in OCT (Tissue-Tek, Sakura Finetek). An aluminium foil cup, was filled with OCT and then the tissue was placed in the cup and manoeuvred to obtain the correct orientation. The cup was placed carefully into a beaker of iso-pentane (2-methyl-butane, BDH Analar, UK) which had been cooled over liquid nitrogen or dry-ice. Frozen blocks were then stored at -20°C until sectioning onto gelatinised slides using a refrigerated microtome (see section 2.4.1).

2.2.7.2 Bouin's Fixative

Bouins fixative was prepared by mixing saturated picric acid (BDH), 40% formaldehyde solution (Fisher Chemicals UK) and glacial acetic acid (BDH) together in the ratio 15:5:1. This fixative can be stored indefinitely once prepared. Following dissection tissue was post-fixed for 7 days in Bouins fixative before being processed for wax embedding.

2.2.7.3 Wax embedding

The tissue was passed through a series of dehydrating alcohols (see Table 2.1 for details), cleared in Histoclear and saturated in paraffin wax using an automated tissue processing carousel (Histokinette model E7326, British American Optical Co.). After completing this process the tissue was embedded in paraffin wax blocks, which were stored at 4°C until sectioning on a benchtop microtome (see section 2.4.1).

Table 2.2.7.3.1 *Wax embedding protocol*

Solution/Medium	Time in each pot (Hours)	
	Mouse brain cycle*	Rat brain cycle
70% Ethanol	5.5	0.5
70% Ethanol	1.5	2.5
80% Ethanol	1.5	2.5
95% Ethanol	1.5	2.5
Absolute Ethanol I	1.5	2
Absolute Ethanol II	1.5	3
Absolute Ethanol III	1.5	3
Histoclear I	1	2
Histoclear II	1.5	3
Histoclear III	2	21
Paraffin Wax I	1	3
Paraffin Wax II	2	2
Total time:	*22 hours*	*47 hours*

*Low volume tissue samples, such as rat spinal cords, are processed on the mouse brain cycle, as the distances required for diffusion are small.

2.2.7.4 Karnovsky's Fixative

This fixative was used in order to perform the Hanker-Yates reaction (see section 2.4.3). To make 1 litre of fixative, 300ml of 4.16% w/v paraformaldehyde solution (dissolved by heating to 60°C and the addition of a small amount of 1M NaOH, cooled before use) was mixed with 100ml glutaraldehyde solution (25%) and the volume made up to 500ml with distilled H_2O. An additional 500ml of 0.2M phosphate buffer was added, and following filtration the solution was adjusted to pH 7.2 and used immediately.

Following perfusion with heparinised saline and Karnovsky's fixative, tissue was post-fixed for 2-3 days and then cryoprotected (see PLP fixation, section 2.2.7.1). Tissue was embedded in OCT as described for PLP fixed tissue, but orientated to produce longitudinal sections (see section 2.3.6.7).

2.3 Methodology II – **Acute physiological measurements in the spinal cord**

2.3.1 Anaesthesia and surgical preparation

Male Wistar rats (Harlan UK) were anaesthetized by administration of urethane (Sigma, UK), 1.2g.kg^{-1} i.p. (urethane formulated in distilled H_2O at 100mg.ml^{-1}, dose volume 12ml.kg^{-1}). This regime produced a consistent anaesthesia with maintenance of blood pressure and respiratory function for at least 3-4 hours (see Laser Doppler Flowmetry below). Body temperature was maintained at ~37°C during the procedure using a homeothermic blanket unit with a rectal temperature probe (Harvard Apparatus, UK). A partial laminectomy was performed at the level of the seventh thoracic vertebra as described in section 2.2.3. In addition a femoral artery was cannulated (Portex 3F intravenous cannula) to enable blood pressure to be measured throughout the procedure. The cannula was filled with either saline or heparinised saline (10 IU.ml^{-1}) and connected to a pressure transducer to record blood pressure and monitor heart rate (Digimed BPA System, Perimed UK). A pre-filled micro-capillary was inserted into the spinal cord via a small hole in the dura using the stereotaxic frame micromanipulator (David Kopf). Animals subsequently underwent one of the following measurement protocols:

2.3.2 Laser Doppler Flowmetry in the spinal cord

Once the capillary was in place a laser Doppler probe (Model 403, Perimed UK) was positioned either adjacent to the micro-injection site or at another rostral or caudal laminectomy site. The probe tip has a fibre separation of 0.5mm, and is believed to measure the blood flow in $1mm^3$ of tissue. Obvious pial vessels were avoided and once a satisfactory flux signal had been obtained the microscope lamp was extinguished to reduce backscatter, and the laminectomy site was filled with KY Jelly (Johnson & Johnson) to limit the drying of the tissue and control bleeding from micro vessels in the site. Baseline recordings of flux were taken for 15minutes before microinjection into the spinal cord, and the capillary remained *in situ* for the duration of the recording (up to 4 hours). The velocity, concentration of moving blood cells (CMBC), perfusion, blood pressure and rectal temperature were recorded using a personal computer running PeriSoft software (Perimed UK). The laser Doppler unit, the blood pressure unit and the homeothermic blanket unit all provided output voltages that were converted from analogue to digital format and sampled by the Perisoft package at a rate of 8Hz. At the end of the recording period animals were killed by i.a. administration of Sagatal (sodium pentobarbitone 60-120mg.rat^{-1}) and the flux measured until a constant baseline had been reached. (For details of the flux measurement protocol see Chapter 3).

2.4 Methodology III – **Immunohistochemistry**

2.4.1 *Preparation of sections and buffers*

PLP fixed tissues were cut on a cryostat as either 50μm ('thick') or 10μm ('thin') sections in the coronal plane for brains and spinal cords and mounted onto gelatinised slides. Following drying overnight at room temperature, slides were stored at -20°C until use. For brain tissue '3-spot' slides were used, whereas for coronal spinal cord sections, '4-spot' slides were employed. For thick sections of either tissue, gelatinised frosted end slides were used.

Bouins fixed spinal cord tissues were cut in the longitudinal plane or the coronal plane as 10μm sections onto SuperFrost+ electrostatically charged slides. Following drying overnight at 37°C these slides were stored at room temperature until use.

2.4.1.1 Phosphate buffer

Standard 0.2M phosphate buffer was prepared by adding 500ml of 0.2M sodium hydrogen orthophosphate to 2 litres of 0.25M potassium dihydrogen phosphate (Sorenson's potassium phosphate, BDH). The resulting solution was adjusted to pH 7.4 as required.

2.4.1.2 Phosphate buffered saline

Phosphate buffered saline (PBS) was prepared by dissolving commercial PBS tablets (PBS (Dulbecco A) Tablets, Oxoid), 1 tablet per 100ml of ddH_2O. Composition of buffer: NaCl 160mM; KCl 3mM; disodium hydrogen phosphate 8mM; potassium dihydrogen orthophosphate 1mM; pH 7.3.

2.4.2 Standard Immunohistochemical method

PLP fixed slides were removed from the freezer and warmed to 37°C in an incubator for at least 10 minutes before proceeding. Bouins fixed slides were de-waxed by immersion in xylene (2 washes of 3 minutes each) followed by two washes in absolute ethanol (2 washes of 3 minutes each).

Endogenous peroxidase activity was quenched by incubating the slides in 1% v/v H_2O_2 in methanol for 20 minutes on a gently oscillating mixer platform. Following a rinse in distilled H_2O the slides were washed twice in PBS/Tween20 (0.05% Tween20 in PBS) for 5 minutes and a wax pen (ImmEdge, DAKO) was used to outline the tissue on the slides to reduce the chance of contaminating control sections with primary antibody and to reduce the total amount of reagents required.

2.4.2.1 Citrate treatment for Bouins fixed tissue

Due to the high degree of cross-linking that occurs as a consequence of this fixation technique, the following step was performed to aid antigen retrieval. Slides were placed into a plastic rack and container, and covered with citrate buffer (2.1g sodium citrate per 1000ml, pH 6.0). This was then placed into a microwave oven and heated at full power (900W, 2450MHz) for 3 minutes. The buffer was then topped up if necessary and the slides left to stand in the container for 5 minutes before repeating

the 3-minute microwave step. A 5 minute wash in PBS/Tween20 was performed before application of blocking serum (see below).

2.4.2.2 Blocking

The slides were tapped dry and placed into a slide tray, and one or two drops of blocking solution was added to each spot (see Table 2.4.2.3.1) and the slides incubated for 30 minutes at room temperature. The slides were tapped to displace the blocking serum before primary antibody or PBS (for negative control sections) was applied to each tissue section (see below for details).

2.4.2.3 Primary antibody and secondary antibody incubation

For 3 spot slides, 50µl of primary antibody solution or control (PBS) was applied to each section; 4 spot slides received 40µl per section. The slides were incubated for 2 hours at room temperature before the primary antibody solution was removed and the slides washed twice in PBS/Tween20 as described above. One drop of secondary antibody (see Table 2.4.3.2.1) was added to each of the spots and the slides incubated for a further 45 minutes.

2.4.2.4 Avidin-Biotin Complex and DAB reaction

Following another 2 washes one drop (60µl) of avidin-biotin-complex (ABC) (1 drop of Reagent A and 1 drop of Reagent B per 5ml of PBS, (ABC Elite, Vector)) was added to each section and incubated for 45 minutes. The ABC reagent was made up at least 45 minutes before it was required in order to allow the components to complex. The slides were washed 3 times in PBS/Tween20 and then reacted with diaminobenzidine (DAB) 0.00001% and 125µl H_2O_2 in 250ml of 0.1M phosphate buffer (1:2 of 0.2M phosphate buffer). The slides were observed regularly until the brown colour development due to DAB oxidation and precipitation was sufficient to identify clearly the cells of interest. Slides were then placed in clean PBS before being counterstained if required, then dehydrated and coverslipped (see below).

2.4.2.5 Counterstaining

Two methods of counterstaining were employed depending on the fixation of the tissue. Bouins fixed and wax processed tissue takes up haematoxylin whereas PLP fixed tissue is more suited to Cresyl fast violet acetate.

2.4.2.5.1 Haematoxylin counterstaining

Slides were taken from PBS and stained with Harris's haematoxylin (Merck BDH) for 10 minutes and rinsed briefly with ddH_2O. The slides were then placed into Scott's tap water (Potassium bicarbonate 2g, magnesium sulphate 20g in 1000ml ddH_2O) until the purple colour of the tissue had become an intense blue colour (at least 2 minutes). Differentiation of the slides in acidified alcohol (1ml glacial acetic acid per 100ml absolute ethanol) for 15 seconds was carried out and then the slides returned immediately to the Scott's tap water to fix the blue colouration. Following a rinse in PBS the slides were ready for dehydration and coverslipping (see section 2.3.2.6).

2.4.2.5.2 Cresyl fast violet acetate

Slides were taken from PBS and placed into acidified water (a few drops of glacial acetic acid in 250ml ddH_2O) for 3 minutes. Next the slides were stained with Cresyl fast violet acetate (Aldrich), 1g per 100ml ddH_2O for 2-5 minutes depending on the age of the solution. Following this the slides were moved quickly (approximately 10 seconds in each solution) through the acidified water and the dehydrating alcohols to xylene (see below).

2.4.2.6 Dehydration and coverslipping

Either directly after DAB colour development or following counterstaining if carried out, the slides were dehydrated by passage through a series of alcohols of increasing concentration: 70%, 80%, 95%, absolute ethanol I and absolute ethanol II. For cresyl violet counterstained tissue the slides need to pass quickly through the more aqueous solutions to prevent destaining. All other slides were passed through each of the alcohols (not including acidified water) for approximately 1 minute, with the exception of absolute ethanol II, which the slides were left in for 5 minutes.

After the alcohols the slides were passed through 2 stages of xylene (xylene I and xylene II) for at least 2 minutes each, and then coverslipped using DePeX mounting medium (BDH) and 50μm coverglasses (BDH).

2.4.3 Modified Hanker-Yates procedure

Horseradish peroxidase (HRP) was administered to the rats i.v. under isofluorane anaesthesia (0.5ml of 30mg.ml^{-1} HRP (Sigma) in sterile saline) via a tail vein, 30 minutes prior to perfusion and fixation with Karnovsky's fixative, and preparation of blocks as described above. Longitudinal 25μm sections were cut from OCT embedded tissue fixed with Karnovsky's fixative (see above), and placed free-floating into PBS. Sections were washed twice in phosphate buffer and then placed in pre-reaction solution (see Table 2.4.3.1) for 10 minutes. After another two washes in phosphate buffer, sections were reacted for 10-20 minutes in Hanker-Yates solution (see Table 2.4.3.1) to which 1 drop of hydrogen peroxide per 100ml has been added. This reaction results in the development of a brown colouration in areas where horseradish peroxidase has extravasated into the tissue parenchyma.

The tissue was then washed in phosphate buffer twice, and floated onto glass slides. These slides were air-dried overnight and then dehydrated through two changes of absolute ethanol, and then two changes of xylene before mounting with DePeX and coverslipping.

Table 2.4.3.1 Reagents for the modified Hanker-Yates procedure

Reagent:	Composition:
0.2M cacodylate buffer	250ml of 42.8mg.l^{-1} Na cacodylate solution
	225ml of 0.2N HCl (4.3ml conc. HCl in 250ml ddH_2O)
	Make up to 1000ml with ddH_2O, pH to 5.1
Hanker-Yates (HY)	250mg p-phenylenediamine
Solution	500mg catechol
	500ml 0.2M cacodylate buffer
Pre-reaction solution	6 parts 1% cobalt chloride
	4 parts 1% ammonium nickel sulphate
	1 part HY solution

Table of reagents required to perform modified Hanker-Yates procedure as described in section 2.4.3

2.5 Methodology IV – **Quantification**

Following immunohistochemistry quantification was carried out either manually using a microscope fitted with an eyepiece graticule, or with a computer based imaging system.

2.5.1 Counting cells using a graticule

The graticule was placed in the eyepiece of a microscope and at a suitable magnification (usually 25x or 40x objective) the field for counting was identified. Cells were counted starting in the top left field of the grid, and only cells that either fell entirely within the field, or crossed the top or left edges of the field were counted. This was repeated for all cells in the graticule field working in a left-to-right, top-down fashion. All measurements for a given set of data were made using the same eyepiece magnification.

Drawings made with a camera lucida established that the field of the graticule at 40x objective magnification was 288μm square with 12x eyepeieces, and 313μm square with 10x eyepieces.

2.5.2 Measurement of area using Leica Qwin

In situations where distinct cell bodies cannot be easily counted, for example where cell bodies may be overlapping or present in very high densities, the Leica Qwin (Leica UK) imaging and analysis system was used. The system comprises a video camera mounted on the head of a microscope via a camera tube, which captures real-time images of the field of view and these can be observed visualised using a PC-based software package.

Once the area of interest is in view at the desired magnification, and the colour balance is adjusted to allow optimum discrimination of the brown DAB signal, the image is acquired and a threshold applied to determine the area of DAB staining. The system can be calibrated using a slide mounted micrometer scale to ensure that for any given combination of lenses or camera adapters the area or length measurements obtained are accurate.

If the threshold, colour balance or intensity settings are not changed, it is possible to make measurements of DAB stain area on a number of slides and treat these data as quantitative.

2.6 Methodology V – **Electron microscopy**

2.6.1 Tissue preparation and fixation

Tissue specimens were prepared for transmission electron microscopy (TEM) by perfusion fixation with 4% v/v paraformaldehyde, 3% v/v glutaraldehyde in 0.1M piperazine-N-N'-bis(2-ethanesolfonic acid) (PIPES) buffer (containing 2% w/v sucrose) after normal perfusion with heparinised saline under terminal pentobarbitone anaesthesia. Perfusion fixation was performed until the soft tissues of the neck and hind-limbs had become completely rigid, indicating that the fixative had penetrated the tissues, and that the spinal cords should also be well fixed.

The spinal cords were dissected out and post fixed for 48 hours before further dissection. From each specimen a 1mm cube of tissue was taken and rinsed in 0.1M PIPES buffer/2% w/v sucrose before being immersed in osmium tetroxide. The blocks were dehydrated and embedded in Spurr resin. Ultra-thin sections were

obtained from these blocks and examined using an Hitachi H7000 electron microscope for evidence of axonal injury. In addition semi-thin sections were stained with toluidine blue and mounted on glass slides for light microscopic examination.

2.6.2 Analysis of EM

Scoring systems were designed to assess the degree of injury to the axoplasm and the myelin sheath by reviewing the images obtained from the electron microscope blindly and picking out representative axons which presented increasing degrees of axonal injury. Further detail of this is provided in Chapter 5.

2.7 Methodology VI –**ELISA quantification of ET-1 and Big-ET-1**

2.7.1 Preparation of samples

Spinal cord samples were prepared by quickly dissecting out a 1cm length of spinal cord, centred on the site of microinjection, from animals that had been perfused with heparinised saline under terminal pentobarbitone anaesthesia. An extraction procedure was then performed to recover the peptide of interest from the spinal cord, based on a protocol provided by the manufacturer of the ET- 1 and Big-ET-1 ELISA kits (IBL-Hamburg, Germany). The tissue was placed into 2ml of cold 0.1% trifluoroacetic acid (TFA), homogenised using a micropestle, and kept on ice until centrifugation at 15krpm (3000 x g) at 4°C. The supernatant was then recovered and passed over a SepPak-plus C18 solid phase extraction mini-column (Waters, UK) which had already been conditioned by washing with 4 x 1ml of 60% acetonitrile/0.1% TFA followed by 4 x 5ml of 0.1% TFA in water. The peptides of interest were retained on the column and eluted off with 3ml of 60% acetonitrile/0.1% TFA into a plastic container. This volume was then divided into 6 x 0.5ml aliquots and dried overnight using a vacuum centrifuge (Univap) which generated a vacuum of ~-1.0 bar (-100kPa) at 21°C. The samples were stored at -20°C until use. Samples of naïve spinal cord, and naïve homogenates spiked with the peptide of interest were also extracted in the same way to determine the recovery of the procedure (for more detail see Chapter 6).

2.7.2 ELISA protocol

The manufacturers instructions were followed when performing the ET-1 and Big-ET-1 ELISA quantification (IBL-Hamburg, Germany), and the protocols were identical unless specified below. Samples that had been prepared as described above were reconstituted with the provided assay buffer (1% bovine serum albumin, 0.05% Tween 20 in PBS) to the their original volumes (0.5ml) and placed in an ultrasonic bath to assist resuspension of the peptides. Subsequent dilution of the samples was performed using the assay buffer. The standards for both ET-1 and Big-ET-1 were prepared in the assay buffer, as a serial 1in 2 dilutions from 100pg.ml^{-1} to 0.78 pg.ml^{-1}. These standards, a zero sample (neat assay buffer), a blank control (no assay buffer or sample) and the diluted reconstituted samples were applied in duplicate to the precoated 96-well plate (100µl per well) and incubated overnight at 4°C. In the ET-1 ELISA kit the wells were precoated with an affinity purified rabbit anti-endothelin-1$^{15-21}$ IgG, and for the Big-ET-1 kit the wells were precoated with an affinity purified rabbit anti-rat big endothelin$^{22-38}$ IgG. The wells were then washed 7 times with wash buffer (0.05% Tween20 in phosphate buffer) before the addition of 100µl of a conjugated secondary antibody solution. For the both the ET-1 and Big-ET-1 ELISAs this was a rabbit anti-endothelin-1 IgG Fab'-horseradish peroxidase (HRP). This solution was incubated for 30 minutes at either 4°C (ET-1) or 37°C (Big-ET-1), and then the wells washed 9 times with wash buffer. At this stage 100µl of a tetramethyl benzidine (TMB) based chromogen reagent containing 0.01% H_2O_2 was added to each well and the plates incubated for 30 minutes at room temperature. At the end of this period 100µl of stop solution (1N H_2SO_4) was added to each well, and the absorbance of each well at 450nm was obtained within 30 minutes using a 96-well plate reader and personal computer based software package (Dynex Revelation 3.2).

2.7.3 Analysis of results

The mean of the duplicates for each of the samples or standard curve points was obtained and used for all further calculations after subtracting the mean of the blank wells. The standard curve was then generated and an equation (second order polynomial) generated in Excel (Microsoft, USA) to calculate the peptide content of the samples from the absorbance values.

Chapter 3 – Laser-Doppler Flowmetry of the spinal cord

3.1 Introduction

The induction of ischaemia in the spinal cord can be accomplished in a number of ways including the use of a blocking weight (Fujimoto *et al.* 2000), radicular artery ligation (Woodward and Freeman 1956) and aortic occlusion (Francel *et al.* 1993) (see Chapter 1 for more detail). However, in order to produce a focal ischaemia without the mechanical trauma or systemic effects associated with these techniques a more subtle approach is required (Corkill and Perry 2001). Endothelin-1 (ET-1) is the most potent vasoconstricting substance identified to date (Yanagisawa *et al.* 1988c), and has been used to generate ischaemic lesions in the rat brain either by direct application onto the mid-cerebral artery (Sharkey and Butcher 1995), or by parenchymal injection to constrict the microcirculation in the striatum (Fuxe *et al.* 1992). The use of ET-1 in inducing spinal cord ischaemia has been limited to intrathecal administration (Hokfelt *et al.* 1989; Westmark *et al.* 1995), which is effective in inducing a reduction in blood flow and generating a lesion. However, intrathecal dosing with large doses of ET-1 does not generate a precise focal ischaemia which can be studied histologically, but rather a more generalised spinal ischaemia with some systemic effects and in some instances mortality. By using a microinjection technique to deliver ET-1, a focal ischaemia can be generated in the spinal cord that is more amenable to investigation of secondary events, such as inflammation and white matter inury, and that does not have a high mortality rate.

3.1.1 Endothelin

The endothelins are a family of peptides (ET-1, ET-2 and ET-3) with roles in development (Baynash *et al.* 1994), blood pressure homeostasis (Mosqueda-Garcia *et al.* 1993) and communication within the CNS (Yoshizawa *et al.* 1990). ET-1 is a 23 amino-acid peptide in its mature form, and acts on two classes of ET receptors that have been classified pharmacologically as ET_A or ET_B. The ET_A receptors are located on the smooth muscle cells of the tunica media of blood vessels and mediate the vasoconstricting effects of ET-1 via a calcium dependent mechanism (Saito *et al.* 1991; Fernandez *et al.* 1995). The ET_B receptors reside on the endothelial cells, and activation of these receptors leads to the synthesis and release of nitric oxide (NO) (Rossi *et al.* 2001) and prostaglandins (Armstead *et al.* 1989) that diffuse through the

basal lamina to act on the smooth muscle cells, causing relaxation. Endothelins contribute to the basal tone of the vasculature through this feedback mechanism, the vasoconstricting and vasodilating actions balancing each other. In response to injury the endothelial cells can release ET-1, which induces vasoconstriction via the ET_A receptors, thereby reducing bleeding and promoting coagulation. If this was unopposed for an extended period of time the tissue could become necrotic, but the ET_B receptors mediate vasodilatation and hence reperfusion of the tissue.

A number of pharmacological tools are available to study the endothelin system *in vivo*. Sarafotoxin-6b (S6b) is a non-selective endothelin receptor agonist originally isolated from the venom of the mole viper *Atractaspis engaddensis*. As it is not cross reactive with antibodies raised against ET-1 or the precursor molecule big-ET-1 it can be used to investigate the role of the endogenous endothelin system during ischaemia using ELISA (see Chapter 6).

A modified form of ET-1 with four substituted Alanine residues in the peptide sequence (4-Ala-ET-1) has been identified which is a selective agonist for the ET_B receptor (Nakamichi *et al.* 1992). This peptide is comparable in size to the normal ET-1 peptide and the snake toxin S6b, and can be used to investigate the role of the ET_B receptor in ET-1 mediated events. The small non-peptide antagonists to ET_A and ET_B receptors such as BQ-123 and BQ-788 (Hiley *et al.* 1992; Koyama *et al.* 1999) are difficult to use without introducing organic solvents such as dimethylsulphoxide (DMSO), which itself causes tissue damage (authors own unpublished observations), and may have free-radical scavenging activity.

3.1.2 Endothelin in the CNS

In addition to the direct vascular effects, ET-1 is also known to have a cardiovascular function in the CNS. For example, in the rat, microinjection of ET-1 into the area postrema (where the blood-brain barrier is incomplete) or the nucleus of the solitary tract (which integrates information from the visceral afferent nerves and forms part of the autonomic reflex circuit) produces a reduction of blood pressure and bradycardia (Mosqueda-Garcia *et al.* 1993). However, not all of the locations where ET_A or ET_B receptors have been observed play an obvious role in cardiovascular homeostasis, and autoradiographic evidence suggests that there are many areas of the brain (Kohzuki *et*

al. 1991; Tayag *et al.* 1996), spinal cord and dorsal root ganglia (DRG) (Kar *et al.* 1991) where these receptors can be found.

ET_B receptors have been found predominantly on astrocytes (Baba 1998; Nakagomi *et al.* 2000) and microglia (McLarnon *et al.* 1999). In contrast, no endothelin receptors were detected on oligodendrocytes (Rogers *et al.* 1997). Certain populations of neurons, specifically the dopaminergic neurons in the rat striatum, express ET_B receptors (Tayag *et al.* 1996; Webber *et al.* 1998; van den Buuse and Webber 2000), supporting the role of endothelin as a signalling peptide in the CNS. The endothelin converting enzyme (ECE), which is required to generate biologically active ET-1 from a precursor molecule (pro-endothelin-1 or big-ET-1), can be found co-localised with ET-1 positive neurons (Sluck *et al.* 1999).

Endogenous endothelin, either produced locally in response to an injury or entering the CNS parenchyma from the circulation through a damaged blood-brain barrier, has been implicated in the development of astrogliosis after an injury to the CNS. ET_B antagonists reduce the astrocytosis seen after injection of ET-1 into the rat striatum (Baba 1998), or after a stab injury to the cerebral cortex (Koyama *et al.* 1999). In a rat spinal cord stab injury model endogenous ET-1 was shown to increase after the insult, and a non-selective ET receptor antagonist, SB209670, reduced reactive gliosis (Uesugi *et al.* 1996). There is evidence from *in vitro* studies that exposing astrocytes to a transient hypoxia and/or hypoglycaemia results in an increased release of ET-1 (Hasselblatt *et al.* 2001), and an increase in the expression of ET_B but not ET_A receptors (Shibaguchi *et al.* 2000). A selective ET_B antagonist results in the potentiation of the post-ischaemic effect of ET-1 *in vitro* (Hasselblatt *et al.* 2001), suggesting that ET_B receptors on astrocytes are involved in clearing excess ET-1 from the injured area.

Although the role of the ET system in CNS pathology following a traumatic or ischaemic insult is complex, ET-1 may provide an efficient investigative tool. The application of ET-1 directly into the CNS parenchyma will activate the ET_A receptors, resulting in a potent vasoconstriction, and hence a focal atraumatic ischaemia. The consequences of astrocytic, microglial or even neuronal ET_B receptor activation are likely to be secondary to the effect of the profound ischaemia induced.

3.1.3 Laser Doppler Flowmetry

The use of laser Doppler (LD) techniques to measure tissue perfusion is now well established and validated with respect to older techniques, such as radiolabelled microspheres (Lindsberg *et al.* 1989), for determining blood flow in the CNS. The LD technique relies on the fact that laser light (like other forms of electromagnetic radiation) of a given wavelength λ will be reflected back from a moving object with a longer or shorter wavelength than that from a stationary object. Thus when a laser of a suitable wavelength is shone into a vascular tissue, some of the laser light that is reflected will be from the stationary components (e.g. connective tissue, smooth muscle cells) and some will be reflected by moving cells such as erythrocytes. The reflected light received by the photodetector will comprise of a distribution of wavelengths, which after subtraction of the non-moving component (i.e. the wavelength of the illuminating laser) will provide us with information concerning the moving cells. The shift in the wavelength will indicate the velocity of the moving cells, and the intensity of the signal will be proportional to the number of moving cells. The non-shifted, backscattered, light signal can reduce the sensitivity of the detector; incident light coming from room or microscope illumination can contribute to this noise and may need to be eliminated or reduced.

The concentration of moving blood cells (CMBC) and the velocity (V) can be used to obtain an indication of the blood flow (flux) in the tissue using the following equation:

$$\text{Flux} = K \times \text{CMBC} \times V$$

The constant K is used to scale the reading appropriately for the equipment used. The flux, or perfusion, value does not have any units as it is a mathematical property of the light reflected and not a direct measure of movement. However, LD perfusion has been repeatedly shown to be a robust correlate of blood flow and is widely accepted as a diagnostic technique in both clinical and experimental settings (Bonner and Nossal 1990; Shepherd 1990; Belcaro and Nicolaides 2000).

This study set out to exploit the sensitivity and non-invasive nature of this technique to measure the changes in spinal cord blood flow induced by microinjection of ET-1 and other related peptides into the ventral spinal cord. By positioning the probe over

the dorsal surface of the cord it was intended that changes in microvascular perfusion in the ventral spinal cord could be observed and recorded over a period of several hours, both at the immediate injection site and at sites 1 or 2 segments distal.

3.2 Methodology

Male Wistar rats (mean weight 336g, range 250-420g) were anaesthetised with urethane (1.2g.kg^{-1} i.p.) and a laminectomy performed to access the spinal cord at the 7th thoracic vertebra (T7) (see Section 2.2). A homeothermic blanket unit (Harvard Apparatus, UK) was used to maintain the rectal temperature of the animal at 37-38°C throughout the procedure. The right femoral artery was cannulated and connected via a heparinised saline (10 U.ml^{-1}) filled cannula to a pressure transducer to record blood pressure and monitor heart rate (Digimed BPA System, Perimed UK). Once the spinal column was immobilised on a modified stereotaxic frame with spinal clamps, a glass micro-capillary (external tip diameter 30-50μm) was lowered into the left ventral horn at T7 (0.5mm lateral, 1.5mm ventral) (see Chapter 2). The capillary was pre-filled with ET-1 (Sigma, UK), 4-Ala-ET-1 (Sigma, UK), Sarafotoxin-6b (Tocris UK) or vehicle (physiological saline). All peptides were resuspended in sterile saline beforehand and stored at -20°C until use. Prior to injection the peptide solutions for injection were adjusted to 60pmol/μl, so that microinjection of 0.25μl delivered 15pmol.

3.2.1 Blood flow measurement

The laser-Doppler (LD) probe (Model 403, tip diameter 0.5mm, Perimed UK) was positioned on the cord surface adjacent to the capillary. In some instances a second laminectomy was performed at T5, T6, T8 or T9 to permit the placing of the LD probe at a different location to the microinjection site (T7). The laminectomy site was filled with KY Jelly (Johnson & Johnson, UK) to prevent the tissue from drying out, and the operating microscope light was extinguished to increase the LD perfusion signal. A 15 minute stable perfusion baseline was obtained prior to the administration of 0.25μl of vehicle, ET-1 (15pmol), 4-Ala-ET-1 (15pmol) or Sarafotoxin-6b (15pmol), and recording continued for at least a further 2 hours. At the end of the experiment euthanasia was induced by i.a. administration of sodium pentobarbitone (60-

120mg.rat^{-1}), and a biological zero flux reading obtained. This is the component of the signal that is purely due to the tissue and not movement of blood cells.

In addition to recording the output from the Perimed PF4001 unit (concentration of moving blood cells (CMBC), velocity (V) and perfusion units (PU)), rectal temperature and instantaneous blood pressure were also recorded. Due to the variation in vascularisation of the tissue and the positioning of the probe, it was necessary to normalise each trace obtained with respect to its baseline value and the biological zero. This was done by subtracting the biological zero PU value from all the data for a given animal, and then calculating each data point as a percentage of the mean baseline reading. The data acquisition was carried out by the personal computer based software system (Perisoft, Perimed UK) at a rate of 32Hz, and subsequently averaged over 20 second periods for analysis.

3.3 Results

3.3.1 Effects of anaesthesia on cardiovascular parameters

Preliminary experiments using Hypnorm/Hypnovel anaesthesia (the regime used in recovery spinal cord microinjection see Section 2.2) revealed that this combination is not suitable for long term anaesthesia due to the cardiovascular effects (see Figure 3.3.3.1). Over the three-hour observation period (which does not include the time taken to cannulate the femoral artery or perform the laminectomy) several top up doses of Hypnorm/Hypnovel were required to maintain anaesthesia. As a result the blood pressure dropped to less than 40mmHg, which is clearly below the normal physiological range for a rat (80-140mmHg). Also during this period respiratory effort reduced dramatically and the animal was tachycardic (heart rate 500 beats per minute). By comparison urethane (1.2g.kg^{-1} i.p.) maintained deep surgical anaesthesia throughout the 3-hour period with only a minimal drop in blood pressure.

Figure 3.3.1.1 Effect of anaesthetic regime on blood pressure

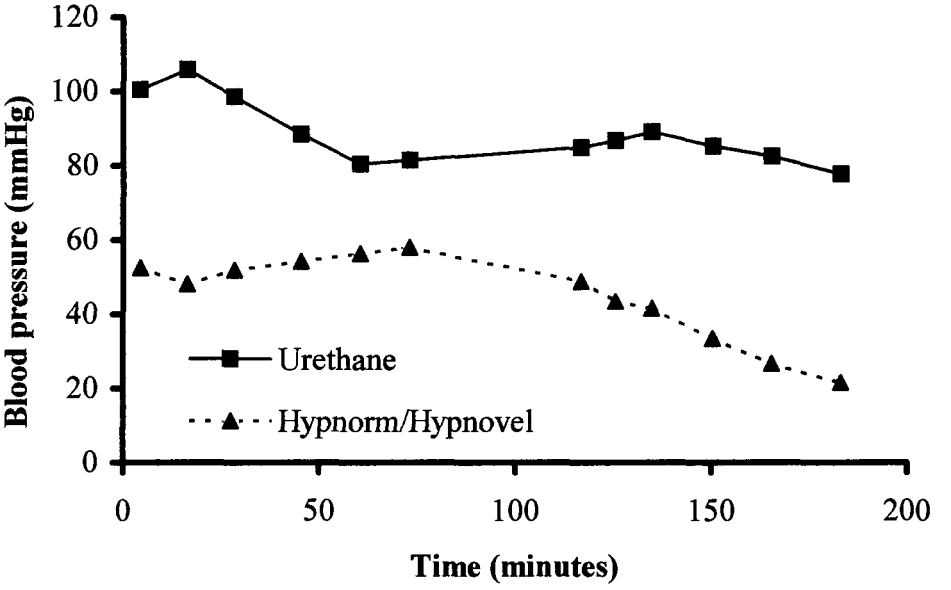

The effects of long-term anaesthesia with two different regimes on the blood pressure of male Wistar rats. Blood pressure was measured as the instantaneous output from the Digimed BPA unit, and reflects systolic rather than mean arterial pressure as the observed pulse pressure was low.

3.3.2 The observed drop in perfusion is due to a reduction in V not CMBC

The perfusion value is derived from both the CMBC and velocity measurements, thus any drop in observed perfusion could be due to a change in the velocity or the CMBC signal. Figure 3.3.2.1 shows an example of a recording obtained from the Perimed PF4001 during the administration of ET-1 (15pmol in 0.25µl). The CMBC value remains constant, although it does become more variable, whereas the velocity decreases following administration of ET-1, and this is reflected in the derived perfusion signal.

3.3.3 ET-1 micro-injection causes a rapid drop in spinal cord perfusion

The local microinjection of ET-1 (15pmol in 0.25µl) into the ventral grey matter leads to an acute drop in perfusion that is measurable from the dorsal surface of the cord using an LD probe (see Figure 3.3.3.1A). Within 30 minutes of injection the perfusion signal dropped to less than 10% of the baseline perfusion signal, and by 2 hours the signal has only recovered to 60% of control.

3.3.4 Sarafotoxin-6b induces a rapid decrease in spinal cord blood flow

In order to confirm that the S6b peptide was capable of mediating an ischaemic event of comparable magnitude to that seen with microinjection of ET-1, an equimolar amount of peptide (15pmol) was microinjected into the spinal cord. The effect of S6b on spinal cord blood flow is shown in Figure 3.3.3.1B.

3.3.5 ET-1 induced ischaemia is not mediated through ET_B receptors

To confirm in our model that the vasoconstriction we were observing was being mediated through the ET_A receptors located on vascular smooth muscle cells an ET_B selective agonist (4-Ala-ET-1) was used at an equimolar dose to the ET-1 microinjections. Figure 3.3.3.1C shows the effect on spinal cord blood flow of microinjection of 15pmol 4-Ala-ET-1.

3.3.6 ET-1 microinjection causes hypoperfusion over 3 segments of cord

The reduction in spinal cord blood flow observed after microinjection of ET-1 described above was measured at a site adjacent to the capillary. In order to determine the rostro-caudal extent of the ET-1 induced ischaemia the protocol was modified so

Figure 3.3.2.1 Example output from Perimed

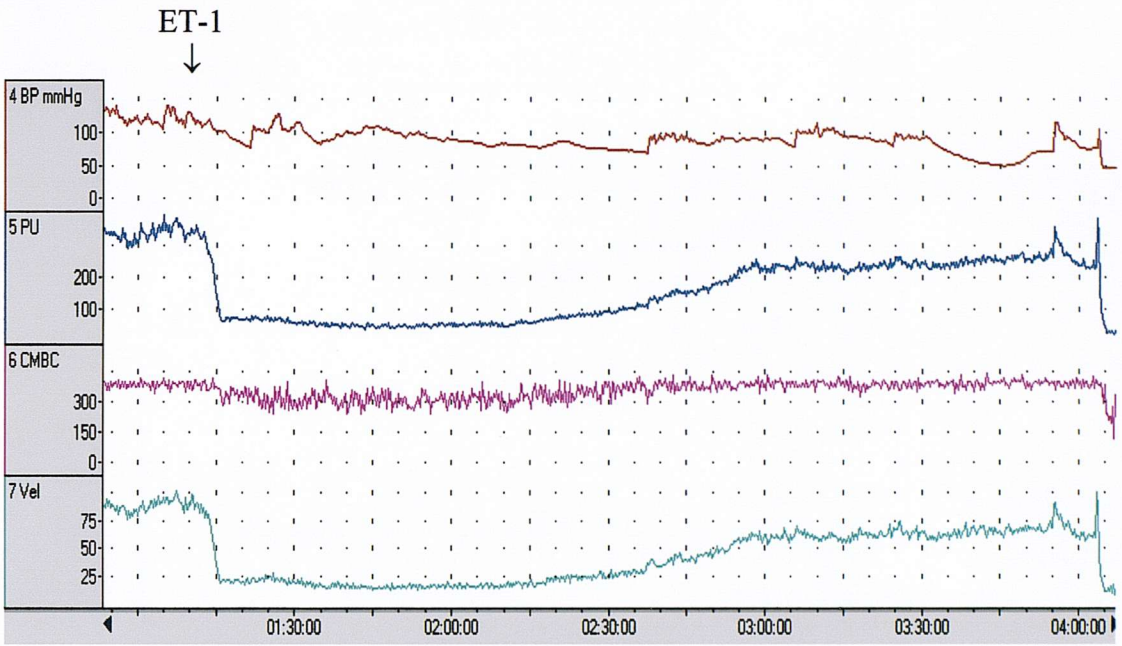

Example of recording trace from an ET-1 injected spinal cord with the LD probe positioned at T7. The x-axis shows time in minutes relative to the start of recording. The perfusion signal (PU) drops after the microinjection of ET-1 (15pmol, 0.25µl) as a result of the drop in velocity (Vel) rather than a drop in CMBC although this signal does become more variable. The instantaneous blood pressure as shown on the top channel remains in the physiological range throughout the procedure although the signal does drop occasionally due to clotting in the arterial cannula.

Figure 3.3.3.1 Effect of ET-1, 4-Ala-ET-1, sarafotoxin-6b or vehicle on spinal cord perfusion

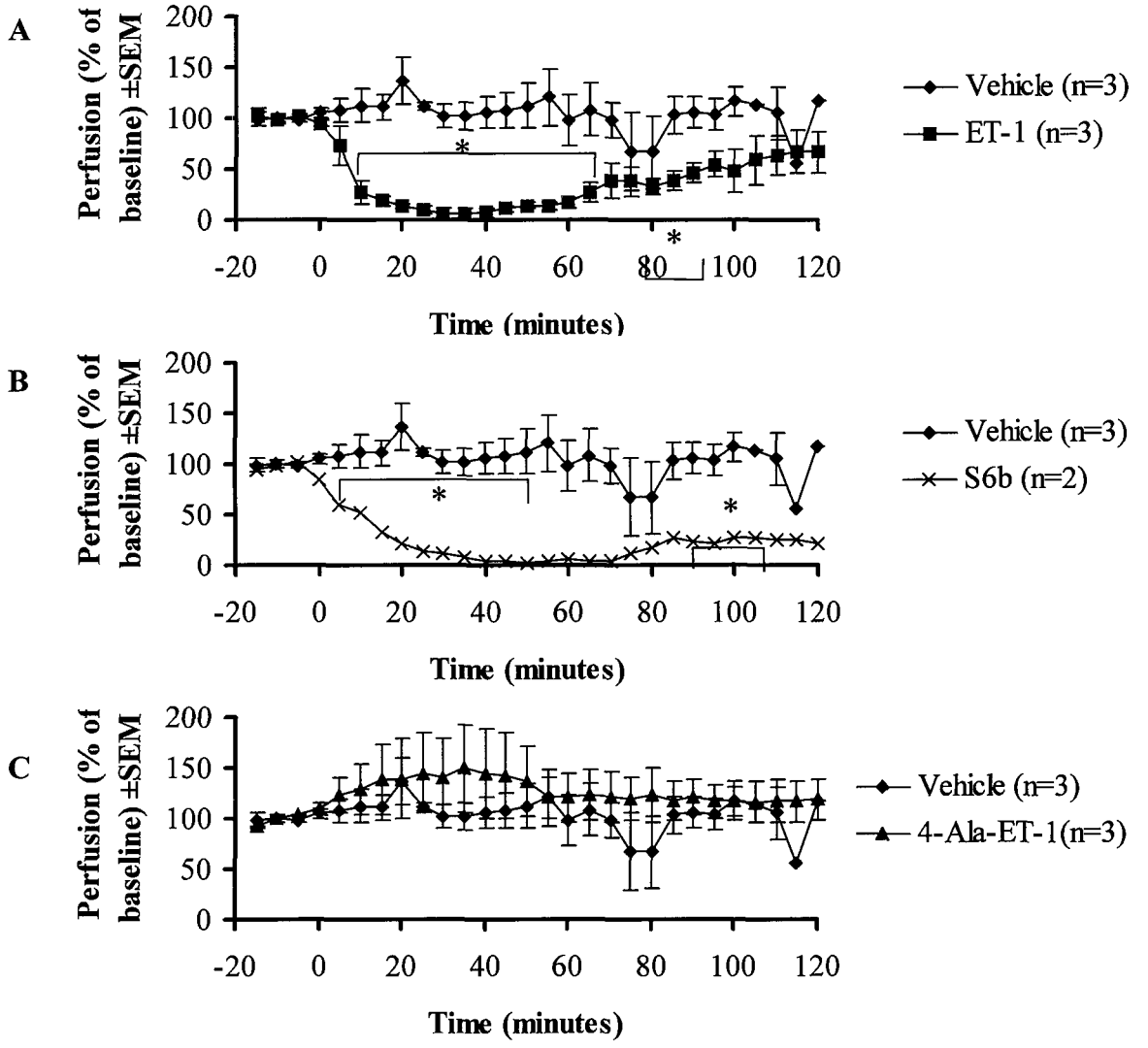

The effect of microinjection of 0.25µl vehicle (saline) into the ventral grey matter of the spinal cord at T7 on spinal cord perfusion as measured by laser Doppler compared to 15pmol of (A) ET-1, (B) Sarafotoxin-6b or (C) 4-Ala-ET-1. Microinjection performed at time zero following a 15-minute baseline period. Error bars as shown are SEM.(* $p<0.05$, one-way ANOVA).

that the LD probe was positioned at sites rostral (T5 or T6) or caudal (T8 or T9) to the site of microinjection (T7). Figure 3.3.6.1 shows the results of these experiments. By 30 minutes after microinjection of ET-1 there was a profound drop in the blood flow measured at T6, T7 and T8, whereas blood flow at T5 and T9 remained at baseline value. The reduction was greatest at T7 and T8, and over the remainder of the observation period these segments remained the most severely affected. Blood flow at T6 appeared to recover over the next 1.5 hours, and the flow at T5 overshot the control measurements.

3.3.7 The drop in spinal cord blood flow is not due to a drop systemic BP

Instantaneous blood pressure was recorded during the experiments in order to ensure that any observed reduction in spinal cord blood flow was not due to a drop in the systemic blood pressure. The Perimed data acquisition system records the absolute arterial blood pressure at a sample rate of 32Hz during the experiment, and from this the arithmetic mean blood pressure is derived, rather than physiological mean arterial blood pressure[1]. To compare the blood pressure stability in the different treatment groups, the percentage change in blood pressure from the baseline period was calculated and these results are shown in Figure 3.3.7.1.

3.4 Discussion

3.4.1 Blood pressure control under anaesthesia

The measurement of a change in blood flow in a discrete area of tissue requires that the background cardiovascular parameters remain as stable as possible. The choice of anaesthetic regime is therefore of considerable importance when optimising a technique such as laser Doppler flowmetry of the spinal cord. Systemic hypotension (or hypertension) may result in a change in the perfusion of tissues and this will be reflected in the LD perfusion signal obtained locally. The drop in blood pressure (BP) observed in preliminary experiments with Hypnorm/Hypnovel anaesthesia (Figure 3.3.3.1) is likely to result in hypoperfusion of the spinal cord. Experimentally induced hypotension has been used as a model of spinal cord ischaemia in primates, where the reduction of blood pressure to 40-50mmHg is sufficient to disrupt normal autoregulation of spinal cord blood flow (Kobrine *et al.* 1979). A drop in BP from

[1] MABP=Diastolic pressure+ $^1/_3$(systolic pressure – diastolic pressure)

Figure 3.3.6.1 Rostrocaudal extent of reduced spinal cord blood flow

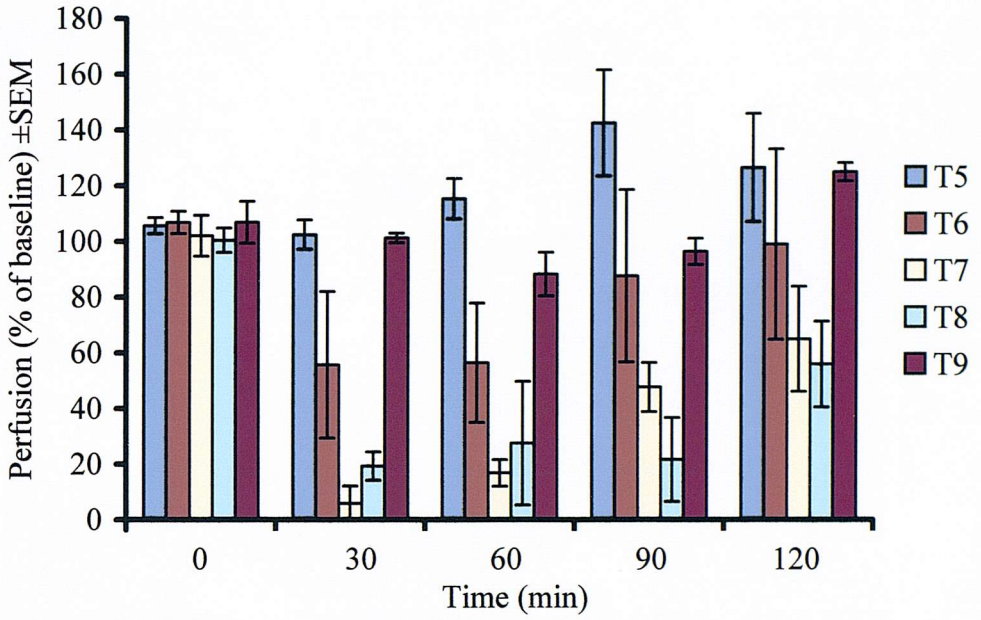

LD perfusion as measured at T5, T6, T7, T8 and T9 following microinjection of 15pmol ET-1 into the ventral grey matter of the spinal cord at T7. Figures shown are % of baseline reading taken 15minutes before microinjection at time zero. All points are n=3.

Figure 3.3.7.1 Comparison of blood pressure changes in blood flow experiments

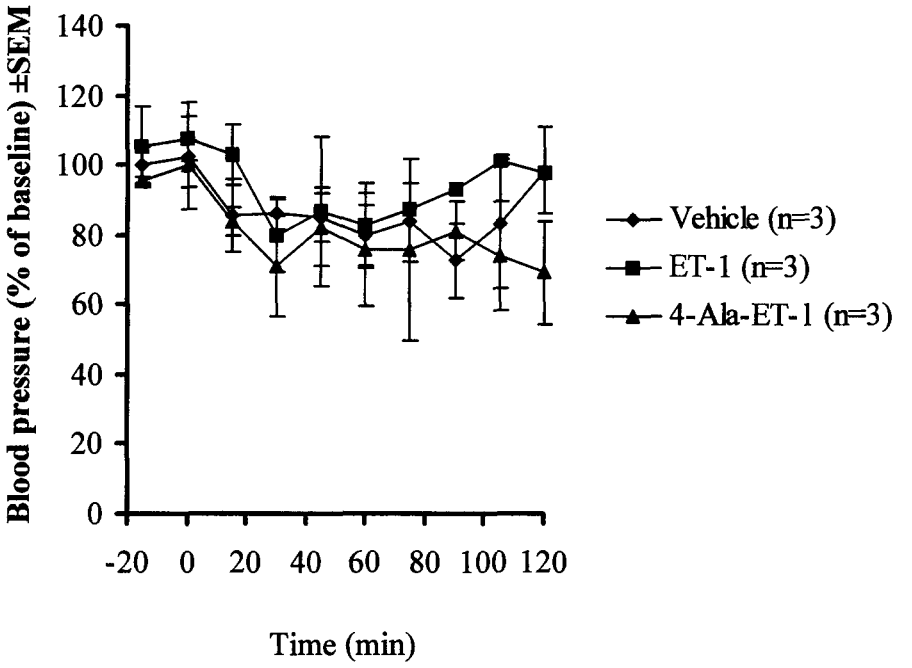

Blood pressure as a percentage of baseline values following microinjection of vehicle (0.25μl), ET-1 (15pmol) or 4-Ala-ET-1 (15pmol) into the grey matter of the ventral spinal cord at T7.

110mmHg to 30mmHg over a three hour period has been observed by others using Hypnorm/Hypnovel (Brammer *et al.* 1993), although earlier reports suggested that this regime was suitable to provide 6-8 hours of surgical anaesthesia (Flecknell and Mitchell 1984).

The average systolic blood pressure in conscious rats is approximately 127mmHg (Buttner *et al.* 1984), and most anaesthetics will reduce this to some extent, particularly over an extended period. Urethane is considered to be one of the most suitable agents to induce and maintain long-term non-recovery surgical anaesthesia without compromising cardiovascular function in rodents (Flecknell 1996) and was therefore used in all the experiments reported.

In addition to maintaining normal cardiovascular parameters, it is important to ensure the body temperature of the animal remains within normal range. Hypothermia is known to be protective in both contusive (Yu *et al.* 2000) and ischaemic (Inamasu *et al.* 2000) models of spinal cord injury. Temperature may also influence the ability of the rat to regulate spinal cord blood flow, and flow may be reduced following hypothermia (Westergren *et al.* 2001).

3.4.2 Endothelin-1 induced changes in blood flow

Although the vasoconstricting properties of ET-1 have been known for many years, it has not been widely used to generate ischaemia in the CNS. As a model of stroke it was used to induce a mid-cerebral artery occlusion (MCAO) by direct application onto the vessel (Sharkey and Butcher 1995), and it has been microinjected into the neostriatum and cortex to induce ischaemia (Willette and Sauermelch 1990; Fuxe *et al.* 1992). Fuxe *et al* (1992) used LD flowmetry to measure a reduction in local blood flow following microinjection of 430pmol of ET-1 into the striatum. Perfusion in the injected area was reduced to approximately 50% for the first 2 hours, reaching only 60% of the control value at the end of a 3 hour observation period. The probe tip (0.45mm diameter) was introduced into the tissue parenchyma in these studies resulting in the inclusion of a large volume of the brain in the blood flow measurements. This may explain why the reported drop in blood flow is less than that seen following microinjection of ET-1 into the spinal cord.

Spinal cord blood flow (SCBF) has been measured in models of spinal trauma in monkeys and cats (Bingham *et al.* 1975; Faden *et al.* 1981) and in a monkey model of spinal ischaemia (Kobrine *et al.* 1979). In these reports blood flow decreases abruptly in the grey matter following injury to the cord, and the blood flow in the white matter either increases or remains at a pre-injury levels. Following intrathecal infusion of 370μM ET-1 to anaesthetised rats there was a 50% reduction in blood flow measured by LD flowmetry (Westmark *et al.* 1995), and lumbar intrathecal doses of 12pmol were sufficient to induce paresis and blood-brain barrier breakdown in conscious rats (Hokfelt *et al.* 1989).

Microinjection of 15pmol ET-1 directly into the grey matter at T7 dramatically reduced blood flow in the spinal cord for at least 2 hours (Figure 3.3.3.1A). This dose of ET-1 was chosen on the grounds that it was sufficient to induce a histologically observable loss of motor neurons without causing gross behavioural manifestations of spinal injury in the animals (see Chapter 4). For the first hour after microinjection the blood flow dropped rapidly and remained below 20% of the baseline. As will be described in detail elsewhere, the reduction in blood flow, and the ensuing ischaemia results in the loss of neurons (including motor neurons in the ventral horns) and injury to the adjacent white matter (see Chapter 4, Chapter 5).

3.4.3 Activation of ET_A not ET_B receptors reduces blood flow

The use of the non-selective endothelin receptor agonist S6b confirmed that the likely mechanism mediating the decrease in spinal cord blood flow was ET_A receptor activation. The profile of spinal cord blood flow following microinjection of S6b was almost identical to that seen after microinjection of ET-1 at an equimolar dose (Figure 3.3.4.2). ET-1 and S6b have similar efficacy at the ET_A receptor (Warner *et al.* 1993) as shown by *in vitro* studies using the rat vas deferens preparation, where both ET-1 and S6b potentiated electrically stimulated twitching at concentrations of 10^{-10}M. However the rank potency of the two agonists does vary, with ET-1 equipotent with S6b at concentrations of below $3x10^{-8}$M, but S6b more potent at this concentration and higher. This difference in receptor activity can be explained by the fact that radiolabelled ET-1 does not dissociate from the ET_A receptor but radiolabelled S6b does (Devadason and Henry 1997), indicating that although they are both ligands for

the same receptor they do not have identical binding properties. These pharmacological differences may account for the toxicity of S6b, as it can dissociate and bind to a number of receptors sequentially, inducing a greater physiological effect than the equivalent dose of ET-1. In the context of the acute physiology of the spinal cord it is clear that the fast and prolonged reduction in spinal cord blood flow is equivalent at least to that caused by microinjection of ET-1, and as such is likely to cause an ischaemic injury. By using S6b to induce the ischaemia it may be possible to assay the tissue for components of the endothelin system, which may be modulated by the ischaemia, without adding endothelin itself. It is known that ET-1 is under the control of the HIF-1 promoter (hypoxia-inducible factor-1) (Yamashita *et al.* 2001) and hence it may be contributing to the development of the ischaemic lesion. Chapter 6 will consider this in more detail.

A modified form of ET-1 with 4 substituted amino acid residues, [$Ala^{1,3,11,15}$]ET-1 (referred to in this text as 4-Ala-ET-1), is a selective ET_B agonist which has been used to distinguish the cardiovascular effects of the ET_A and ET_B receptors in the anaesthetised rat (Bigaud and Pelton 1992).

The ET_B selective agonist 4-Ala-ET-1 failed to elicit a drop in blood flow (Figure 3.3.3.1B), as would be predicted from the evidence that vasoconstriction is mediated by ET_A receptors on smooth muscle cells (Pierre and Davenport 1998). It would appear from Figure 3.3.31B that there is a high degree of variability in the response to 4-Ala-ET-1, which is due to one of the three animals used responding to the peptide with a transient increase in perfusion. It is possible that this effect was an artefact caused by some of the peptide reaching the endothelial cells through a ruptured vessel wall and inducing a NO or prostaglandin mediated vasodilation through ET_B receptors.

3.4.4 ET-1 induced ischaemia is measurable over 3 vertebral levels

Although it has already been stated that the ET-1 dose used was known to induce a lesion characterised by loss of neurons and injury to the white matter, it was not clear how widespread the induced ischaemia might be along the rostro-caudal axis of the spinal cord. The graph in Figure 3.3.6.1 shows the changes in blood flow measured at T5, T6, T7, T8 and T9 (the 5^{th} to 9^{th} thoracic vertebral levels of the spinal cord). At

the time of microinjection (T=0) the blood flow in all segments is 100% relative to the 15 minute baseline recording, but 30 minutes later the blood flow at the level of T7 and T8 is reduced dramatically, to less than 20% of the control value. The segment rostral to the injection site, T6, also has a dramatic reduction in blood flow to approximately 50% by this time. The most distal segments, T5 and T9, do not experience such a reduction and in fact there may be some evidence of hyperaemia in the rostral segment (T5) at 90 and 120 minutes. The T7 perfusion remains reduced for the duration of the observation period, as does T8, but the T6 segment perfusion increases at 90 and 120 minutes. By the end of the recording period, the most rostral and caudal segments appear to be hyperperfused (120% perfusion) while the central segments, specifically T7 and T8 remain at only 60% of baseline perfusion.

Previous studies which have addressed the issue of local spinal perfusion following spinal cord injury have not addressed the question of the rostro-caudal extension of the ischaemia. It has been assumed that the size of the lesion following impact trauma is due to physical disruption of the tissue resulting from the contusion. The non-contusive ischaemic models, for example occlusion of the aorta with a balloon catheter (Yamada *et al.* 1998), rely on inducing a widespread ischaemia rather than a focal injury. The results presented in the previous section have been obtained by using an atraumatic focal ischaemia, and it would not necessarily be assumed that microinjection of 0.25µl of a vasoconstrictor into one thoracic segment would produce such profound changes in blood flow over at least 10mm of the spinal cord. There are a number of possible explanations for this phenomena including spread of exogenous ET-1 in the tissue parenchyma, local induction of endogenous ET-1 or disruption of local autoregulatory mechanisms. These issue will be addressed in further detail in Chapter 6.

The reduction in spinal cord perfusion seen after microinjection of ET-1 is not due to a reduction in systemic blood pressure (Figure 3.3.7.1). Blood pressure did decrease over the course of the experiment but not in response to the microinjection of ET-1. The vehicle and 4-Ala-ET-1 results overlie the ET-1 profile, demonstrating that although there was a profound change in spinal perfusion, systemic perfusion was not affected. Confirmation of this also comes from the rostro-caudal profile of spinal cord

ischaemia shown in Figure 3.3.6.1, which would not be possible if microinjection of ET-1 caused a drop in systemic blood pressure.

3.5 Conclusions

It is clear from these experiments that microinjection of ET-1 into the ventral grey matter of the spinal cord induces a profound and prolonged drop in perfusion which will undoubtedly lead to the development of ischaemia in the affected tissue. Although the involvement of astrocytic ET_B receptors cannot be ruled out with respect to the activation of astrocytes in the developing lesion, the profound physiological effects following microinjection of ET-1 are due to an ET_A receptor mediated vasoconstriction.

Previous attempts to produce such ischaemic insults in the cord relied upon traumatic injuries, such as weight drop (Carlson *et al.* 1998) or blocking weight models (Fujimoto *et al.* 2000), or non-specific spinal ischaemia induced by aortic occlusion (Hirose *et al.* 2000) or multiple radicular artery ligation (Woodward and Freeman 1956). This model presents an opportunity to examine in detail the relationship between the drop in blood flow, and the development of an ischaemic lesion. The pathological effects of this ischaemia on the structures and cellular composition of both the grey and white matter of the spinal cord are discussed in the next chapter.

Chapter 4 – Acute inflammation and glial pathology in endothelin-1 induced spinal cord ischaemia

4.1 Introduction

4.1.1 Spinal cord injury

It has long been understood that ischaemia is one of the components of a traumatic spinal cord injury (SCI), and experimentally induced spinal cord ischaemia can reproduce much of the tissue destruction seen in the human injury (Woodward and Freeman 1956). Lesions often have a necrotic haemorrhagic centre, which spreads both rostro-caudally in the grey matter and radially into the white matter (Liu *et al.* 1997). Although the loss of neurons in the grey matter can have serious effects for the patient such as the development of autonomic dysreflexia, it is the damage to ascending and descending axons in the adjacent white matter that is likely to result in paralysis.

Much of the work carried out to model SCI has been performed using impact models, where a force is applied to the cord to induce a contusion injury (for examples see Happel *et al.* 1981; Liu *et al.* 1997; Carlson *et al.* 1998). During such procedures tissue damage is inflicted with the physical force of the impact, and structural components of the cord are damaged. Direct physical disruption of the brain or spinal cord may, for example, result in the release of arachidonic acid metabolites (Xu *et al.* 1990), haemorrhage (Woodward and Freeman 1956) and the destruction of axons (Buki *et al.* 2000). This limits the ability to dissect the underlying pathological mechanisms experimentally, and in particular the ability to discern the contribution of the acute inflammatory response to the injury.

4.1.2 Acute inflammation

The acute inflammatory response is the first line of defence for an organism that has been injured or invaded by a pathogen, and is usually characterised by the presence of polymorphonuclear (PMN) cells or neutrophils. These cells have the capacity to phagocytose bacteria and kill them by fusing the phagosome (the membrane vesicle containing the pathogen) with cytoplasmic granules, which contain a variety of degradative enzymes. The two main classes of granules are the azurophil and specific granules, both of which contain enzymes possessing antimicrobial activity

(e.g. lysozyme), and enzymes capable of degrading the extracellular matrix (e.g. elastase and collagenase).

In addition to the phagocytic function, neutrophils can launch a non-specific attack on pathogens by secreting their granule contents into their immediate environment following stimulation. This allows the neutrophil to rapidly attack the pathogen without having to phagocytose it first. Neutrophil granule release may also contribute to the generation of classical inflammation (rubor, calor and tumour) by causing extravasation of plasma and vasodilatation. However, the presence of such powerful enzymes as collagenase, elastase and myeloperoxidase in the tissue parenchyma can have negative consequences for the host, and in many situations, especially those involving trauma and ischaemia, neutrophils are now considered to be contributory to the injury (Bednar *et al.* 1997).

Another major phagocytic cell of the acute inflammatory response is the mononuclear phagocyte or macrophage, which removes debris and can also secrete growth factors to stimulate repair or regeneration in some tissues. These cells usually arrive at the site of injury after the neutrophils, and unlike the neutrophils they may persist for some time afterwards (Mathers and Falconer 1991; Leskovar *et al.* 2000). Many tissues have resident populations of macrophages that can be activated by infection or injury, such as the Kuppfer cells in the liver, and in the central nervous system these are the microglia (Kreutzberg 1996; Perry and Gordon 1997). Fully activated resident microglia are morphologically and immunologically indistinguishable from infiltrating monocyte derived macrophages, but can be differentiated by using bone-marrow chimeric animals. It has been shown using this technique that in the contused rat spinal cord the resident macrophages are the predominant population in the lesion for at least the first 3 days, and that the hematogenous monocytes do not penetrate the white matter in any significant numbers (Popovich and Hickey 2001).

The phagocytosis of debris or pathogens which have been coated with antibodies or opsonised is mediated through Fc-receptors and complement C3b receptors on macrophages respectively. Once the particle or pathogen is fully enclosed in a phagosome, it is fused with a lysosome containing destructive enzymes including proteinases and lipases. Like neutrophils, the macrophages are capable of secreting a

number of pro-inflammatory products into the local environment, such as lysozyme, IL-1, TNFα, PAF and hydroxyl radicals. It is these substances that may, in certain circumstances, contribute to the ongoing injury rather than destroy an invading pathogen. Macrophages can also contribute to the resolution of an inflammatory response by releasing protease inhibitors (e.g. α2-macroglobulin) and growth factors (e.g. PDGF). The persistence of these activated microglia/macrophages in an injured area can exacerbate the initial injury. It has, for example, been shown that depletion of macrophages reduces the motor deficit after a traumatic spinal cord injury in the rat (Popovich *et al.* 1999).

The current therapy used in clinical acute spinal cord injury is high dose methylprednisolone (Bracken *et al.* 1990), which does not affect neutrophil recruitment or activation. Methylprednisolone is believed to act as an inhibitor of lipid peroxidation when used acutely in high doses (Behrmann *et al.* 1994), although it has been ascribed other properties including the ability to reduce TNFα induction and NFκB activation after SCI (Xu *et al.* 1998). It is clear that novel therapies, that can modulate the acute inflammatory response in such injuries, could be of great importance (Taoka and Okajima 1998, 2000).

It has also been noted that the rodent spinal cord appears to react to physical injury (Schnell *et al.* 1999a) or direct injection of pro-inflammatory cytokines (Schnell *et al.* 1999b) with a more pronounced acute inflammatory response than the brain. It would therefore be of interest to see if these two areas of the CNS respond to an ischaemic injury in a similarly unequal fashion.

The blood-spinal cord barrier (BSCB), which is analogous to the blood-brain barrier (BBB) elsewhere in the CNS, is maintained by the presence of tight junctions between endothelial cells in spinal cord blood vessels. These junctions prevent the movement of proteins and cells into the spinal cord parenchyma under normal conditions (Perry *et al.* 1997). Under pathological conditions such as following a contusion injury (Mustafa *et al.* 1995) the BSCB can fail, thus facilitating the free movement of solutes and some cell populations into the spinal cord parenchyma. Microinjection of inflammatory cytokines such as TNFα and IL-1β into the spinal cord can also induce

BSCB failure (Schnell *et al.* 1999b), which implies that although mechanical trauma may directly injure some of the vasculature, the inflammatory response may have a role.

4.1.3 Glial cell pathology

The tissue matrix in which the neurons and axons are supported consists of a number of cell types including astrocytes, microglia and oligodendrocytes. It is known that following SCI there are distinct pathological changes in astrocytes (Du *et al.* 1999), microglia and oligodendrocytes (Shuman *et al.* 1997).

Astrocytes play an important role in metabolic support for neurons, and in maintaining the extracellular environment by buffering neurotransmitters and potassium. The response of astrocytes to injury is rapid, as changes in morphology (enlarged branched processes) and increases in the glial fibrillary acidic protein (GFAP) can be seen within 1 hour following a spinal cord lesion (Hadley and Goshgarian 1997). These cells are sensitive to changes in the extracellular milieu, and there is evidence that in SCI the acidification of the microenvironment can induce reactive gliosis (Du *et al.* 1999). It has also been shown that following a stab injury to the rat brain, treatment with the ET_B receptor antagonist BQ-788 reduces the astrogliosis, suggesting that endogenous endothelin may contribute to the cellular upregulation of GFAP after injury (Koyama *et al.* 1999). Astrocytes possess gap junctions that allow them to communicate over significant distances, and as a result injury in one location may produce an extended area of astrocyte upregulation. The enlargement of astrocytes and the thickening of their processes changes the nature of the microenvironment, effectively inducing a glial scar. In addition to providing structural support this scar is non-permissive to axonal regeneration (Davies *et al.* 1997), and may prevent inappropriate axonal sprouting.

The myelin sheaths that insulate certain populations of axons and enable them to conduct action potentials using fast saltatory conduction are formed from the processes of oligodendrocytes. These cells, unlike their equivalent in the peripheral nervous system, the Schwann cell, extend their processes over a number of different axons (Morell and Norton 1980). One of the consequences of this is that axons unaffected by the initial mechanical trauma become demyelinated as oligodendrocytes

undergo apoptosis following injury to their myelin processes or loss of some of the ensheathed axons (Shuman *et al.* 1997; Casha *et al.* 2001). This axonal degeneration takes place several days after the injury as the axon undergoes Wallerian degeneration.

By inducing focal ischaemia in the rodent spinal cord with minimum trauma it is possible to examine the acute inflammatory response and the responses of the resident glial cells without the complications of a mechanical injury. In Chapter 3 it was demonstrated that microinjection of endothelin-1 (ET-1) into the ventral grey matter of the spinal cord caused a dramatic drop in blood flow for at least 2 hours. The present chapter describes the observed effects of this ischaemia with respect to neuronal loss, inflammatory cell recruitment, blood-spinal cord barrier breakdown and glial pathology.

4.2 Methodology

4.2.1.1 Tissue preparation

Male Wistar rats were anaesthetised with Hypnorm/Hypnovel and microinjected with vehicle (sterile saline) or endothelin-1 (ET-1, 15pmol) into the caudate putamen (striatum) or the ventral horn grey matter of the spinal cord at the level of the 7th thoracic vertebra (See Chapter 2). At 6 hours, 24 hours, 72 hours, 7 days or 21 days following microinjection the animals were anaesthetised with pentobarbitone and perfusion-fixed with either periodate-lysine paraformaldehyde (PLP) or Bouins fixative (See Chapter 2). Tissues were prepared for wax-embedding (Bouins fixed tissue) or freezing (PLP fixed tissue), and stored until 10μm sections were prepared (see Chapter 2). PLP fixed sections were cut using a cryostat and stored at -20°C until use. Paraffin embedded Bouins fixed sections were cut on a benchtop microtome and stored at room temperature until use.

4.2.1.2 Blood spinal cord barrier status

The status of the blood spinal cord barrier (BSCB) was ascertained in a series of animals by visualising the extravasation of horseradish peroxidase (HRP). The HRP was administered i.v. (via the tail vein) under isoflurane anaesthesia 30 minutes before perfusion. Microinjection of ET-1 (15pmol) or vehicle was carried out as described

above, 6h, 24h or 72h prior to HRP in 3 animals per treatment per timepoint. Perfusion fixation was carried out using heparinised saline followed by Karnovsky's fixative (see Chapter 2), and the tissue was post-fixed, cryoprotected and embedded in OCT before 25μm sections were cut. Areas of blood-spinal cord barrier disruption were revealed using a modified Hanker-Yates procedure (Perry and Linden 1982) as described in Chapter 2. This uses the enzymic activity of the HRP to develop a brown precipitate, indicating areas of the tissue where HRP has entered the parenchyma. Qualitative assessment of spinal cord status was made by analysing images of the spinal cord sections which had been acquired using a personal computer based video camera and software package (Leica Qwin, Leica UK).

4.2.2 Immunohistochemistry

Immunohistochemistry was carried out using the general methodology described in Chapter 2. Bouins fixed tissue required microwave treatment in citrate buffer (2.1g sodium citrate per 1000ml, pH 6.0) and this step was performed before blocking. For neutrophil staining the rabbit anti-rat neutrophil polyclonal antiserum MBS-1 (CNS Inflammation Group, University of Southampton) was used at a dilution of 1:2000. Activated macrophages were identified using the monoclonal mouse antibody ED-1 (Serotec, UK) which recognises mononuclear phagocyte lysosomal enzymes (Damoiseaux *et al.* 1994). A polyclonal rabbit anti-cow glial fibrillary acidic protein (GFAP) antibody (Dako) was used to identify astrocytes. Early changes in microglial morphology were assessed by using the mouse monoclonal antibody OX-42 (Serotec UK), which is specific for CD11b, the complement CR3 receptor, at a dilution of 1:1000.

Biotinylated goat anti-rabbit and horse anti-mouse secondary antibodies (Vector, UK) were used with the polyclonal (MBS-1, GFAP) and monoclonal (ED-1, OX-42) antibodies respectively. Subsequent amplification of the signal was achieved by the use of an avidin-biotin horseradish peroxidase complex (ABC Elite, Vector UK) which enabled visualisation using diaminobenzidine (DAB), resulting in a brown precipitate.

Figure 4.2.2.1 shows examples of ED-1 positive macrophage staining and MBS-1 positive neutrophil staining. The macrophages have a distinctive 'foamy' appearance consistent with high phagocytic activity; ED-1 is known to be specific for lysosomal proteins (Damoiseaux *et al.* 1994). The neutrophil nuclei are multi-lobed, and the antibody appears to bind to an extracellular epitope.

4.2.3 Counterstaining

Counterstaining of tissue sections was carried out using either haematoxylin (Bouins fixed wax sections) or cresyl violet fast acetate (PLP fixed sections) to enable visualisation of nuclei as described in Chapter 2. Both of the staining techniques used reveal Nissl substance (rough endoplasmic reticulum), nuclei and background staining of the neuropil. Haematoxylin counterstaining also enabled quantification of pyknotic nuclei observed in the white matter. These are dense 'droplet-like' structures formed as a result of condensation of nuclear chromatin during apoptosis. The presence of pyknotic nuclei is indicative of on-going cell death by apoptosis, as the nuclei only adopt this morphology for a brief period during degeneration.

4.2.4 Quantification

4.2.4.1 Neutrophils

In the coronal, PLP fixed, brain and spinal cord sections neutrophils were counted at 25x objective magnification using a microscope fitted with an eyepiece graticule. The three highest density fields per slide were counted and the arithmetic mean calculated; this was repeated for 3 slides per animal, and the mean of the resulting values was used as the count for that individual.

For the longitudinal Bouins fixed spinal cord sections the counting was partitioned between the white and grey matter (see Figure 4.2.4.1.1). Neutrophils were counted at 40x objective magnification using a microscope fitted with a graticule. Seven fields were counted in the both the grey and white matter at 1mm intervals rostral and caudal from the microinjection site (i.e. 15 fields per section, in both the white and grey matter). For each animal 3 non-adjacent sections from the ventral spinal cord were counted and the values for the corresponding rostro-caudal fields were totalled, so that for each animal there was a single count value for each 1mm interval, representing the summed counts at three dorso-ventral levels.

Figure 4.2.2.1 Macrophage and neutrophil immunohistochemistry

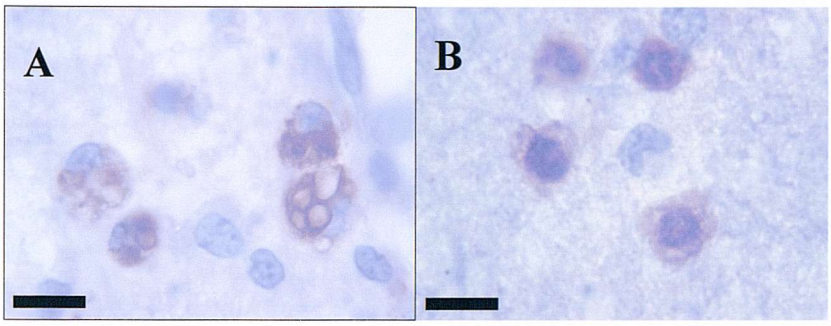

Representative images of (A) macrophage immunohistochemistry using ED-1, (B) neutrophil immunohistochemistry using MBS-1. Bar = 10μm

Figure 4.2.4.1.1 White and grey matter leukocyte counting

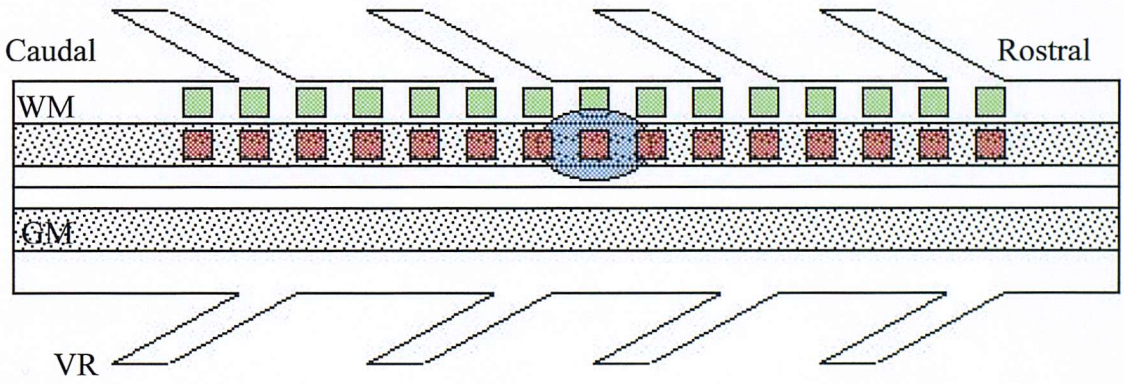

Diagrammatic representation of fields counted for analysis of rostro-caudal and white matter-grey matter distribution of inflammatory cells in longitudinal sections of the spinal cord. VR= ventral roots; GM= grey matter; WM= white matter; Green and red boxes represent location of counting fields (graticule field at 40x objective magnification= 313x313μm) 1mm apart in both white and grey matter; blue ellipse is microinjection site

4.2.4.2 Macrophages

Macrophages were quantified in the coronal, PLP fixed, sections using a computer based image-capture system (Qwin, Leica UK). Images of the regions of interest were captured at 25x objective magnification, and a threshold applied to measure the area of dark brown DAB staining only, which in this case was macrophage ED-1 staining. The mean of the 5 highest density fields for each of three sections per animal was recorded and used as the count for that individual.

In the longitudinal, Bouins fixed, sections ED-1 positive macrophages were counted in 15 non-adjacent fields in the grey and white matter using a graticule as described above for neutrophils.

4.2.4.3 Pyknotic nuclei

Pyknotic nuclei were quantified in the lateral white matter of longitudinal Bouins fixed haematoxylin counterstained sections using a graticule as described above for neutrophils. The lateral white matter on both edges of each section was examined at 1mm intervals along the length of the lesion (centred at the microinjection site, total of 15 fields) and at each interval the field with the highest number of pyknotic nuclei recorded. The criteria for designation as a pyknotic nuclei that the nuclei needed to be highly dense and of spheroid appearance with little or no cytoplasm visible (see Figure 4.2.4.3.1).

4.2.4.4 Neuronal loss

The rostro-caudal length of the ischaemic spinal cord lesion was assessed by observing the maximum extent of neuronal loss in longitudinal sections. Haematoxylin stained Bouins fixed spinal cord sections were examined using a 25x objective, and the loss of normal neuronal staining (characterised by a dense nucleus surrounded by a Nissl stained cytoplasm) was assessed. Areas of the spinal cord where the neurons had lost these characteristics, or the neurons were no longer visible, were classified as lesion. The length of neuronal loss along the spinal cord was obtained by recording the co-ordinates of the extreme ends of the area of neuronal loss from the microscope stage, and calculating the distance between them. This

Figure 4.2.4.3.1 **Pyknotic nuclei**

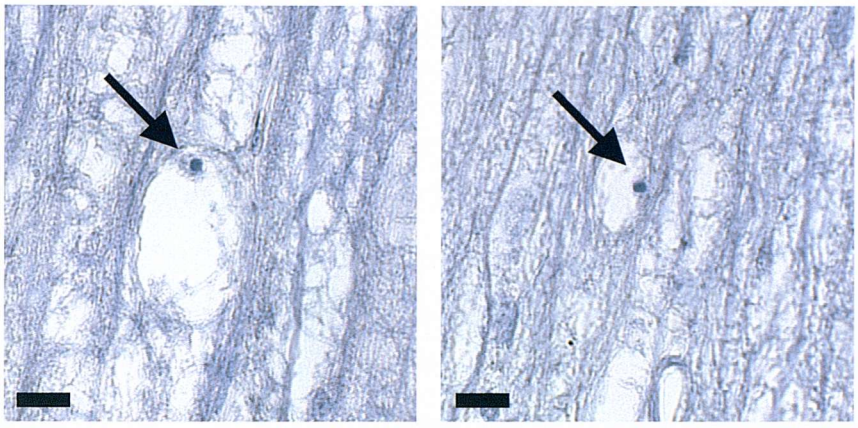

Examples of pyknotic nuclei visible in lateral white matter 7 days after microinjection of ET-1 (15pmol) into the ventral grey matter at T7. Sections are haematoxylin stained Bouins fixed spinal cords, 10μm thick. Arrows indicate position of pyknotic nuclei, which are associated with vacuolation of the white matter. Scale bar = 10μm.

assessment was carried out in lesions at 6 hours, 24 hours and three days after microinjection of ET-1 (15pmol).

4.2.5 Statistical analysis

Statistically significant differences in cell counts were tested for by ANOVA (SAS v8.2, SAS Institute). The results for ED-1 staining in section 4.3.3 are expressed as an area rather than cell counts. As the number of ED-1 positive macrophages increases they may overlap considerably, so that for example a doubling in ED-1 positive area does not equate to a doubling in the number of cells present. In this case the data is best interpreted on an ordinal rather than an interval scale, and hence the Mann-Whitney U-test (StatView) was used to test for statistically significant differences. Student's T-test was used to determine statistically significant differences between treatments for the pyknotic nuclei data.

4.2.6 Qualitative analysis

Representative images of OX-42 positive activated microglia and GFAP positive astrocytes were obtained using a personal computer based image acquisition system (Leica Qwin) attached to a microscope and video camera. Where necessary, images were adjusted *post-hoc* only to increase contrast or to reduce background distortion using picture editing software (Photoshop, Adobe).

4.3 Results

4.3.1 ET-1 induced ischaemia destroys neurons

Microinjection of ET-1 into the caudate putamen (striatum) results in the loss of normal neuronal staining at 6 hours after microinjection. The medium spiny neurons in Panel A of Figure 4.3.1.1 are of normal appearance, whereas those in Panel B have a shrunken, necrotic morphology. The blue colouration seen in the striatal sections is due to the presence of a dye (Monastral Blue) co-injected with the ET-1 or vehicle to reveal the microinjection site. In the spinal cord the large neurons (α-motor neurons) of the ventral horn can be seen in Panel A of Figure 4.3.1.2 at 6 hours following microinjection of vehicle. In Panel B, 6 hours after microinjection of ET-1 the cell bodies and nuclei are no longer distinct.

Figure 4.3.1.1 Normal and necrotic striatal neurons

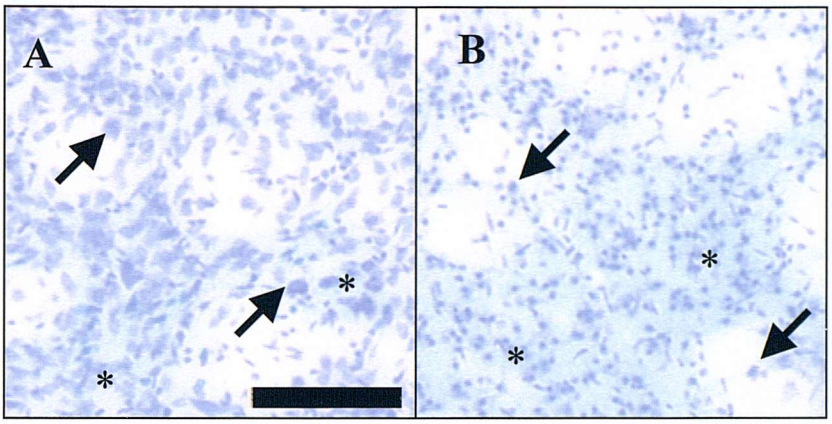

Cresyl fast violet acetate staining of rat striatum (coronal 10μm section) 6 hours after microinjection with: (A) Vehicle (sterile saline 0.25μl) and (B) ET-1 (15pmol, 0.25μl). Bar = 100μm. Cresyl violet fast acetate reveals Nissl substance. Blue colour (*) in both panels is dye (Monastral Blue) co-injected with ET-1 or vehicle to show injection site. Arrows in panel A indicate normal medium spiny neurons; arrows in panel B indicate 'sickly' or necrotic neurons.

Figure 4.3.1.2 Normal and necrotic spinal cord motor neurons

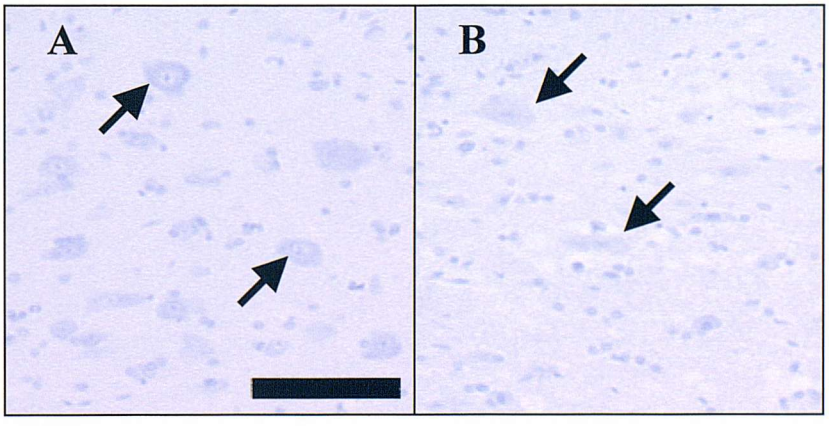

Haematoxylin staining of rat spinal cord grey matter (longitudinal 10μm section) 6 hours after microinjection with: (A) Vehicle (sterile saline 0.25μl) and (B) ET-1 (15pmol, 0.25μl). Bar = 100μm. Arrows in panel A indicate normal α-motor neurons; arrows in panel B indicate 'sickly' or necrotic neurons.

4.3.2 Cell loss in the spinal cord extends along the rostro-caudal axis

As previously discussed in Chapter 3, the ischaemia extends rostrally and caudally from the microinjection site by at least one vertebral level. The rostro-caudal extent of the area of neuronal loss was measured in haematoxylin-stained sections at 6, 24 and 72 hours post microinjection and shown in Figure 4.3.2.1. ANOVA comparison of the three sets of lesions revealed no significant difference between the timepoints ($p=0.8175$). In the vehicle injected animals there was no significant loss of neurons at any time-point (data not shown).

4.3.3 Neutrophils and macrophages are recruited after focal ischaemia

In the period following ET-1 microinjection neutrophils are recruited into the parenchyma of the spinal cord peaking at 24 hours (Figure 4.3.3.1), but no significant recruitment into the brain parenchyma is observed at this time. The number of neutrophils in the striatum remains unchanged over the three time-points, while in the spinal cord there is a clear increase at 24 hours which has subsided at 72 hours.

The recruitment of ED-1 positive macrophages into the spinal cord is more extensive than into the striatum (Figure 4.3.3.2), particularly at the 3 day time-point where there is more than a 4-fold difference in the area of ED-1 positive staining in the spinal cord compared to the brain.

4.3.4 Blood spinal cord barrier is disrupted at 24h post ET-1

The blood spinal cord barrier (BSCB) is not compromised after microinjection of vehicle at 6 hours, 24 hours or 72 hours, as visualised by the lack of extravasation of HRP into the tissue parenchyma (Figure 4.3.4.1). Microinjection of ET-1 results in the failure of the BSCB at 24 hours but not at the 6 hour or 3 day time-points. At 24 hours after microinjection of ET-1 the horseradish peroxidase has clearly entered the tissue parenchyma in the ischaemic lesion as indicated by DAB precipitation, which is visible in both the grey and white matter. The grey matter shows marked recruitment of macrophages at 72 hours after microinjection of ET-1 (see 4.3.7 below), which are likely to be phagocytosing cellular debris and tissue matrix. For this reason the grey matter of the sections is extremely fragile, even though the tissue has been fixed, and hence the overt tissue damage seen in Figure 4.3.4.1.

Figure 4.3.2.1 Rostrocaudal extent of cell loss

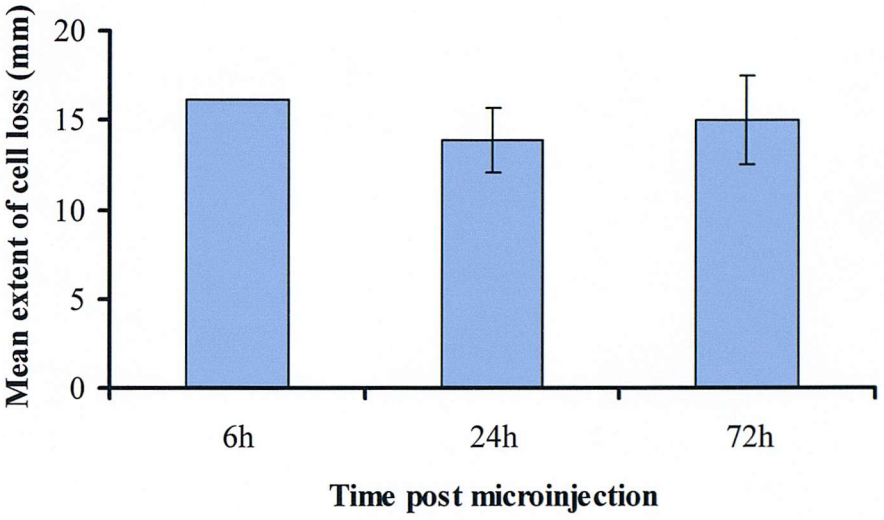

Length of lesion as seen by loss of gross neuronal staining (Haematoxylin) in longitudinal spinal cord sections after microinjection of ET-1 (15pmol, 0.25µl). All n=3 except 6h time point where n=2.

Figure 4.3.3.1 Neutrophil recruitment in the spinal cord and striatum

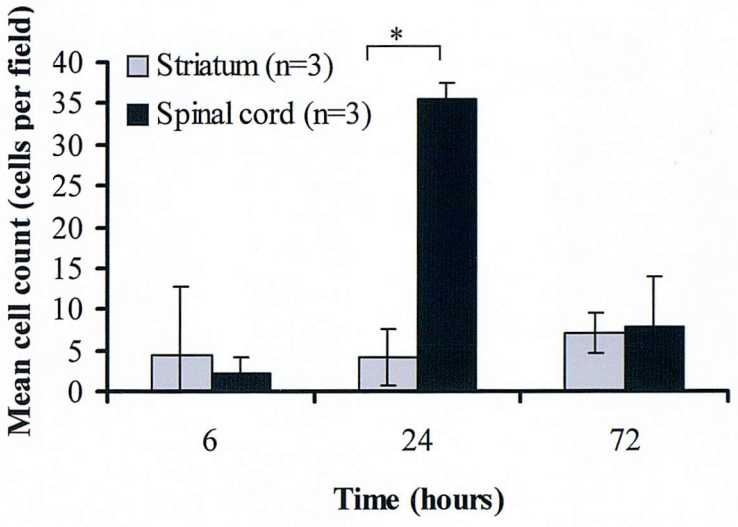

MBS-1 positive neutrophil counts in the striatum and spinal cord following microinjection of ET-1 (15pmol, 0.25µl). (* $p<0.05$ ANOVA one way).

Figure 4.4.3.2 Macrophage recruitment in the spinal cord and striatum

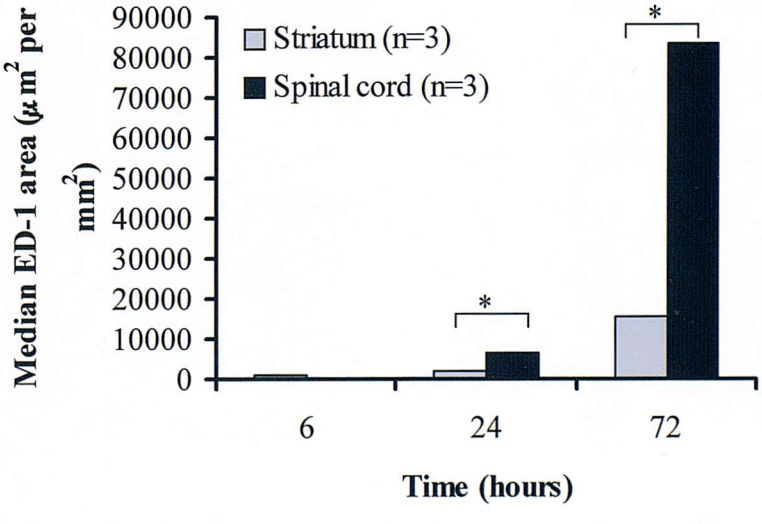

ED-1 positive macrophages quantified as the area of ED-1 positive staining in the striatum and spinal cord following microinjection of ET-1 (15pmol, 0.25µl). (* $p<0.05$ Mann-Whitney U-test).

Figure 4.3.4.1 Blood-spinal cord barrier breakdown

Representative sections showing blood brain barrier breakdown (horseradish peroxidase extravasation visualised using a modified Hanker-Yates procedure) in the spinal cord 6, 24 and 72 hours after microinjection with vehicle (sterile saline 0.25μl) or ET-1 (15pmol, 0.25μl).

4.3.5 Neutrophils are preferentially recruited to the spinal grey matter

The earlier sections presented data from coronal sections of spinal cord or brain and compared the neutrophil and macrophage recruitment between these two compartments. The further characterisation of ET-1 induced focal brain ischaemia is described elsewhere (Hughes *et al* 2003, manuscript in preparation).

A more detailed analysis of the profile of neutrophil recruitment into the spinal cord is presented in Figure 4.3.5.1, where the rostro-caudal and temporal pattern of recruitment into both the white and grey matter of the spinal cord is described. Following microinjection of vehicle there is no neutrophil recruitment into the grey matter, other than a few cells at the microinjection site at 24 hours (Figure 4.3.5.1A). Microinjection of ET-1 does not result in the recruitment of neutrophils into the grey matter at 6 hours, but by 24 hours significant numbers of neutrophils are present. These are visible along a 15mm length of spinal cord, centred on the microinjection site. By 3 days after microinjection the number of neutrophils in the grey matter has decreased, and only a few cells are present caudal to the microinjection site.

The absolute numbers of neutrophils recruited into the white matter of the spinal cord following microinjection of ET-1 are very low (Figure 4.3.5.1B), but they are present along the length of the lesion. Apart from a very small number of neutrophils present at the microinjection site, the microinjection of vehicle into the grey matter of the spinal cord resulted in no recruitment of neutrophils into the white matter. The few cells that are present after the microinjection of ET-1 follow the same temporal pattern as those recruited into the grey matter, i.e. none at 6 hours, peak numbers at 24 hours which are greatly reduced by 3 days.

4.3.6 Microglial activation

Immunohistochemistry for OX-42 shows the presence of activated microglia in the white and grey matter of the spinal cord (Figure 4.3.6.1). In the grey matter 24 hours after vehicle microinjection there is OX-42 positive staining associated with distinct microglial cells. They are not as elongated as those seen in the white matter, but they do have processes. In contrast the OX-42 staining in the ET-1 microinjected spinal cords does not have such a distribution. There is staining around the cell bodies of

activated microglia, but there is little evidence of the fine processes seen in the vehicle-injected animals. The cell bodies appear to have thickened and retracted their fine processes. Three days after microinjection of vehicle, the microglia in the grey matter are largely unchanged, with perhaps a few cells appearing to have a more stellate appearance with fine processes. The ET-1 microinjected grey matter has by this time become densely packed with OX-42 positive cells possessing distinct round nuclei visible by cresyl violet counterstaining.

Microglia are visible in the lateral white matter 24 hours and 3 days after microinjection of vehicle into the ventral grey matter (Figure 4.3.6.1). The cells have a stellate appearance, with some processes lying along the longitudinal axis of the white matter, between axons. In ET-1 microinjected spinal cords the microglia in the white matter do not have these processes, and instead have a more compact rounded appearance at both the 24-hour and 3 day time points. This suggests that the cells have retracted their processes and are adopting a phagocytic macrophage phenotype.

4.3.7 Macrophage recruitment

ED-1 positive phagocytic macrophages, which could be activated resident microglia or haematogenous monocytes, are present in both the grey and white matter of the spinal cord following microinjection of ET-1 (Figure 4.3.7.1, Figure 4.3.7.2). Microinjection of vehicle resulted in minimal recruitment of macrophages into the grey matter at any of the time points examined (Figure 4.3.7.1). There is no recruitment of macrophages until 3 days after microinjection of ET-1, at which time the distribution of ED-1 postive macrophages in the grey matter is more pronounced caudally ($p<0.05$ ANOVA comparison of total counts in the rostral versus caudal fields, excluding the centre three fields). At the later time points (7 and 21 days) the asymmetry is lost. In the grey matter the macrophage numbers peak at 7 days post ET-1, although even at 21 days a population of macrophage persists in higher numbers than were present at 3 days.

Microinjection of vehicle into the ventral grey matter resulted in minimal recruitment of macrophages into the white matter at any time point (Figure 4.3.7.2). Microinjection of ET-1 did lead to the recruitment of ED-1 positive macrophages into the spinal cord white matter, although lower in absolute numbers than that seen in the

grey matter. Macrophages appear in significant numbers 3 days after microinjection of ET-1 and is symmetrical with respect to the site of microinjection. The number of ED-1 positive macrophages is greatly increased in the white matter at the 7 day timepoint compared to the 3 day result. However, unlike the grey matter, between 7 and 21 days the number of macrophages present does not decrease.

4.3.8 Astrogliosis is evident after ischaemia

At 24 hours after the microinjection of ET-1 there was a dramatic change in the morphology of astrocytes in the white matter as visualised by GFAP immunohistochemistry (see Figure 4.3.8.1). Vehicle microinjection resulted in minimal changes in the appearance of astrocytes at this time. In the ET-1 injected spinal cords the white matter fibrous astrocytes had enlarged cell bodies and thickened processes compared to vehicle injections. Also at this time in the ET-1 injected cords, protoplasmic astrocytes were absent from the ischaemic grey matter lesion area. In intact grey matter adjacent to the lesion the astrocytes were slightly enlarged in appearance. The grey matter of vehicle injected spinal cords showed little GFAP reactivity at 24 hours.

Ischaemically injured grey matter remained devoid of astrocyte staining at 3 days, while astrocytes in adjacent intact grey matter, and the grey matter of vehicle injected cords, remained highly GFAP positive. White matter astrocytes in vehicle and ET-1 microinjected groups showed some evidence of up regulation of GFAP and hypertrophy.

By 7 days post injection a marked reduction in the GFAP staining was evident in the vehicle injected grey matter and white matter. In areas of intact grey matter adjacent to the lesion in ET-1 injected cords there was a high degree of GFAP staining in enlarged protoplasmic astrocytes. White matter astrocytes in the ET-1 injected cords appear to be more up regulated at this timepoint compared to the vehicle-injected animals. GFAP staining in the lesioned grey matter is absent at this timepoint.

At 21 days post microinjection of ET-1, GFAP positive astrocytes were reappearing in the lesioned grey matter, although in the vehicle injected cords the GFAP signal was minimal in both the grey and white matter. A few enlarged GFAP positive astrocytes

Figure 4.3.5.1 Rostrocaudal distribution of neutrophils

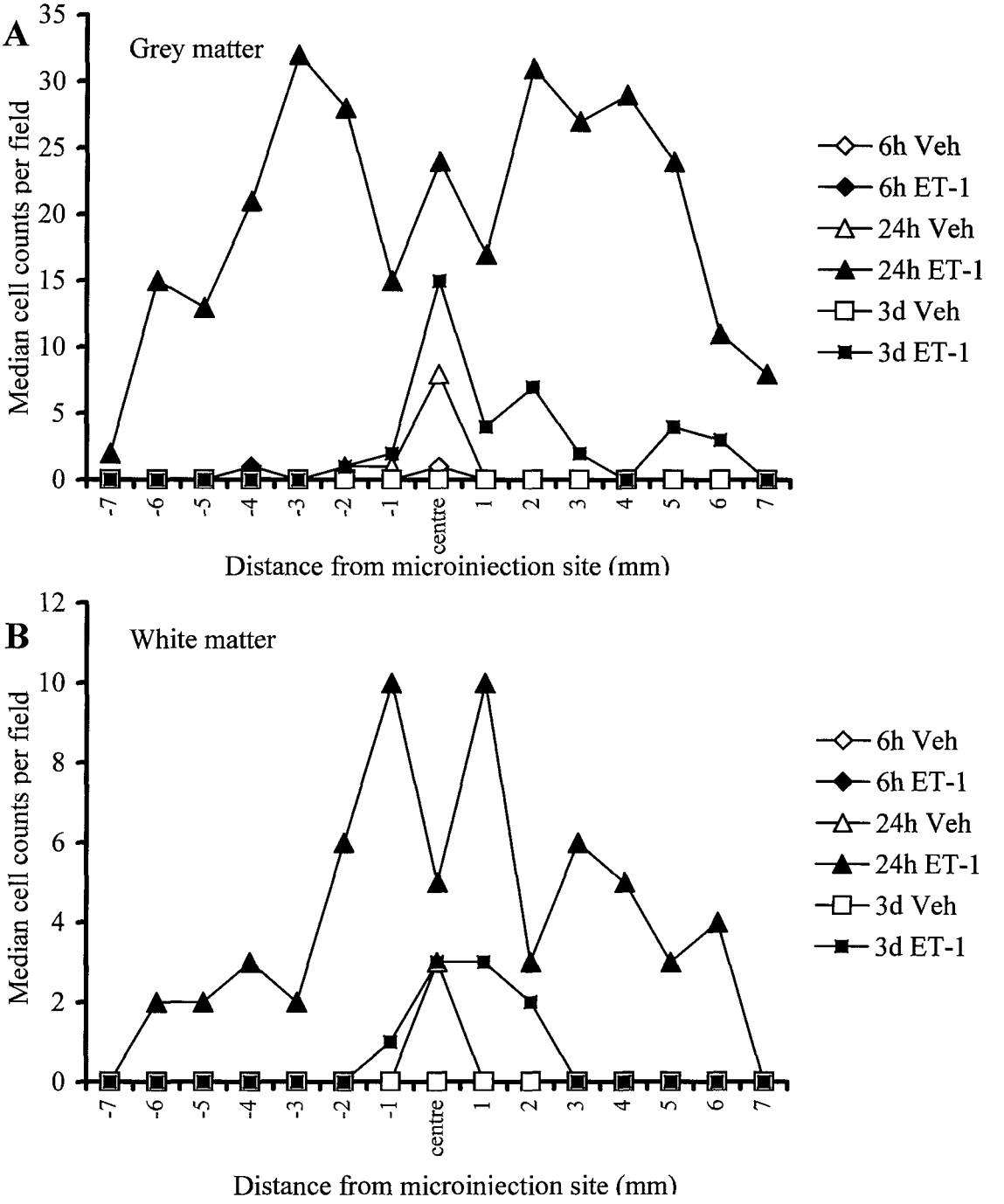

Rostro-caudal distribution of MBS-1-positive neutrophils in the grey (A) and white (B) matter following microinjection of vehicle (0.25µl) or ET-1 (15pmol) into the ventral spinal cord at T7. All points n=3 animals, 3 non-adjacent sections per animal counted and summed.

Figure 4.3.6.1 Microglial activation

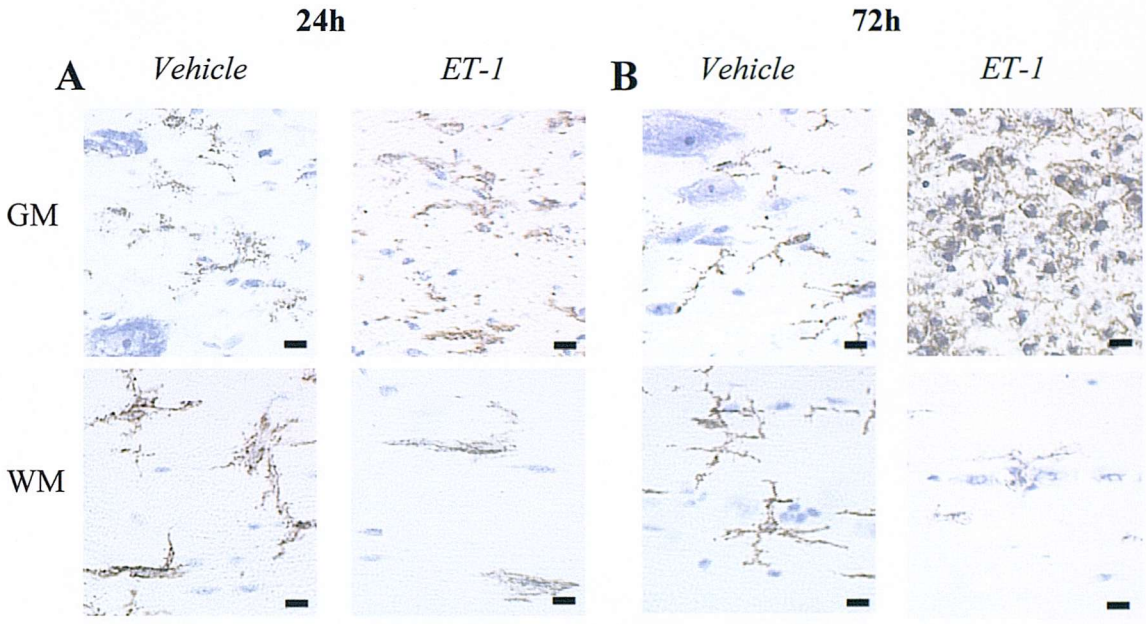

Representative images of OX-42 positive microglia in the grey matter (GM) and white matter (WM) after microinjection of vehicle (0.25µl) or ET-1 (15pmol) into the ventral spinal cord at T7. Examples shown are at 24 hours (Panel A) or 72 hours (Panel B) after microinjection. Scale bar = 10µm.

Figure 4.3.7.1 Rostrocaudal distribution of macrophages in the grey matter

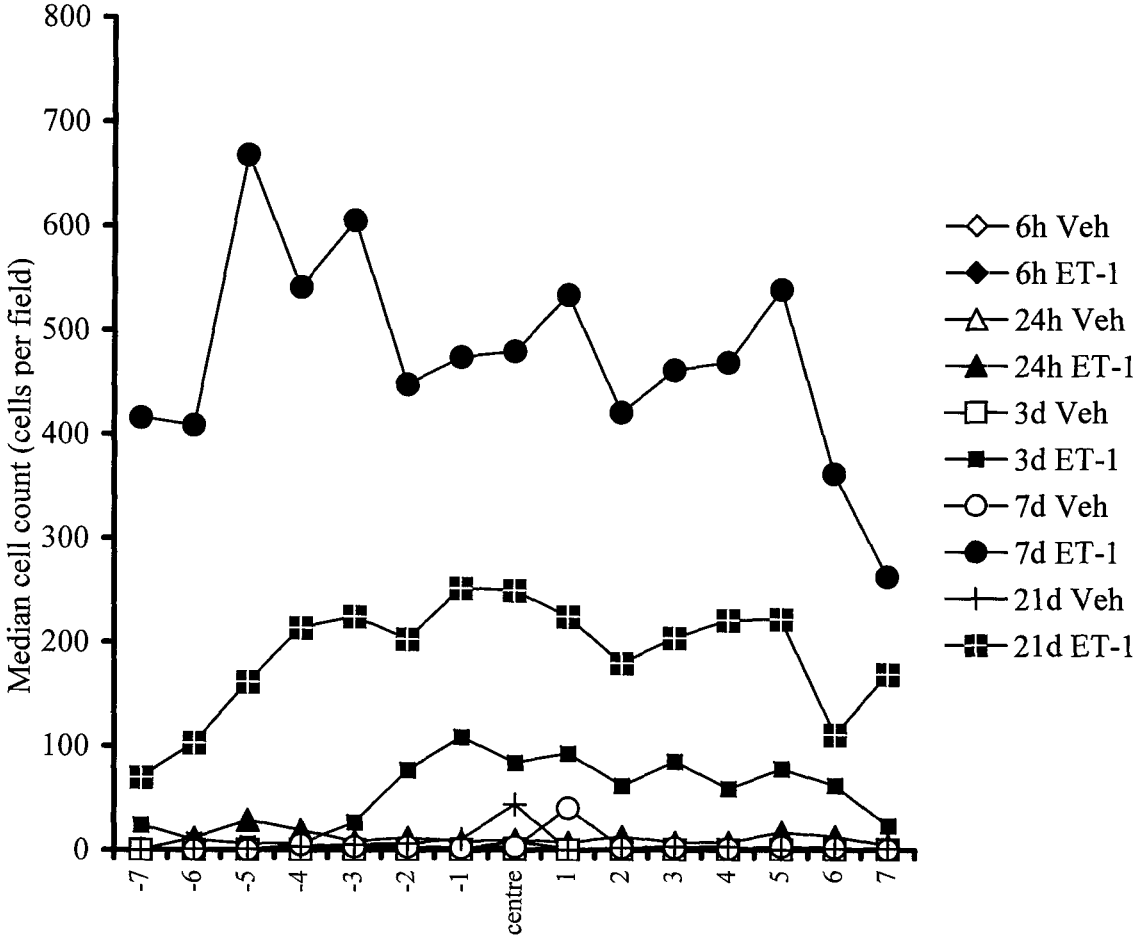

Rostro-caudal distribution of ED-1-positive macrophages in the grey matter following microinjection of vehicle (0.25µl) or ET-1 (15pmol) into the ventral spinal cord at T7. All points n=3 animals, 3 non-adjacent sections per animal counted and summed.

Figure 4.3.7.2 Rostrocaudal distribution of macrophages in the white matter

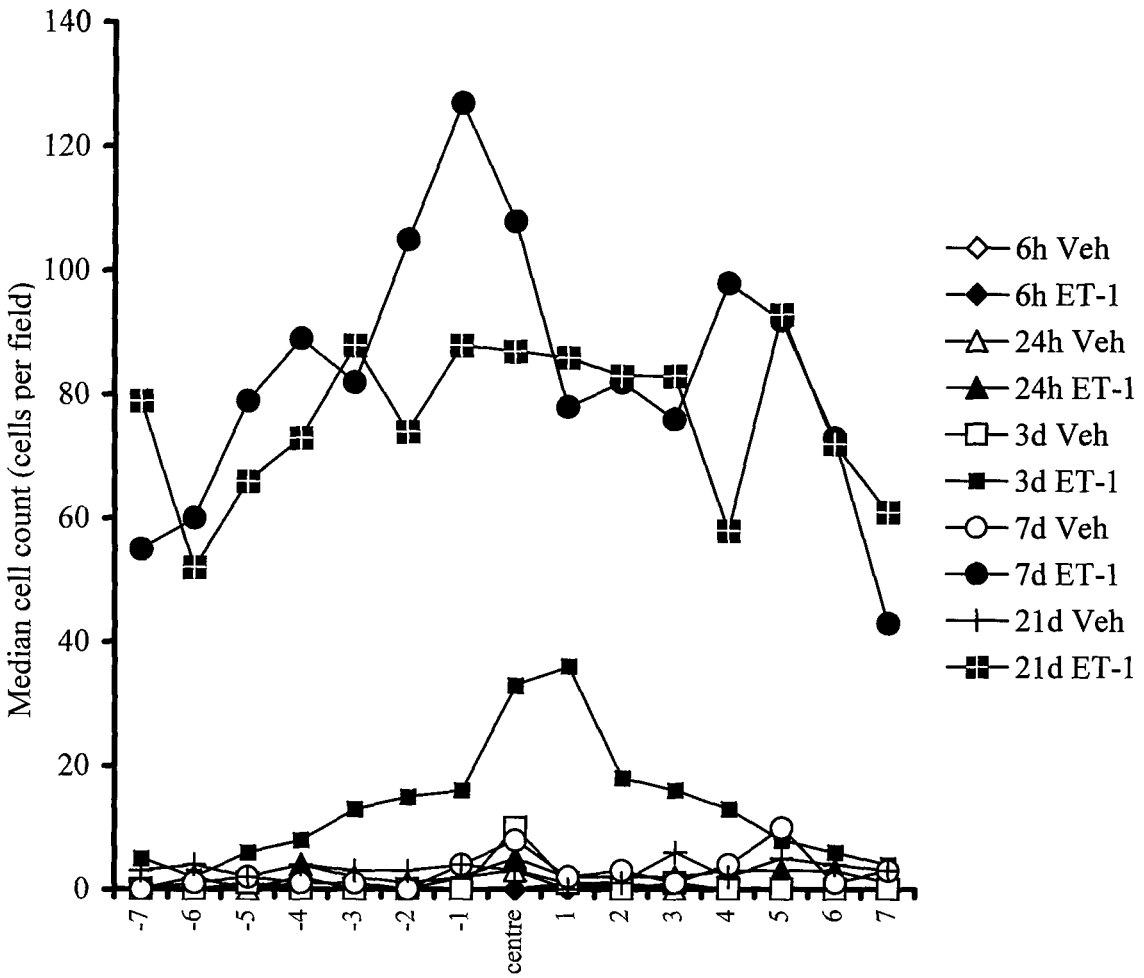

Rostro-caudal distribution of ED-1-positive macrophages in the white matter following microinjection of vehicle (0.25µl) or ET-1 (15pmol) into the ventral spinal cord at T7. All points n=3 animals, 3 non-adjacent sections per animal counted and summed.

were present in the white matter of ET-1 injected, but not the vehicle injected, spinal cords.

4.3.9 Pyknotic nuclei in white matter

Pyknotic nuclei were present in the lateral white matter of vehicle and ET-1 microinjected spinal cords at 3, 7 and 21 days after microinjection (Figure 4.3.9.1). There was no difference between the vehicle and ET-1 microinjected spinal cords with respect to the number of pyknotic nuclei present in the white matter at 3 days. By 7 days there was a statistically significant difference in the number of pyknotic nuclei in the ET-1 injected cords ($p<0.005$, Student's T-test) when compared to the vehicle injected cords, and this was maintained at 21 days ($p<0.005$, Student's T-test).

4.4 Discussion

4.4.1 Neuronal loss as a result of focal ischaemia

Within six hours of microinjection of 15pmol ET-1 into the parenchyma of the brain or spinal cord there is a loss of neuronal cell bodies in the immediate area around the microinjection site (Figure 4.3.1.1 and Figure 4.3.1.2). The reduction of blood flow in the spinal cord following microinjection of 15pmol ET-1 has been demonstrated to be statistically significant for at least 2 hours (Chapter 3), and this certainly appears sufficient to kill α-motor neurons in the ventral grey matter (Figure 4.3.1.2). The clearly visible nucleus and nucleolus of the large neurons in panel A are absent in panel B, indicating that these cells are no longer viable and are degenerating. Pyknotic nuclei are not seen in these cells, which confirms that they are undergoing a rapid necrosis and have not had time to initiate apoptotic cell death.

Ventral motor neurons are lost following a dorsal spinal contusion injury in the rat (Grossman *et al.* 2001). The motor neurons undergo changes characteristic of necrosis, such as cell swelling and loss of membrane integrity but some of the adjacent glial cells in the injured grey matter do undergo apoptosis. However in a murine model of non-impact spinal ischaemia and reperfusion, where the left subclavian artery is clamped and then released, there was evidence of apoptosis in the neurons of the ventral horn (Matsushita *et al.* 2000). These authors measured activated caspase-8, which is an enzyme in the early part of the apoptotic cascade, and

Figure 4.3.8.1 Changes in astrocyte morphology

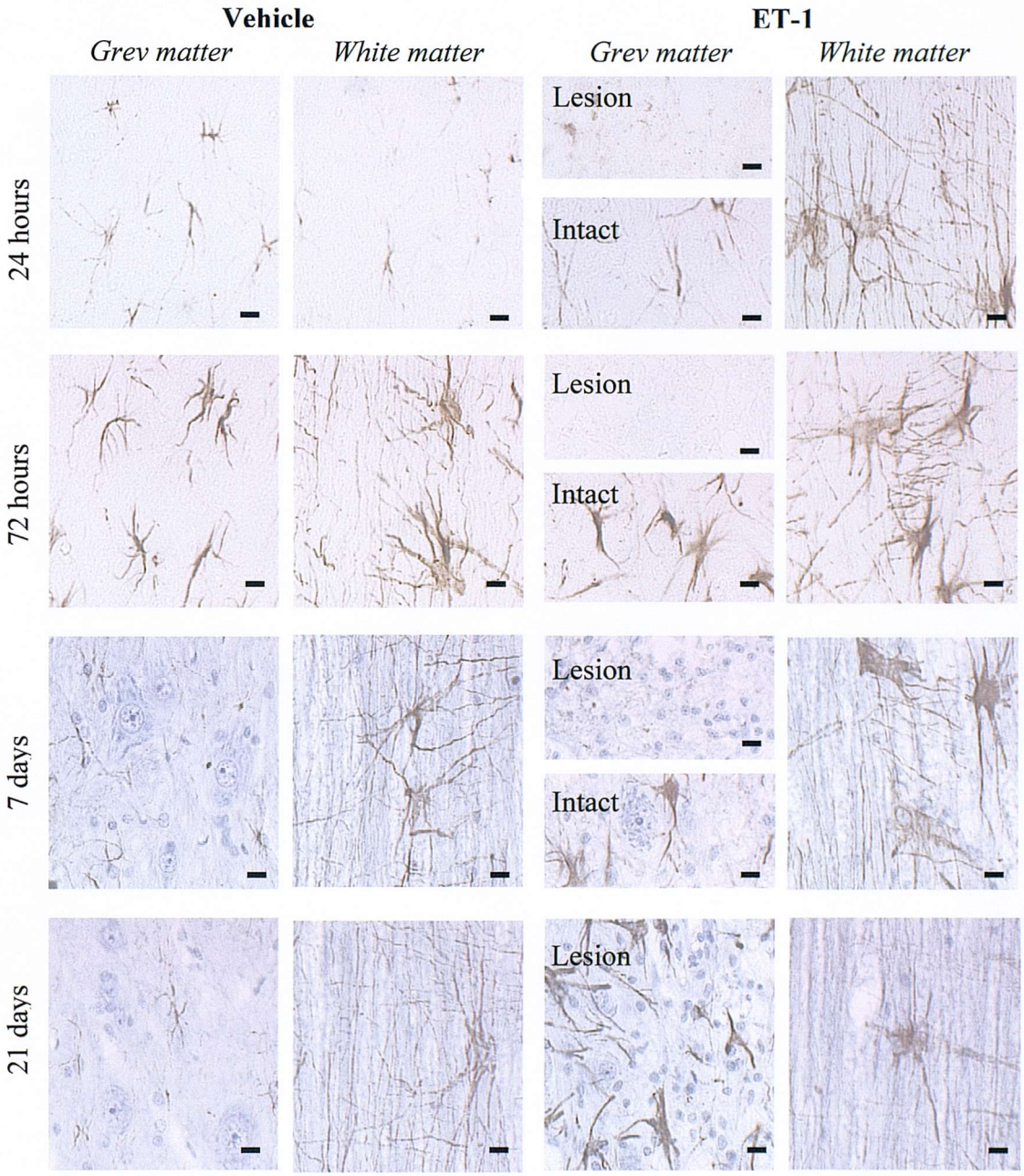

Representative images of GFAP positive astrocytes in the grey matter and white matter at 24 hours, 72 hours 7 days and 21 days after microinjection of vehicle (0.25µl) or ET-1 (15pmol) into the ventral spinal cord at T7. Areas of both intact and lesioned grey matter following ET-1 microinjection are shown. Scale bar = 10µm.

Figure 4.3.9.1 Distribution of pyknotic nuclei in lateral white matter

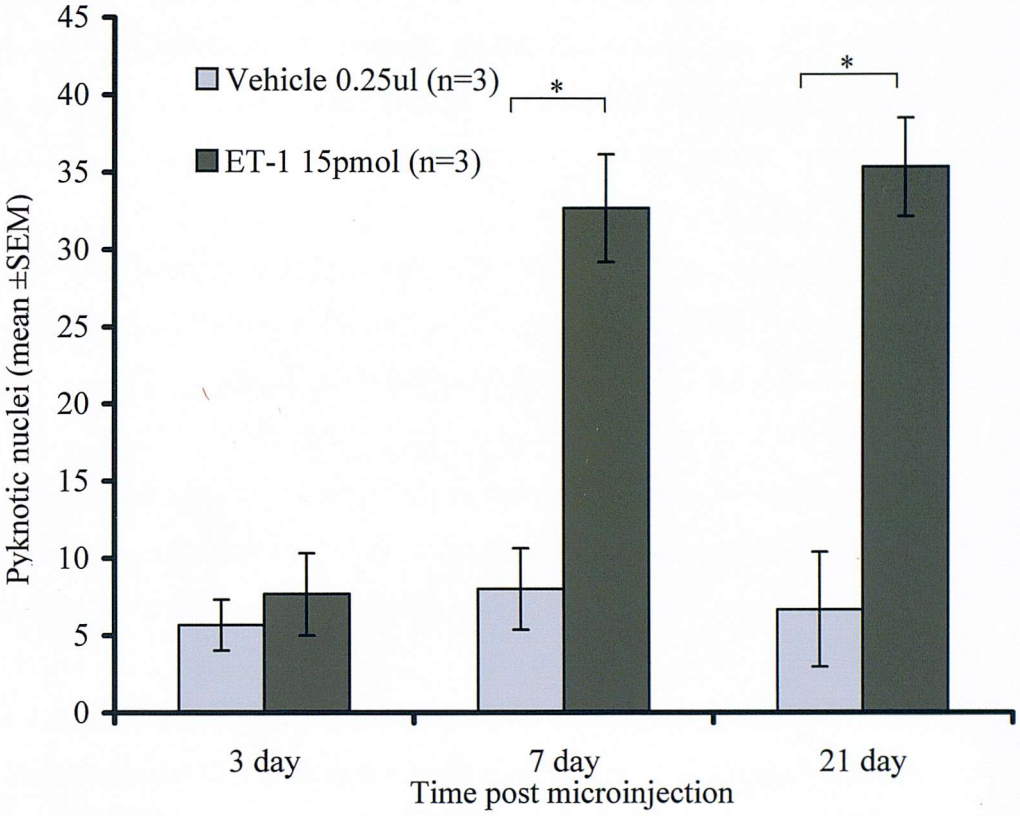

Pyknotic nuclei in the lateral white matter 3, 7 and 21 days after microinjection with vehicle (0.25µl) or ET-1 (15pmol). Pyknotic nuclei were counted in 15 fields per section at 1mm intervals centred on the microinjection site. For each animal the total number of pyknotic nuclei from three sections was calculated. *$p<0.05$ Students T-test.

also later components, such as mitochondrial cytochrome-c, in neurons of the ventral spinal cord. These reports suggest that in a complex spinal cord injury where both physical trauma and ischaemia (as a result of haemorrhage, coagulation and vasoconstriction) are present, both necrotic and apoptotic mechanisms of neuronal cell death might be involved. It would appear that the neurons destroyed in the ventral horn of the spinal cord in the present study are killed by a necrotic mechanism based on their morphology.

Fuxe *et al* found that 3 hours after a large dose of ET-1 (430pmol) was injected into the rat striatum, there was a lesion visible histologically as an area of cells displaying chromatolysis (Fuxe *et al.* 1992). At later time-points neuronal cell bodies were absent, but the overall lesion volume remained constant. The amount of ET-1 used in the present study, 15pmol, is much less but appears to have had a very similar effect. Medium spiny neurons are absent in the area where ET-1 was microinjected into the striatum, but not vehicle (Figure 4.3.1.1).

4.4.2 Neuronal cell loss in the spinal cord is extensive but stable

The rostro-caudal extent of the ischaemia, observed in Chapter 3, correlates well with the length of the spinal cord over which loss of neurons is observed (Figure 4.2.2). The distance between adjacent vertebral laser Doppler observations was approximately 5mm, and as the most severe ischaemia was observed at the three central locations (T6, T7 and T8) we would expect the lesion to be at least 10mm long. The observed mean lesion length was 15mm, suggesting that the reduction in blood flow observed over the central three segments did result in an ischaemic lesion only in this area, and not any further in the rostral or caudal direction. The lesion length is stable from 6 hours until at least 72 hours after microinjection of ET-1, suggesting that in the first three days the loss of motor neurons and other cells in the ventral horns of the spinal cord is solely due to the acute ischaemia.

4.4.3 Neutrophils are recruited into the spinal cord parenchyma after ET-1

Following a traumatic injury to the rodent spinal cord neutrophils can be identified in the necrotic lesion area, with a peak in numbers at 24 hours after impact (Carlson *et al.* 1998). The spinal cord recruits more neutrophils into a mechanically injured area than an equivalent area of similarly injured brain tissue (Schnell *et al.* 1999a),

suggesting that there may be some differences between areas of the CNS in their responses to injury. Following a spinal cord contusion injury (Streit *et al.* 1998) or focal ischaemia in the parietal cortex (Jander *et al.* 2000), TNFα and IL-1β mRNAs are increased transiently, returning to baseline values within 24 hours. The direct microinjection of these proinflammatory cytokines (TNFα or IL-1β) into the brain and spinal cord also results in a differential inflammatory response, with a more pronounced neutrophil recruitment in the spinal cord than the brain (Schnell *et al.* 1999b). There is evidence that at least some part of this difference may be due to the differential upregulation of chemokines in the spinal cord compared to the brain (Campbell *et al.* 2002).

Ischaemia and reperfusion alone, in the absence of a mechanical injury, can recruit neutrophils into the spinal cord (Hirose *et al.* 2000). These authors used inflation of an aortic balloon catheter to produce ischaemia over multiple spinal cord segments in the rat. Depletion of leukocytes by administration of nitrogen mustard resulted in the preservation of motor function and a reduction in neutrophil myeloperoxidase in the spinal cord. This sort of gross ischaemia of the spinal cord and much of its surrounding tissue may reproduce the type of injury observed following infra-renal clamping of the aorta during surgical removal of aneurysms, but this is not the typical pattern of ischaemia seen in traumatic spinal cord injury.

Twenty-four hours after a focal ischaemic insult capable of destroying neurons in the spinal cord and striatum (Figures 4.3.1.1 and 4.3.1.2) there is a profound recruitment of neutrophils into the spinal cord but not the striatum (Figure 4.3.3.1). The reason for this difference is not clear, although it is apparent that there is also a difference in blood-brain barrier permeability at this time point (see 4.3.4.1). It has been reported that the enhanced recruitment of neutrophils into the spinal cord compared to the brain after parenchymal injection of IL-1β can be explained by differential synthesis of the chemokine CINC-1 (Campbell *et al.* 2002). The relationship between the recruitment of neutrophils and the breakdown of the blood-brain barrier (BBB) has been explored in an IL-1β driven neutrophil recruitment model (Anthony *et al.* 1997). Neutrophil depletion prevents the BBB breakdown normally associated with neutrophil influx after parenchymal IL-1β microinjection in the juvenile rat brain.

This suggests that in this context the neutrophils are contributing to the BBB breakdown. Neutrophils are believed to mediate the breakdown of the blood brain barrier by a number of mechanisms including the release of glutamate, which acts on endothelial cell metabotropic glutamate receptors (Collard *et al.* 2002). The recruitment of neutrophils into the tissue parenchyma is dependent on the attachment and rolling of these cells along the endothelium lined lumen of blood vessels. Using selective antibodies against the adhesion molecule P-selectin reduced the neutrophil recruitment in an IL-1β driven neutrophil recruitment model (Bernardes-Silva *et al.* 2001).

4.4.4 Macrophages in cord but not striatum at 72h after ET-1

Macrophages, like neutrophils, appear in the spinal cord after ET-1 induced ischaemia but not the brain, with a large number of ED-1 positive cells present in the spinal cord at 72 hours after insult (Figure 4.3.3.2). The phagocytosis of debris following the necrotic death of neurons at the lesion site is important for restoration of tissue homeostasis, and would be expected to occur at both sites with equal vigour. However, it is possible that the extent of the lesion in the spinal cord results in a more pronounced activation of resident microglia than in the brain. Evidence from bone marrow chimeric rats suggests that even up to 3 days after a contusion injury, the vast majority of macrophages in the spinal cord are microglia derived (Popovich and Hickey 2001). Whether the variability in macrophage response is caused in part by a difference in microglial sensitivity is not clear, but it has been reported that microglia in the white matter become activated during Wallerian degeneration by a complement-independent mechanism, implying that microglial activation may be location sensitive (Watanabe *et al.* 1999). Other explanations could include differential tissue production of chemokines. Macrophage chemo-attractant protein-1 (MCP-1) mRNA is increased from 1 to 7 days after injury in contused spinal cord (Le *et al.* 2000), and this chemokine would be expected to recruit haematogenous monocytes.

4.4.5 Blood-spinal cord barrier breakdown

Following a traumatic contusion injury to the spinal cord, blood-spinal cord barrier (BSCB) breakdown can be observed over a wide area and for at least 3-7 days (Popovich *et al.* 1996). Microinjection of ET-1 into the ventral horn of the spinal cord

results in an increase in horseradish peroxidase extravasation, a marker of BSCB breakdown, at 24 hours (Figure 4.3.4.1). This time-point is coincident with the peak number of neutrophils, and neutrophil infiltration is associated with damage to the BSCB as these cells can secrete collagenases, which degrade the extracellular matrix, in order to extravasate to the site of injury. The microinjection of a high dose of ET-1 (160pmol) into the striatum resulted in no significant breakdown of the blood-brain barrier (BBB) (Corkill *et al.* 2001). This is consistent with the finding that IL-1β or TNFα microinjected into the brain fail to induce BBB breakdown at doses which cause profound leakage of plasma proteins in the spinal cord (Schnell *et al.* 1999b). The reasons for this difference are not yet clear; it may be that there are structural differences in the BBB composition between areas of the CNS, or that the endothelial cell tight junctions in the spinal cord are more likely to break down in response to inflammatory or ischaemic stimuli.

Other studies have described BSCB breakdown occurring very early after an injury. In one instance following an incision injury to the dorsal cord, BSCB leakage was identified within 5 hours (Mustafa *et al.* 1995). This type of injury, where a sharp instrument is used to cut the tissue, results in a mechanical trauma to blood vessels immediately around the incision, and in bleeding. Both of these factors may lead to the extravasation of an injected protein at early time points after injury. A previous study using intrathecal administration of an ET-1 solution (Westmark *et al.* 1995) found BSCB leakage after 3 hours of ET-1 induced spinal ischaemia. However Westmark *et al* injected the marker of BSCB breakdown, horseradish peroxidase (HRP), before the application of ET-1. As ET-1 causes a profound vasoconstriction it is possible that the HRP has been excluded from the ischaemic tissue at 6 hours in the studies presented above. Perfusion of the spinal cord within 6 hours of microinjection of ET-1 results in inadequate penetration of fixative. This can be visualised when using Bouins fixative, which has a bright yellow colour due to the presence of picric acid. The area of the spinal cord around the microinjection site appears paler. All tissues taken for immunohistochemistry were also post-fixed, so this phenomenon does not result in a lack of fixation within the lesion and subsequent loss of section quality.

4.4.6 Neutrophil recruitment in the spinal cord

Having established that neutrophils enter the spinal cord parenchyma following ET-1 microinjection, it would be useful to understand which compartment, white matter (WM) or grey matter (GM), the cells preferentially move into. In this model the ET-1 is microinjected into the grey matter and is believed to act on the micro-vessels supporting the neurons in this part of the tissue. However, given the wide rostro-caudal extent of the ischaemia, it would not be unreasonable to expect the ischaemia to also affect tissue radially, and ischaemia of the adjacent white matter may result in substantial damage to axons and can lead to functional impairment (Petty and Wettstein 1999). The presence of neutrophils in the white matter would indicate that there is potential for some additional damage, and this may be amenable to pharmacological or other therapeutic intervention.

In Figure 4.3.5.1 it is clear that there is some recruitment of neutrophils into both the grey and white matter compartments of the spinal cord at 24 hours after microinjection of ET-1. The recruitment appears to be roughly symmetrical around the lesion site, and to extend 7mm rostrally and caudally. The number of cells present at 3 days after microinjection of ET-1 is low, but is more pronounced in the caudal direction in both the grey and white matter. Of all the vehicle-injected groups only the 24-hour time-point showed any neutrophil recruitment; this was limited to the microinjection site and was probably due to minor mechanical damage. This confirms that the microinjection procedure causes minimal trauma.

In the central field of the lesion there is a statistically significant difference between the vehicle and ET-1 treated grey matter neutrophil counts at 24 hours and 3 days after microinjection ($p<0.05$, Students T-test comparison between treatments using the sum of the three central fields). Apparent differences in neutrophil recruitment in the white matter of the central field are not statistically different at any time-point, but it is clear from Figure 4.3.5.1B that these cells are recruited into the white matter following ET-1 but not vehicle.

The absolute numbers of neutrophils in the white matter 24 hours after ET-1 are quite low (10 cells per field) even at the centre of the lesion (Figure 4.3.5.1B). These numbers are one-third of the value reached in the grey matter at the same time-point.

This result may be due to the fact that the grey matter is more vascular than the white matter (Koyanagi *et al.* 1993a). Increased cellular damage (and hence more chemotactic signals such as C5a, LTB_4 and chemokines) and a greater vascular area for cells to extravasate from may result in an increased number of neutrophils in the grey rather than the white matter. The microinjection of ET-1 into the grey matter causes a profound ischaemia along the rostrocaudal axis of the spinal cord (Chapter 3). Given the extent of the ischaemia along this axis, it is likely that the ventral and ventrolateral white matter, which is served by a vascular system contiguous with that in the grey matter, may also experience ischaemia. This will result in tissue damage and an acute inflammatory response.

It is unclear in rodent studies where neutrophil inhibition is employed as a therapeutic strategy, whether the functional benefit obtained is due to the survival of more motor neurons or the protection of white matter (Taoka and Okajima 1998, 2000). In stroke, where ischaemia-reperfusion results in neutrophil influx and damage to cells in the penumbral region, the contribution of neutrophils to the injury may be more straightforward (Barone and Feuerstein 1999). Axonal injury that is not directly related to the destruction of cell bodies in the grey matter may be due to a combination of ischaemia induced excitotoxicity (Li *et al.* 1999), hypoxia and inflammation.

4.4.7 Macrophage recruitment in the spinal cord

The resident macrophages of the CNS, the microglia, perform a surveillance function, responding to the presence of invading pathogens, cellular debris or apoptotic cells by adopting a phagocytic phenotype (Kreutzberg 1996; Perry and Gordon 1997). The complement receptor CR3 is present on microglia and this is one of the ways in which the rapid response to tissue debris is mounted. In addition the key recognition molecule C1q, which initiates the classical complement cascade, is up-regulated in microglia in the brain after a transient ischaemic insult (Schafer *et al.* 2000).

The microinjection of zymosan, which is a ligand for the complement CR3 receptor, into the rat spinal cord results in the activation of microglia and the formation of an inflammatory lesion (Popovich *et al.* 2002). Injection of zymosan into white matter tracts (lateral and ventral funiculi) resulted in axonal injury, although the authors report that by 3 days the majority of macrophages in the lesion are haematogenous in

origin. This is in contrast to a contusion injury, where the microglia constitute the majority of macrophages in the lesion for the first 3 days (Popovich and Hickey 2001).

In addition to stimulation by complement fragments, microglia can be activated by other mechanisms. Evidence from *in vitro* studies suggests that human microglia respond to stimulation by ET-1 in a calcium-dependent manner via the ET_B receptor (McLarnon *et al.* 1999). This would provide a mechanism for the tissue macrophages to be responsive to vascular injury or hypoxia, both of which can induce ET-1 production. Microglial activation is present in the non-traumatic photochemically induced cortical ischaemia model (Schroeter *et al.* 1999). Microglial activation has been observed following ET-1 induced focal ischaemia in the spinal cord (Figure 4.3.6.1). The normally quiescent microglia change in their morphology, from a stellate appearance with antler-like processes, to a more rounded shape with fewer, thicker processes. This occurs in both the grey and white matter of the spinal cord following microinjection of ET-1 but not vehicle.

Experiments using the ET_B antagonist BQ-788 in the rat cortical stab model showed no reduction in macrophage recruitment (Koyama *et al.* 1999), although the drug had reduced astrocyte activation, suggesting that the trauma was sufficient to induce a full phagocytic response. The nuclear transcription factor NFκB, a key molecule in the regulation of inflammatory and proliferative events, is upregulated in spinal cord microglia, in addition to endothelial cells and neurons, following a contusion injury (Bethea *et al.* 1998).

Other signalling systems, including cytokines and chemokines are involved in the response of microglia to inflammatory stimuli in their microenvironment. Microglia have chemokine receptors (Bacon and Harrison 2000) including the CX_3CR1 receptor that is specific for fractalkine, and as neurons are one of the main sources of fractalkine in the CNS, it is hypothesised that this chemokine may be involved in neuron-microglial communication.

It has been shown *in vitro* that mouse microglia contain the mRNA for the CXCR3 receptor, and this enables them to respond to secondary lymphoid-tissue chemokine (SLC) by chemotaxis (Biber *et al.* 2001). These authors also provide evidence that neuronal-microglial signalling can occur through chemokine, as SLC mRNA was present in neurons from the ischaemic cortex of mice that had undergone mid-cerebral artery occlusion (MCAO).

The temporal and spatial profile of macrophage recruitment into the spinal cord following an impact injury has been reported previously (Carlson *et al.* 1998; Leskovar *et al.* 2000). The established pattern is that macrophages do not appear in large numbers until 3 days after the injury, and they are present in both the grey and white matter, particularly in the dorsal white matter at the site of impact.

In a non-traumatic ischaemic injury that develops after microinjection of ET-1 there is recruitment into both the grey and white matter of the spinal cord after 3 days (Figure 4.3.7.1, Figure 4.3.7.2). There is a difference between the grey and white matter in both the absolute numbers of cells recruited and their spatial distribution. In the white matter the maximum number of cells recruited per field is only one third of the peak observed in an adjacent area of grey matter, and this is likely to be due to the fact that this area is more vascular and contains degenerating cells in abundance. The apparent peak at the lesion centre in the white matter at three days cannot be accounted for by mechanical injury caused by the microinjection technique as a vehicle injection resulted in minimal recruitment of macrophages at the same time-point. This suggests that the very pronounced macrophage response seen by Carlson was a direct result of the mechanical trauma, and not any secondary pathological events (Carlson *et al.* 1998).

The difference in white matter macrophage recruitment between ET-1 and vehicle injection at 3 days after microinjection is not statistically significant. However, from Figure 4.3.7.2 it is clear that there is a pattern of recruitment of macrophages into the white matter at 3 days following ET-1 microinjection that does not occur following vehicle microinjection. Even more significant increases in macrophage numbers occur by 7 days, and although in the grey matter these are reduced by 21 days, in the white matter there is no reduction in macrophage presence at 21 days. The persistence

of macrophages in the white matter over long periods following an injury is to be expected as axonal tracts degenerate (Kosel *et al.* 1997). There is potential for this longer term macrophage response to cause further axonal or myelin damage (Coleman and Perry 2002).

The recruitment of macrophages into the grey matter is robust, with large numbers of cells filling the ventral horns at 3 days post ET-1 microinjection. The recruitment at this time appears to be asymmetrical, and statistical analysis of the counts obtained either side of the injection site reveal a statistically significant difference ($p<0.05$). The minimal macrophage recruitment seen in vehicle injected cords resolves quickly, and as a result there is a highly significant difference between vehicle and ET-1 injected groups at the 7 and 21 day timepoints. The reduction in macrophage numbers may be due in part to the successful clearance of debris after a prolonged period of active phagocytosis, or the formation of a gliotic scar in the area which was formerly occupied by grey matter. The proliferation and repopulation of this area by astrocytes may reduce the ability of macrophages to move into the area or proliferate.

4.4.8 Astrogliosis

The pattern of astrocyte up-regulation seen following microinjection of ET-1 is consistent with the known behaviour of astrocytes after injury, i.e. a rapid loss of GFAP staining at the lesion focus, and thickening of astrocyte processes associated with up-regulation of the intermediate filament protein GFAP immunoreactivity in adjacent areas. This can happen within 1 hour following a spinal cord lesion (Hadley and Goshgarian 1997). There is clear evidence of classic astrocytic hypertrophy in the spinal cord white and grey matter following the microinjection of ET-1, and to a lesser extent vehicle (Figure 4.3.8.1). Hypoxia is toxic to astrocytes *in vitro*, and causes them to undergo an apoptic death (Yu *et al.* 2001), and in vivo at the epicentre of an ischaemic or mechanical lesion there is an absence of GFAP staining (Grossman *et al.* 2001).

It is now clear that one of the key molecules involved in astrocytic activation in hypoxia and trauma is ET-1. A number of studies have identified astrocytes as a source of ET-1 in ischaemia *in vitro* and *in vivo* (Jiang *et al.* 1993; Pluta *et al.* 1997; Petrov *et al.* 2002). In addition astrocytes express the ET_B receptor and increase

expression of this receptor under hypoxic conditions (Shibaguchi *et al.* 2000; Hasselblatt *et al.* 2001). The use of specific ET_B receptor antagonists such as BQ-788 has shown that the activation of these receptors leads to the characteristic astrogliosis seen after injury (Uesugi *et al.* 1996; Hama *et al.* 1997; Koyama *et al.* 1999), and *in vitro* studies have demonstrated that this process is calcium dependent (Du *et al.* 1999).

Astrocytes are not the only source of ET-1 in an injured tissue, and it has been shown in a rodent model of traumatic brain injury (TBI) that endothelial cells rapidly supersede them as the source of ET-1in the lesion (Petrov *et al.* 2002). Microinjection of ET-1 would be expected to activate astrocytes by its direct action on ET_B receptors, but as the microinjection also produces a dramatic reduction in blood flow (see Chapter 3), it is likely that the astrocyte pathology seen is due to the focal ischaemia and its consequences, possibly including local synthesis and release of ET-1 (see Chapter 6).

As astrocytes communicate via gap junctions (Venance *et al.* 1998), the stimulation of a single astrocyte could lead to many others being stimulated by spreading activation (Stoll *et al.* 1998). This probably explains why astrocytes many millimetres distal to the microinjection site appear to by upregulated. At the edges of the lesion, both along the lateral edges in contact with the white matter and at the distal ends adjacent to intact grey matter, the astrocytes remain highly GFAP positive at day 21. This is the outer edge of a glial scar, which acts as a physical barrier and also prevents inappropriate axonal sprouting. At the latest time point examined (21 days) the lesioned grey matter, which until this time was dominated by macrophages, appears to have astrocytes extending their processes into the lesion from the glial scar. This may ultimately lead to the repopulation of the grey matter area with a complete glial scar.

4.4.9 Pyknotic nuclei

Dense, spherical structures were seen in the lateral white matter at the 7 and 21 day time-points (Figure 4.3.9.1). Based on their location and morphology, they are most probably the pyknotic nuclei of apoptotic oligodendrocytes. It has been reported that oligodendrocytes undergo apoptosis along degenerating axons after spinal cord injury in the rat (Shuman *et al.* 1997; Casha *et al.* 2001) and in primates (Crowe *et al.* 1997).

Shuman reported that the cell death seen was maximal at 8 days, however it can be seen in Figure 4.3.9.1 that the number of pyknotic nuclei remains constant from 7 to 21 days following microinjection of ET-1. An interesting observation arising from the analysis of these spinal cord sections is that even in vehicle injected spinal cords or at the earlier time-points there are a few pyknotic nuclei present. Whether this is indicative of normal turnover or post-natal development, or reflects some artefact is not known at this time.

There is no evidence from the immunohistochemistry for macrophages and astrocytes that these cells are the source of the pyknotic nuclei, and there was no co-localisation of inflammatory cells with these structures. This is in agreement with Frei, who observed no association between macrophages/activated microglia and death of ventral white matter oligodendrocytes up to 2 weeks following a contusion injury (Frei *et al.* 2000).

4.5 Conclusions

It is clear from the data presented above that following ET-1 induced focal ischaemia there is a profound acute inflammatory response in the spinal cord, in comparison to the effect in the striatum. It is unlikely that these differences can be accounted for simply by the size of the ischaemic lesion as the direct injection of pro-inflammatory cytokines has also failed to elicit a significant inflammatory response in the brain (Schnell *et al.* 1999b).

The pattern of neuronal cell death and neutrophil recruitment in the spinal cord after microinjection of ET-1 mimics that observed following an impact injury. Macrophage recruitment is less than that seen after an impact injury as it is not enhanced by the effects of physical trauma, and reflects perhaps the true tissue injury caused by the ischaemic lesion. The recruitment of microglia and their phenotypic change into phagocytes is consistent with the situation following trauma, although it is not clear whether it is the ischaemia which triggers the activation directly or if necrotic cells releasing their cell contents initiate the complement cascade and thereby activate the microglia. The ischaemic lesion also induces astrocytes to undergo their characteristic changes in morphology and GFAP expression, and oligodendrocytes appear to be

undergoing apoptosis over an extended timescale as a result of axonal degeneration in the white matter.

These results indicate that this model is a useful tool to investigate spinal cord injury, as it comprises all the major components of classical SCI such as necrosis, inflammation, blood-brain barrier breakdown and gliosis, but without a significant mechanical component. This makes it a good setting to investigate aspects of SCI which can be difficult to address in mechanical injury models, such as axonal injury as a result of secondary mechanisms.

Chapter 5 – Axonal injury

5.1 Introduction

It has been understood for many years that injury to the spinal cord results in paralysis of systems below the level of the lesion. This is due to the loss of axons in the white matter tracts, which normally communicate between the periphery and the CNS. Although spinal cord injury has been studied for many years, it is only relatively recently that there has been renewed interest in the underlying mechanisms and patterns of axonal pathology. As these events become more fully understood the potential for finding interventions that could prevent some of the axonal injury, and hence functional loss, may be found.

The previous chapters have described how microinjection of ET-1 induces a profound focal ischaemia of the spinal cord, resulting in neuronal loss, acute inflammation, reactive gliosis and loss of oligodendrocytes over an extended period. The present chapter will focus on the white matter axons and their myelin sheaths, and also investigate the contributions of ischaemia and excitotoxicity to the observed pathology.

5.1.1 Mechanical injury to axons

Axons can be injured in the immediate trauma of a spinal cord injury, for example as the mechanical force of a penetrating bone fragment enters the vertebral lumen. Axons do have some capacity to stretch, and hence avoid transection, but only at relatively low velocities; high-speed displacement of axons ($0.5 – 1 m.s^{-1}$) within the white matter can cause immediate injury (Honmou and Young 1995). As a result, axons that are not physically transacted by a sharp bone fragment or penetrating object can still be irreversibly damaged.

Other forms of CNS injury also result in axonal pathology, for example diffuse axonal injury (DAI), where rapid deceleration of the head, such as that which occurs during a motor vehicle accident, causes the brain to move within the skull and impact against it. The resulting pressure waves and tissue stretching can damage axons (Povlishock and Christman 1995). The characteristic histopathology of DAI consists of axonal swellings throughout the brain parenchyma, where the proximal segments of severed axons continue to accumulate organelles and neurofilaments from the cell body by fast

anterograde axonal transport. Although some of the axons will be transected immediately, there is evidence that secondary mechanisms are also involved (see below).

It has been demonstrated in animal models of traumatic brain injury (TBI) where DAI is observed that calcium entry into the injured axon can damage mitochondria, leading to cytochrome-c release and the activation of caspase-3 (Buki *et al.* 2000), which are events likely to lead to axonal degeneration. There is *in vitro* evidence that calcium entry does not occur through mechanically generated pores, but rather through voltage gated calcium channels and as a result of reversal of the sodium/calcium exchanger (Wolf *et al.* 2001). Mechanical injury to axons results in the opening of voltage gated sodium channels, which allows entry of sodium into the axon and depolarises the membrane. This depolarisation opens voltage gated calcium channels, and the change in sodium gradient forces the Na^{+}/Ca^{2+} exchanger to reverse, resulting in additional calcium influx. It has been known for some time that sodium channel blocking agents are protective in white matter ischaemia (Stys *et al.* 1992) and Wolf *et al* propose that the mechanically induced opening of the channels is reduced by these drugs, thus preventing this sodium influx.

5.1.2 Immune mediated axon injury

Inflammation within the CNS can generate axonal injury. There is evidence that immune mediated axon injury occurs in multiple sclerosis (Trapp *et al.* 1998; Perry and Anthony 1999), although it is still not fully understood by what mechanism this happens. In multiple sclerosis auto-reactive T-cells target the myelin sheath and the result is plaques in the white matter where demyelination has occurred. The mechanism responsible for the damage to the axon are currently not clear, but could include direct injury to the axon by NO/peroxynitrite (Touil *et al.* 2001), or matrix metalloproteinases (Newman *et al.* 2001) generated by inflammatory cells within the plaques. Macrophages and T-cells have been observed in areas of axonal injury (Bitsch *et al.* 2000), as indicated by APP immunohistochemistry in human multiple sclerosis. In particular there was association of CD8-positive T-cells in the areas of APP accumulation, and these can behave as cytolytic T-lymphocytes (CTLs), releasing the pore-forming protein perforin and destructive serine esterases (granzymes) (Roitt *et al.* 2001).

The acute inflammatory response may contribute to the axonal damage seen after spinal cord injury. Depletion of haematogenous macrophages with clodronate loaded liposomes resulted in an improved behavioural outcome for rats following a contusion injury, and increased preservation of axons (Popovich *et al.* 1999). Inhibition of neutrophil derived enzymes, such as elastase (Tonai *et al.* 2001), reduces the behavioural deficit, although it is unclear how much of this benefit is due to preservation of axons.

5.1.3 Ischaemic injury to axons

One of the key features of ischaemic injury to white matter *in vivo* is the injury to astrocytes, oligodendrocytes and myelin (Pantoni *et al.* 1996; Yam *et al.* 1998; Wakita *et al.* 2002). The white matter requires less energy relative to the high metabolic demands of grey matter, but it is nevertheless vulnerable to ischaemia (Petty and Wettstein 1999). This has been demonstrated in studies examining the effect of cerebral ischaemia on brain white matter in the rat. Myelin disruption (Pantoni *et al.* 1996) and amyloid precursor protein (APP) positive end bulbs (Yam *et al.* 1997) were present in the white matter twenty-four hours after mid-cerebral artery occlusion.

In addition to the mechanically mediated mechanism described earlier, ischaemia can also cause an influx of calcium into the axon. Energy is required to maintain the Na^+/K^+ gradients used by the axon to generate action potentials, and if these gradients fail as a result of ischaemia, calcium can enter the axon through voltage dependent calcium channels and the reversal of the Na^+/Ca^{2+} exchanger. This calcium can activate degradative enzymes, such as calpains, to trigger axonal destruction (Stys 1998). Mitochondria will also be disrupted in an ischaemic axon, and release their contents into the axoplasm, including cytochrome-c and caspase-3 (Buki *et al.* 2000).

One of the key events now understood to occur in ischaemic/hypoxic axons is the reversal of the Na^+/Ca^{2+} transporter, which normally uses the high $[Na^+]_{EC}$ to pump Ca^{2+} out of the axoplasm (Stys 1998). The Na^+/Ca^{2+} transporter has been observed in the white matter, and immuno-gold electron microscopy has confirmed that it is present at the nodes of Ranvier of CNS axons (Steffensen *et al.* 1997). A series of *in vitro* experiments using rat tissue has shown that calcium entry into the axoplasm is

responsible for the loss of function seen after a period of ischaemia. Removal of extracellular calcium with the ion chelating agent EGTA preserved the compound action potential (CAP) in the optic nerve after 1 hour of anoxia (Waxman *et al.* 1991) and use of a calcium free perfusate protected the CAP in isolated spinal cord dorsal columns by 90% against glutamate toxicity (Li and Stys 2000). The voltage gated calcium channel antagonists verapamil and omega-cono toxin also enhanced the CAP recovery following a mechanical injury in an isolated dorsal white matter preparation (Agrawal *et al.* 2000).

5.1.4 Glutamate and myelin injury

It has been proposed that the injury to myelin and oligodendrocytes seen in models of SCI is not a result of inflammation (Frei *et al.* 2000), as no temporal or spatial correlation was seen between glial and myelin injury and the appearance of inflammatory cells. The myelin sheath is formed from the wrapping of oligodendrocyte processes around axons, and forms a dense electrically insulating layer essential for saltatory conduction (Morell and Norton 1980).

Glutamate is an excitatory amino acid that is synthesised in neuronal cell bodies and transported to axon terminals where it is used as a neurotransmitter. In addition to synaptic communication, glutamate can be released into the extracellular milieu where it can have potent effects on other neuronal, glial or endothelial cells that possess glutamate receptors. Glutamate is scavenged from the extracellular environment by astrocytes to prevent the accumulation of this potent excitatory molecule.

Receptors for glutamate can be ionotropic (for example the NMDA receptor which is located on neuronal cell bodies (Dumuis *et al.* 1988)), or metabotropic (for example mGluR1 which is found on endothelial cells (Collard *et al.* 2002)). The ionotropic receptors are constructed from a number of subunits, some of which are common to more than one receptor (Dingledine *et al.* 1999). They are classified pharmacologically according to the rank order of potency of the synthetic agonists N-methyl-D-aspartate (NMDA), alpha-amino-3-hydroxy-5-methyl-4-isoxazole propionic acid (AMPA) and kainic acid (KA).

Under pathological conditions, such as trauma or ischaemia, glutamate is released by neurons as a result of a reversed uptake mechanism (Rossi *et al.* 2000). This results in excitotoxicity, as the released glutamate opens the NMDA receptors, allowing calcium to enter the cell. The glutamate will also activate the AMPA/Kainate receptors, which are sodium channels, thus depolarising the membrane and opening the voltage dependent calcium channels, resulting in additional calcium entry (Szatkowski and Attwell 1994). If the calcium is not cleared or buffered by the cell, cell death may ensue as a result of the activation of proteases, such as the calpains, and mitochondrial dysfunction.

Pharmacological intervention in models of SCI with certain glutamate antagonists, which would be expected to protect neurons in the grey matter from excitotoxic injury, result in a reduction in white matter injury. This occurs because ionotropic glutamate receptors are not restricted to synapses, and can be found in many areas within the CNS. Kainic acid and AMPA receptors, two classes of non-NMDA receptors, can be found on astrocytes (Agrawal and Fehlings 1997). AMPA receptors are also found on the myelin and oligodendrocytes (Li and Stys 2000). These receptors function as they would in a neuronal membrane, allowing depolarising sodium into the cell, and potassium out, and as a result ischaemic cells, which cannot maintain their Na^+/K^+ gradients are vulnerable to excitotoxicity. The source of glutamate in this scenario has been identified as the axon cylinder itself (Li *et al.* 1999), which possesses a Na^+/glutamate transporter that normally moves glutamate into the axoplasm using the Na^+ gradient. Under ischaemic conditions where the Na+/K+ gradient is compromised, the glutamate flows out of the axon where it can act on receptors in the local micro-environment, namely the AMPA and KA receptors on oligodendrocytes and astrocytes.

Electrophysiological studies using rat dorsal columns *in vitro* have shown that compression, which mimics the trauma and ischaemia of SCI (Agrawal and Fehlings 1997; Li *et al.* 1999), or direct application of glutamate (Li and Stys 2000) both result in a reduction of the CAP. Addition of the AMPA antagonists NBQX or GYKI52466, or the removal of calcium ions from the perfusate resulted in an improved recovery of the CAP when the compression or agonist was removed. The NMDA receptor antagonists MK801 or APV did not offer any protection, confirming that the

AMPA/KA receptors mediate toxicity in these conditions. Mouse brain slices *in vitro* are also vulnerable to ischaemia, and the resulting white matter injury and electrophysiological dysfunction can be ameliorated by NBQX or the removal of calcium (Tekkok and Goldberg 2001).

The protection seen *in vitro* has been reproduced in some *in* vivo models of SCI. Direct microinjection of the AMPA antagonist NBQX reduced the number of oligodendrocytes destroyed following a T8 contusion injury (Rosenberg *et al.* 1999), whilst i.v. infusion of the drug 15 minutes (Wrathall *et al.* 1996) or 4 hours (Wrathall *et al.* 1997) after contusion significantly reduced the behavioural deficits observed. In a non-contusive model of SCI, where the aorta is occluded with a balloon-tipped catheter, rendering much of the spinal column ischaemic, intrathecal NBQX was also shown to preserve axons in the ventral and ventrolateral white matter (Kanellopoulos *et al.* 2000). As the drug is not acting on the axon, which lacks ionotropic glutamate receptors, it is likely that the effects of the injury on axons is reduced by preventing damage to glial cells. In particular it has been proposed that astrocytes have a key role in supplying energy to myelinated axons in the form of lactate (Stys 1998).

The previous chapters have demonstrated that ET-1 is capable of producing a focal ischaemia of the spinal cord sufficient to cause neuronal loss and the initiation of an acute inflammatory response. The present chapter describes the effects of this lesion on the axons within ventral white matter of the spinal cord at the light and electron microscopic level. In addition an excitotoxic lesion induced by microinjection of NMDA into the ventral grey matter is described. Comparison of the ischaemic lesion with a purely excitotoxic lesion will be used to assess the likely contributions of direct ischaemia from those resulting from the efflux of glutamate during ischaemia.

5.2 Methodology

5.2.1 Microinjection of ET-1 and NMDA for immunohistochemistry

Male Wistar rats were anaesthetised with Hypnorm/Hypnovel and microinjected with vehicle (sterile saline) endothelin-1 (ET-1, 15pmol) or *N*-methyl-D-aspartate (NMDA, 20nmol) into the ventral horn of the spinal cord at the level of the 7th thoracic vertebra (See Chapter 2). At predetermined intervals following microinjection (6 hours to 21 days) the animals were anaesthetised with pentobarbitone and perfusion-fixed with

Bouins fixative (See Chapter 2). Bouins fixed tissues were wax-embedded and stored until 10μm sections were cut on a bench-top microtome (see Chapter 2). In order to assess the histopathology of the NMDA induced spinal cord lesion immunohistochemistry was performed to detect neutrophils (MBS-1), macrophages (ED-1) and astrocytes (GFAP) as described in the previous chapter.

5.2.2 Immunohistochemistry for APP

Immunohistochemistry was performed as described in Chapter 2 using a mouse monoclonal antibody against the β-amyloid precursor protein (APP) LN-27 (Zymed, USA). A biotinylated horse anti-mouse secondary antibody (Vector,UK) and horseradish-peroxidase labelled avidin-biotin complex (ABC-Elite, Vector, UK) were used to visualise the primary antibody localisation by DAB preciptation (see Chapter 2 for details).

5.2.3 Quantification of APP staining

For the ET-1 and vehicle microinjected spinal cords, the area of APP staining was obtained using a microscope equipped with a video camera, and a personal computer software package for image acquisition (Leica Qwin, Leica UK). Briefly, the sections were inspected by the operator at 25x magnification and the five highest intensity fields were captured electronically and a threshold, which remained constant for all the analysis, was applied to enable the area of DAB staining to be measured. The analysed images were stored for reference and illustrative purposes. For each animal, 3 non-adjacent sections were analysed and the areas summed to provide a single value representing the amount of APP visible. For the NMDA injected cords, representative images were obtained and captured using the same system.

5.2.4 Transmission electron microscopy

For the transmission electron microscopic (TEM) studies, animals were prepared as described and injected with vehicle (0.25μl), ET-1 (15pmol) or NMDA (20nmol) into the ventral horn of the spinal cord at the level of the 7th thoracic vertebra (See Chapter 2). Animals were anaesthetised with pentobarbitone 72 hours later and perfused with ~100ml of heparinised saline (5 IU.ml^{-1}) as described in Chapter 2. Following this,

animals were perfusion fixed using the same line with electron microscopy (EM) fixative (see Chapter 2).

The spinal cords were promptly dissected with minimal flexion, post-fixed for 48 hours and processed to produce resin embedded tissue blocks. The final blocks contained spinal cord material 5mm caudal to the microinjection site.

Coronal ultra-thin (90-150 nm) sections were cut using an ultra-microtome and mounted on grids. The ultra-thin sections were stained with uranyl-acetate and lead nitrate prior to imaging with an Hitachi H 7000 electron microscope at 3000x magnification. Selected fields were photographed and printed with 2x magnification resulting in a final magnification of 6000x. At least 12 non-overlapping fields were obtained for each tissue specimen.

The semi-thin sections (240nm) were taken onto glass slides and stained with toluidine blue, mounted in DePeX and cover-slipped (see Chapter 2). These sections were then examined using a light microscope to determine the macroscopic extent of white matter injury. Representative drawings indicating the areas of axonal injury were made and digital images were obtained using the computer and video camera system described in the above section.

5.2.5 Analysis of TEM images

The scoring system was generated by examining the photomicrographs and recording examples of myelinic and axonal disruption. The photomicrographs were scanned into a personal computer using an Epson Perfection 1250 scanner at full size, with a resolution of 300 pixels per inch (118.11 pixels per cm). A montage was created by copying the morphological examples for each score into a single new image at the same resolution and size. This scoring sheet was used as a reference during the analysis of the photomicrographs to ensure consistency (see Figure 5.2.5.1). Photomicrographs were analysed for axonal and myelin disruption using a scoring system based on morphological characteristics visible at the TEM level. For each animal 16 axons in each of 12 photomicrographs were given a score of 0, 1 or 2 for the condition of myelin, and a score of 0, 1 or 2 for the condition of the axoplasm. A score of 0 indicates the normal range of appearance, including fixation artefacts

present in non-injured tissue. A score of 2 indicates complete disruption, i.e. a complete absence of axoplasm, or for the myelin, vacuolation and splitting. The intermediate score of 1 was used to represent the range of morphologies that were clearly different to normal (i.e. non-0) but were not fully disrupted (i.e. non-2). This included axoplasm that had become dense and was undergoing degeneration, and myelin which was disrupted to some extent but not vacuolated.

A grid was marked onto an acetate sheet so that when overlayed onto a photomicrograph the picture was divided into a 5x5 grid, and a dot was placed at the intersection points that did not fall at the edges of the image (i.e. the central 4x4 points). This provided 16 points to analyse on each photomicrograph (see Figure 5.2.5.2). If there was no axon present under the dot or the axon had already been analysed, the next nearest axon was selected. The scores obtained for each treatment were normalised (score per axon) for analysis.

5.3 Results

5.3.1 APP is present in the white matter after ET-1

A qualitative assessment of the APP immunohistochemistry reveals axonal end bulbs and swollen axon cylinders in the lateral white matter from 24 hours after microinjection of ET-1 but not vehicle (Figure 5.3.1.1). At 6 hours after microinjection some evidence of APP accumulation was present in both the vehicle and ET-1 injected spinal cords. By 24 hours the amount of APP present in the ET-1 injected cords was much greater than that seen in the vehicle injected cords, but by 72 hours this was greatly reduced.

5.3.2 APP accumulation is visible up to 3 days after ET-1

Quantification of APP staining shows that although there is evidence of APP accumulation at 24 hours and 3 days after microinjection of ET-1, there is no significant APP staining at 7 or 21 days (Figure 5.3.2.1).

Figure 5.2.5.1 Examples of axonal injury scoring

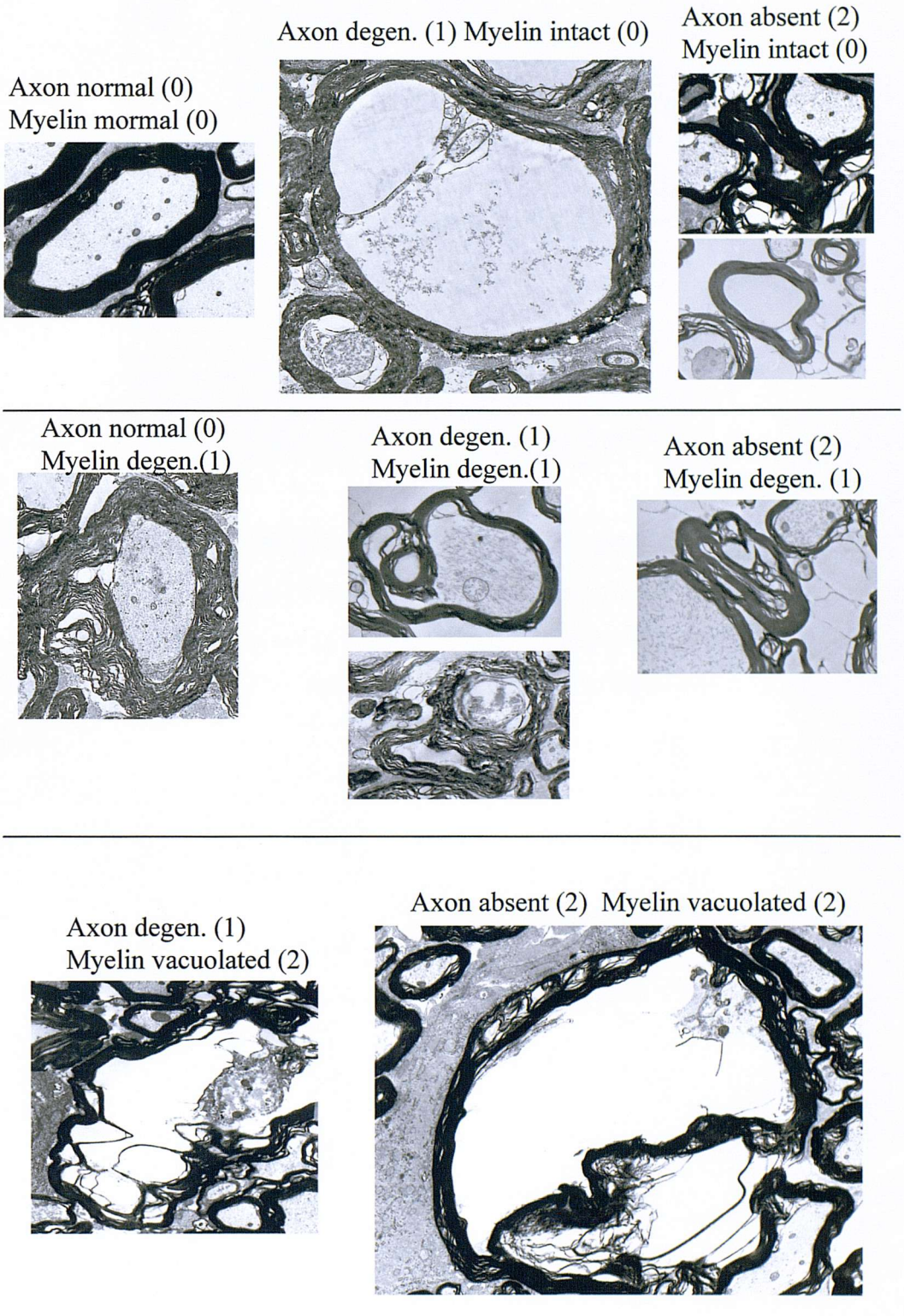

Examples images of degenerating axons, and their axoplasm injury and myelin injury scores. Key: Degen.=degeneration. All images shown at the same scale.

Figure 5.2.5.2 Scoring grid for TEM

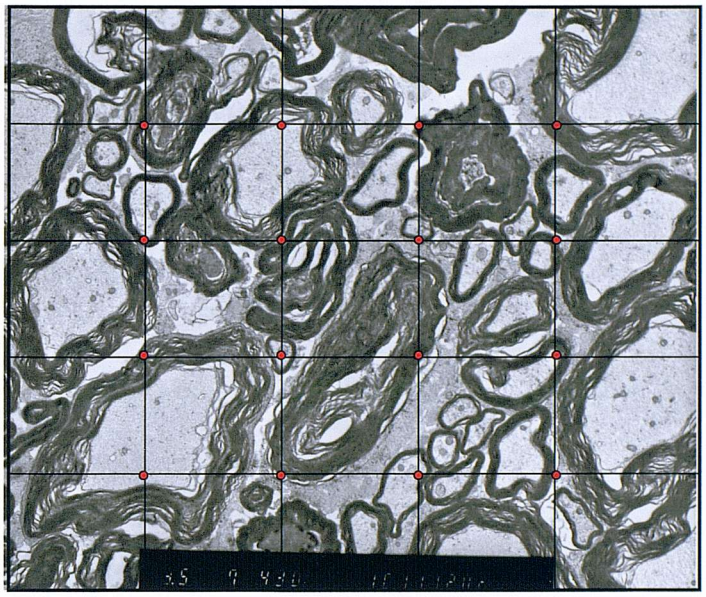

The grid was marked out on an acetate transparency, and aligned with the corners of each electron photomicrograph. The intersecting points at the centre of the grid (indicated by red dots) form a 4x4 grid of their own. Each axon (or next nearest if the axon had already been scored or was not present) was scored on two axes as described in the text.

Figure 5.3.1.1 APP is present in the lateral white matter after ET-1

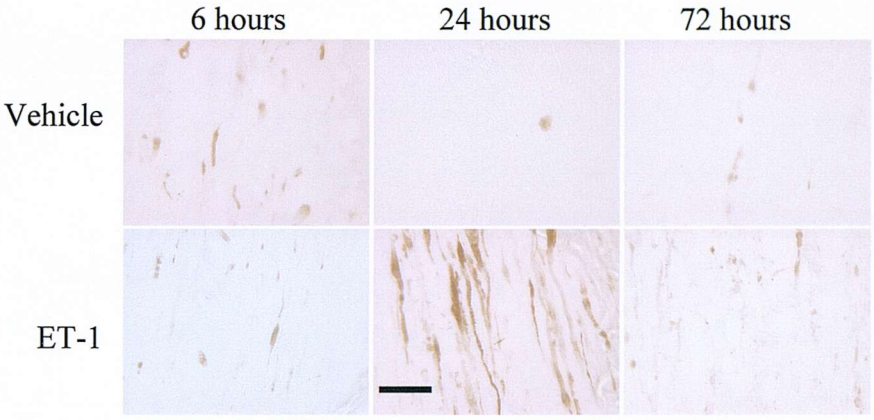

Representative images of APP immunohistochemistry in the spinal cord white matter 6, 34 and 72 hours after microinjection of vehicle (0.25ml) or ET-1 (15pmol) into the ventral grey matter of the spinal cord at T7. Scale bar = 50μm.

Figure 5.3.2.1 Graph of APP after ET-1 from 6h to 21d

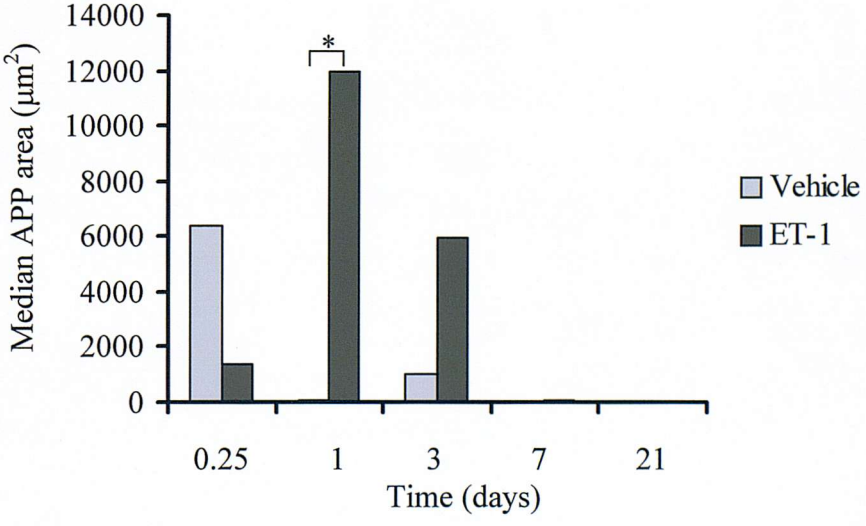

Area of APP present in the lateral white matter of the spinal cord after microinjection of vehicle (0.25μl) or ET-1 (15pmol). All groups n=3 except vehicle at 7 & 21 days, where n=1. *p<0.05 Mann-Whitney U-Test.

5.3.3 APP end-bulbs after NMDA

Microinjection of NMDA results in an excitotoxic lesion in the ventral grey matter (Figure 5.3.3.1), and the appearance of APP positive elements in the ventral white matter (Figure 5.3.3.2). Panels A-C of Figure 5.3.3.1 show the grey matter stained for macrophages after microinjection of vehicle (0.25μl) and NMDA (20nmol). In the vehicle injected grey matter (Panel A) the neuronal cell bodies are still clearly visible due to the haematoxylin counterstain. Following NMDA the neuronal cell bodies are absent or indistinct (Panel B), and ED-1 positive macrophages are appearing in the lesioned area at 24 hours, and are present in great numbers by 3 days (Panel C). Panel D shows some neutrophil recruitment has occurred at 24 hours, but this has declined by 3 days (not shown). In the white matter (Panel E), astrocytes have become activated and adopted a distinct morphology with thickened, highly GFAP positive cell bodies and processes (see Chapter 4).

There is evidence of APP accumulation in the white matter adjacent to the lesioned grey matter (Figure 5.3.3.2). In addition vacuolation of the white matter has occurred in the areas where APP positive axons and axon end bulb structures are located.

5.3.4 TEM studies

Microinjection of vehicle resulted in very little damage to the axoplasm or the myelin as assessed at 7h hours using the scoring system described above (Figure 5.3.4.1). Microinjection of ET-1 resulted in damage to both the axoplasm and the myelin sheath, although there was more axoplasmic injury present than was seen after microinjection of either NMDA or vehicle (Figure 5.3.4.1). Microinjection of NMDA also damaged the myelin sheath and the axoplasm, but there was more myelin injury than that observed after microinjection of either ET-1 or vehicle.

Figure 5.3.3.1 Microinjection of NMDA induces a lesion in the spinal cord

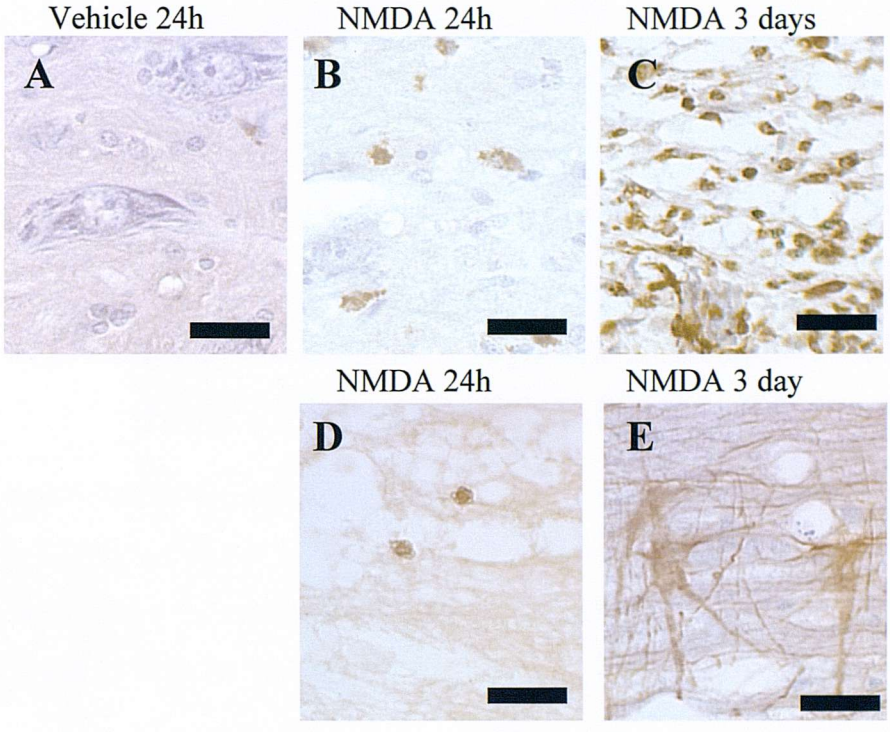

Representative images of the histopathology of an excitotoxic spinal cord lesion. Panels A-C shows immunohistochemistry for macrophages (ED-1) in haematoxylin counterstained sections 24h after microinjection of vehicle (0.25µl) (A), and 24h (B) and 3 days (C) after microinjection of NMDA (20nmol). Panel D shows immunohistochemistry for neutrophils (MBS-1) at 24 hours after microinjection of NMDA (20nmol), and Panel E astrocytes (GFAP) 3 days after microinjection of NMDA (20nmol). Scale bar =50µm.

Figure 5.3.3.2 APP is present in the lateral white matter after NMDA

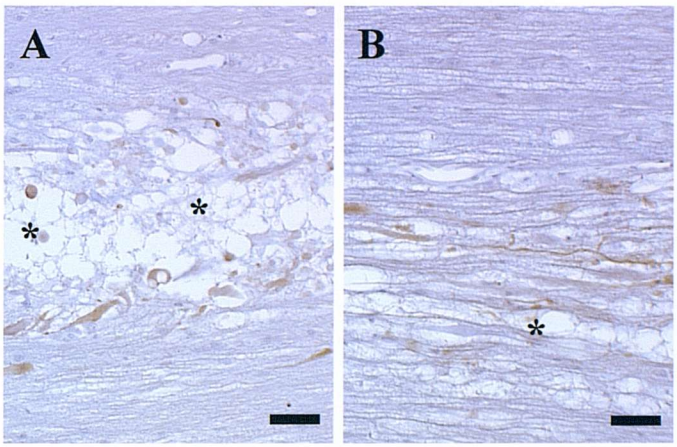

Representative images of APP immunohistochemistry in the ventral spinal cord at 24 hours (A) and 3 days (B) after micro-injection of NMDA (0.25µl, 20nmol). Sections are counterstained with haematoxylin. Areas of vacuolated white matter are indicated with an asterisk (*). Scale bar =50µm.

Figure 5.3.4.1 Myelin and axoplasm scores

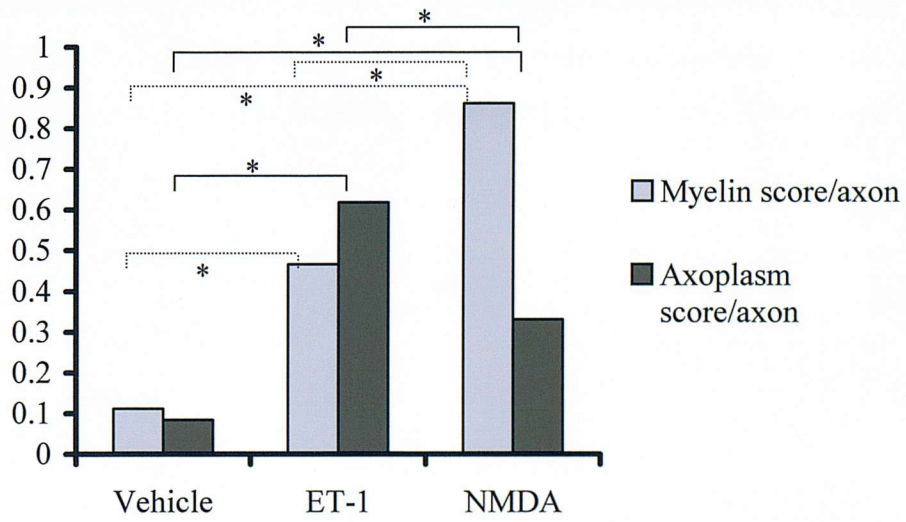

Normalised axon injury scores from ventral white matter 5mm caudal to microinjection site 3 days after microinjection of vehicle (0.25µl), ET-1 (15pmol) or NMDA (20nmol). *p=<0.05 Anova.

The frequency of zero scores for both myelin and axoplasmic injury is highest for the vehicle-injected cords (Figure 5.3.4.2A). In the ET-1 injected group very few axons have the highest score (2) for myelin injury but there are more scoring 2 for axoplasmic injury (Figure 5.3.4.2B). The reverse is true for axons in the NMDA injected cords, which score highly on the myelin injury axis but not the axoplasmic injury axis (Figure 5.3.4.2C).

Representative areas of white matter injury observed in the toluidine blue stained semi-thin sections were acquired at 100x magnification to observe myelin disruption (Figure 5.3.4.3A). Areas of frank axonal injury observed at the light microscope level in these sections were mapped onto a standardised diagram of the rat thoracic spinal cord (Figure 5.3.4.3B). The vehicle-injected cords have very little disruption, the NMDA injected cords have disruption confined to the ventral white matter ipsilateral to the microinjection site and the ET-1 injected cords have widespread bilateral injury to the white matter, particularly is areas adjacent to the grey matter.

In addition to the quantitative analysis of pathology, the photomicrographs were examined to identify features that may add to the understanding of the lesion. Figure 5.3.4.4 shows an image of a macrophage enclosed within a ring of intact myelin

Figure 5.3.4.2 Frequencies of scores

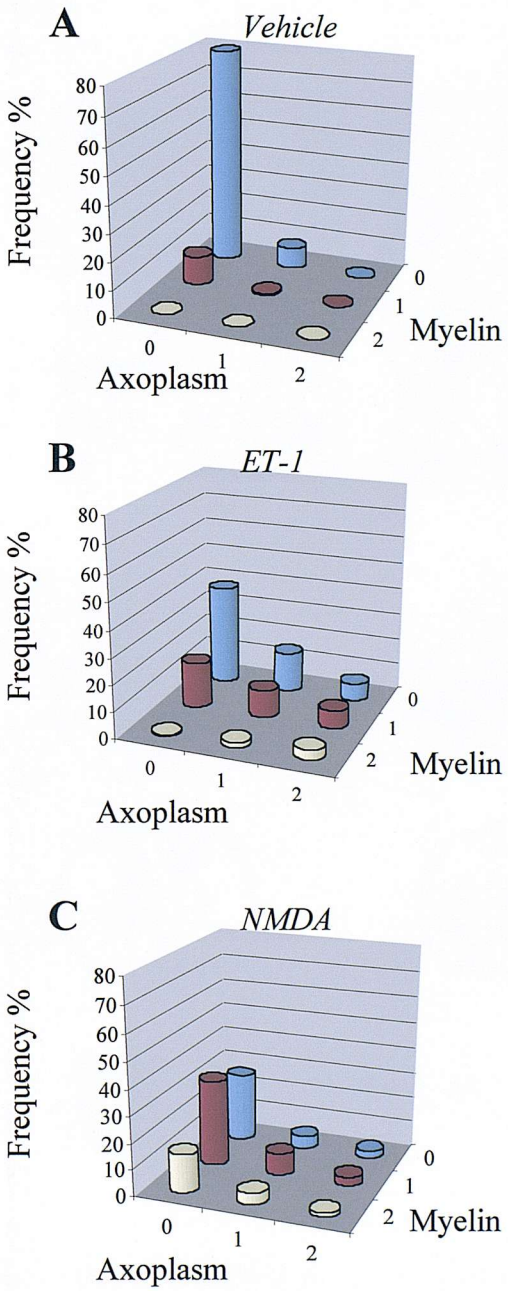

The associations between axoplasmic and myelin injury as assessed by analysis of electron photomicrographs of ventral white matter 5mm caudal to the microinjection site 3 days after microinjection of 0.25ml of vehicle (A), 15pmol ET-1 (B) or 20nmol NMDA (C). All groups n=3 rats. A total of 16 axons in each of 12 fields per animal were assessed using a scoring system, and assigned a score of 0,1 or 2 for the condition of the axoplasm and myelin. Values are expressed as a percentage of all axons scored for that treatment.

Figure 5.3.4.3 Macroscopic distribution of axonal injury

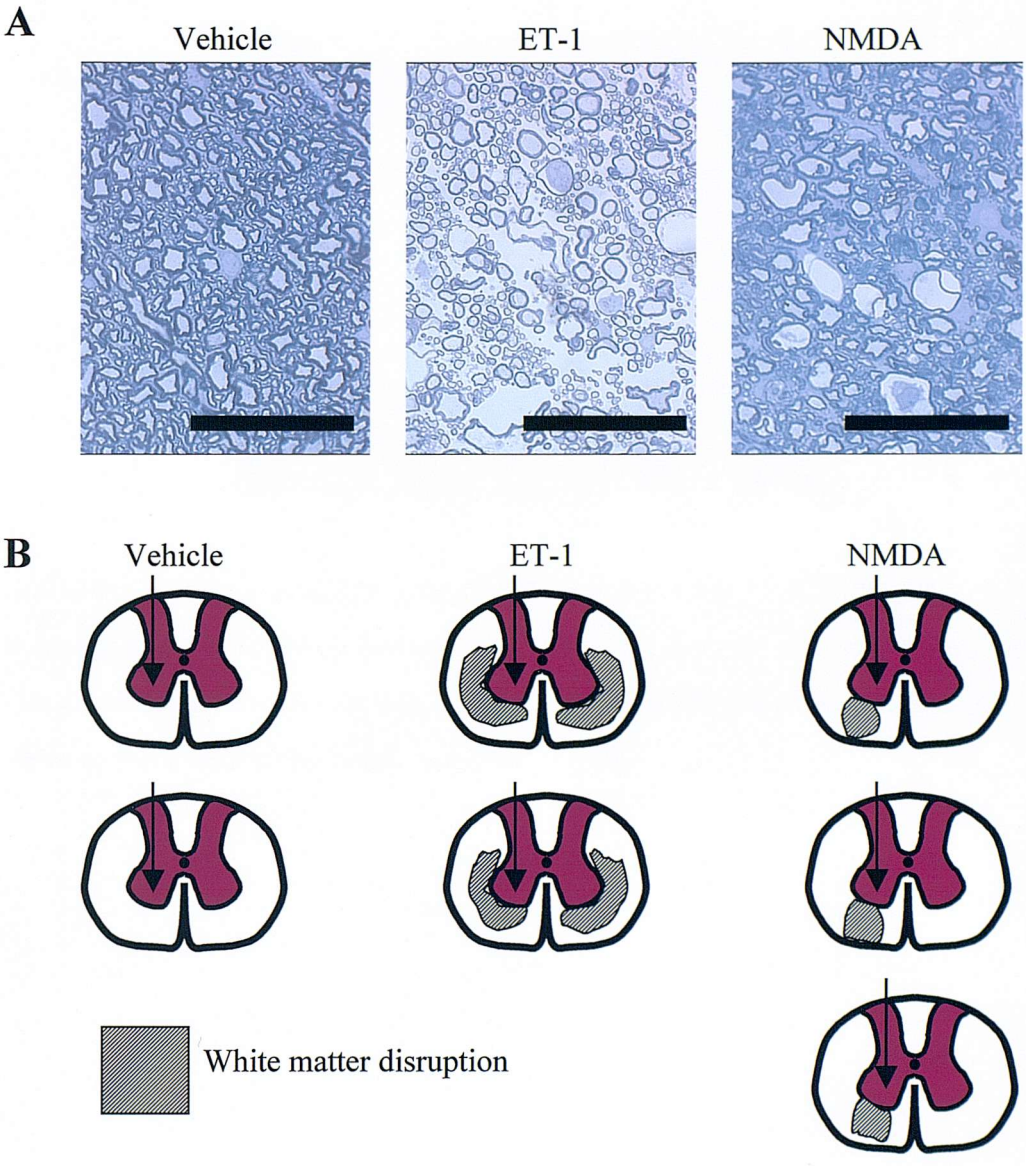

White matter disruption present in toluidine-blue stained semi-thin sections taken 5mm caudal to microinjection site at 3 days after microinjection of vehicle (0.25ml), ET-1 (15pmol) and NMDA (20nmol). Panel A shows representative images of the ventral white matter in these sections. Scale bar = 50μm. Panel B shows areas of frank white matter injury present in whole coronal sections mapped onto a schematic of the thoracic spinal cord. Black arrows indicate the microinjection site.

Figure 5.3.4.4 Macrophages can enter the lumen of a CNS axon

Electron photomicrograph of ventral white matter in the coronal plane 3 days after the microinjection of ET-1 (15pmol). The image was obtained from a block taken 5mm caudal to the microinjection site. A macrophage is present within the lumen of the axon in the centre of the field. Scale bar = 5μm.

5.4 Discussion

5.4.1 White matter after ischaemia

White matter pathology in the brain has been characterised following mid-cerebral artery occlusion (MCAO), and is known to include myelin disruption (Pantoni *et al.* 1996), and the appearance of amyloid precursor protein (APP) positive end bulbs (Yam *et al.* 1997). The ischaemia induced by MCAO also affects neuronal cell bodies, which makes interpretation of the white matter pathology more difficult. Experiments in the spinal cord have established that axon injury can occur independently of neuronal death (Kanellopoulos *et al.* 2000), and there is *in vitro* evidence that oligodendrocytes can be damaged by anoxia (Stys 1998). These results indicate that ischaemia alone is sufficient to induce white matter damage, and in particular lead to axonal injury. However it is not clear from these studies which mechanisms might be responsible for the pathology seen.

Ischaemia can result in an increase in extracellular glutamate (Rossi *et al.* 2000), mainly through the reversal of the glutamate transporters on neuronal cell bodies. This glutamate contributes to the toxicity of the ischaemic insult, resulting in an increasing likelihood of excitotoxic cell death. In ET-1-induced focal ischaemia of the spinal cord it is clear that there is a rapid necrosis of the grey matter, and pathology of the adjacent white matter. This is evident histologically from the appearance of APP filled end-bulbs, which are only visible under pathological conditions in the CNS (see below). In addition there is vacuolation of the white matter, which indicates areas where the white matter is under stress, and may reflect oedema, or the separation of the myelin from the axoplasm.

APP positive swollen axons and end-bulb structures appeared in the white matter within 6 hours of the microinjection of ET-1 or vehicle (Figure 5.3.1.1), indicating that there was an initial disruption in the axonal transport of APP. The continued movement of APP along the fast anterograde axon transport mechanism results in the formation of these end bulbs. Vesicles containing APP are carried along the microtubules away from the cell body by kynesin molecules, which are ATP dependent molecular motors. In locations where the axon has become transected, or ischaemia disables the molecular motors, the vesicles accumulate and the normally undetectable APP becomes visible by immunohistochemistry, revealing the end-bulb

structures. The appearance of APP end-bulbs in the vehicle injected animals at 6 hours is surprising, although not statistically significant, given the lack of trauma seen histologically (Chapter 4).

Maximal APP accumulation was seen at 24 hours, although there was still a significant amount of APP visible at 3 days. By 7 and 21 days after microinjection there was no appreciable amount of APP visible in the white matter, although rare APP positive axon profiles were still seen in the ET-1 injected cords at 21 days, indicating that axon injury may be an on-going process even at this time.

The laser Doppler technique has been used to assess the reduction of blood flow in the spinal cord following microinjection of ET-1 (Chapter 3). Blood flow is reduced by more than 80% within 15 minutes of administration, and remains below 50% for at least 1.5 hours. This represents a rapid and pronounced ischaemic insult, comparable to that seen in rodent models of stroke such as MCAO, where the onset of ischaemia is immediate. In a transection lesion model of spinal cord injury, where the ascending axons of the rat dorsal spinal columns are severed with a pair of fine iridectomy scissors, APP appears in end bulb structures within 6 hours of injury (data not shown). This implies that acute ischaemia can lead to as rapid an injury to the axons as a mechanical trauma, and that the interruption to normal axonal physiology may be severe following microinjection of ET-1.

5.4.2 Excitotoxicity

Given the appearance of white matter pathology, and the rapid destruction of the grey matter, it was of interest to determine whether the white matter pathology is the result of excitotoxic injury (due to the release of glutamate from the adjacent grey matter) or direct ischaemia of the white matter mediated by vasoconstriction of the penetrating vessels. In order to address this issue NMDA, a glutamatergic agonist (Watkins 1962), was microinjected into the ventral horn in the same manner as ET-1, and immunohistochemistry performed to examine the pathology generated. As would be expected, the microinjection of NMDA resulted in an area of neuronal loss in the grey matter within 24 hours (see Figure 5.3.3.1), which recruited few neutrophils and induced a macrophage response (Corkill D.J., W. Gomez-Leal & V.H. Perry 2003, manuscript in preparation). White matter pathology in the form of extensive

vacuolation and APP positive swollen axons and end bulbs was also visible by 24 hours after microinjection in the areas adjacent to the microinjection of NMDA (see Figure 5.3.3.2). Previous studies have used glutamatergic agonists such as NMA (N-methyl aspartate), kainic acid and quisqualic acid to induce an excitotoxic lesion in the cervical region of the dorsal spinal cord of the rat (Pisharodi and Nauta 1985). These authors report a loss of neurons in the grey matter associated with a loss of function in the ipsilateral forelimb, and a sparing of axons in the adjacent white matter as assessed by silver staining 2 weeks after injury. The apparent lack of axon injury could be due to the anatomical variation, given the large amount of grey matter present in the cervical enlargement where Pisharodi *et al* injected and the smaller grey matter area present at T7 where the microinjection was performed in these studies.

5.4.3 Electron microscopic analysis of WM damage

Having confirmed that excitotoxicity could injure the white matter directly, transmission electron microscopy (TEM) was used to examine the extent and nature of the white matter pathology at 3 days after microinjection of NMDA, ET-1 or vehicle. A wide variety of axonal and myelinic pathologies were observed following these treatments, and a scoring system that considered these two components separately was constructed (Figure 5.2.5.1). Axons ranged from being completely normal, with intact dense myelin and an axoplasm containing distinct neurofilaments and microtubules, to severely injured with a degenerating or absent axoplasm, and extensive disruption of the myelin. The relationship between myelin and axon injury was not straightforward in that some axons had completely normal myelin and yet no axoplasm, and others had a normal axoplasm and severely damaged myelin.

Some apparent axon and myelin disruption was seen in the vehicle treated spinal cords, and this suggests that there is background level of fixation artefacts (Figure 5.3.4.1). These can arise as a result of uneven perfusion of the tissue, which limits the amount of fixative entering the parenchyma. Insufficient fixation could then lead to some myelin splitting when the tissue is dehydrated and processed. As the concentric layers of myelin have not been bonded to each other Spurr resin can pass into the inter-lamella spaces to generate the artefact. In the ET-1 microinjected cords there is a statistically significant increase in the axoplasmic pathology compared to either the vehicle injected or NMDA injected spinal cords (Figure 5.3.4.1). The reverse was

seen for myelin pathology, in that the NMDA injected cords had a statistically significant increase in myelin scores compared to either the vehicle or ET-1 injected cords. This confirms that there is a difference in the white matter injury following an ischaemic or excitotoxic insult, and suggests that the injury seen following microinjection of ET-1 cannot be accounted for by an excitotoxic mechanism alone.

In order to see if there were any qualitative associations between the treatments and the pathologies described in the scoring system, an analysis of the frequency of each of the scores for each of the treatments was carried out (Figure 5.3.4.2). Chi-squared analysis of the frequencies of the scores shows that the treatment and axon pathology observed are not independent ($p<0.005$), indicating that the scoring system was able to detect differences between the treatment groups. In the vehicle injected specimens 80% of scores were zero for both axon and myelin injury. A minority of axons (<5%) scored a 1 for axonal and myelinic pathology. The remainder consisted of a score of 1 for either axon or myelin score, and no axons scored a 2 on either axis, indicating that there was very little axonal injury present.

Microinjection of ET-1 did not lead to the disruption of all axons (Figure 5.3.4.2). More than 35% of axons analysed in the ventral white matter exhibited no evidence of myelinic or axonal injury. A much larger proportion of axons scored a 1 for either axoplasmic or myelinic injury, or both, than in the vehicle-injected cords. There are a number of animals that scored 2 for axoplasmic injury and either a 0,1 or 2 for myelin injury. Fewer axons displayed evidence of severe myelin injury (score of 2) with moderate or absent axoplasmic injury.

It can be seen in Figure 5.3.4.2C that 25% of axons were spared from any injury following excitotoxic lesioning by the microinjection of NMDA. However it can be seen that there are very few axons with an axoplasmic score of 1 or 2, demonstrating that the axoplasm is relatively intact after excitotoxic lesioning. However a large proportion of axons analysed scored a 1 or a 2 for myelin injury. This shows that the axoplasmic injury was lower in the excitotoxic lesions relative to the ischaemic lesion.

In this study the sections were analysed in the coronal plane in order to visualise the ascending and descending axons in cross-section. The edges of the myelin at the

nodes of Ranvier possess cytoplasm and organelles, and they maintain the tight junctions essential for electrical insulation of the myelin. Depolarising glutamate from an ischaemic axon, under conditions where the oligodendrocyte myelin is also ischaemic, may lead to the entry of calcium and the breakdown of the cytoplasm. The resulting loss of tight junctions would allow extracellular fluid to enter the myelin, resulting in splitting and vacuolation. Glutamate release from the axon has been demonstrated in an ischaemic lesion (Li *et al.* 1999), and AMPA receptors located on myelin and oligodendrocytes (Li and Stys 2000) can be activated by this glutamate. The myelin injury observed in the electron photomicrographs, i.e. the splitting of the dense concentric layers of myelin and in extreme cases the vacuolation (see Figure 5.2.5.1 for examples), is likely to be caused by the separation of the myelin layers at the paranode.

Microinjection of the glutamatergic agonist NMDA resulted in more severe injury to the myelin than the ischaemic lesion (Figure 5.4.3.1). Excitotoxicity in the oligodendrocyte myelin resulting from over-activation of AMPA receptors is the likely cause of this damage. The ionotropic glutamate receptors are classified pharmacologically by the rank potency of various agonists (NMDA, AMPA and KA). However at high local concentrations the pharmacological specificity could be lost, allowing non-NMDA receptors to be activated by NMDA, or by glutamate released by the adjacent grey matter. The amount of NMDA microinjected in this study, 20nmol, was delivered in a small volume 0.25µl, and hence a high concentration was required (80nmol.µl^{-1} is equivalent to 80mmol.l^{-1}). This dose was selected as lower amounts failed to produce a significant grey matter lesion. The very high concentration of NMDA locally in the white matter may have overcome the relative selectivity of the AMPA receptors and activated them, leading to myelin injury.

Another explanation for the focal injury induced by microinjection of NMDA is direct damage due to acidity. Microinjection of the inactive enantiomer of NMDA, N-methyl-L-aspartate (NMLA) resulted in a smaller lesion (data not shown). Both NMDA and NMLA were dissolved in sterile saline and brought to physiological pH before storage at -20°C, and subsequently diluted in phosphate buffered saline before microinjection. This suggests that NMLA does have a weak agonist activity, or that

there is some component of the lesion that is due to the chemical properties of the solution.

5.4.4 Macroscopic features of white matter injury

Following microinjection of ET-1 there is a profound change in the structure of the white matter 5mm caudal to the injection site. The toluidine-blue stained semi-thin sections clearly show that the ventrolateral white matter is disrupted (Figure 5.3.4.3A). In the vehicle injected spinal cords there is no evidence of white matter disruption. Closer examination by light microscopy reveals that in the injured white matter of the ET-1 injected cords there is loss of glial cells and a number of myelin profiles are devoid of axoplasm. The axons in the vehicle-injected cords have a very different appearance, with dense compact myelin surrounding intact axoplasm. Microinjection of NMDA results in less injury to the glial cells, but evidence of myelin vacuolation is present. This is in agreement with the observations made on the electron photomicrographs from the same specimens.

The areas of white matter that were injured by the microinjection of ET-1 or NMDA were markedly different (Figure 5.3.4.3). Unilateral microinjection of ET-1 into the spinal cord induced bilateral axonal injury, which affected the ventral, ventrolateral and lateral regions of the spinal cord 5mm caudal to the injection site. This region of the cord is likely to contain axons belonging to the spinothalamic tract (STT), which passes through the ventrolateral white matter (Giesler *et al.* 1981). In contrast, microinjection of NMDA caused damage only ipsilateral to the injection site, and only in the ventral white matter. This could be due to differences in the mechanism of injury. In the ET-1 injected spinal cords a profound ischaemia over at least 3 segments was seen using laser Doppler blood flow measurement (Chapter 3) and the subsequent lesion is bilateral (Chapter 4). The excitotoxic lesion, because it relies on the diffusion of NMDA or released glutamate within the grey matter, behaves differently. Near the lesion centre there may be sufficient NMDA and released glutamate to diffuse from one ventral horn across to the other. As the lesion extends rostro-caudally the likelihood of released glutamate crossing to the opposite horn by diffusion reduces, in part as a result of the medial-ventral movement of extracellular fluid in the ventral horn.

5.4.5 Intra-axonal macrophages

In the CNS the resident macrophages, the microglia, can become activated by a number of mechanisms including complement receptor (CR3) activation to become phagocytic macrophages in response to tissue trauma and cell death (Kreutzberg 1996; Perry and Gordon 1997). It has been demonstrated (see Chapter 4) that following microinjection of ET-1 the microglia in the white matter change their morphology, the cellular processes retract and the cell body takes on a more rounded shape. By 3 days after ET-1 there is a significant macrophage response in the grey and white matter, although the number go on to increase in the white matter at 7 and 21 days. Given this, it would not have been unexpected to observe macrophages in the injured white matter, phagocytosing myelin and other debris.

The observation that there were macrophages enclosed within the myelin, in the space normally occupied by the axoplasm (Figure 5.3.4.4) was unexpected. The presence of macrophages within peripheral motor axons injured as a result of Guillain-Barré syndrome has been reported previously (Griffin *et al.* 1996). This is a potentially fatal acute disease often associated with prior infection with *Campylobacter jejuni*, which presents clinically with varying degrees of demyelination and axonal pathology. The stimulus for this macrophage response is an autoimmune reaction, as *C. jejuni* may possess some epitopes that cause antibodies to be raised which can target axonal proteins and initiate complement activation. Post-mortem dorsal root samples were obtained from individuals who had died from the disease, and these specimens were examined at the electron microscopic level. Griffin *et al* observed a lengthening of the node of Ranvier, and macrophages located close to the node in axons sectioned longitudinally. Macrophages could clearly be seen within the lumen of axons in cross-section. Given the prior association with the nodes of Ranvier it is likely that this is the site of macrophage entry into the axon.

The finding that macrophages can enter axons following an ischaemic CNS lesion is unusual, and requires further investigation. The distal segment of an axon transected as a result of mechanical, anoxic or inflammatory injury undergoes Wallerian degeneration (George and Griffin 1994), which is an active degenerative process (Coleman and Perry 2002). Following dorsal rhizotomy, axons that ascend in the dorsal columns and terminate in the gracile nucleus of the rat spinal cord degenerated

at a rate of 2.5-3.0mm.h^{-1} (George and Griffin 1994). In addition there was no overt macrophage response and axonal debris persisted in the white matter for at least 90 days. In the results presented earlier (Chapter 4) it was shown that following an ischaemic lesion induced by microinjection of ET-1 there was a profound macrophage response in the spinal cord at three days. The large numbers of active phagocytes in the lesion, and the presence of axonal debris may explain the observation of macrophages within the axonal lumen. However, this phenomenon was not reported following a focal inflammatory lesion of the brain induced by a non-CNS antigen (Matyszak *et al.* 1997), where demyelination and Wallerian degeneration of axons occurs and macrophages are present. Further investigation of the axonal degeneration and macrophage behaviour in these two settings may be needed to explain this difference.

5.4.6 Functional consequences of axonal injury

The immunohistochemical and electron microscopic data presented above describe a range of axonal pathologies that would be expected to have some functional consequences. In these studies no formal attempt was made to identify or measure locomotor performance, sensory loss or allodynia. Some animals did display a transient post-operative paraparesis, but no animals showed signs of post-operative pain or overt behavioural changes.

The ventro-lateral white matter in the thoracic spinal cord does not contain motor axons but does contain the spinothalamic tract (STT) (Giesler *et al.* 1981) which conveys pain and temperature information from the periphery to the thalamus. This pathway was identified by the injection of horse-radish peroxidase into the lateral thalamus, which results in the labelling of axons in the ventro-lateral white matter in the thoracic spinal cord (Giesler *et al.* 1981). The ventrolateral white matter in the thoracic spinal cord also contains other tracts, including descending projections from the raphe obscurus nucleus (Loewy 1981).

The white matter lesion generated by focal ischaemia of the ventral spinal cord results in a substantial degree of white matter axonal injury without inducing overt behavioural deficits. Existing models of spinal cord injury that rely on spinal cord contusion produce a more debilitating injury, and the animals often need intensive

intervention, for example the manual emptying of bowels and bladders, in order to survive. The use of focal spinal cord ischaemia therefore represents a useful alternative model in which white matter pathology can be assessed with a much-reduced impact on the welfare of the animal.

5.4.7 AMPA antagonists in SCI

It has been established that the spinal cord white matter contains non-NMDA receptors, namely the KA receptors on astrocytes, and the AMPA receptors on both oligodendrocytes and astrocytes (Agrawal and Fehlings 1997; Li and Stys 2000). The results presented above demonstrate that a focal ischaemic lesion in the spinal cord, or a focal excitotoxic lesion, can damage the myelin and result in axonal injury. AMPA-selective glutamatergic antagonists have been assessed in *in vitro* models of traumatic (Agrawal and Fehlings 1997) and ischaemic (Li *et al.* 1999) spinal cord injury. In these models the antagonists NBQX and GYKI52466 were shown to enhance the recovery of compound action potentials in compressed and anoxic white matter respectively. Further studies *in vivo* have shown improvements in behavioural and/or histological outcomes when the AMPA antagonist NBQX was administered systemically (Wrathall *et al.* 1996) or locally (Wrathall *et al.* 1997) following a mechanical contusion injury (weight drop at T8). A more detailed analysis of the white matter sparing effects of NBQX showed that treatment with the antagonist resulted in a high degree of protection for oligodendrocytes (Rosenberg *et al.* 1999). In a purely ischaemic model of SCI, where the aorta is occluded and the whole spinal column is rendered ischaemic, NBQX treatment reduced the number of axons lost and improved locomotor function (Kanellopoulos *et al.* 2000).

Clearly it would be of great interest to use an AMPA antagonist in the ET-1 microinjection model to see if the axoplasmic and myelin injury can be reduced. The prevention of some of the myelin damage could offer protection to axons, but it may also be important to consider the preservation of astrocytes.

5.5 Conclusion

Following microinjection of ET-1 or NMDA there is clearly a spectrum of white matter pathology in the ventral spinal cord. Focal ischaemia induced by microinjection of ET-1 results in the rapid appearance of APP positive end-bulb

structures, which are not associated with inflammatory cells. These structures are visible for at least three days in the ET-1 injected spinal cords but not the vehicle microinjected cords, which suggests that there is ongoing axonal injury over this period. Excitotoxicity also results in the appearance of APP positive axons, vacuolation and overt evidence of loss of structural integrity.

Detailed examination of the white matter three days after microinjection by electron microscopy reveals that there is a different pattern of white matter pathology in the two lesion types. The excitotoxic lesions are largely confined to the ipsilateral ventral white matter, whereas the ischaemic lesions have affected the ventral and ventrolateral white matter bilaterally. Ischaemia results in dramatic loss of axoplasm and some myelin injury, whereas excitotoxicity appears to spare the axoplasm but results in more substantial myelin injury. This is consistent with the literature, which suggests that axonal membranes do not contain any ionotropic glutamate receptors, but oligodendrocyte myelin and astrocytes do. The injury to myelin seen in the ischaemic lesion may be due to reversal of an axonal glutamate pump that reverses in ischaemia and releases glutamate into the microenvironment.

This model of focal ischaemia provides an important tool to further our understanding of the mechanisms of axon and myelin injury in ischaemic spinal cord injury. Using an experimental system which has had the mechanical component of injury eliminated will facilitate the investigation of new therapeutic strategies for spinal cord injury, including the use of AMPA antagonists.

Chapter 6 – Mechanisms of lesion development

6.1 Introduction

In Chapter 3 it was demonstrated that microinjection of ET-1 into the ventral grey matter of the spinal cord resulted in a significant reduction in blood flow over 3 spinal segments. This generated an ischaemic lesion and an acute inflammatory response involving neutrophil recruitment, blood-spinal cord barrier breakdown and macrophage recruitment as reported in Chapter 4. It was noted that although the volume of ET-1 injected into the spinal cord was small (0.25μl), the lesion extended symmetrically more than 10mm along the rostro-caudal axis, centred on the site of microinjection. No explanation of the underlying mechanisms responsible for these phenomena was offered. This chapter aims to explore these mechanisms further, as further understanding of the processes which generate the lesion following microinjection of ET-1 is essential when considering the effects of novel treatments and therapeutic strategies. In addition new insights into the pathological mechanisms involved in ischaemic spinal cord injury may be generated.

6.1.1 Diffusion of microinjected substances

Microinjection of a solution into a tissue will result in the diffusion of the solute into the extracellular fluid as Brownian motion of the liquid causes the solute to move. Although the microinjected volume will displace extracellular fluid in the immediate area around the capillary tip, the pressure of the injected liquid will be rapidly dissipated, and so movement of the solution is not a result of the injection pressure. The ability of a solute to move into the tissue down its concentration gradient will depend on a number of variables, including the volume of the extracellular space, the path length between two points (tortuosity) and the presence of non-specific uptake mechanisms (Sykova *et al.* 1994; Zoli *et al.* 1999). If the solute is a protein, then the size and charge of the protein will also affect diffusion through the extracellular space. Microinjection of solutions is performed slowly to allow equilibration of any pressure difference within the tissue that would lead to rupturing of the tissue and reflux of the solution along the injection track.

Fluorescent low molecular weight (3kD) dextran has been used previously to study the movement of solutes in the extracellular space of the striatum (Jansson *et al.* 1999).

Microinjection of a fluorescent dextran into the spinal cord will provide useful information concerning the limits of diffusion in this model, and determine if this can explain the size and rapid development of the lesion.

6.1.2 Induction and release of ET-1

Endothelin-1 is the most potent vasoconstricting substance known and was first identified in the supernatant of cultured aortic endothelial cells (Yanagisawa *et al.* 1988a; Yanagisawa *et al.* 1988b; Yanagisawa *et al.* 1988c). Endothelial cells possess ET_B receptors that mediate vasodilatation, and these cells are in close proximity to ET_A receptor bearing smooth muscle cells which contract in response to ET-1. These autocrine and paracrine mechanisms contribute to the maintenance of vascular tone and thus blood pressure homeostasis.

The endothelin system is also involved in the tissue response to injury. Vascular endothelial cells contain secretory granules called Weibel-Palade bodies (WPB), which are filled with the pro-coagulant protein Von-Willebrand Factor (VWF). In addition to VWF these granules also contain the chemokine IL-8, the adhesion molecule P-selectin and the vasoconstricting peptide ET-1 (van Mourik *et al.* 2002). This ET-1 mediated vasoconstriction plays a major role in stopping blood loss from injured vessels.

A further mechanism by which ET-1 may become involved is by the induction of ET-1 gene expression during hypoxia. It has been demonstrated that ET-1 is under the control of the hypoxia inducible factor-1 (HIF-1) (Yamashita *et al.* 2001) in endothelial cells. Within the CNS another source of ET-1 during ischaemia (Pluta *et al.* 1997) or injury (Petrov *et al.* 2002) are the astrocytes. The up-regulation of the endothelin-1 gene results in the increased expression of the ET-1 precursor molecule big-ET-1, which is in turn cleaved by proteases and the specific endothelin converting enzymes (ECEs).

This would suggest that within an ischaemic lesion in the CNS there may be both release of ET-1 by WPBs in endothelial cells, and increased synthesis of ET-1 by astrocytes and endothelial cells. These sources of ET-1 may be contributing to the development of the lesion. As areas of the grey matter become ischaemic the

synthesis and release of ET-1 into neighbouring areas may result in further vasoconstriction and ischaemia. The spread of the grey matter lesion is limited by the white matter laterally and ventrally, and by the vascular architecture, which in the medial and dorsal parts of the cord is supplied by the dorsal spinal arteries. This results in the rostro-caudal elongation of the lesion.

It may be possible to determine if local synthesis and release of these peptides is contributing to the lesion expansion by measuring the amount of ET-1 or big-ET-1 present in the spinal cord during the developing lesion using commercially available ELISA kits. Exogenous ET-1 introduced into the spinal cord to induce a lesion would be detected by these assays. The non-selective endothelin receptor agonist sarafotoxin-6b (S6b), is a potent vasoconstricting toxin originally identified in the venom of the mole viper *Atractaspis engaddensis*. Although it has a high potency at the ET_A receptor (Devadason and Henry 1997) and it is a peptide, it does not have sufficient structural homology to cross-react with certain antibodies raised against ET-1. Microinjection of S6b results in a profound reduction in spinal cord blood flow within minutes of administration (Chapter 3). This combination of ischaemic potency and lack of cross reactivity makes it highly suitable for use in these studies where early events in the developing ischaemic lesion are examined.

Immunohistochemistry for ET-1 may also enable the qualitative description of the temporal and spatial distribution of ET-1 within the ischaemic lesion. The pharmacological properties of S6b are not identical to ET-1 with respect to clearance and receptor occupancy. ET-1 is cleared by the ET_B receptor, which internalises after binding ET-1, whereas S6b dissociates from ET receptors and can therefore activate more receptors (Devadason and Henry 1997). This makes using S6b to study later events more difficult, as it persists and does not mimic the activity of ET-1. For this reason microinjection of ET-1 is more suitable to generate lesions for examination by immunohistochemistry.

By measuring ET-1 or the precursor molecule big-ET-1 within an acutely ischaemic lesion and then examining the cellular distribution of ET-1 in the hours and days following, it may be possible to explore the hypotheses that ET-1 plays a role in both

the immediate generation of the lesion and the secondary events such as gliosis and neovascularisation.

6.2 Methodology

6.2.1 Microinjection of fluorescent low molecular dextran

Male Wistar rats were anaesthetised with Hypnorm/Hypnovel and microinjection into the ventral grey matter of the spinal cord at the level of the 7th thoracic vertebra was performed as described in Chapter 2. The fluorescent marker used was a soluble fluorescein conjugated 3kD dextran (D-3306, Molecular Probes) which is anionic and lysine fixable, and is comparable in size to ET-1 which has a molecular weight of 2492. This was co-injected in a total volume of 0.25µl with either vehicle (sterile saline) or ET-1 (15pmol) so that each injection delivered 0.125µg of the dextran. At 3 hours after microinjection the animals received terminal anaesthesia (sodium pentobarbitone (Sagatal) 100mg/rat i.p.), were perfused with heparinised saline (5 IU.ml^{-1}) and then perfusion fixed with 4% paraformaldehyde solution. The spinal cords were removed and post-fixed for a further 6 hours before being cryoprotected (see Chapter 2). A 2-3cm length of spinal cord centred on the microinjection site was embedded in OCT medium and 20µm longitudinal sections were cut onto gelatinised glass slides using a microtome. Some sections were counterstained with a 10µg.ml^{-1} solution of 4,6-diamidino-2-phenylindole dihydrochloride (DAPI) in PBS, which is a dye that fluoresces when bound to DNA, enabling the visualisation of nuclei.

The fluorescein-dextran and DAPI staining were visualised with an argon laser confocal microscope (Enterprise). Images of the spinal cord were obtained at low power to show the extent of dextran diffusion from the microinjection site.

6.2.2 ELISA measurement of ET-1 and big ET-1

Male Wistar rats were anaesthetised with Hypnorm/Hypnovel and prepared for microinjection into the ventral grey matter of the spinal cord at the level of the 7th thoracic vertebra as described in Chapter 2. Microinjection of 0.25µl of vehicle (sterile saline) or 15pmol of sarafotoxin 6b (S6b) was performed as described earlier for recovery surgery. S6b has a molecular weight of 2564, which is very similar to ET-1, which has a molecular weight of 2492. At 1 hour after microinjection the

animals received terminal anaesthesia (sodium pentobarbitone (Sagatal) 100mg/rat i.p.) and were then perfused with heparinised saline (5 $IU.ml^{-1}$). The spinal cord was removed and a 1cm section centred on the microinjection site was isolated and prepared for ET-1 and big-ET-1 extraction as directed by the ELISA kit protocol (described in Chapter 2). Briefly, the tissue was homogenised and the supernatant passed over a solid phase extraction column (C18 Sep-Pak Plus, Waters UK) to retain the small hydrophobic peptides. These were then eluted off the column using acetonitrile, and the samples dried down overnight in a vacuum centrifuge (Univap). A new column was used to extract the peptides for each of the supernatant samples.

The ET-1 or big ET-1 content of each of the spinal cords was then assayed using commercially available ELISA kits (IBL Hamburg, Germany) as described in Chapter 2. The samples were reconstituted in assay buffer and applied to a 96-well plate pre-coated with a rabbit anti-rat ET-1 or big-ET-1 polyclonal antibody to capture the peptide of interest. The presence of bound peptide was measured using a secondary anti-ET-1 antibody conjugated to horseradish peroxidase. When a chromogenic substrate was added to the wells the amount of colour (measured as absorbance) generated by the bound enzyme conjugate was proportional to the concentration of ET-1 or big ET-1 present in the samples. A standard curve was generated as directed by the manufacturer to enable the concentration of peptide to be determined. The efficiency of the extraction procedure was investigated by placing a known amount of ET-1 or big-ET-1 into a homogenate of naïve spinal cord and then performing the extraction procedure as described above.

6.2.3 Immunohistochemistry for ET-1

Male Wistar rats were anaesthetised with Hypnorm/Hypnovel and prepared for microinjection into the ventral grey matter of the spinal cord at the level of the 7^{th} thoracic vertebra as described in Chapter 2. Microinjection of 0.25µl of vehicle (sterile saline) or 15pmol of ET-1 (15pmol) was performed as described earlier for recovery surgery. At specific times after microinjection, ranging from 6 hours to 21 days after microinjection, the animals received terminal anaesthesia (sodium pentobarbitone (Sagatal) 100mg/rat i.p.) and were perfused with heparinised saline (5 $IU.ml^{-1}$) followed by Bouins fixative (see Chapter 2). The spinal cords were dissected

and post-fixed in Bouins fixative for 1 week, and then processed to wax (see Chapter 2). Sections (10μm) were cut using a benchtop microtome and mounted on electrostatically charged slides (Superfrost Plus, BDH), and stored at room temperature until use.

The standard immunohistochemistry protocol described in Chapter 2 was used, and is summarised below with specific details of the anti-ET-1 antibody. The sections were dewaxed in xylene and rehydrated before endogenous peroxidase was quenched using methanol and hydrogen peroxide. A wax pen (ImmEdge, Vector) was used to outline the sections before the microwave citrate buffer antigen retrieval step was performed. After blocking with 10% normal goat serum in PBS, the primary antibody, a polyclonal rabbit anti-rat ET-1 (IHC6901, Peninsula Laboratories) was applied to the sections at a dilution of 1:2000. After 2 hours at room temperature the primary antibody was washed off and a secondary antibody, biotinylated goat anti-rabbit IgG (Vector Labs, UK) was added to the sections. Visualisation of the bound primary antibody was achieved by using an HRP conjugated avidin biotin complex, which was added to the sections after washing off unbound secondary antibody, followed by DAB substrate which results in a brown precipitate in areas of primary antibody labelling. Sections of naïve spinal cord, from animals which had not undergone the microinjection protocol, were also examined using IHC6901 to determine the normal distribution of ET-1 visible by this technique. Some sections were counterstained with haematoxylin to enable visualisation of cell types and tissue structures.

In addition to IHC6901 staining for ET-1, in some adjacent sections astrocytes were identified using a rabbit anti-cow glial fibrillary associated protein (GFAP) as described in Chapter 2. The specificity of IHC6901 for ET-1 was examined by pre-absorbing the primary antibody with ET-1 or big ET-1 in 1% bovine serum albumin (BSA) for 2 hours prior to application onto the sections.

All sections were dehydrated through a series of ethanol solutions and xylene, mounted with DePeX and coverslipped. A qualitative assessment of the presence and distribution of ET-1 was made by examining each section and noting the cellular location of positive staining. Representative images were obtained using a personal

computer based image acquisition and analysis system (Qwin, Leica UK). Images were obtained of the naïve tissue IHC6901 staining, the pre-absorbed primary antibody staining and the GFAP stained adjacent sections using the same system.

6.3 Results

6.3.1 Movement of low molecular weight dextran within the spinal cord

Microinjection of the low molecular weight dextran alone into the ventral grey matter at T7 resulted in the presence of fluorescent signal over several millimetres from the injection site by 3 hours (Figure 6.3.1.1A). Co-injection of ET-1 (15pmol) with the dextran resulted in a reduced area of spread (Figure 6.3.1.1B). The grey matter of the spinal cord appears narrower in the ET-1 injected spinal cord (Figure 6.3.1.1D) than in the vehicle injected cord (Figure 6.3.1.1C).

6.3.2 ET-1 and Big-ET-1 in the spinal cord 1 hour after microinjection of S6b

One hour after microinjection of vehicle into the ventral grey matter of the spinal cord a very small amount of ET-1 (~3pg.ml^{-1}) was detectable in 2/3 spinal cord samples using a specific ELISA assay. Microinjection of S6b reduced the amount of ET-1 peptide to below the limit of detection in all 3 spinal cords. Big-ET-1 remained at the limits of detection in all spinal cord samples taken at 1 hour following microinjection of S6b or vehicle. The recovery of ET-1 and big-ET-1 from spiked spinal cord homogenates was 0.3% and 0.6% respectively.

6.3.3 Specificity of IHC6901 for ET-1 is confirmed

Immunohistochemistry was performed on adjacent 10μm Bouins fixed spinal cord sections from animals that had been microinjected with ET-1 (15pmol) into the ventral grey matter 72 hours before perfusion. The IHC6901 antibody was co-incubated at room temperature for 2 hours with either 1% BSA alone (control), ET-1 in 1% BSA or big-ET-1 in 1% BSA. This step removed free anti-ET-1 or anti-big-ET-1 antibodies from the polyclonal antibody solution in order to confirm that the observed staining was specific to these peptides. The distinct pattern of cellular staining seen in the control section was reduced when the IHC6901 antibody was pre-absorbed with big-ET-1 (Figure 6.3.3.1). Pre-absorption with ET-1 resulted in a complete loss of cellular staining in the section.

Figure 6.3.1.1 Movement of dextran within the spinal cord

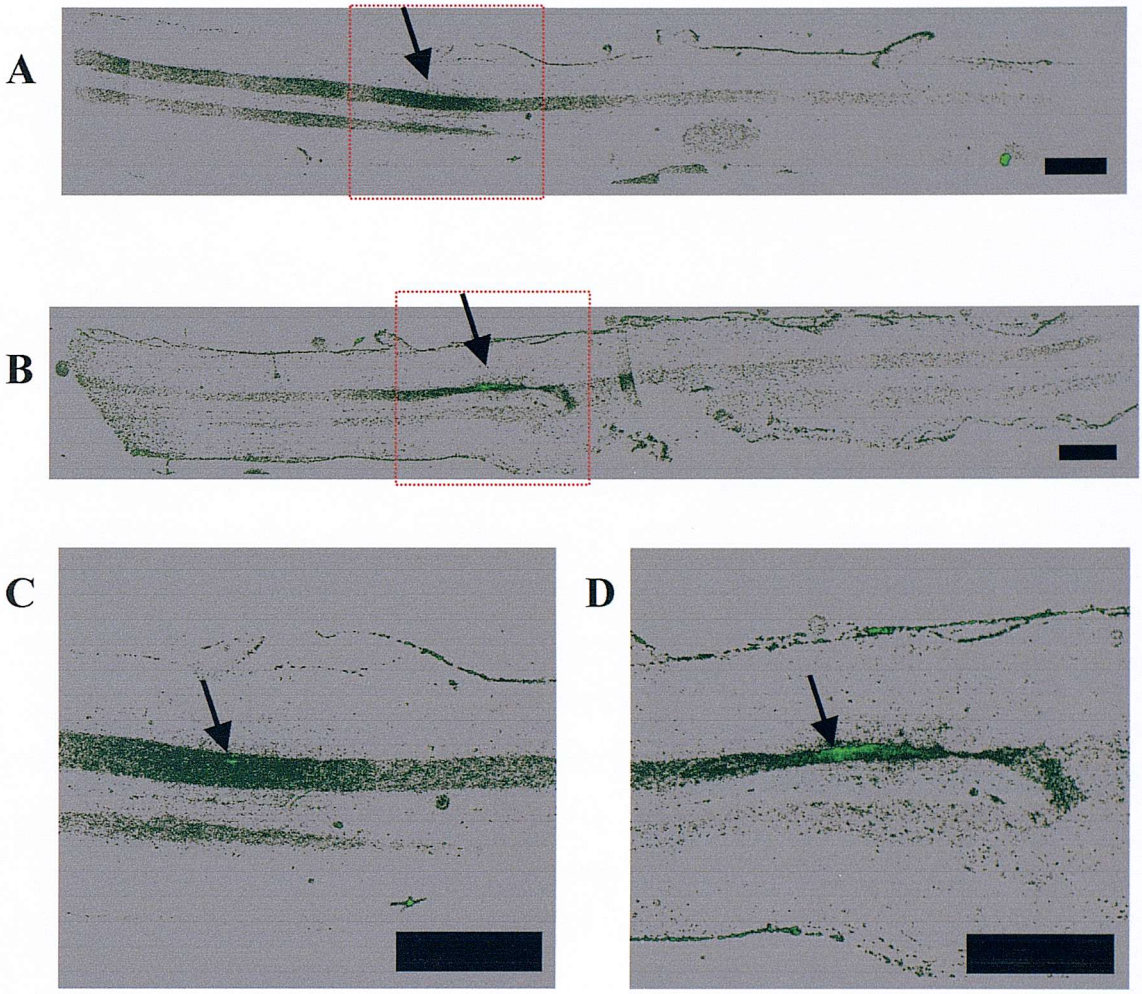

Reconstructed confocal microscope images of the rat spinal cord in longitudinal section following microinjection of fluorescein conjugated 3kD dextran with vehicle (Panel A) or ET-1 (15pmol) (Panel B). False colour has been used to show the fluorescein as green and the background as grey. Black arrows indicate the microinjection site. Panels C and D are enlargements of the microinjection site (area shown bounded by the red dashed line on panels A and B). The sections are oriented with the caudal direction to the right. Scale bar=1000μm.

Figure 6.3.3.1 Specificity of IHC6901 for ET-1 is confirmed by absorption

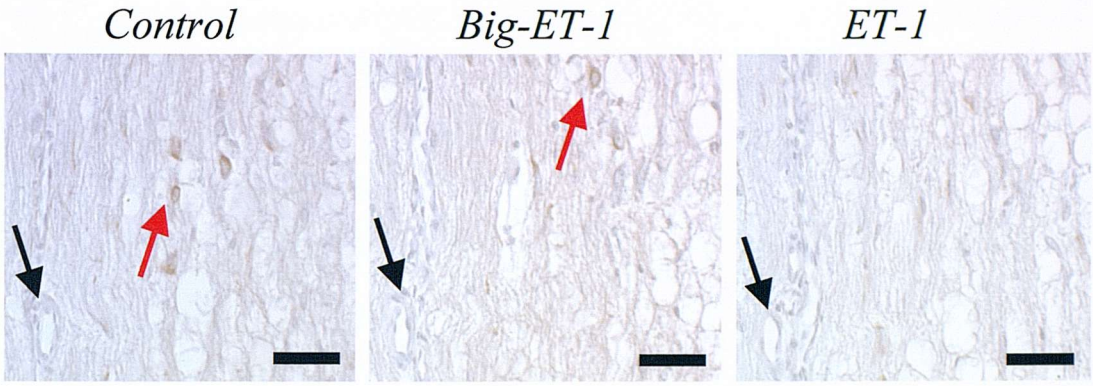

Representative sections from a set of adjacent 10μm sections which had been used to confirm the specificity of the primary antibody IHC6901. The first panel shows the pattern of DAB staining present when the primary antibody was co-incubated with 1% BSA in PBS. The middle panel is an adjacent section using the antibody under identical conditions, with the exception that big-ET-1 was present in the 1% BSA solution. The right hand panel is the next adjacent section, and the IHC6901 antibody had been co-incubated with ET-1 in 1% BSA. The red arrows indicate cellular staining with IHC6901. The black arrow indicates a blood vessel that was used as morphological landmark as it was present in all sections. Scale bar =25μm.

6.3.4 ET-1 is present in cells of the central canal in the naïve spinal cord

The presence of ET-1 in the naïve spinal cord was examined using the IHC6901 antibody on coronal sections of naïve spinal cord (Figure 6.3.4.1). Control sections, which were subject to the complete immunohistochemistry procedure with the exception that no primary antibody was applied, showed no evidence of DAB staining. Using the IHC6901 primary antibody revealed a distinct pattern of cellular staining in the central canal (Figure 6.3.4.1, central panel). Astrocytes, identified with GFAP immunohistochemistry, did not co-localise with the IHC6901 staining.

6.3.5 ET-1 is present in endothelial cells and glia following ischaemia

Immunohistochemistry using IHC6901 revealed a distinct temporal and spatial pattern of staining following the microinjection of ET-1 (15pmol) or vehicle (0.25µl) into the ventral spinal cord (Figure 6.3.5.1). At 6 and 24 hours after microinjection of ET-1 into the spinal cord ventral grey matter, some microvessels of the ventral grey matter within the lesion are positive for ET-1 (Figure 6.3.5.1A). ET-1 is also detectable in astrocytes, both in the intact grey matter and the lateral white matter. Panel B shows a representative section of lateral white matter stained with GFAP for astrocytes and an adjacent section stained for ET-1 with ICH6901 (Figure 6.3.5.1B). The pattern of staining is similar in both sections suggesting that the ET-1 staining is present on astrocytes.

The distribution of ET-1 detected by immunohistochemistry varied depending on both the time post microinjection and whether vehicle or ET-1 was injected. All the sections stained as described in the previous section were examined using a microscope to enable qualitative assessment of the histology. The results of this assessment are shown in Table 6.3.5.2.

Figure 6.3.4.1 Location of ET-1 in the naïve spinal cord

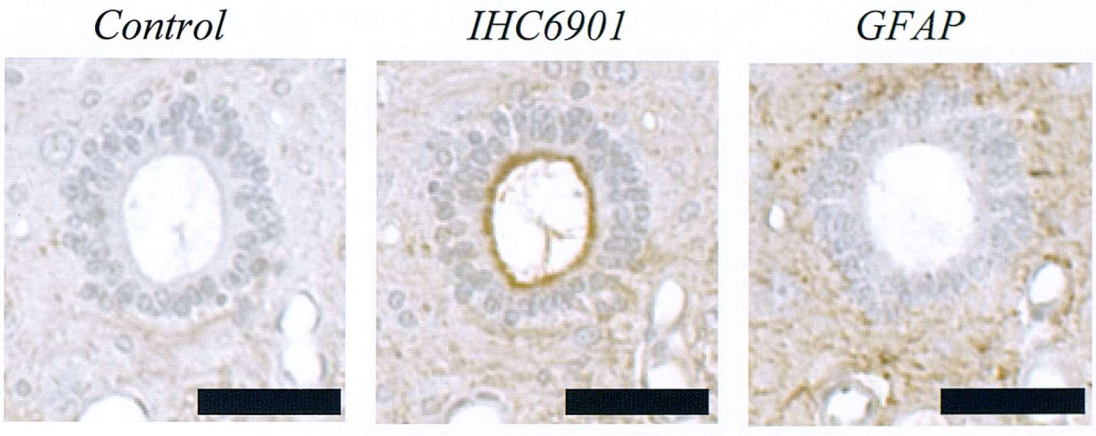

Representative images of immunohistochemistry performed on coronal sections of naïve rat spinal cord. The leftmost panel shows a control section with no primary antibody, the middle panel shows IHC6901 staining for ET-1, and the rightmost panel is GFAP staining for astrocytes. All sections were counterstained with haematoxylin. Scale bar=25μm.

Figure 6.3.5.1 Location of ET-1 in the spinal cord following ischaemia

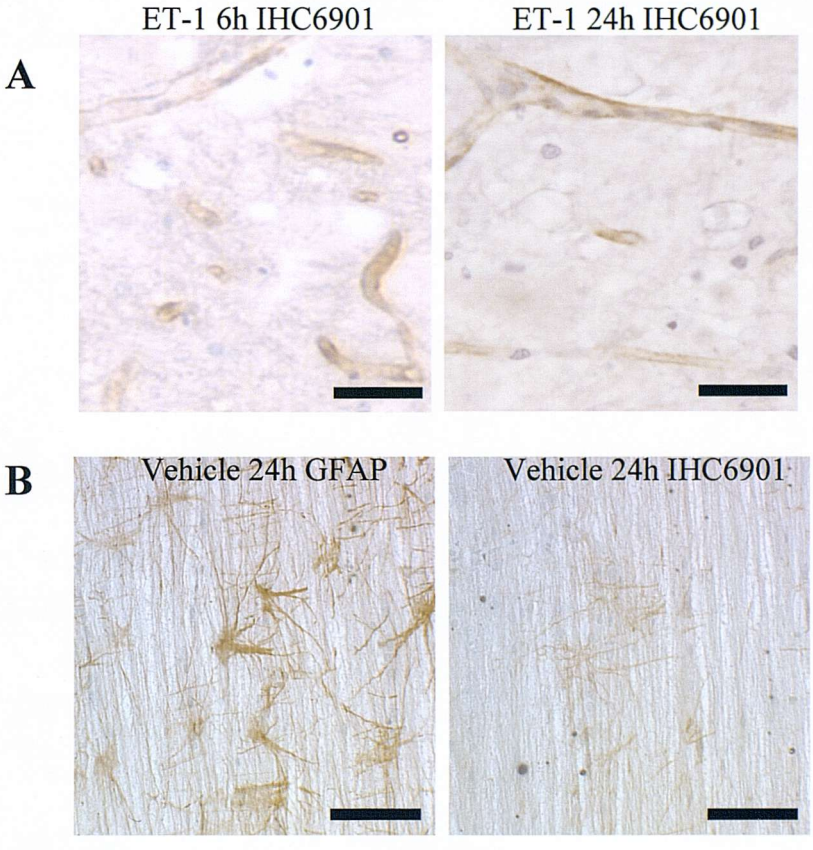

Representative images of immunohistochemistry performed using the IHC6901 anti-ET-1 primary antibody. Panel A shows the positive staining using IHC6901 in the microvasculature within the lesion at 6 hours and 24 hours after microinjection of ET-1 (15pmol) into the ventral grey matter at T7. Panel B shows the typical pattern of GFAP staining for astrocytes in the lateral white matter 24 hours after microinjection of vehicle (0.25µl), and in an adjacent section the staining for IHC6901. All scale bars=25µm.

Table 6.3.5.2 Summary of ET-1 immunohistochemistry results

	Vehicle			ET-1		
Time	*GM Astrocytes*	*GM Vessels*	*WM Astrocytes*	*GM Astrocytes*	*GM Vessels*	*WM Astrocytes*
6h	Few astro processes caudal to injection (2/3) Few astrocytes (1/3)	No signal (3/3)	Light signal (3/3)	Few spots (1/3)	In lesion (2/3)	Light signal (3/3)
24h	Few processes (1/3)	In gm (2/3)	Light signal (3/3)	No signal (3/3)	In lesion (3/3)	Light signal (3/3)
3d	Processes (1/3)	No signal (3/3)	Light signal (3/3)	Processes in GM tissue adjacent to lesion (1/3)	In lesion (3/3)	Light signal (3/3)
7d	No signal (1/1)	No signal (1/1)	Light signal (1/1)	No signal (3/3)	Occasional lesion (3/3)	Light signal (3/3)
21d	Rare processes (1/1)	No signal (1/1)	Light signal (1/1)	Processes in intact GM tissue (2/3)	No signal (3/3)	Light signal (3/3)
Naive	No signal (1/1)	No signal (1/1)	Light signal (1/1)			

The above table summarises the observations made on the immunohistochemistry performed with IHC6901 for ET-1. For each section the presence of staining in grey matter astrocytes (*GM astrocytes* on the table), grey matter vessels (*GM vessels* on the table) and the white matter astrocytes (*WM astrocytes* on the table) was noted. The number of animals in which the described staining was observed is recorded in parentheses in each case. All treatment groups were n=3 except for the naïve, and the 7 and 21 day vehicle groups which are n=1.

6.4 Discussion

6.4.1 Movement of microinjected substances in the spinal cord

The movement of small molecules through the extracellular space (ECS) in the CNS parenchyma has been studied previously by injecting tetramethyl ammonium (TMA) into the rat striatum (Jansson *et al.* 1999) or spinal cord (Sykova *et al.* 1994). Three parameters, the extracellular space fraction (α), tortuosity (λ) and non-specific uptake (k') can be used to describe the features of the extracellular environment which govern the ability of a molecule to move in the ECS. The extracellular space fraction (α) expresses the actual volume in which the molecule can move within, whereas tortuosity (λ) is a measure of the path length a molecule would need to travel between two points. Non-specific uptake (k') accounts for the movement of the molecule out into the vasculature or uptake by cells. These three parameters can be measured following the microinjection of TMA into the CNS parenchyma by using an ion selective electrode that will return a voltage proportional to the concentration of TMA in the vicinity of the electrode tip.

Iontophorectic application of TMA into the striatum resulted in a spherical diffusion pattern, and by 10 minutes after injection TMA was measurable in a sphere of radius 1.5mm centred on the injection site (Jansson *et al.* 1999). Although the movement of TMA in the striatum was visualised as a sphere, this is not absolutely correct, as the presence of white matter fascicles through the tissue leads to uneven diffusion, or anisotropy, as movement is more restricted in some directions. The derived values of α, λ an k' were very similar to those obtained in an experiment in the rat spinal cord (Sykova *et al.* 1994) using the same technique. This would suggest that in the spinal cord the movement of TMA would follow the same kinetics, and therefore diffusion 1-2mm from the injection site would be predicted within 10 minutes. Given the structure of the spinal cord, anisotropic diffusion is likely to occur which may aid rostro-caudal diffusion.

Although TMA can be used to define the mathematical properties of the ECS, it is small (it has a molecular weight of 77D) and diffuses rapidly and cannot be used to compare the spread of larger molecules over longer periods of time. Biotinylated dextrans have been used to investigate the movement of substances in the ECS of the

striatum (Jansson *et al.* 1999). The dextrans used in these studies have a small molecular weight (3kD), which allows them to move freely in the ECS, and the biotin conjugation permits the visualisation of the distribution using immunohistochemical techniques. Jansson *et al* found that the diffusion of biotinylated dextrans is concentration-dependent, and the volume of distribution increases to $66mm^3$ at 2 hours after the microinjection of 0.1µl of a $30\mu g.ml^{-1}$ solution. If this was a perfect sphere it would have a radius of 2.5mm.

In the fluorescein conjugated dextran experiments reported in the previous section, the microinjection of 0.25µl of dextran solution resulted in a visible spread through the grey matter of the ventral spinal cord (Figure 6.3.1.1A). This appeared to have spread 2-3mm in both the rostral and caudal directions. Co-injection of ET-1 (15pmol) with the same dextran solution resulted in a markedly different distribution (Figure 6.3.1.1B). There appears to be a much higher signal in the microinjection site and subsequently less diffusion rostrally and caudally. Another interesting observation is that the grey matter appears to have reduced in width. This could be evidence of the potent vasoconstriction induced by ET-1, causing the shortening of blood vessels by the constriction of the smooth muscle cells. Microinjection of ET-1 into the ventral grey matter of the spinal cord causes a potent reduction in blood flow over at least 1 hour (Chapter 3). Perfusion of the animals at 3 hours after microinjection indicates that there are profound morphological changes in the grey matter at this time, and it can also be seen in Figure 6.3.1.1B that an area adjacent to the intense fluorescent signal is damaged, and this is likely to have occurred due to poor perfusion with fixative due to ongoing vasoconstriction.

It is not possible to derive any of the diffusion parameters discussed above from this fluorescent dextran experiment, although Sykova *et al* did measure these parameters in the spinal cord during ischaemia (progressive exsanguination) and terminal anoxia using the TMA method (Sykova *et al.* 1994). In addition extracellular K^+ was measured as an indicator of the progressive ischaemia. The extracellular space fraction, α, and the non-specific uptake *k'* both decreased during ischaemia. Tortuosity, λ, did not change until the extracellular K^+ concentration increased dramatically. The decrease in extracellular space is likely to be due to the swelling of

glia and neurones, as they lose their ability to control ionic gradients across their membranes. Hypotension caused by exsanguination reduced the perfusion of the tissue, resulting in decreased clearance of TMA and hence a drop in *k'*. When the tissue was under severe ischaemic stress the tissue K^+ concentration increased from 3-4mM to 60-70mM, and at this time the tortuosity increased as a result of the further swelling of neurons and glia.

In Chapter 3 spinal cord perfusion was measured using the laser Doppler technique following microinjection of ET-1 into the ventral spinal cord at T7. In addition to the rapid decrease in blood flow immediately adjacent to the microinjection site, blood flow in the spinal cord segments rostral and caudal to this site was also affected. This is summarised in Figure 6.4.1.1A. The decrease in blood flow is measurable in the two spinal segments adjacent to the microinjection site, T6 and T8, but not two segments away at T5 and T9. In addition to confirming that the effect is due to local and not systemic changes in perfusion, there is clearly a lag time between the drop in perfusion at T7 and the other segments. The time taken to reach 75, 50 and 25% of control perfusion values is shown in table form in Figure 6.4.1.1B. There is a delay of approximately 12 minutes in the time taken to reach 75% of control values between the microinjection site at T7 and both of the adjacent vertebral sites at T8 and T6. The rostral segment, T6, takes another 30 minutes to decrease to 50% of control, and blood flow does not reduce any further (Figure 6.4.1.1A,B). The caudal segment, T8, has a similar blood flow profile to T7 (Figure 6.4.1.1A) following microinjection of ET-1, although the time taken to drop from 75% of control to 25% of control is 12 minutes compared to 6 minutes at T7. The distance between the laser Doppler probe sites along the spinal cord was 5mm. If the time taken to reach 75% of control is used in the calculation, the velocity of the spreading vasoconstriction is $0.4mm.min^{-1}$. Using the 50 and 25% values, velocities of 0.301 and $0.269mm.min^{-1}$ are obtained. These values are much higher than the diffusion rates calculated for TMA reported above, which only diffuses 1-2mm in 10 minutes ($0.1\text{-}0.2mm.min^{-1}$) (Sykova *et al.* 1994). This strongly suggests that diffusion of ET-1 injected into the spinal cord cannot account for the rapid elongation of the ischaemic lesion.

Figure 6.4.1.1 Spread of rostro-caudal ischaemia

A

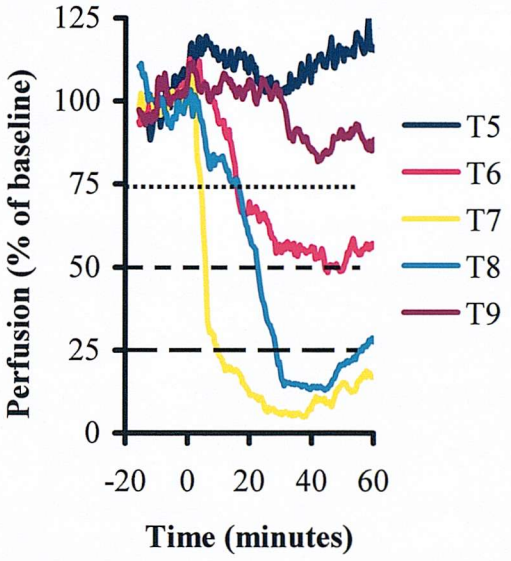

B

Blood flow

	75%	*50%*	*25%*
T5	-	-	-
T6	15.6	44.3	-
T7	4.3	6	10
T8	16.3	22.6	28.6
T9	-	-	-

These data from Chapter 3 depict spinal cord blood flow as measured by laser Doppler flowmetry following microinjection of ET-1 (15pmol) into the ventral grey matter at T7. The graph in Panel A shows the profile of perfusion at the 5th to 9th thoracic vertebra (T5-T9) following microinjection of ET-1 at T7 (n=3 for each profile). The dashed lines indicate 75%, 50% and 25% of control blood flow. The table in Panel B was constructed by reading off the mean time taken to reach 75%, 50% and 25% of control blood flow. Dashes indicate that spinal cord blood flow did not drop to this level.

These data suggest that some of the differences in fluorescein dextran distribution following microinjection of ET-1 could be due to changes in the extracellular space parameters. In addition simple diffusion cannot account for the speed at which the spinal cord blood flow decreases along the spinal cord. Consideration of these properties of the extracellular space will be essential when new therapeutic strategies, especially those involving large molecules, are considered.

6.4.2 Changes in ET-1 content in the spinal cord following ischaemic injury

An increase in the tissue ET-1 content has been reported following a traumatic injury to the rat spinal cord (Salzman *et al.* 1996). Within 30 minutes of a weight drop injury at T10, the concentration of ET-1 measured in an extract of the spinal cord by radio-immuno assay (RAI) was 165% of the value obtained in sham operated animals. After this time the amount of ET-1 decreased to sham levels by 48 hours after injury. In the data presented in the previous section it was shown that the recovery of the ET-1 ELISA was very low, and there were barely detectable amounts of ET-1 present in the vehicle injected spinal cords, but none in the sarafotoxin-6b injected spinal cords. In view of the literature cited above, and the known up-regulation of ET-1 during hypoxia *in vitro* (see below), this was not as expected.

The contusion injury used by Salzman *et al* would have resulted in the immediate mechanical disruption of the spinal cord vasculature, involving haemorrhage and coagulation, as well as the secondary development of tissue ischaemia. The microinjection of sarafotoxin-6b did not generate any traumatic damage, but did result in a profound reduction in blood flow (see Chapter 3). This difference in lesion generation may explain some of the discrepancy between the two experiments. After the weight drop injury the spinal cord was not perfused before processing, and therefore the assay also measured ET-1 present in blood at the haemorrhagic centre of the lesion. Following microinjection of sarafotoxin-6b the animals were perfused, and the ET-1 measured was that which remained in the tissue, i.e. within the spinal cord parenchyma or within cells.

The ET-1 peptide was originally purified from the supernatant of cultured porcine endothelial cells (Yanagisawa *et al.* 1988c), and is also produced by endothelial cells within the CNS vasculature (Yoshimoto *et al.* 1990). Although ET-1 is known to

have a role in maintaining vascular tone under normal physiological conditions (Rossi *et al.* 2001) and is secreted by endothelial cells by a constitutive pathway (Russell *et al.* 1998), it does have an additional important function during injury. Endothelial cells posses excretory granules called Weibel-Palade bodies (WPBs) (Weibel and Palade 1964) which contain large amounts of the pro-coagulant protein von-Willebrand factor (VWF) (Goerge *et al.* 2002) and histamine (Doi *et al.* 1995). These granules undergo exocytosis in response to injury or ischaemia and ensure that platelet aggregation and the formation of clot occur. It is now understood that in addition to VWF, the WPBs also contain ET-1 (Ozaka *et al.* 1997; van Mourik *et al.* 2002). This ET-1 causes rapid vasoconstriction to restrict bleeding at a site of trauma.

This would suggest that the reduction in ET-1 seen in sarafotoxin-6b injected spinal cords is due to the release of ET-1 from WPBs in the endothelial cells during ischaemia. Vehicle microinjection would not trigger the release of WPB contents and hence the amount of ET-1 present in these spinal cords is greater.

The extraction procedure for both the ET-1 and big-ET-1 assays was carried out according to the manufacturers instructions for tissue samples. However the very low recovery values (<1%), obtained from spiking naïve homogenate with a known amount of ET-1 prior to extraction, indicate that this process was not optimal. The ELISA assays used were sensitive and specific enough to detect the small amount of ET-1 present only in the extracted homogenates of the vehicle- microinjected spinal cords. The inability to measure big-ET-1 in any of the extracted spinal cord samples indicates that there is scarce big-ET-1 present in the perfused tissue, and given the very low recovery observed (<1%), it may not have been possible to measure it even if it was present. A high-performance liquid chromatography study using extracts of porcine spinal cord found that big-ET-1 content was less than 1% of measured ET-1 (Shinmi *et al.* 1989), which supports this suggestion.

6.4.3 Immunohistochemistry for ET-1 following injury

Before attempting to describe the cellular location of ET-1 seen after an ischaemic lesion, it is essential to determine the specificity of the antibody for the ET-1 peptide (Figure 6.3.3.1). The primary antibody, IHC6901, has a reported cross reactivity with big-ET-1 so it was important to know if big-ET-1 could be contributing to the

observed signal. Pre-absorption of the antibody with big-ET-1 resulted in a minor decrease in cellular staining compared to that seen in an adjacent section which was pre-absorbed with a control solution containing only BSA. Pre-absorption of IHC6901 with ET-1 led to an absence of cellular staining (Figure 6.3.3.1). This specific absorption confirmed that using this antibody for immunohistochemistry would allow the visualisation of the ET-1 peptide in Bouins fixed tissue.

A distinctive pattern of ET-1 staining was present in naïve spinal cord tissue (Figure 6.3.4.1). The apical surfaces of the ependymal cells, which form the central canal of the spinal cord, stained intensely for ET-1. These ependymal cells are engaged in pinocytosis, and studies using intraventricular injection of HRP have shown that they are capable of transporting HRP from the lumen of the central canal into the tissue extracellular spaces (Cifuentes *et al.* 1992). There is a higher concentration of ET-1 in the CSF (39 +/- 3 pg/ml), which flows down the central canal, than in the plasma (10 +/- 3 pg/ml) of normotensive rats (Mosqueda-Garcia *et al.* 1993). The possibility that this ET-1 may play a role in cardiovascular control is suggested by the observation that the concentration of ET-1 in the CSF decreased in response to a drop in systemic blood pressure. Thus the ET-1 staining seen in these ependymal cells at the apical surface could be due to active sampling of the ET-1 rich CSF by pinocytosis.

In addition to this mechanism, it is known that ependymal cells contain the mRNA for ET_B receptors (Hori *et al.* 1992; Nakagomi *et al.* 2000) but not ET_A receptors. These receptors are believed to be responsible for the clearance of ET-1 (Fukuroda *et al.* 1994), as binding of ET-1 to the ET_B receptor is almost irreversible and leads to receptor internalisation. These internalised receptors do not get recycled, and are passed into the late endosomal/lysosomal pathway (Oksche *et al.* 2000). However, it is unlikely that the ET-1 staining observed in the experiments presented above is due to this clearance mechanism.

The presence of ET-1 within the CNS parenchyma following a traumatic injury has been demonstrated by immunohistochemistry with other primary antibodies in the spinal cord (McKenzie *et al.* 1995) and in the brain (Petrov *et al.* 2002). McKenzie *et al* reported that the cellular location of ET-1 at 24 hours post-injury was in the neurons of the ventral spinal cord. In contrast Petrov *et al* observed ET-1 in

endothelial cells, macrophages and neurons in the brain at this time after a traumatic brain injury (TBI).

At 24 hours after an ischaemic injury induced by microinjection of ET-1 into the ventral grey matter of the spinal cord there was clear pattern in the distribution of ET-1 as visualised by immunohistochemistry (Figure 6.3.5.1). The endothelial cells within the lesion were ET-1 positive (as they had been at 6 hours also) and clearly outline the vessels (Figure 6.3.5.1A). Endothelial cell production of ET-1 is known to be up-regulated during hypoxia, and this is due to the presence of the hypoxia-inducible factor-1 (HIF-1) binding domain upstream of the ET-1 coding gene (Hu *et al.* 1998; Yamashita *et al.* 2001). The presence of ET-1 in the tissue at this time is likely to aid neovascularisation, as ET-1 is an endothelial cell mitogen. ET-1 is also known to induce gliosis (Koyama *et al.* 1999) through the ET_B receptor. Lack of glial ET_B receptors results in an enhanced amount of cell death following mid cerebral artery occlusion (Siren *et al.* 2002), and blockade of ET_B receptors with BQ-788 following a stab lesion in the cortex reduces gliosis (Koyama *et al.* 1999). ET_B receptors are involved in the clearance of ET-1, as after binding this ligand the receptor internalises (Oksche *et al.* 2000). By removing ET-1 from the CNS parenchyma the astrocytes may be preventing unwanted interaction between ET receptors present on neurons and at the same time maintaining the astrocytic gliosis.

Cells with an astrocytic morphology also stained positively for ET-1, particularly in the lateral white matter. To confirm that these cells were astrocytes, immunohistochemistry was performed using GFAP on adjacent sections to ET-1 staining with IHC6901 (Figure 6.3.5.1B). The profile of the GFAP stained astrocytes looks very similar to the ET-1 staining, although the ET-1 staining looks fainter and may be restricted to the cell surface unlike GFAP, which is intracellular.
Whether the staining seen is the result of ET-1 clearance by astrocytes, or due to increased ET-1 synthesis by these cells is unclear. There is *in vitro* evidence that astrocytes release mature ET-1 under ischaemic conditions and then clear it via an ET_B receptor mediated mechanism (Hasselblatt *et al.* 2001). In contrast an animal model of TBI reveals the expression of ET-1 to be in astrocytes pre-injury, but post injury ET-1 is localised in the endothelial cells and macrophages (Petrov *et al.* 2002).

Astrocytes in the normal optic nerve of the pig and human have also been shown to have ET-1 mRNA and immunoreactive protein (Ripodas *et al.* 2001).

The temporal profile of ET-1 positive immunohistochemistry is summarised in Table 6.3.5.2. Microinjection of vehicle (0.25µl) into the ventral horn grey matter at T7 resulted in ET-1 being detectable on some astrocytes in the grey matter at early time points (6 and 24 hours). Endothelial cells in the microvasculature also showed some ET-1 positive staining at 24 hours, but this did not persist. The lateral white matter astrocytes revealed a pattern of staining identical to that seen in the naïve spinal cord, namely a light ET-1 signal.

Microinjection of ET-1 (15pmol) into the ventral grey matter causes a rapid decrease in blood flow (Chapter 3) that results in neuronal loss and glial activation (Chapter 4). Within 6 hours of microinjection, the endothelial cells in the grey matter vasculature show an increased ET-1 signal that persists for at least 3 days. Astrocytes within the grey matter at the margins of the lesion show ET-1 staining at 3 days and 21 days. Astrocytes are destroyed by ischaemia in the lesion, and it is only at the later time-points (7 and 21 days) that there is evidence of astrocyte repopulation (Chapter 4).

The pattern of ET-1 immunohistochemistry seen in the above experiments most closely resembles that seen in the brain following TBI (Petrov *et al.* 2002), with the exception that ET-1 positive macrophages were also observed in that report. The findings of McKenzie *et al,* that ET-1 was present on grey matter neurons are not supported by the present results. These authors also noted that the pattern of ET-1 staining seen was identical to the areas of blood-spinal cord barrier breakdown observed by i.v. administration of HRP (McKenzie *et al.* 1995). This raises the possibility that the ET-1 observed in the ventral grey matter may be the result of ET-1 entry into the tissue through the disrupted barrier.

It is difficult to interpret these results without knowing for certain whether the observed ET-1 staining on astrocytes is due to the clearance of ET-1 from the extracellular milieu or release of ET-1 from the astrocytes. If resting astrocytes contain a pool of ET-1, which is released during injury to initiate gliosis in other

astrocytes, we would expect to see ET-1 in astrocytes within the grey matter of vehicle injected or naïve spinal cords. In the results above, ET-1 is not seen in the naïve spinal cord astrocytes, and following vehicle injection it is seen on only a few astrocyte processes. It is possible that as ET-1 is extremely potent, only small amounts are present in these cells, which makes it difficult to visualise using immunohistochemistry.

Endothelial cell production of ET-1 in the lesion is consistent with the known behaviour of these cells and the function of ET-1 in an ischaemic lesion. Production and secretion of ET-1 by endothelial cells stimulates mitosis, thus promoting the repair and extension of microvessels within the tissue parenchyma. This ET-1 may interact with astrocytes at the edges of the lesion to induce the observed gliosis. In addition, clearance of this ET-1 by astrocytes, as a means of limiting the exposure of the intact CNS to ET-1, may explain the ET-1 positive staining seen in astrocytes at the margins of the lesion. The observation of ET-1 positive astrocytes at later time-points (21 days) when there is no endothelial cell staining in the lesion suggests that astrocytes may be generating their own ET-1 or that the secretory pathway for ET-1 in the endothelial cells has increased, preventing the visualisation of ET-1 in these cells.

6.4.4 Other mechanisms

There are other mechanisms which may be involved the development of the lesion but that were not addressed in the experimental work presented above. In addition to VWF and ET-1, the Weibel-Palade bodies also contain histamine (Doi *et al.* 1995), and histamine itself is a powerful stimulus for exocytosis of Weibel-Palade bodies (van Mourik *et al.* 2002). Intrathecal injection of the peptidic substance-P antagonist spantide results in a rapid local decrease in spinal cord blood flow (Freedman *et al.* 1988). This effect was later determined to be due to stimulation of histamine release, as pre-treatment with antihistamines blocked the drop in spinal cord blood flow (Hoover ; Hakanson *et al.* 1990). It has been established that the vasoconstricting effect of systemically administered ET-1 on the cerebral vasculature can be inhibited with the ET_A receptor antagonist BQ-123 (Fernandez *et al.* 1998), which suggests a direct pharmacological connection between ET-1 and vasoconstriction. This does not exclude the possibility that histamine is involved in the propagation of an ET-1-induced focal ischaemia as the reductions in blood flow observed by Fernandez *et al*

were not pathological. There is also the suggestion that ET-1 may enhance the sensitivity of smooth muscle to histamine, although this was seen in bronchial smooth muscle rather than vascular it may be a contributing factor (Kanazawa *et al.* 1992). The pre-treatment of animals with antihistamine drugs, such as cetirizine, prior to microinjection of ET-1 into the spinal cord may reveal the involvement of histamine in the observed changes in blood flow.

The control of blood flow within the spinal cord is also subject to the influence of direct innervation. Histochemical studies have identified aminergic nerve fibres on the intraparenchymal vessels of the cat spinal cord (Itakura 1983), and the major vessels of the rat spinal cord also have adrenergic innervation (Amenta *et al.* 1987). This suggests a role for sympathetic regulation of blood flow in the spinal cord that could become dysregulated under pathological conditions, particularly if the cell bodies of these nerves become ischaemic. In the cat, electrical stimulation of the cervical sympathetic nerve resulted in the constriction of pial arteries penetrating the surface of the brain (Sercombe and Wahl 1982), which confirms that the vasculature of the CNS can be subject to some sympathetic input. There is also evidence that some of the nerve fibres found on the cerebral vasculature contain ET-1 (Milner *et al.* 2000), and these originate in sympathetic ganglia, suggesting that ET-1 may have a direct role in autonomic function.

6.5 Conclusion

In this novel model of ischaemia induced by ET-1 or the known $ET_{A/B}$ agonist sarafotoxin there is a reduction in the tissue ET-1 content 1 hour after the initiation of the lesion, which is likely to be due to release of granules (Weibel-Palade bodies) from endothelial cells. In addition, the spread of the lesion rostrally and caudally is unlikely to be due to movement of the microinjected ET-1 through the extracellular space of the grey matter. Co-injection of ET-1 with a fluorescein conjugated low molecular weight dextran resulted in spread over only a few millimetres. From 6 hours to 21 days after microinjection a distinct distribution of ET-1 is revealed by immunohistochemistry. Vascular endothelial cells in the grey matter lesion, astrocytes in the intact grey matter and astrocytes in the lateral white matter adjacent to the lesion all stain positively for ET-1 during the development of the lesion, with almost complete resolution by 21 days. This ongoing production of ET-1 may be

contributing to the revascularisation of the lesion, and also to the development of the gliotic scar.

Given these data, it is conceivable that there are other mechanisms that drive the rapid expansion of the lesion. These may include histamine release from the endothelium and possibly the involvement of the local nervous control of blood vessels. Future investigations into these mechanisms may aid the complete understanding of the pathological mechanisms in play during a spinal cord injury, and lead to effective acute therapy.

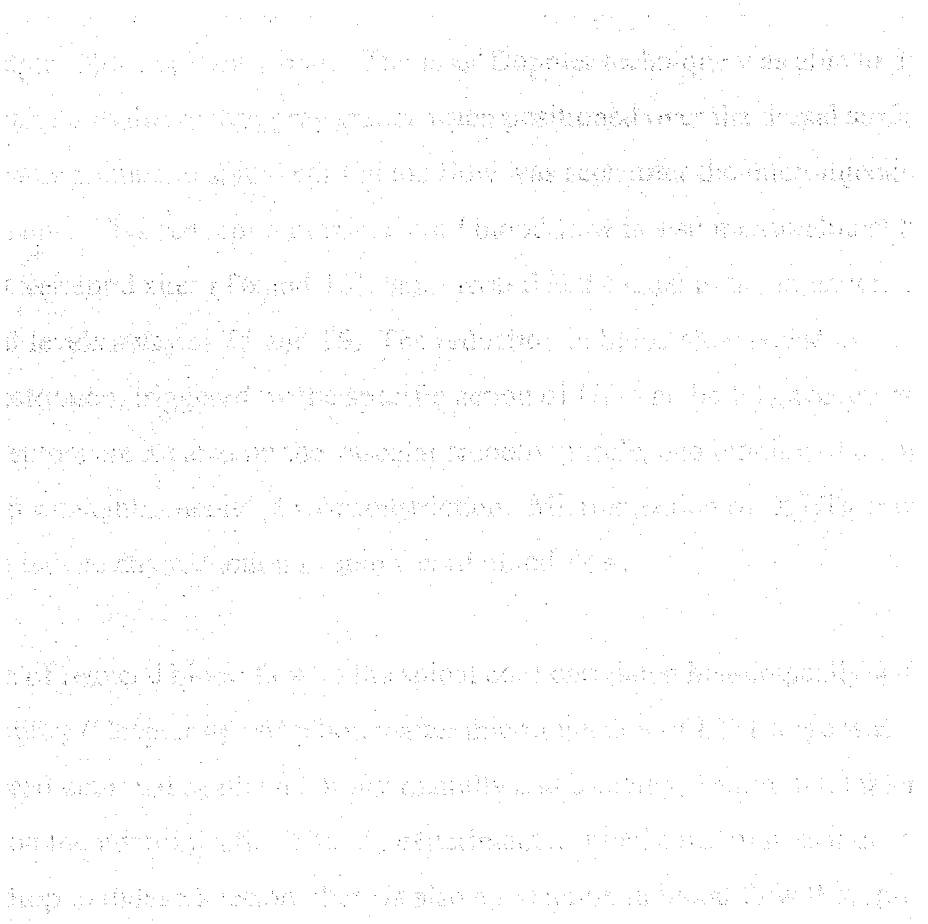

Chapter 7 – Discussion and future work

7.1 Introduction

Focal ischaemia induced by microinjection of ET-1 has been shown to generate a lesion in the spinal cord that destroys grey matter and results in substantial white matter axon pathology without significant mechanical injury to the spinal cord. The aim of this chapter is to integrate the results of the previous chapters and discuss their wider implications for future investigation of spinal cord injury and the testing of novel therapeutic strategies.

7.2 Spinal cord ischaemia as a model of SCI

7.2.1 Grey matter injury

The microinjection of ET-1 (15pmol) into the ventral spinal cord at the level of the 7th thoracic vertebra (T7) clearly causes a statistically significant decrease in blood flow (see Chapter 3) for at least 1 hour. The laser Doppler technique was able to detect these changes in the ventral grey matter when positioned over the dorsal surface of the cord, and no change in spinal cord blood flow was seen after the microinjection of sterile saline. This reduction of spinal cord blood flow is also measurable at the adjacent vertebral sites (T6 and T8), 5mm rostral and caudal to the injection, but not 2 vertebral levels away at T5 and T9. The reduction in blood flow is due to vasoconstriction, triggered by the specific action of ET-1 at the ET_A receptors. These ET_A receptors are located on the vascular smooth muscle, and binding of an agonist results in a calcium-mediated vasoconstriction. Microinjection of an ET_B agonist failed to induce any reduction in spinal cord blood flow.

The area of reduced blood flow in the spinal cord correlated histologically with grey matter injury (Chapter 4). At 6 hours after microinjection of ET-1 there was widespread neuronal death and injury rostrally and caudally, 15mm in total length, centred on the microinjection site. In experimental spinal cord injuries induced using weight drop to induce a lesion, there is also a reduction in blood flow that spreads above and below the impact site (Tator and Fehlings 1991). One study that has addressed this elongation phenomenon was reported by Grossman *et al*, who observed a lesion, characterised by loss of ventral motor neurons, which is 9mm in length 15 minutes after impact, and which extends to 12mm at 24 hours (Grossman *et al.* 2001).

In my experiments, the ET-1 was microinjected in a small volume (250nl), yet profound changes in blood flow were measured over 3 segments centred on the injection site. This corresponds to vasoconstriction along a 10-15mm length of spinal cord. There are a number of possible explanations for this phenomenon including the diffusion of exogenous ET-1, the induction or release of endogenous ET-1, or the activation of other mechanisms by the ET-1.

7.2.2 Diffusion of ET-1 in the spinal cord

To address the question of whether the ET-1 is diffusing through the parenchyma of the spinal cord to induce vasoconstriction at adjacent sites, a fluorescein-conjugated dextran (molecular weight 3000) of a similar size to ET-1 (molecular weight 2492) was co-injected with ET-1 (15pmol) or vehicle (Chapter 6). Microinjection of the dextran with sterile saline vehicle resulted in diffusion of the dextran 2-3mm rostrally and caudally after 3 hours. Co-injection with ET-1 reduced the apparent diffusion of the dextran and the ET-1 appeared to cause a constriction of the grey matter at the injection site. This suggests that the ET-1 induced vasoconstriction may limit the movement of ET-1 following microinjection through a reduction in the extracellular space. In addition, the vasoconstriction induced by the action of ET-1 on vascular smooth muscle cells is sufficiently powerful to disrupt the morphology of the grey matter, and this may also contribute to the developing ischaemia. These data indicate that diffusion of microinjected ET-1 is unlikely to account for the vasoconstriction and neuronal death seen at the adjacent vertebral levels.

The rapid spread of the vasoconstriction is also illustrated by the rate at which spinal cord blood flow decreases at the adjacent vertebral levels after microinjection of ET-1 at T7 (Chapter 3 and Chapter 6). The velocity of this spread into the adjacent caudal segment was calculated using the time taken to reach 25% of control blood flow, and a value of ~0.3mm.min^{-1} was obtained. This is more rapid than the passive diffusion of tetramethyl ammonium, a small water-soluble molecule (molecular weight 74), which moves at a speed of 0.1-0.2mm.min^{-1} in the spinal cord parenchyma (Sykova *et al.* 1994). As such a small molecule as TMA would be expected to diffuse more rapidly than a protein such as ET-1, these findings further support the proposition that diffusion of microinjected ET-1 cannot explain the size of the lesion.

7.2.3 Local changes in endogenous ET-1

Another possibility is that the local vasculature responds to the focal ischaemia by propagating the vasoconstriction rostro-caudally. This could be mediated either by the local release of ET-1, or the local release of other vasoconstricting substances that would lead to a 'domino-effect' along the vasculature. It is known that ischaemic endothelial cells can produce ET-1 (Yamashita *et al.* 2001), and the local concentration of ET-1 has been shown to increase in the spinal cord following a mechanical injury (McKenzie *et al.* 1995). To explore the possibility that ET-1 is released locally in the tissue in an ischaemic lesion, sarafotoxin-6b (S6b), a potent non-selective ET receptor agonist was microinjected in the same manner as the previous ET-1 experiments. S6b produces a dramatic reduction in spinal cord blood flow following microinjection with a very similar profile to that seen after microinjection of ET-1 (Chapter 3). This peptide does not cross-react with commercially available ET-1 and big-ET-1 ELISA assays (Chapter 6), which made it useful for experiments to quantify the possible ischaemia-induced levels of endogenous ET-1.

Unfortunately, the results were inconclusive, as the recovery of ET-1 and big-ET-1 was very poor despite the use of a number of solid phase extraction protocols. An interesting qualitative observation was that all of the S6b injected spinal cords had undetectable amounts of ET-1, whereas 2/3 of the vehicle injected spinal cords had very low but measurable amounts of ET-1. Vascular endothelial cells contain Weibel-Palade bodies (WPBs), which are secretory granules that contain many substances including the pro-coagulant protein von Willebrand Factor (VWF), histamine and ET-1. These granules are released following injury to the vasculature to promote coagulation and to stop bleeding. The release of ET-1 from these granules as a result of ischaemic injury may explain both the increase in ET-1 seen following impact trauma (McKenzie *et al.* 1995) and the lack of measurable ET-1 in the S6b injected cords. In the mechanical injury model the spinal cord tissue was taken without perfusion of the animal, and therefore the homogenate produced would include the ET-1 released into the microcirculation in the injured area. Following microinjection of S6b, the animals were perfused with heparinised saline, which would flush the microcirculation, removing any released ET-1.

In addition to this acute release of ET-1 by the endothelial cells, ET-1 is secreted constitutively in order to contribute to the basal vasoconstricting tone. Following injury, endothelial cells can increase their output of ET-1 as it is an endothelial cell mitogen and can therefore promote the regeneration of blood vessels. The distribution of ET-1 in the CNS parenchyma following spinal cord (McKenzie *et al.* 1995) and brain (Petrov *et al.* 2002) trauma has been described using immunohistochemistry. McKenzie *et al* reported that the ET-1 was present in the neurons of the ventral spinal cord at 24 hours post-injury, and Petrov *et al* observed ET-1 in endothelial cells, macrophages and neurons in the brain at this time after a traumatic brain injury (TBI). There is also evidence in the literature that ET-1 can be released by astrocytes under normal and pathological conditions (Hasselblatt *et al.* 2001; Ripodas *et al.* 2001).

The cellular distribution report by Petrov *et al* and McKenzie *et al* is at odds with that observed following focal ischaemia of the spinal cord (Chapter 6). Immunohistochemistry with a polyclonal anti-ET-1 antibody was performed to determine the temporal and spatial distribution of ET-1 following a focal ischaemic lesion. ET-1 is present in endothelial cell WPBs in intact tissue, although positive immunohistochemical staining of endothelial cells was not observed in control animals in this study. Previous studies that identified ET-1 in WPBs have used immuno-electron microscopy (Ozaka *et al.* 1997), which suggests that immunohistochemistry may not be adequate to detect ET-1 within secretory granules in naïve tissue, possibly because they are small and few in number. Following injury or ischaemia there is likely to be a release of the WPBs followed by an increase in ET-1 production by endothelial cells, which would improve the ability to detect the peptide by immunohistochemistry. In the grey matter, vascular endothelial cells within the lesion stained positively for ET-1 during the first 3 days after microinjection of ET-1. Astrocytes in the intact grey matter adjacent to the lesion also stain positively for ET-1 after this time. This ongoing production of ET-1 may be contributing to the revascularisation of the lesion, and also to the development of the gliotic scar via the activation of ET_B receptors on astrocytes. As astrocytes can effectively clear ET-1 from the extracellular milieu this mechanism may represent a way of limiting the penetration of ET-1 into the intact CNS parenchyma.

7.2.4 Acute inflammation

The rapid destruction of the grey matter of the spinal cord, which follows the ET-1 induced vasoconstriction, generates a robust inflammatory response (Chapter 4). It has previously been demonstrated that microinjection of the proinflammatory cytokine TNFα into the spinal cord causes more inflammation than the microinjection of the same dose of TNFα into the striatum (Schnell *et al.* 1999b). Mechanical injury to the mouse spinal cord and brain also results in a greater number of inflammatory cells being recruited to the spinal cord (Schnell *et al.* 1999a). Microinjection of ET-1 (15pmol) into the caudate putamen (striatum) of the rat results in the loss of medium spiny neurons, but no neutrophils are recruited (Chapter 4). Microinjection of the same amount of ET-1 into the ventral grey matter of the spinal cord also caused the destruction of neurons. However, this injury led to a pronounced neutrophil recruitment, which was maximal at 24 hours after microinjection. This recruitment coincided with blood-spinal cord barrier breakdown, which does not occur in the striatum. The neutrophils were almost exclusively present in the grey matter, and the few neutrophils seen in the white matter were closely associated with blood vessels, which demonstrates that these cells do not enter the white matter in significant numbers.

Spinal cord ischaemia also activated the resident macrophages of the spinal cord, the microglia. These cells changed their phenotype from quiescent immobile cells to actively phagocytic ED-1 positive macrophages (Chapter 4). Blood derived monocytes are also recruited into the lesion with an ED-1 positive macrophage phenotype, but it is not possible to distinguish between the two populations of cells in these results. Macrophages did not appear in the lesion in appreciable numbers until 3 days after microinjection of ET-1. At this time there was an asymmetry in the distribution of macrophages in the grey matter, with more in the caudal end of the lesion than in the rostral end. This asymmetry was lost by 7 days after microinjection, and the extent of macrophage recruitment was shown to be coextensive with the 15mm length of the injured grey matter. The grey matter macrophages peaked in number at day 7, but in the white matter the number of macrophages remained the same at 7 and 21 days after microinjection. The absolute numbers of macrophages in the white matter were consistently lower than in the grey matter, which may reflect

both the large amount of necrosis in the grey matter and the lower vascularity of the white matter. The presence of macrophages in the white matter at 21 days after ischaemic injury suggests that the phagocytosis of axonal debris is a prolonged event. This has also been observed in human tissue, where macrophages remain in the spinal white matter for several years after a stroke, as axonal tracts degenerate (Kosel *et al.* 1997). Actively phagocytic macrophages in the white matter are essential for the clearance of axonal and glial debris following injury, but they may induce further axonal injury by releasing destructive enzymes and free radicals, although this remains to be shown (Coleman and Perry 2002).

7.2.5 White matter pathology

7.2.5.1 Inflammation

Although the ventral grey matter of the spinal cord contained large numbers of neutrophils at 24 hours post injury, there was no evidence of axon injury, in the form of amyloid precursor peptide (APP) positive axonal swellings or 'end bulbs', in the white matter immediately adjacent to the grey matter. APP-positive axons were present in the white matter at 24 hours, but they were distributed within the ventro-lateral white matter with no obvious relationship to the inflammation in the grey matter (Chapter 5). The APP signal was still present in the white matter at 3 days after microinjection of ET-1, although by 7 days it was no longer present.
Although there is a lack of evidence for ongoing axonal injury as assessed by APP immunohistochemistry, the white matter is still undergoing pathological changes up to 21 days after microinjection of ET-1. Pyknotic nuclei, which are likely to be apoptotic oligodendrocytes on the basis of their distribution, are present along the length of the ventrolateral white matter from 7 days until at least 21 days after focal ischaemia (Chapter 4). Wallerian degeneration results in the apoptosis of oligodendrocytes which had previously ensheathed the axons (Warden *et al.* 2001). As oligodendrocytes ensheathe multiple axons with myelin, this loss of cells is likely to result in the demyelination of otherwise normal axons, which could have functional consequences.

7.2.5.2 Ischaemia and excitotoxicity

The lack of a simple spatial relationship between the inflammatory cells and the axonal damage suggests that other mechanisms, including glutamate toxicity and

direct ischaemia of the white matter may be involved. One of the consequences of white matter ischaemia *in vitro* and *in vivo* is the loss of conductance of action potentials (Waxman *et al.* 1991). This is believed to be mediated in part by extracellular potassium, which is normally buffered by astrocytes (Young *et al.* 1982). Under ischaemic conditions the astrocytes are unable to maintain this function and the concentration of extracellular potassium rises, preventing the conduction of action potentials along axons. The propagation of action potentials along axons, especially myelinated axons where saltatory conduction occurs, requires relatively little energy compared to the large metabolic demands of neuronal cell bodies. However, energy failure in the axons is still a likely consequence of prolonged ischaemia, and could ultimately lead to irreversible axon damage due to entry of calcium into the axoplasm and the activation of proteases (Chapter 5).

The link between axonal conduction failure and degeneration is not necessarily certain, as axons may be able to withstand a limited amount of ischaemia and transient loss of function without degenerating (Stys 1998). It is however well known that metabolic failure can result in the depolarisation of the axonal membrane and the entry of calcium through voltage-gated calcium channels (Imaizumi *et al.* 1999) and the reversed sodium-calcium transporter (Petty and Wettstein 1999; Li *et al.* 2000). This calcium entry activates proteases, such as the calpains, which can degrade the structural components of the axon.

The other secondary mechanism investigated was excitotoxicity. This could arise from the presence of glutamate released from the necrotic neurons in the grey matter, and as a result of glutamate efflux from axons during ischaemia or following trauma (Li *et al.* 1999). Axons themselves do not have glutamate receptors (Li and Stys 2000), but the oligodendrocytes and their myelin have AMPA receptors. Excitotoxicity at these sites could result in myelin damage, which would then expose axons to injury and dysfunction. Electron microscopy was used to examine axons and their myelin in the ventral white matter caudal to the microinjection site (Chapter 5). In addition to ET-1 and vehicle microinjections, a series of animals received microinjections of NMDA, a synthetic glutamatergic agonist which would be expected to destroy grey matter neurons without inducing any changes in spinal cord blood flow.

Analysis of the damage sustained by the axoplasm and myelin after these treatments revealed differences in the pattern of injury following microinjection of ET-1 or NMDA. The ischaemic lesion was characterised by moderate injury to the myelin, but a high degree of axon degeneration. In the excitotoxic lesion the myelin was severely damaged while the axoplasm remained relatively intact. This indicates that although excitotoxicity can injure axons, it makes a minor contribution to the axonal degeneration seen after ischaemia.

7.3 Future experiments

The ability to generate these non-mechanical spinal cord lesions presents a unique opportunity to investigate a variety of pathological and physiological systems involved in the development of SCI.

7.3.1 Electrophysiological assessment of axon ischaemia

It has been known for many years that axonal ischaemia results in a loss of conduction, but the relationship between this ischaemia and the onset of axonal degeneration have only been understood relatively recently (Waxman *et al.* 1991; Stys 1998; Li *et al.* 2000). Given the profound reduction in blood flow in the spinal cord following microinjection of ET-1, it is likely that direct ischaemia of the white matter is occurring. It would be of great interest to determine if the focal ischaemia induced by microinjection of ET-1 into the grey matter of the spinal cord is capable of inducing functional changes in adjacent white matter axons.

7.3.1.1 In vivo electrophysiology

The axonal membrane, which is exposed at the nodes of Ranvier, can be depolarised by applying current with a stimulating electrode, and if this is of sufficient amplitude an action potential (AP) can be induced which moves symmetrically away from the electrode to the axon terminal (orthodromic conduction) and the neuronal cell body (antidromic conduction). When using field stimulation the initial electrical stimulus can depolarise a number of axons simultaneously, and if these axons are of a similar calibre they will transmit the action potential synchronously, producing a compound action potential (CAP). A recording electrode placed on another part of the same axon, or group of axons, can be used to measure the CAP as it passes.

This technique can be used to determine the physiological status of the axons, as loss of CAP conduction implies energy failure in the white matter. Metabolic failure or restriction will lead to the inability to conduct action potentials, and ultimately to calcium entry and axon destruction. Previous reports using aortic occlusion to induce ischaemia of the whole spinal column in the cat demonstrated a loss of CAP conductance after 20 minutes of ischaemia (Yamada *et al.* 1998).

7.3.1.2 Pilot investigations

Preliminary experiments have been performed to assess the feasibility of applying this technique to the microinjection protocol already established, where physiological recordings can be made with the rat fixed in a stereotaxic frame and access to the spinal cord obtained via laminectomies under urethane (non-recovery) anaesthesia (see Chapter 3). Briefly, a recording electrode, consisting of two non-insulated silver wires, was positioned under the sciatic nerve using a micromanipulator. The stimulating electrode (a pair of insulated silver wires with exposed tips) was placed on the surface of the dura at T5 using a micromanipulator and connected to a stimulator unit (Harvard). The recording electrode and the stimulator were connected to an integrated signal amplifier and processor (BIOPAC MP150), and recordings were obtained using a personal computer based software package (AcqKnowledge, BIOPAC).

Stimulating voltages (pulse duration 0.1msec) were optimised for each animal in order to obtain a consistent compound action potential (range 7-25V). Once a stable action potential (AP) had been obtained baseline recordings were taken for at least 10 minutes (approximately 12 events per minute). After this time ET-1 or vehicle were microinjected into the dorsal grey matter, and the AP recording continued for at least 1 hour to observe any changes in the waveform. At the end of the experiment animals were killed by i.a. administration of Sagatal (sodium pentobarbitone 60-120mg.rat^{-1}), and the cessation of AP was confirmed.

In these preliminary experiments microinjection of 0.25μl vehicle into the dorsal grey matter resulted in little change to the recorded CAP. However dorsal microinjection

of ET-1 induced an apparent loss of CAP within 10-20 minutes of administration (data not shown). In two out of the three recordings, the CAP was absent by 30 minutes post microinjection, and in the third it was markedly reduced by this time. In one of the animals the CAP was lost within 10 minutes of microinjection of ET-1. It was established in separate experiments that microinjection of 15pmol ET-1 into the dorsal grey matter resulted in a significant reduction in spinal cord blood flow as assessed by laser Doppler flowmetry at the injection site (data not shown). In addition axon injury in the adjacent white matter, as indicated by the appearance of APP positive axon profiles, was present 24 hours following dorsal microinjection of 15pmol ET-1 but not vehicle (data not shown).

Whilst these results are not conclusive, they do suggest that spinal cord ischaemia induced by microinjection of ET-1 into the grey matter may place the adjacent white matter under sufficient physiological stress to prevent the conduction of action potentials. Further experiments to clarify this observation will be essential if the correlation of *in vivo* hypoperfusion and subsequent axonal dysfunction and pathology is to be demonstrated.

7.3.2 Control of spinal cord blood flow

There are mechanisms other than release of ET-1 that could contribute to the vasoconstriction seen in the spinal cord after microinjection of ET-1. It is known that the spinal cord blood flow is autoregulated over a wide range of systemic blood pressures (Kobrine *et al.* 1979), but the contribution of descending sympathetic innervation and local innervation is unclear. There have been conflicting reports on the significance of the sympathetic innervation, with some authors suggesting that chemical sympathectomy with guanethidine treatment does not affect the spinal cord blood flow reflexes (Kinoshita and Monafo 1993), while others have shown that adrenalectomy or abdominal sympathectomy do affect the ability of the spinal cord to autoregulate (Iwai *et al.* 1991). The cholinergic system could also be involved as motor neurons in the ventral horn release acetylcholine as they undergo necrosis, and this may act locally on post-synaptic parasympathetic effector sites, such as arteriolar smooth muscle, or autonomic ganglia (Brown and Taylor 1996) . Autonomic neurons in the guinea pig trachea are responsive to ET-1 (Takimoto *et al.* 1993), so it is

possible that some smooth muscle contraction may be due to direct activation of sympathetic neurons by ET-1.

The identification and manipulation of this system could provide new insights into the underlying mechanisms involved in post-injury vasoconstriction in the spinal cord. There are very few reports describing the networks of fibres innervating the spinal vasculature of the adult rat, although a recent report has described ET-1 containing axonal varicosities in sympathetic nerves of the brain vasculature (Milner *et al.* 2000). This group used electron microscopy to identify neurons in the trigeminal ganglia of the rat that send ET-1 positive sensory fibres to the basilar artery. The presence of ET-1 positive axonal varicosities on the human middle-cerebral artery has since been confirmed (Loesch and Burnstock 2002). The release of ET-1 from axonal varicosities along the major vessels of the ventral spinal cord following injury would need to be demonstrated, but if this is a major mechanism driving lesion development it may represent a new therapeutic target. The ET-1 induced focal ischaemia model may provide a useful tool to investigate these phenomena. The quality of histological samples obtained acutely following ischaemia is likely to be high due to the minimal trauma involved, and this is particularly important for electron microscopy.

Milner et al produced sensory denervation by the administration of capsaicin to the young rat, which resulted 12 weeks later in a reduction in the number of ET-1 positive cells in the trigeminal ganglia, and a reduction in the number of ET-1 positive nerve fibres on the vasculature (Milner *et al.* 2000). Conversely, chemical sympathectomy by the administration of 6-hydroxydopamine (6-OHDA) for three days to 12-week-old rats resulted in an increase in the ET-1 containing axon profiles. These techniques could be used to manipulate the ET-1 content of the axons innervating the spinal vasculature in advance of an ET-1 induced focal ischaemia. If this source plays an important role in the development of the lesion, the size of the lesion or the rate of lesion progression rostrally and caudally may be reduced in the denervated animals and increased in the 6-OHDA treated animals.

7.3.3 Recovery of axonal function

If, as suggested above, focal ischaemia of the spinal cord is capable of disrupting the conduction of compound action potentials *in vivo*, it will be important to know to what

extent the axonal dysfunction is reversible. This could be investigated by extending the length of the observation period in these experiments to see if compound action potential conduction is recovered. Refinement of the recording techniques, for example by using suction electrodes or single fibre recordings, may increase the quality of the recordings made over longer periods. Other ways of examining the physiology of the spinal cord could also be introduced, including potassium sensitive microelectrodes (Sykova *et al.* 1994) to monitor the extracellular potassium concentration in the white matter in relation to axonal failure and recovery *in vivo*. The development of small, commercially available, oxygen sensitive electrodes opens the possibility of measuring the functional ischaemia directly in this setting. The correlation of ischaemia with functional loss and subsequent axon pathology *in vivo* in the rat would be of interest, as it may be useful to know if strategies which prevent conduction failure also reduce axon pathology.

7.3.4 Apoptosis in the lesion

It was suggested earlier (Chapter 4) that neuronal death seen in this model is largely mediated through necrotic mechanisms, but the actual mode of death for any cell type has not been determined as yet in this model. The loss of supporting cells, such as oligodendrocytes and astrocytes, due to apoptosis in the white matter may contribute to the ongoing lesion pathology. TUNEL (terminal deoxynucleotidyl transferase (TdT)-mediated deoxyuridine triphosphate (dUTP)-biotin nick end labelling) staining has been used by a number of authors to identify apoptotic cells (Liu *et al.* 1997) in injured CNS tissues. This technique relies on DNA fragmentation, which is a hallmark of apoptosis in the cell body, which makes it unsuitable to the detection of axonal injury. Although there is evidence that caspase-3, a key enzyme in the apoptotic cascade is present in degenerating axons in the brain following a traumatic injury (Buki *et al.* 2000), it has recently been shown that the ubiquitin-proteasome system plays a major role in axon degeneration (Zhai *et al.* 2003). Optic nerve transection was performed to induce axonal degeneration, and treatment with MG132, a ubiquitin-proteasome inhibitor, resulted in delayed degeneration of axons as assessed by immunohistochemistry for microtubules and neurofilaments. It is clear that if the enzymes that are key to the structural disintegration of the axon can be identified, then the development of axon-protective inhibitors may be possible.

7.3.5 Immune mediated white matter injury

As yet, the hypothesis that the acute inflammatory response, which follows the ET-1 induced ischaemia, contributes to white matter injury has not been tested, although it was noted that there is no spatial correlation between the inflammatory cells and axon injury (Chapter 5). Several authors have reported beneficial effects of anti-neutrophil interventions (Taoka *et al.* 1997; Taoka *et al.* 1998; Fujimoto *et al.* 2000) on behavioural and histological outcomes following experimental spinal cord injury. Whole animal irradiation could be used to ablate the bone marrow, resulting in the depletion of all granulocytes prior to the induction of focal ischaemia in the spinal cord. This could reveal the extent to which both neutrophils and non-microglial phagocytic macrophages contribute to the white matter injury in this model. Light and electron microscopy could be used to observe any changes in axon pathology.

If leukocyte ablation reveals a role for acute inflammation in producing damage to axons or other white matter structures, this could be further dissected by using neutrophil inhibiting techniques, such as anti-neutrophil antibodies in this model. Suppression of the local inflammatory response after injury by administration of the anti-inflammatory cytokine IL-10 has been investigated in an impact model of spinal cord injury (Brewer *et al.* 1999). These authors reported both a positive and negative effect on neurological recovery. Systemic administration was beneficial but local injection made the lesion worse. The ET-1 microinjection model, which is minimally traumatic, may provide a suitable setting to investigate these phenomena further.

7.3.6 Excitotoxic injury to white matter

It is now widely recognised that a number of non-neuronal cells in the spinal cord have glutamate receptors, and could be vulnerable to the high concentrations of extracellular glutamate found in the ischaemic lesion. The NMDA-receptor antagonist MK-801 is neuroprotective in experimental models of stroke, but does not confer protection against excitotoxic injury to the white matter, which contains only AMPA/kainate-type glutamate receptors (Li and Stys 2000). A number of *in vitro* and *in vivo* studies have confirmed that antagonists that act at these non-NMDA glutamate receptors can protect the white matter from ischaemic injury (Wrathall *et al.* 1996; Li and Stys 2000).

Microinjection of the glutamatergic agonist NMDA into the grey matter of the spinal cord has enabled the contribution of excitotoxicity to the axonal injury to be examined (Chapter 5). The profile of axon pathology was consistent with the location of glutamate receptors on oligodendrocyte myelin, and not axons. The preservation of myelin in the white matter following spinal cord injury may lead to the prevention of some functional loss. Recently it has been demonstrated that a combined use-dependent sodium channel blocker and voltage-gated calcium channel blocker, HP184, can improve spinal cord function in rodents even 35 days after a mechanical SCI (Rathbone *et al.* 2002). This suggests that demyelination and alterations in axonal electrophysiology may be contributing to the functional loss seen clinically. This drug has also been shown to be neuroprotective in acute SCI, as blockade of sodium channels prevents the depolarisation of the axon and the subsequent entry of calcium into the axoplasm (Khan *et al.* 2002). Focal ischaemia induced by microinjection of ET-1 into the spinal cord provides an ideal setting to investigate this strategy further, because as there is no mechanical injury, the axon pathology seen is the result of ischaemic and post-ischaemic events.

Another way to reduce injury to the white matter may be to use AMPA/kainate antagonists, such as NBQX (von Euler *et al.* 1994) and GYKI53655 (Chizh *et al.* 1994). These compounds have been shown to protect astrocytes (Agrawal and Fehlings 1997) and oligodendrocytes (Li and Stys 2000), which are known to bear AMPA- and kainate specific glutamate receptor subunits, from injury following mechanical or ischaemic insults. The electron microscopic assessment of axonal pathology reported earlier (Chapter 5) was carried out at 3 days after microinjection of ET-1, NMDA or vehicle. As neuronal destruction appears to be under way by 6 hours after microinjection of ET-1, it would be of interest to see if myelin damage is occurring within 6-24 hours of injury. Pharmacological intervention with AMPA antagonists could be tested to see if this acute myelin damage can be ameliorated.

7.4 Conclusions

The generation of focal ischaemia of the spinal cord by microinjection of ET-1 provides a model of SCI with unique advantages over existing techniques, particularly the absence of mechanical injury. The biology of this model has been characterised in detail, including the temporal and spatial progression of ET-1-induced focal ischaemia

and the induction of an acute inflammatory response. In spite of the absence of mechanical injury, axon pathology was observed in the ventrolateral white matter, which was consistent with ischaemic injury.

This experimental system offers distinct advantages over the widely used mechanical injury models. Firstly, although the ischaemia is severe enough to cause substantial grey matter injury and injury to axons in the adjacent white matter, it does not result in overt behavioural or physiological changes in the animals. Conventional SCI rats require a high degree of maintenance, as their bladders and colons need to be manually emptied. The ability to generate anatomically and physiologically relevant axonal injury *in vivo* without causing paralysis is also advantageous from an animal welfare perspective.

Secondly, as there is minimal mechanical injury to the spinal cord, any axonal or vascular injury seen must be the consequence of ischaemia or other secondary mechanisms. In the context of a mechanical injury to the spinal cord, ischaemia itself is a secondary mechanism. This model may also be useful in that it mimics the behaviour of the margins of a traumatic spinal cord lesion, which expand to include tissue that was not affected by the impact. This is precisely the tissue that therapeutic strategies for acute spinal cord injury will need to salvage, and the lack of mechanical injury may provide a larger window in which to measure any beneficial effects.

Thirdly, this model may provide a means of investigating further the biology of axonal degeneration *in vivo*. The processes which contribute to axonal scission following ischaemia are not fully understood, and as this model provides an ischaemic insult to axons it may be possible to dissect these mechanisms more fully in an anatomically relevant part of the CNS. Although axonal degeneration has been observed for many decades, it is only relatively recently that existence of a mutant mouse, which exhibits slow degeneration of axons after transection, has demonstrated the active nature of Wallerian degeneration (Coleman and Perry 2002).

Current therapy for SCI is far from adequate, and even modest protection of axons may generate significant improvements in the quality of life for the many thousands of people who suffer a spinal cord injury each year. It is hoped that this model will

contribute to the further understanding of the pathological mechanisms causing axonal damage in spinal cord injury, and to the subsequent development of novel therapeutic strategies that will bring benefit to individuals with acute spinal cord injury.

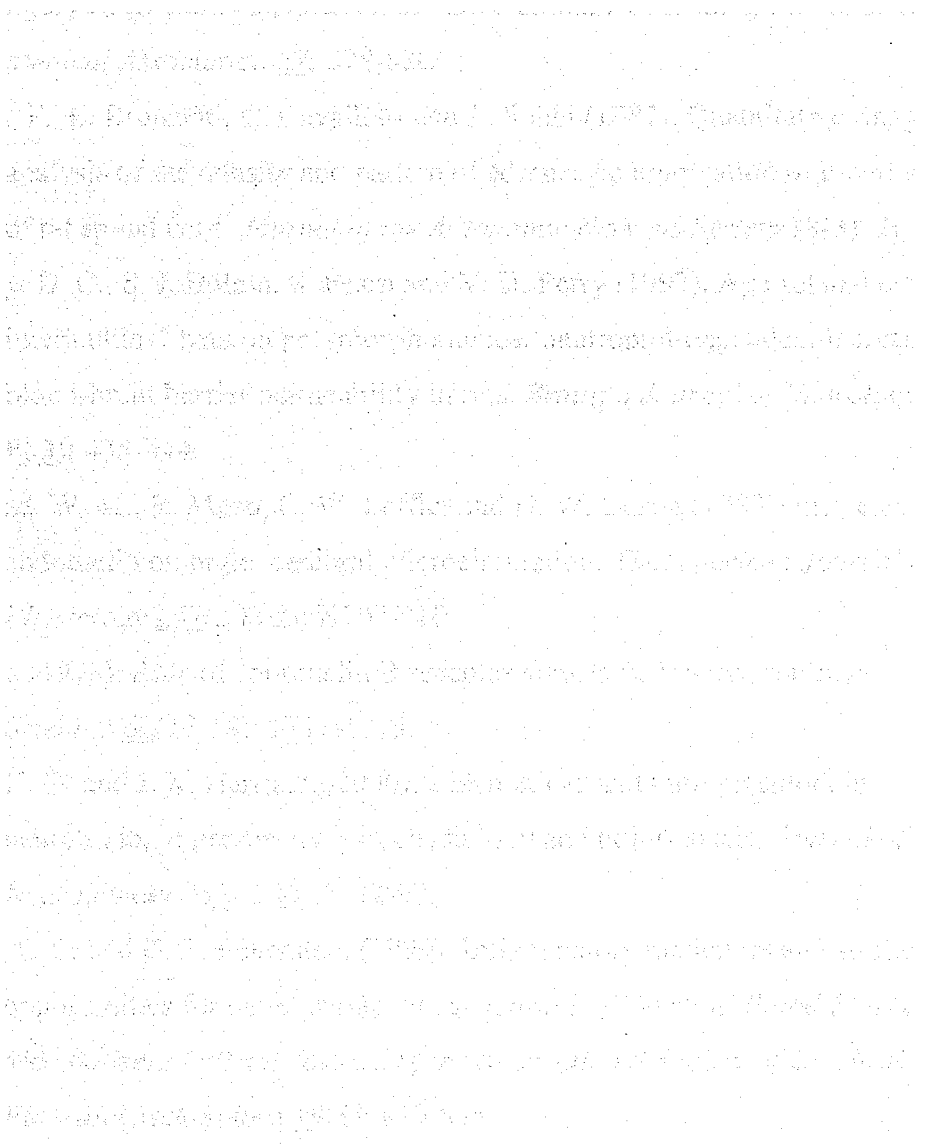

References:

Agrawal, S. K. and M. G. Fehlings (1997). Role of NMDA and non-NMDA ionotropic glutamate receptors in traumatic spinal cord axonal injury. *Journal of Neuroscience* 17(3): 1055-1063.

Agrawal, S. K., R. Nashmi and M. G. Fehlings (2000). Role of L- and N-type calcium channels in the pathophysiology of traumatic spinal cord white matter injury. *Neuroscience* 99(1): 179-188.

Allen, A. R. (1911). Surgery of experimental lesion of spinal cord equivalent to crush injury of fracture disclocation of spinal column. *Journal of the American Medical Association* 57: 878-880.

Amenta, F., E. Bronzetti, C. Cavallotti and L. Felici (1987). Quantitative image analysis of the density and pattern of adrenergic innervation of blood vessels of rat spinal cord. *Journal of the Autonomic Nervous System* 18(3): 261-264.

Anthony, D. C., S. J. Bolton, S. Fearn and V. H. Perry (1997). Age-related effects of interleukin-1 beta on polymorphonuclear neutrophil-dependent increases in blood-brain barrier permeability in rats. *Brain; a Journal of Neurology* 120 (Pt 3): 435-444.

Armstead, W. M., R. Mirro, C. W. Leffler and D. W. Busija (1989). Influence of endothelin on piglet cerebral microcirculation. *The American Journal of Physiology* 257(2 Pt 2): H707-710.

Baba, A. (1998). Role of endothelin B receptor signals in reactive astrocytes. *Life Sciences* 62(17-18): 1711-1715.

Bacon, K. B. and J. K. Harrison (2000). Chemokines and their receptors in neurobiology: perspectives in physiology and homeostasis. *Journal of Neuroimmunology* 104(1): 92-97.

Barone, F. C. and G. Z. Feuerstein (1999). Inflammatory mediators and stroke: new opportunities for novel therapeutics. *Journal of Cerebral Blood Flow and Metabolism : Official Journal of the International Society of Cerebral Blood Flow and Metabolism* 19(8): 819-834.

Baynash, A. G., K. Hosoda, A. Giaid, J. A. Richardson, N. Emoto, R. E. Hammer and M. Yanagisawa (1994). Interaction of endothelin-3 with endothelin-B receptor is essential for development of epidermal melanocytes and enteric neurons. *Cell* 79(7): 1277-1285.

Bednar, M. M., C. E. Gross, D. B. Howard and M. Lynn (1997). Neutrophil activation in acute human central nervous system injury. *Neurological Research* 19(6): 588-592.

Behrmann, D. L., J. C. Bresnahan and M. S. Beattie (1994). Modeling of acute spinal cord injury in the rat: neuroprotection and enhanced recovery with methylprednisolone, U-74006F and YM-14673. *Experimental Neurology* 126(1): 61-75.

Belcaro, G. and A. N. Nicolaides (2000). Laser Doppler Flowmetry: Principles of Technology and Clinical Applications. *Non-invasive Investigations in Vascular Disease*. London, Imperial College Press: 123-147.

Bernardes-Silva, M., D. C. Anthony, A. C. Issekutz and V. H. Perry (2001). Recruitment of neutrophils across the blood-brain barrier: the role of E- and P-selectins. *Journal of Cerebral Blood Flow and Metabolism* 21(9): 1115-1124.

Bethea, J. R., M. Castro, R. W. Keane, T. T. Lee, W. D. Dietrich and R. P. Yezierski (1998). Traumatic spinal cord injury induces nuclear factor-kappaB activation. *Journal of Neuroscience* 18(9): 3251-3260.

Biber, K., A. Sauter, N. Brouwer, S. C. Copray and H. W. Boddeke (2001). Ischemia-induced neuronal expression of the microglia attracting chemokine Secondary Lymphoid-tissue Chemokine (SLC). *Glia* 34(2): 121-133.

Bigaud, M. and J. T. Pelton (1992). Discrimination between ETA- and ETB-receptor-mediated effects of endothelin-1 and [Ala1,3,11,15]endothelin-1 by BQ-123 in the anaesthetized rat. *British Journal of Pharmacology* 107(4): 912-918.

Bingham, W. G., H. Goldman, S. J. Friedman, S. Murphy, D. Yashon and W. E. Hunt (1975). Blood flow in normal and injured monkey spinal cord. *Journal of Neurosurgery* 43(2): 162-171.

Bitsch, A., J. Schuchardt, S. Bunkowski, T. Kuhlmann and W. Bruck (2000). Acute axonal injury in multiple sclerosis. Correlation with demyelination and inflammation. *Brain* 123 (Pt 6): 1174-1183.

Blight, A. R. (1992). Macrophages and inflammatory damage in spinal cord injury. *Journal of Neurotrauma* 9 Suppl 1: S83-91.

Bonner, R. F. and R. Nossal (1990). Principles of Laser-Doppler Flowmetry. *Laser-Doppler Blood Flowmetry*. A. P. Shepherd and P. A. Oberg. London, Kluwer: 17-45.

Bracken, M. B., M. J. Shepard, W. F. Collins, T. R. Holford, W. Young, D. S. Baskin, H. M. Eisenberg, E. Flamm, L. Leo-Summers, J. Maroon and e. al (1990). A randomized, controlled trial of methylprednisolone or naloxone in the treatment of acute spinal-cord injury. Results of the Second National Acute Spinal Cord Injury Study [see comments]. *New England Journal of Medicine* 322(20): 1405-1411.

Bradbury, E. J., L. D. Moon, R. J. Popat, V. R. King, G. S. Bennett, P. N. Patel, J. W. Fawcett and S. B. McMahon (2002). Chondroitinase ABC promotes functional recovery after spinal cord injury. *Nature* 416(6881): 636-640.

Brammer, A., C. D. West and S. L. Allen (1993). A comparison of propofol with other injectable anaesthetics in a rat model for measuring cardiovascular parameters. *Laboratory Animals* 27(3): 250-257.

Brewer, K. L., J. R. Bethea and R. P. Yezierski (1999). Neuroprotective effects of interleukin-10 following excitotoxic spinal cord injury. *Experimental Neurology* 159(2): 484-493.

Brown, J. H. and P. Taylor (1996). Muscarinic receptor agonists and antagonists. *Goodman & Gilmans The Pharmacological Basis of Therapeutics*. J. G. Hardman and L. E. Limbird. London, McGraw-Hill: 141-160.

Buki, A., D. O. Okonkwo, K. K. Wang and J. T. Povlishock (2000). Cytochrome c release and caspase activation in traumatic axonal injury. *Journal of Neuroscience* 20(8): 2825-2834.

Buttner, D., H. Hackbarth, F. Wollnik and H. Borggreve (1984). Blood pressure in rats: a comparison of a multifactorial experimental design to measurements in an outbred stock. *Laboratory Animals* 18(2): 110-114.

Campbell, S. J., D. C. Wilcockson, A. G. Butchart, V. H. Perry and D. C. Anthony (2002). Altered chemokine expression in the spinal cord and brain contributes to differential interleukin-1beta-induced neutrophil recruitment. *Journal of Neurochemistry* 83(2): 432-441.

Carlson, S. L., M. E. Parrish, J. E. Springer, K. Doty and L. Dossett (1998). Acute inflammatory response in spinal cord following impact injury. *Experimental Neurology* 151(1): 77-88.

Casha, S., W. R. Yu and M. G. Fehlings (2001). Oligodendroglial apoptosis occurs along degenerating axons and is associated with FAS and p75 expression following spinal cord injury in the rat. *Neuroscience* 103(1): 203-218.

Cassada, D. C., J. J. Gangemi, J. M. Rieger, J. Linden, A. K. Kaza, S. M. Long, I. L. Kron, C. G. Tribble and J. A. Kern (2001). Systemic adenosine A2A agonist ameliorates ischemic reperfusion injury in the rabbit spinal cord. *The Annals of Thoracic Surgery* 72(4): 1245-1250.

Chalmers-Redman, R. M., A. D. Fraser, W. Y. Ju, J. Wadia, N. A. Tatton and W. G. Tatton (1997). Mechanisms of nerve cell death: apoptosis or necrosis after cerebral ischaemia. *International Review of Neurobiology* 40: 1-25.

Chen, M. S., A. B. Huber, M. E. van der Haar, M. Frank, L. Schnell, A. A. Spillmann, F. Christ and M. E. Schwab (2000). Nogo-A is a myelin-associated neurite outgrowth inhibitor and an antigen for monoclonal antibody IN-1 [see comments]. *Nature* 403(6768): 434-439.

Chizh, B. A., M. J. Cumberbatch and P. M. Headley (1994). A comparison of intravenous NBQX and GYKI 53655 as AMPA antagonists in the rat spinal cord. *British Journal of Pharmacology* 112(3): 843-846.

Cifuentes, M., P. Fernandez_LLebrez, J. Perez, J. M. Perez_Figares and E. M. Rodriguez (1992). Distribution of intraventricularly injected horseradish peroxidase in cerebrospinal fluid compartments of the rat spinal cord. *Cell and Tissue Research* 270(3): 485-494.

Coleman, M. and V. Perry (2002). Axon pathology in neurological disease: a neglected therapeutic target. *Trends in Neurosciences* 25(10): 532.

Collard, C. D., K. A. Park, M. C. Montalto, S. Alapati, J. A. Buras, G. L. Stahl and S. P. Colgan (2002). Neutrophil-derived Glutamate Regulates Vascular Endothelial Barrier Function. *The Journal of Biological Chemistry* 277(17): 14801-14811.

Corkill, D. J., D. C. Anthony and V. H. Perry (2001). Contrasting inflammatory responses in endothelin-1 induced ischaemic lesions in rat brain and spinal cord. *British Neuroscience Association Abstracts* 16: P12.07.

Corkill, D. J. and V. H. Perry (2001). A model to dissociate the ischaemic and mechanical components of spinal cord injury. *Journal of Neuroimmunology* 118(1): Pr 59.

Crowe, M. J., J. C. Bresnahan, S. L. Shuman, J. N. Masters and M. S. Beattie (1997). Apoptosis and delayed degeneration after spinal cord injury in rats and monkeys [published erratum appears in Nat Med 1997 Feb;3(2):240]. *Nature Medicine* 3(1): 73-76.

Damoiseaux, J. G., E. A. Dopp, W. Calame, D. Chao, G. G. MacPherson and C. D. Dijkstra (1994). Rat macrophage lysosomal membrane antigen recognized by monoclonal antibody ED1. Immunology. ENGLAND. **83:** 140-147.

Damon, D. H. (1998). Postganglionic sympathetic neurons express endothelin. *American Journal of Physiology* 274(3 Pt 2): R873-878.

David, S. and A. J. Aguayo (1981). Axonal elongation into peripheral nervous system "bridges" after central nervous system injury in adult rats. *Science* 214(4523): 931-933.

Davies, S. J., M. T. Fitch, S. P. Memberg, A. K. Hall, G. Raisman and J. Silver (1997). Regeneration of adult axons in white matter tracts of the central nervous system. *Nature* 390(6661): 680-683.

Devadason, P. S. and P. J. Henry (1997). Comparison of the contractile effects and binding kinetics of endothelin-1 and sarafotoxin S6b in rat isolated renal artery. *British Journal of Pharmacology* 121(2): 253-263.

Dewar, D., P. Yam and J. McCulloch (1999). Drug development for stroke: importance of protecting cerebral white matter. *European Journal of Pharmacology* 375(1-3): 41-50.

Dingledine, R., K. Borges, D. Bowie and S. F. Traynelis (1999). The glutamate receptor ion channels. *Pharmacological Reviews* 51(1): 7-61.

Dohrmann, G. J., F. C. Wagner and P. C. Bucy (1971). The microvasculature in transitory traumatic paraplegia. *Journal of Neurosurgery* 35: 263-271.

Doi, Y., T. Ozaka, M. Katsuki, H. Fukushige, E. Toyama, Y. Kanazawa, K. Arashidani and S. Fujimoto (1995). Histamine release from Weibel-Palade bodies of toad aortas induced by endothelin-1 and sarafotoxin-S6b. *The Anatomical Record* 242(3): 374-382.

Du, S., A. Rubin, S. Klepper, C. Barrett, Y. C. Kim, H. W. Rhim, E. B. Lee, C. W. Park, G. J. Markelonis and T. H. Oh (1999). Calcium influx and activation of calpain I mediate acute reactive gliosis in injured spinal cord. *Experimental Neurology* 157(1): 96-105.

Ducker, T. B. and P. L. J. Perot (1971). Spinal cord oxygen and blood flow in trauma. *Surgical Forum* 22: 413-415.

Dumuis, A., M. Sebben, L. Haynes, J. P. Pin and J. Bockaert (1988). NMDA receptors activate the arachidonic acid cascade system in striatal neurons. *Nature* 336(6194): 68-70.

Faden, A. I., T. P. Jacobs, E. Mougey and J. W. Holaday (1981). Endorphins in experimental spinal injury: therapeutic effect of naloxone. *Annals of Neurology* 10(4): 326-332.

Faden, A. I. and S. Salzman (1992). Pharmacological strategies in CNS trauma. *Trends in Pharmacological Sciences* 13(1): 29-35.

Faden, A. I. and R. P. Simon (1988). A potential role for excitotoxins in the pathophysiology of spinal cord injury. *Annals of Neurology* 23(6): 623-626.

Feldman, R. S., J. S. Meyer and L. F. Quenzer (1997). Neurons and Glial Cells. *Principles of Neuropsychopharmacology*. Sunderland, Massachusetts, Sinauer Associates: 75-109.

Fernandez, N., L. Monge, J. L. Garcia, A. L. Garcia-Villalon, B. Gomez and G. Dieguez (1998). In vivo and in vitro action of endothelin-1 on goat cerebrovascular bed. *European Journal of Pharmacology* 348(2-3): 199-211.

Fernandez, N., L. Monge, A. L. Garcia-Villalon, J. L. Garcia, B. Gomez and G. Dieguez (1995). Endothelin-1-induced in vitro cerebral venoconstriction is mediated by endothelin ETA receptors. *European Journal of Pharmacology* 294(2-3): 483-490.

Fitch, M. T., C. Doller, C. K. Combs, G. E. Landreth and J. Silver (1999). Cellular and molecular mechanisms of glial scarring and progressive cavitation: in vivo and in vitro analysis of inflammation-induced secondary injury after CNS trauma. *Journal of Neuroscience* 19(19): 8182-8198.

Flecknell, P. (1996). *Laboratory Animal Anaesthesia*. London, Academic Press.

Flecknell, P. A. and M. Mitchell (1984). Midazolam and fentanyl-fluanisone: assessment of anaesthetic effects in laboratory rodents and rabbits. *Laboratory Animals* 18(2): 143-146.

Fournier, A., T. GrandPre and S. M. Strittmatter (2001). Identification of a receptor mediating Nogo-66 inhibition of axonal regeneration. *Nature* 409: 341-346.

Francel, P. C., B. A. Long, J. M. Malik, C. Tribble, J. A. Jane and I. L. Kron (1993). Limiting ischemic spinal cord injury using a free radical scavenger 21-aminosteroid and/or cerebrospinal fluid drainage. *Journal of Neurosurgery* 79(5): 742-751.

Freedman, J., C. Post, J. Kahrstrom, A. Ohlen, P. Mollenholt, C. Owman, L. Alari and T. Hokfelt (1988). Vasoconstrictor effects in spinal cord of the substance P antagonist [D-Arg, D-Trp7,9 Leu11]-substance P (Spantide) and somatostatin

and interaction with thyrotropin releasing hormone. *Neuroscience* 27(1): 267-278.

Frei, E., I. Klusman, L. Schnell and M. E. Schwab (2000). Reactions of oligodendrocytes to spinal cord injury: cell survival and myelin repair. *Experimental Neurology* 163(2): 373-380.

Fujimoto, T., T. Nakamura, T. Ikeda and K. Takagi (2000). Potent protective effects of melatonin on experimental spinal cord injury. *Spine* 25(7): 769-775.

Fukuroda, T., T. Fujikawa, S. Ozaki, K. Ishikawa, M. Yano and M. Nishikibe (1994). Clearance of circulating endothelin-1 by ETB receptors in rats. *Biochemical and Biophysical Research Communications* 199(3): 1461-1465.

Fukuroda, T., K. Noguchi, S. Tsuchida, M. Nishikibe, F. Ikemoto, K. Okada and M. Yano (1990). Inhibition of biological actions of big endothelin-1 by phosphoramidon. *Biochemical and Biophysical Research Communications* 172(2): 390-395.

Fuxe, K., N. Kurosawa, A. Cintra, A. Hallstrom, M. Goiny, L. Rosen, L. F. Agnati and U. Ungerstedt (1992). Involvement of local ischemia in endothelin-1 induced lesions of the neostriatum of the anaesthetized rat. *Experimental Brain Research* 88(1): 131-139.

George, E. B., J. D. Glass and J. W. Griffin (1995). Axotomy-induced axonal degeneration is mediated by calcium influx through ion-specific channels. *Journal of Neuroscience* 15(10): 6445-6452.

George, R. and J. W. Griffin (1994). The proximo-distal spread of axonal degeneration in the dorsal columns of the rat. *Journal of Neurocytology* 23(11): 657-667.

Giesler, G. J., H. R. Spiel and W. D. Willis (1981). Organization of spinothalamic tract axons within the rat spinal cord. *The Journal of Comparative Neurology* 195(2): 243-252.

Goerge, T., A. Niemeyer, P. Rogge, R. Ossig, H. Oberleithner and S. W. Schneider (2002). Secretion pores in human endothelial cells during acute hypoxia. *The Journal of Membrane Biology* 187(3): 203-211.

Griffin, J. W., C. Y. Li, C. Macko, T. W. Ho, S. T. Hsieh, P. Xue, F. A. Wang, D. R. Cornblath, G. M. McKhann and A. K. Asbury (1996). Early nodal changes in the acute motor axonal neuropathy pattern of the Guillain-BarrÃ© syndrome. *Journal of Neurocytology* 25(1): 33-51.

Grill, R., K. Murai, A. Blesch, F. H. Gage and M. H. Tuszynski (1997). Cellular delivery of neurotrophin-3 promotes corticospinal axonal growth and partial functional recovery after spinal cord injury. *Journal of Neuroscience* 17(14): 5560-5572.

Grossman, S. D., L. J. Rosenberg and J. R. Wrathall (2001). Temporal-spatial pattern of acute neuronal and glial loss after spinal cord contusion. *Experimental Neurology* 168(2): 273-282.

Guth, L., C. P. Barrett, E. J. Donati, S. S. Deshpande and E. X. Albuquerque (1981). Histopathological reactions an axonal regeneration in the transected spinal cord of Hibernating squirrels. *Journal of Comparative Neurology* 203(2): 297-308.

Guth, L., P. J. Reier, C. P. Barret and E. J. Donati (1983). Repair of the mammalian spinal cord. *Trends in Neurosciences* 6: 20-24.

Hadley, S. D. and H. G. Goshgarian (1997). Altered immunoreactivity for glial fibrillary acidic protein in astrocytes within 1 h after cervical spinal cord injury. *Experimental Neurology* 146(2): 380-387.

Hakanson, R., S. Leander, N. Asano, D. M. Feng and K. Folkers (1990). Spantide II, a novel tachykinin antagonist having high potency and low histamine-releasing effect. *Regulatory Peptides* 31(1): 75-82.

Hama, H., Y. Kasuya, T. Sakurai, G. Yamada, N. Suzuki, T. Masaki and K. Goto (1997). Role of endothelin-1 in astrocyte responses after acute brain damage. *Journal of Neuroscience Research* 47(6): 590-602.

Happel, R. D., K. P. Smith, N. L. Banik, J. M. Powers, E. L. Hogan and J. D. Balentine (1981). Ca2+-accumulation in experimental spinal cord trauma. *Brain Research* 211(2): 476-479.

Hasselblatt, M., P. Lewczuk, B. M. Loffler, H. Kamrowski_Kruck, N. von_Ahsen, A. L. Siren and H. Ehrenreich (2001). Role of the astrocytic ET(B) receptor in the regulation of extracellular endothelin-1 during hypoxia. *Glia* 34(1): 18-26.

Hiley, C. R., D. J. Cowley, J. T. Pelton and A. C. Hargreaves (1992). BQ-123, cyclo(-D-Trp-D-Asp-Pro-D-Val-Leu), is a non-competitive antagonist of the actions of endothelin-1 in SK-N-MC human neuroblastoma cells. *Biochemical and Biophysical Research Communications* 184(1): 504-510.

Hirose, K., K. Okajima, Y. Taoka, M. Uchiba, H. Tagami, K. Nakano, J. Utoh, H. Okabe and N. Kitamura (2000). Activated protein C reduces the

ischemia/reperfusion-induced spinal cord injury in rats by inhibiting neutrophil activation. *Annals of Surgery* 232(2): 272-280.

Hoffman, F. M., P. Chen, R. Jeyaseelan, F. Incardona, M. Fisher and R. Zidovetzki (1998). Endothelin-1 induces production of the neutrophil chemotactic factor interleukin-8 by human brain-derived endothelial cells. *Blood* 92(9): 3064-3072.

Hokfelt, T., C. Post, J. Freedman, J. M. Lundberg and L. Terenius (1989). Endothelin induces spinal lesions after intrathecal administration. *Acta Physiologica Scandinavica* 137(4): 555-556.

Holland, L. Z. and N. D. Holland (1999). Chordate origins of the vertebrate central nervous system. *Current Opinion in Neurobiology* 9(5): 596-602.

Honmou, O. and W. Young (1995). Traumatic injury of spinal axons. The Axon: Structure Function and Pathophysiology. S. G. Waxman, J. D. Kocsis and P. K. Stys, Oxford University Press: 480-503.

Hoover, D. B. Effects of spantide on guinea pig coronary resistance vessels. *Peptides* 12(5): 983-988.

Hori, S., Y. Komatsu, R. Shigemoto, N. Mizuno and S. Nakanishi (1992). Distinct tissue distribution and cellular localization of two messenger ribonucleic acids encoding different subtypes of rat endothelin receptors. *Endocrinology* 130(4): 1885-1895.

Horner, P. J. and F. H. Gage (2000). Regenerating the damaged central nervous system. *Nature* 407: 963-970.

Hosli, E. and L. Hosli (1991). Autoradiographic evidence for endothelin receptors on astrocytes in cultures of rat cerebellum, brainstem and spinal cord. *Neuroscience Letters* 129(1): 55-58.

Hu, J., D. J. Discher, N. H. Bishopric and K. A. Webster (1998). Hypoxia regulates expression of the endothelin-1 gene through a proximal hypoxia-inducible factor-1 binding site on the antisense strand. *Biochemical and Biophysical Research Communications* 245(3): 894-899.

Hu, S., P. K. Peterson and C. C. Chao (1997). Cytokine-mediated neuronal apoptosis. *Neurochemistry International* 30(4-5): 427-431.

Hurlbert, R. J. (2000). Methylprednisolone for acute spinal cord injury: an inappropriate standard of care [see comments]. *Journal of Neurosurgery* 93(1 Suppl): 1-7.

Imaizumi, T., J. D. Kocsis and S. G. Waxman (1999). The role of voltage-gated Ca2+ channels in anoxic injury of spinal cord white matter. *Brain Research* 817(1-2): 84-92.

Inamasu, J., S. Suga, S. Sato, T. Horiguchi, K. Akaji, K. Mayanagi and T. Kawase (2000). Post-ischemic hypothermia delayed neutrophil accumulation and microglial activation following transient focal ischemia in rats. *Journal of Neuroimmunology* 109(2): 66-74.

Itakura, T. (1983). Aminergic and cholinergic innervations of the spinal cord blood vessels of cats. A histochemical study. *Journal of Neurosurgery* 58(6): 900-905.

Iwai, A., W. W. Monafo and S. G. Eliasson (1991). Effect of adrenalectomy or sympathectomy on spinal cord blood flow in hypothermic rats. *The American Journal of Physiology* 260(3 Pt 2): H827-831.

Jander, S., M. Schroeter and G. Stoll (2000). Role of NMDA receptor signaling in the regulation of inflammatory gene expression after focal brain ischemia. *Journal of Neuroimmunology* 109(2): 181-187.

Jansson, A., T. Mazel, B. Andbjer, L. Rosen, D. Guidolin, M. Zoli, E. Sykova, L. F. Agnati and K. Fuxe (1999). Effects of nitric oxide inhibition on the spread of biotinylated dextran and on extracellular space parameters in the neostriatum of the male rat. *Neuroscience* 91(1): 69-80.

Jiang, M. H., A. Hoog, K. C. Ma, X. J. Nie, Y. Olsson and W. W. Zhang (1993). Endothelin-1-like immunoreactivity is expressed in human reactive astrocytes. *Neuroreport* 4(7): 935-937.

Kanazawa, H., N. Kurihara, K. Hirata, H. Fujiwara, H. Matsushita and T. Takeda (1992). Low concentration endothelin-1 enhanced histamine-mediated bronchial contractions of guinea pigs in vivo. *Biochemical and Biophysical Research Communications* 187(2): 717-721.

Kanellopoulos, G. K., X. M. Xu, C. Y. Hsu, X. Lu, T. M. Sundt and N. T. Kouchoukos (2000). White matter injury in spinal cord ischemia: protection by AMPA/kainate glutamate receptor antagonism. *Stroke* 31(8): 1945-1952.

Kar, S., J. G. Chabot and R. Quirion (1991). Quantitative autoradiographic localisation of [125I]endothelin-1 binding sites in spinal cord and dorsal root ganglia of the rat. *Neuroscience Letters* 133(1): 117-120.

Karaki, H., S. A. Sudjarwo, M. Hori, K. Sakata, Y. Urade, M. Takai and T. Okada (1993). ETB receptor antagonist, IRL 1038, selectively inhibits the endothelin-induced endothelium-dependent vascular relaxation. *European Journal of Pharmacology* 231(3): 371-374.

Khan, M., S. Jiang, P. Middlemis, S. Kang, C. P. Smith and M. Rathbone (2002). HP184 is neuroprotective and improves locomotor function after moderate acute spinal crush injury in rats. *Journal of Neurotrauma* 19(10): 1375 P1512.

Kinoshita, Y. and W. W. Monafo (1993). Guanethidine chemical sympathectomy: spinal cord and sciatic nerve blood flow. *The American Journal of Physiology* 265(4 Pt 2): H1155-1159.

Kobrine, A. I., D. E. Evans and H. V. Rizzoli (1979). The effects of ischemia on long-tract neural conduction in the spinal cord. *Journal of Neurosurgery* 50(5): 639-644.

Kohzuki, M., S. Y. Chai, G. Paxinos, A. Karavas, D. J. Casley, C. I. Johnston and F. A. Mendelsohn (1991). Localization and characterization of endothelin receptor binding sites in the rat brain visualized by in vitro autoradiography. *Neuroscience* 42(1): 245-260.

Kosel, S., R. Egensperger, K. Bise, S. Arbogast, P. Mehraein and M. B. Graeber (1997). Long-lasting perivascular accumulation of major histocompatibility complex class II-positive lipophages in the spinal cord of stroke patients: possible relevance for the immune privilege of the brain. *Acta Neuropathol (Berl)* 94(6): 532-538.

Koyama, Y., M. Takemura, K. Fujiki, N. Ishikawa, Y. Shigenaga and A. Baba (1999). BQ788, an endothelin ET(B) receptor antagonist, attenuates stab wound injury-induced reactive astrocytes in rat brain. *Glia* 26(3): 268-271.

Koyanagi, I., C. H. Tator and P. J. Lea (1993a). Three-dimensional analysis of the vascular system in the rat spinal cord with scanning electron microscopy of vascular corrosion casts. Part 1: Normal spinal cord. *Neurosurgery* 33(2): 277-283; discussion 283-284.

Koyanagi, I., C. H. Tator and P. J. Lea (1993b). Three-dimensional analysis of the vascular system in the rat spinal cord with scanning electron microscopy of vascular corrosion casts. Part 2: Acute spinal cord injury. *Neurosurgery* 33(2): 285-291; discussion 292.

Krajewski, S., M. Krajewska, L. M. Ellerby, K. Welsh, Z. Xie, Q. L. Deveraux, G. S. Salvesen, D. E. Bredesen, R. E. Rosenthal, G. Fiskum and J. C. Reed (1999). Release of caspase-9 from mitochondria during neuronal apoptosis and cerebral ischemia. *Proceedings of the National Academy of Sciences of the United States of America* 96(10): 5752-5757.

Kreutzberg, G. W. (1996). Microglia: a sensor for pathological events in the CNS. *Trends in Neurosciences* 19(8): 312-318.

Kumar, S. and S. B. Hedges (1998). A molecular timescale for vertebrate evolution. *Nature* 392(6679): 917-920.

Kurosawa, M., K. Fuxe, A. Hallstrom, M. Goiny, A. Cintra and U. Ungerstedt (1991). Responses of blood flow, extracellular lactate, and dopamine in the striatum to intrastriatal injection of endothelin-1 in anesthetized rats. *Journal of Cardiovascular Pharmacology* 17 Suppl 7: S340-342.

Kurtel, H. and S. Ghandour (1999). Endothelins and inflammation: the gastrointestinal system. *Pathophysiology* 6: 77-89.

Le, Y. L., K. Shih, P. Bao, R. S. Ghirnikar and L. F. Eng (2000). Cytokine chemokine expression in contused rat spinal cord. *Neurochemistry International* 36(4-5): 417-425.

Leigh, L. E., B. Ghebrehiwet, T. P. Perera, I. N. Bird, P. Strong, U. Kishore, K. B. Reid and P. Eggleton (1998). C1q-mediated chemotaxis by human neutrophils: involvement of gClqR and G-protein signalling mechanisms. *Biochemical Journal* 330 (Pt 1): 247-254.

Leskovar, A., L. J. Moriarty, J. J. Turek, I. A. Schoenlein and R. B. Borgens (2000). The macrophage in acute neural injury: changes in cell numbers over time and levels of cytokine production in mammalian central and peripheral nervous systems. *Journal of Experimental Biology* 203 Pt 12: 1783-1795.

Li, S., Q. Jiang and P. K. Stys (2000). Important role of reverse Na(+)-Ca(2+) exchange in spinal cord white matter injury at physiological temperature. *Journal of Neurophysiology* 84(2): 1116-1119.

Li, S., G. A. Mealing, P. Morley and P. K. Stys (1999). Novel injury mechanism in anoxia and trauma of spinal cord white matter: glutamate release via reverse Na+-dependent glutamate transport. *J Neurosci (Online)* 19(14): RC16.

Li, S. and P. K. Stys (2000). Mechanisms of ionotropic glutamate receptor-mediated excitotoxicity in isolated spinal cord white matter. *Journal of Neuroscience* 20(3): 1190-1198.

Lindsberg, P. J., J. T. O_Neill, I. A. Paakkari, J. M. Hallenbeck and G. Feuerstein (1989). Validation of laser-Doppler flowmetry in measurement of spinal cord blood flow. *The American Journal of Physiology* 257(2 Pt 2): H674-680.

Liu, T., P. R. Young, P. C. McDonnell, R. F. White, F. C. Barone and G. Z. Feuerstein (1993). Cytokine-induced neutrophil chemoattractant mRNA expressed in cerebral ischemia. *Neuroscience Letters* 164(1-2): 125-128.

Liu, X. Z., X. M. Xu, R. Hu, C. Du, S. X. Zhang, J. W. McDonald, H. X. Dong, Y. J. Wu, G. S. Fan, M. F. Jacquin, C. Y. Hsu and D. W. Choi (1997). Neuronal and glial apoptosis after traumatic spinal cord injury. *Journal of Neuroscience* 17(14): 5395-5406.

Loesch, A. and G. Burnstock (2002). Endothelin in human cerebrovascular nerves. 103 Suppl 48: 404S-407S.

Loewy, A. D. (1981). Raphe pallidus and raphe obscurus projections to the intermediolateral cell column in the rat. *Brain Research* 222(1): 129-133.

LoPachin, R. M. and E. J. Lehning (1997). Mechanism of calcium entry during axon injury and degeneration. *Toxicology and Applied Pharmacology* 143(2): 233-244.

Marketos, S. G. and P. Skiadas (1999a). Hippocrates. The father of spine surgery. *Spine* 24(13): 1381-1387.

Marketos, S. G. and P. K. Skiadas (1999b). Galen: a pioneer of spine research. *Spine* 24(22): 2358-2362.

Masaki, T., S. Miwa, T. Sawamura, H. Ninomiya and Y. Okamoto (1999). Subcellular mechanisms of endothelin action in vascular system. *European Journal of Pharmacology* 375(1-3): 133-138.

Mathers, D. A. and R. J. Falconer (1991). The electrolytic lesion as a model of spinal cord damage and repair in the adult rat. *Journal of Neuroscience Methods* 38(1): 15-23.

Matsushita, K., Y. Wu, J. Qiu, L. Lang-Lazdunski, L. Hirt, C. Waeber, B. T. Hyman, J. Yuan and M. A. Moskowitz (2000). Fas receptor and neuronal cell death after spinal cord ischemia. *Journal of Neuroscience* 20(18): 6879-6887.

Matyszak, M. K., M. J. Townsend and V. H. Perry (1997). Ultrastructural studies of an immune-mediated inflammatory response in the CNS parenchyma directed against a non-CNS antigen. *Neuroscience* 78(2): 549-560.

McKenzie, A. L., J. J. Hall, N. Aihara, K. Fukuda and L. J. Noble (1995). Immunolocalization of endothelin in the traumatized spinal cord: relationship to blood-spinal cord barrier breakdown. *Journal of Neurotrauma* 12(3): 257-268.

McLarnon, J. G., X. Wang, J. H. Bae and S. U. Kim (1999). Endothelin-induced changes in intracellular calcium in human microglia. *Neuroscience Letters* 263(1): 9-12.

McTigue, D. M., P. J. Horner, B. T. Stokes and F. H. Gage (1998). Neurotrophin-3 and brain-derived neurotrophic factor induce oligodendrocyte proliferation and myelination of regenerating axons in the contused adult rat spinal cord. *Journal of Neuroscience* 18(14): 5354-5365.

Mennicken, F., R. Maki, E. B. de Souza and R. Quirion (1999). Chemokines and chemokine receptors in the CNS: a possible role in neuroinflammation and patterning. *Trends in Pharmacological Sciences* 20(2): 73-78.

Milner, P., A. Loesch and G. Burnstock (2000). Endothelin immunoreactivity and mRNA expression in sensory and sympathetic neurones following selective denervation. *International Journal of Developmental Neuroscience : the Official Journal of the International Society For Developmental Neuroscience* 18(8): 727-734.

Mitsuhashi, T., T. Ikata, T. Morimoto, T. Tonai and S. Katoh (1994). Increased production of eicosanoids, TXA2, PGI2 and LTC4 in experimental spinal cord injuries. *Paraplegia* 32(8): 524-530.

Moncada, S., R. J. Flower and J. R. Vane (1985). Prostaglandins, prostacyclin, thromboxane A2 and leukotrienes. *Goodman and Gilman's The Pharmacological Basis of Therapeutics*. A. G. Gilman, L. S. Goodman, T. W. Rall and F. Murad, Macmillan Publishing Co.: 660-673.

Morell, P. and W. T. Norton (1980). Myelin. *Scientific American* 242(5): 88-96.

Mosqueda-Garcia, R., T. Inagami, M. Appalsamy, M. Sugiura and R. M. Robertson (1993). Endothelin as a neuropeptide. Cardiovascular effects in the brainstem of normotensive rats. *Circulation Research* 72(1): 20-35.

Mustafa, A., H. S. Sharma, Y. Olsson, T. Gordh, P. Thoren, P. O. Sjoquist, P. Roos, A. Adem and F. Nyberg (1995). Vascular permeability to growth hormone in the rat central nervous system after focal spinal cord injury. Influence of a new anti-oxidant H 290/51 and age. *Neuroscience Research* 23(2): 185-194.

Nagata, S. (1997). Apoptosis by death factor. *Cell* 88(3): 355-365.

Nakagomi, S., S. Kiryu_Seo and H. Kiyama (2000). Endothelin-converting enzymes and endothelin receptor B messenger RNAs are expressed in different neural cell species and these messenger RNAs are coordinately induced in neurons and astrocytes respectively following nerve injury. *Neuroscience* 101(2): 441-449.

Nakamichi, K., M. Ihara, M. Kobayashi, T. Saeki, K. Ishikawa and M. Yano (1992). Different distribution of endothelin receptor subtypes in pulmonary tissues revealed by the novel selective ligands BQ-123 and [Ala1,3,11,15]ET-1. *Biochemical and Biophysical Research Communications* 182(1): 144-150.

Nambi, P., M. Pullen and G. Feuestein (1990). Identification of endothelin receptors in various regions of rat brain. *Neuropeptides* 16: 195-199.

Newman, T. A., S. T. Woolley, P. M. Hughes, N. R. Sibson, D. C. Anthony and V. H. Perry (2001). T-cell- and macrophage-mediated axon damage in the absence of a CNS-specific immune response: involvement of metalloproteinases. *Brain* 124(Pt 11): 2203-2214.

Nicholls, D. and D. Attwell (1990). The release and uptake of excitatory amino acids. *Trends in Pharmacological Sciences* 11(11): 462-468.

NSCIC (2001). Spinal cord injury: Facts and figures at a glance. Birmingham, Alabama, USA, National Spinal Cord Injury Statistical Center, University of Alabama, USA.

Oksche, A., G. Boese, A. Horstmeyer, J. Furkert, M. Beyermann, M. Bienert and W. Rosenthal (2000). Late endosomal/lysosomal targeting and lack of recycling of the ligand-occupied endothelin B receptor. *Molecular Pharmacology* 57(6): 1104-1113.

Oliver, M., G. Zarb, J. Silver, M. Moore and V. Salisbury (1988). *Walking into darkness: The experience of spinal cord injury*, Macmillan Press Scientific & Medical.

Osterholm, J. L. (1974). The pathophysiological response to spinal cord injury. The current status of related research. *Journal of Neurosurgery* 40(1): 5-33.

Ozaka, T., Y. Doi, K. Kayashima and S. Fujimoto (1997). Weibel-Palade bodies as a storage site of calcitonin gene-related peptide and endothelin-1 in blood vessels of the rat carotid body. *The Anatomical Record* 247(3): 388-394.

Pantoni, L., J. H. Garcia and J. A. Gutierrez (1996). Cerebral white matter is highly vulnerable to ischemia. *Stroke; a Journal of Cerebral Circulation* 27(9): 1641-1646; discussion 1647.

Perry, V. H. and D. C. Anthony (1999). Axon damage and repair in multiple sclerosis. *Philosophical Transactions of the Royal Society of London. Series B: Biological Sciences* 354(1390): 1641-1647.

Perry, V. H., D. C. Anthony, S. J. Bolton and H. C. Brown (1997). The blood-brain barrier and the inflammatory response. *Molecular Medicine Today* 3(8): 335-341.

Perry, V. H. and S. Gordon (1997). Microglia and Macrophages. Immunology of the Nervous System. R. W. Keane and W. F. Hickey. Oxford, Oxford University Press: 155-172.

Perry, V. H. and R. Linden (1982). Evidence for dendritic competition in the developing retina. *Nature* 297(5868): 683-685.

Petrov, T., J. Steiner, B. Braun and J. A. Rafols (2002). Sources of endothelin-1 in hippocampus and cortex following traumatic brain injury. *Neuroscience* 115(1): 275-283.

Petty, M. A. and J. G. Wettstein (1999). White matter ischaemia. *Brain Research. Brain Research Reviews* 31(1): 58-64.

Pierre, L. N. and A. P. Davenport (1998). Relative contribution of endothelin A and endothelin B receptors to vasoconstriction in small arteries from human heart and brain. *Journal of Cardiovascular Pharmacology* 31(Suppl 1): S74-76.

Pisharodi, M. and H. J. W. Nauta (1985). An animal model for neuron-specific spinal cord lesions by the microinjection of N-methylaspartate, kainic acid and quisqualic acid. *Applied Neurophysiology* 48: 226-233.

Pluta, R. M., R. J. Boock, J. K. Afshar, K. Clouse, M. Bacic, H. Ehrenreich and E. H. Oldfield (1997). Source and cause of endothelin-1 release into cerebrospinal fluid after subarachnoid hemorrhage. *Journal of Neurosurgery* 87(2): 287-293.

Popovich, P. G., Z. Guan, V. McGaughy, L. Fisher, W. F. Hickey and D. M. Basso (2002). The neuropathological and behavioral consequences of intraspinal

microglial/macrophage activation. *Journal of Neuropathology and Experimental Neurology* 61(7): 623-633.

Popovich, P. G., Z. Guan, P. Wei, I. Huitinga, N. van Rooijen and B. T. Stokes (1999). Depletion of hematogenous macrophages promotes partial hindlimb recovery and neuroanatomical repair after experimental spinal cord injury. *Experimental Neurology* 158(2): 351-365.

Popovich, P. G. and W. F. Hickey (2001). Bone marrow chimeric rats reveal the unique distribution of resident and recruited macrophages in the contused rat spinal cord. *Journal of Neuropathology and Experimental Neurology* 60(7): 676-685.

Popovich, P. G., P. J. Horner, B. B. Mullin and B. T. Stokes (1996). A quantitative spatial analysis of the blood-spinal cord barrier. I. Permeability changes after experimental spinal contusion injury. *Experimental Neurology* 142(2): 258-275.

Povlishock, J. T. and C. W. Christman (1995). Diffuse axonal injury. *The Axon: Structure Function and Pathophysiology*. S. G. Waxman, J. D. Kocsis and P. K. Stys, Oxford University Press: 504-529.

Raineteau, O., K. Fouad, P. Noth, M. Thallmair and M. E. Schwab (2001). Functional switch between motor tracts in the presence of the mAb IN-1 in the adult rat. *Proceedings of the National Academy of Sciences of the United States of America* 98(12): 6929-6934.

Ramer, M. S., G. P. Harper and E. J. Bradbury (2000). Progress in spinal cord research - a refined strategy for the International Spinal Research Trust. *Spinal Cord* 38(8): 449-472.

Rathbone, M., S. Jiang, M. Khan, Y. Lu, J. Buttigieg, D. Lee, J. Harvey, K. Paulseth, R. Bain, A. Safdar, S. Wang, J. Saoud, D. Rampe, M. Petty and C. P. Smith (2002). HP184, a combined sodium and potassium channel blocker, improves locomotor scores 35 days after a moderate spinal cord injury in the rat. *Journal of Neurotrauma* 19(10): 1337 P1358.

Ripodas, A., J. A. de Juan, M. Roldan-Pallares, R. Bernal, J. Moya, M. Chao, A. Lopez, A. Fernandez-Cruz and R. Fernandez-Durango (2001). Localisation of endothelin-1 mRNA expression and immunoreactivity in the retina and optic nerve from human and porcine eye. Evidence for endothelin-1 expression in astrocytes. *Brain Research* 912(2): 137-143.

Rogers, S. D., E. Demaster, M. Catton, J. R. Ghilardi, L. A. Levin, J. E. Maggio and P. W. Mantyh (1997). Expression of Endothelin-B receptors by glia *in vivo* is increased after CNS injury in rats, rabbits, and humans. *Experimental Neurology* 145: 180-195.

Roitt, I., J. Brostoff and D. Male (2001). Cell-mediated cytotoxicity. *Immunology*. London, Mosby: 163-172.

Rosenberg, L. J., Y. D. Teng and J. R. Wrathall (1999). 2,3-Dihydroxy-6-nitro-7-sulfamoyl-benzo(f)quinoxaline reduces glial loss and acute white matter pathology after experimental spinal cord contusion. *Journal of Neuroscience* 19(1): 464-475.

Rossi, D. J., T. Oshima and D. Attwell (2000). Glutamate release in severe brain ischaemia is mainly by reversed uptake. *Nature* 403(6767): 316-321.

Rossi, G. P., T. M. Seccia and G. G. Nussdorfer (2001). Reciprocal regulation of endothelin-1 and nitric oxide: relevance in the physiology and pathology of the cardiovascular system. *International Review of Cytology* 209: 241-272.

Rothwell, N. J. (1997). Sixteenth Gaddum Memorial Lecture December 1996. Neuroimmune interactions: the role of cytokines. *British Journal of Pharmacology* 121(5): 841-847.

Russell, F. D., J. N. Skepper and A. P. Davenport (1998). Evidence using immunoelectron microscopy for regulated and constitutive pathways in the transport and release of endothelin. *Journal of Cardiovascular Pharmacology* 31(3): 424-430.

Saito, A., R. Shiba, M. Yanagisawa, T. Masaki, S. Kimura, K. Yamada, T. Mima, T. Shigeno and K. Goto (1991). Endothelins: vasoconstrictor effects and localization in canine cerebral arteries. *British Journal of Pharmacology* 103(1): 1129-1135.

Salmon, J. A. and G. A. Higgs (1994). The eicosanoids: generation and action. *Textbook of Immunopharmacology*. M. M. Dale, J. C. Foreman and D. T. Fan. Oxford, Blackwell Scientific: 131-142.

Salzman, S. K., R. Acosta, G. Beck, J. Madden, B. Boxer and E. H. Ohlstein (1996). Spinal endothelin content is elevated after moderate local trauma in the rat to levels associated with locomotor dysfunction after intrathecal injection. *Journal of Neurotrauma* 13(2): 93-101.

Schafer, M. K., W. J. Schwaeble, C. Post, P. Salvati, M. Calabresi, R. B. Sim, F. Petry, M. Loos and E. Weihe (2000). Complement C1q is dramatically up-regulated in brain microglia in response to transient global cerebral ischemia. *Journal of Immunology* 164(10): 5446-5452.

Schnell, L., S. Fearn, H. Klassen, M. E. Schwab and V. H. Perry (1999a). Acute inflammatory responses to mechanical lesions in the CNS: differences between brain and spinal cord. *European Journal of Neuroscience* 11(10): 3648-3658.

Schnell, L., S. Fearn, M. E. Schwab, V. H. Perry and D. C. Anthony (1999b). Cytokine-induced acute inflammation in the brain and spinal cord. *Journal of Neuropathology and Experimental Neurology* 58(3): 245-254.

Schroeter, M., S. Jander, O. W. Witte and G. Stoll (1999). Heterogeneity of the microglial response in photochemically induced focal ischemia of the rat cerebral cortex. *Neuroscience* 89(4): 1367-1377.

Sercombe, R. and M. Wahl (1982). Inhibition of the pial artery constriction induced by sympathetic stimulation by local microapplication of a cholinomimetic agent. *Journal of Cerebral Blood Flow and Metabolism : Official Journal of the International Society of Cerebral Blood Flow and Metabolism* 2(4): 451-456.

Sharkey, J. and S. P. Butcher (1995). Characterisation of an experimental model of stroke produced by intracerebral microinjection of endothelin-1 adjacent to the rat middle cerebral artery. *Journal of Neuroscience Methods* 60: 125-131.

Shepherd, A. P. (1990). History of Laser-Doppler Flowmetry. Laser-Doppler Blood Flowmetry. A. P. Shepherd and P. A. Oberg. London, Kluwer Academic Publishers: 1-16.

Shibaguchi, H., A. Himeno, K. Shigematsu, Y. Kataoka and M. Niwa (2000). Transient hypoxia/hypoglycemia upregulates endothelin B receptors in cultured rat astrocytes. *Glia* 31(1): 91-94.

Shinmi, O., S. Kimura, T. Yoshizawa, T. Sawamura, Y. Uchiyama, Y. Sugita, I. Kanazawa, M. Yanagisawa, K. Goto and T. Masaki (1989). Presence of endothelin-1 in porcine spinal cord: isolation and sequence determination. *Biochemical and Biophysical Research Communications* 162(1): 340-346.

Shohami, E., T. P. Jacobs, J. M. Hallenbeck and G. Feuerstein (1987). Increased thromboxane A2 and 5-HETE production following spinal cord ischemia in the rabbit. *Prostaglandins, Leukotrienes and Medicine* 28(2): 169-181.

Shuman, S. L., J. C. Bresnahan and M. S. Beattie (1997). Apoptosis of microglia and oligodendrocytes after spinal cord contusion in rats. *Journal of Neuroscience Research* 50(5): 798-808.

Sim, E. (1994). Complement. *Textbook of immunopharmacology*. M. M. Dale, J. C. Foreman and D. T. Fan. Oxford, Blackwell Scientific: 155-169.

Simon, R. P., J. H. Swan, T. Griffiths and B. S. Meldrum (1984). Blockade of N-methyl-D-aspartate receptors may protect against ischemic damage in the brain. *Science* 226(4676): 850-852.

Siren, A. L., P. Lewczuk, M. Hasselblatt, C. Dembowski, L. Schilling and H. Ehrenreich (2002). Endothelin B receptor deficiency augments neuronal damage upon exposure to hypoxia-ischemia in vivo. *Brain Research* 945(1): 144-149.

Sluck, J. M., R. C. Lin, L. I. Katolik, A. Y. Jeng and J. C. Lehmann (1999). Endothelin converting enzyme-1-, endothelin-1-, and endothelin-3-like immunoreactivity in the rat brain. *Neuroscience* 91(4): 1483-1497.

Steffensen, I., S. G. Waxman, L. Mills and P. K. Stys (1997). Immunolocalization of the Na(+)-Ca2+ exchanger in mammalian myelinated axons. *Brain Research* 776(1-2): 1-9.

Stoll, G., S. Jander and M. Schroeter (1998). Inflammation and glial responses in ischemic brain lesions. *Progress in Neurobiology* 56(2): 149-171.

Streit, W. J., S. L. Semple-Rowland, S. D. Hurley, R. C. Miller, P. G. Popovich and B. T. Stokes (1998). Cytokine mRNA profiles in contused spinal cord and axotomized facial nucleus suggest a beneficial role for inflammation and gliosis. *Experimental Neurology* 152(1): 74-87.

Stys, P. K. (1998). Anoxic and ischemic injury of myelinated axons in CNS white matter: from mechanistic concepts to therapeutics. *Journal of Cerebral Blood Flow and Metabolism* 18(1): 2-25.

Stys, P. K., B. R. Ransom and S. G. Waxman (1992). Tertiary and quaternary local anesthetics protect CNS white matter from anoxic injury at concentrations that do not block excitability. *Journal of Neurophysiology* 67(1): 236-240.

Sykova, E., J. Svoboda, J. Polak and A. Chvatal (1994). Extracellular volume fraction and diffusion characteristics during progressive ischemia and terminal anoxia in the spinal cord of the rat. *Journal of Cerebral Blood Flow and Metabolism :*

Official Journal of the International Society of Cerebral Blood Flow and Metabolism 14(2): 301-311.

Szatkowski, M. and D. Attwell (1994). Triggering and execution of neuronal death in brain ischaemia: two phases of glutamate release by different mechanisms. *Trends in Neurosciences* 17(9): 359-365.

Takimoto, M., T. Inui, T. Okada and Y. Urade (1993). Contraction of smooth muscle by activation of endothelin receptors on autonomic neurons. *Febs Letters* 324(3): 277-282.

Taoka, Y. and K. Okajima (1998). Spinal cord injury in the rat. *Progress in Neurobiology* 56(3): 341-358.

Taoka, Y. and K. Okajima (2000). Role of leukocytes in spinal cord injury in rats. *Journal of Neurotrauma* 17(3): 219-229.

Taoka, Y., K. Okajima, K. Murakami, M. Johno and M. Naruo (1998). Role of neutrophil elastase in compression-induced spinal cord injury in rats. *Brain Research* 799(2): 264-269.

Taoka, Y., K. Okajima, M. Uchiba, K. Murakami, S. Kushimoto, M. Johno, M. Naruo, H. Okabe and K. Takatsuki (1997). Gabexate mesilate, a synthetic protease inhibitor, prevents compression-induced spinal cord injury by inhibiting activation of leukocytes in rats [see comments]. *Critical Care Medicine* 25(5): 874-879.

Tator, C. H. and M. G. Fehlings (1991). Review of the secondary injury theory of acute spinal cord trauma with emphasis on vascular mechanisms [see comments]. *Journal of Neurosurgery* 75(1): 15-26.

Tayag, E. C., A. Y. Jeng, P. Savage and J. C. Lehmann (1996). Rat striatum contains pure population of ETB receptors. *European Journal of Pharmacology* 300(3): 261-265.

Tekkok, S. B. and M. P. Goldberg (2001). Ampa/kainate receptor activation mediates hypoxic oligodendrocyte death and axonal injury in cerebral white matter. *The Journal of Neuroscience : the Official Journal of the Society For Neuroscience* 21(12): 4237-4248.

Tonai, T., K. Shiba, Y. Taketani, Y. Ohmoto, K. Murata, M. Muraguchi, H. Ohsaki, E. Takeda and T. Nishisho (2001). A neutrophil elastase inhibitor (ONO-5046) reduces neurologic damage after spinal cord injury in rats. *Journal of Neurochemistry* 78(5): 1064-1072.

Tonai, T., Y. Taketani, N. Ueda, T. Nishisho, Y. Ohmoto, Y. Sakata, M. Muraguchi, K. Wada and S. Yamamoto (1999). Possible involvement of interleukin-1 in cyclooxygenase-2 induction after spinal cord injury in rats. *Journal of Neurochemistry* 72(1): 302-309.

Touil, T., M. S. Deloire_Grassin, C. Vital, K. G. Petry and B. Brochet (2001). In vivo damage of CNS myelin and axons induced by peroxynitrite. *Neuroreport* 12(16): 3637-3644.

Trapp, B. D., J. Peterson, R. M. Ransohoff, R. Rudick, S. Mork and L. Bo (1998). Axonal transection in the lesions of multiple sclerosis. *New England Journal of Medicine* 338(5): 278-285.

Uesugi, M., Y. Kasuya, H. Hama, M. Yamamoto, K. Hayashi, T. Masaki and K. Goto (1996). Endogenous endothelin-1 initiates astrocytic growth after spinal cord injury. *Brain Research* 728(2): 255-259.

van den Buuse, M. and K. M. Webber (2000). Endothelin and dopamine release. *Progress in Neurobiology* 60: 385-405.

van Mourik, J. A., T. Romani_de_Wit and J. Voorberg (2002). Biogenesis and exocytosis of Weibel-Palade bodies. *Histochemistry and Cell Biology* 117(2): 113-122.

Venance, L., J. Premont, J. Glowinski and C. Giaume (1998). Gap junctional communication and pharmacological heterogeneity in astrocytes cultured from the rat striatum. *Journal of Physiology* 510 (Pt 2): 429-440.

Victorino, G. P., D. H. Wisner and V. L. Tucker (2000). Basal release of endothelin-1 and the influence of the ETB receptor on single vessel hydraulic permeability. *The Journal of Trauma* 49(2): 314-319.

von Euler, M., A. Seiger, L. Holmberg and E. Sundstrom (1994). NBQX, a competitive non-NMDA receptor antagonist, reduces degeneration due to focal spinal cord ischemia. *Experimental Neurology* 129(1): 163-168.

Wakita, H., H. Tomimoto, I. Akiguchi, A. Matsuo, J. X. Lin, M. Ihara and P. L. McGeer (2002). Axonal damage and demyelination in the white matter after chronic cerebral hypoperfusion in the rat. *Brain Research* 924(1): 63-70.

Wang, C. X., J. A. Olschowka and J. R. Wrathall (1997). Increase of interleukin-1beta mRNA and protein in the spinal cord following experimental traumatic injury in the rat. *Brain Research* 759(2): 190-196.

Wang, K. C., V. Koprivica, J. A. Kim, R. Sivasankaran, Y. Guo, R. L. Neve and Z. He (2002). Oligodendrocyte-myelin glycoprotein is a Nogo receptor ligand that inhibits neurite outgrowth. *Nature* 417(6892): 941-944.

Warden, P., N. I. Bamber, H. Li, A. Esposito, K. A. Ahmad, C. Y. Hsu and X. M. Xu (2001). Delayed glial cell death following wallerian degeneration in white matter tracts after spinal cord dorsal column cordotomy in adult rats. *Experimental Neurology* 168(2): 213-224.

Warner, T. D., G. H. Allcock, E. J. Mickley and J. R. Vane (1993). Characterization of endothelin receptors mediating the effects of the endothelin/sarafotoxin peptides on autonomic neurotransmission in the rat vas deferens and guinea-pig ileum. *British Journal of Pharmacology* 110(2): 783-789.

Watanabe, T., T. Yamamoto, Y. Abe, N. Saito, T. Kumagai and H. Kayama (1999). Differential activation of microglia after experimental spinal cord injury. *Journal of Neurotrauma* 16(3): 255-265.

Watkins, J. C. (1962). The synthesis of some acidic amino acids possessing neuropharmacological activity. *Journal of Medicinal and Pharmaceutical Chemistry* 5: 1187-1199.

Waxman, S. G., B. R. Ransom and P. K. Stys (1991). Non-synaptic mechanisms of Ca(2+)-mediated injury in CNS white matter. *Trends in Neurosciences* 14(10): 461-468.

Webber, K. M., J. N. Pennefather, G. A. Head and M. van den Buuse (1998). Endothelin induces dopamine release from rat striatum via endothelin-B receptors. *Neuroscience* 86(4): 1173-1180.

Weibel, E. R. and G. E. Palade (1964). New cytoplasmic components in arterial endothelia. *The Journal of Cell Biology* 23: 101-112.

Weidner, N., A. Blesch, R. J. Grill and M. H. Tuszynski (1999a). Nerve growth factor-hypersecreting Schwann cell grafts augment and guide spinal cord axonal growth and remyelinate central nervous system axons in a phenotypically appropriate manner that correlates with expression of L1. *Journal of Comparative Neurology* 413(4): 495-506.

Weidner, N., R. J. Grill and M. H. Tuszynski (1999b). Elimination of basal lamina and the collagen scar after spinal cord injury fails to augment corticospinal tract regeneration. *Experimental Neurology* 160(1): 40-50.

Westergren, H., M. Farooque, Y. Olsson and A. Holtz (2001). Spinal cord blood flow changes following systemic hypothermia and spinal cord compression injury: an experimental study in the rat using Laser-Doppler flowmetry. *Spinal Cord* 39(2): 74-84.

Westmark, R., L. J. Noble, K. Fukuda, N. Aihara and A. L. McKenzie (1995). Intrathecal administration of endothelin-1 in the rat: impact on spinal cord blood flow and the blood-spinal cord barrier. *Neuroscience Letters* 192(3): 173-176.

Willette, R. N. and C. F. Sauermelch (1990). Abluminal effects of endothelin in cerebral microvasculature assessed by laser-Doppler flowmetry. *American Journal of Physiology* 259(6 Pt 2): H1688-1693.

Wolf, J. A., P. K. Stys, T. Lusardi, D. Meaney and D. H. Smith (2001). Traumatic axonal injury induces calcium influx modulated by tetrodotoxin-sensitive sodium channels. *The Journal of Neuroscience : the Official Journal of the Society For Neuroscience* 21(6): 1923-1930.

Woodward, J. S. and L. W. Freeman (1956). Ischemia of the spinal cord: an experimental study. *Journal of Neurosurgery* 13: 63-72.

Wrathall, J. R., Y. D. Teng and D. Choiniere (1996). Amelioration of functional deficits from spinal cord trauma with systemically administered NBQX, an antagonist of non-N-methyl-D-aspartate receptors. *Experimental Neurology* 137(1): 119-126.

Wrathall, J. R., Y. D. Teng and R. Marriott (1997). Delayed antagonism of AMPA/kainate receptors reduces long-term functional deficits resulting from spinal cord trauma. *Experimental Neurology* 145(2 Pt 1): 565-573.

Xu, J., G. Fan, S. Chen, Y. Wu, X. M. Xu and C. Y. Hsu (1998). Methylprednisolone inhibition of TNF-alpha expression and NF-kB activation after spinal cord injury in rats. *Brain Research. Molecular Brain Research* 59(2): 135-142.

Xu, J. A., C. Y. Hsu, T. H. Liu, E. L. Hogan, P. L. J. Perot and H. H. Tai (1990). Leukotriene B4 release and polymorphonuclear cell infiltration in spinal cord injury. *Journal of Neurochemistry* 55(3): 907-912.

Yam, P. S., J. Patterson, D. I. Graham, T. Takasago, D. Dewar and J. McCulloch (1998). Topographical and quantitative assessment of white matter injury following a focal ischaemic lesion in the rat brain. 2(4): 315-322.

Yam, P. S., T. Takasago, D. Dewar, D. I. Graham and J. McCulloch (1997). Amyloid precursor protein accumulates in white matter at the margin of a focal ischaemic lesion. *Brain Research* 760(1-2): 150-157.

Yamada, T., T. Morimoto, H. Nakase, H. Hirabayashi, K. Hiramatsu and T. Sakaki (1998). Spinal cord blood flow and pathophysiological changes after transient spinal cord ischemia in cats. *Neurosurgery* 42(3): 626-634.

Yamasaki, Y., Y. Matsuo, J. Zagorski, N. Matsuura, H. Onodera, Y. Itoyama and K. Kogure (1997). New therapeutic possibility of blocking cytokine-induced neutrophil chemoattractant on transient focal ischemic brain damage in rats. *Brain Research* 759: 103-111.

Yamashita, K., D. J. Discher, J. Hu, N. H. Bishopric and K. A. Webster (2001). Molecular regulation of the endothelin-1 gene by hypoxia. Contributions of hypoxia-inducible factor-1, activator protein-1, GATA-2, AND p300/CBP. *Journal of Biological Chemistry* 276(16): 12645-12653.

Yanagisawa, M., A. Inoue, T. Ishikawa, Y. Kasuya, S. Kimura, S. Kumagaye, K. Nakajima, T. X. Watanabe, S. Sakakibara, K. Goto and e. al (1988a). Primary structure, synthesis, and biological activity of rat endothelin, an endothelium-derived vasoconstrictor peptide. *Proceedings of the National Academy of Sciences of the United States of America* 85(18): 6964-6967.

Yanagisawa, M., H. Kurihara, S. Kimura, K. Goto and T. Masaki (1988b). A novel peptide vasoconstrictor, endothelin, is produced by vascular endothelium and modulates smooth muscle Ca2+ channels. *Journal of Hypertension. Supplement* 6(4): S188-191.

Yanagisawa, M., H. Kurihara, S. Kimura, Y. Tomobe, M. Kobayashi, Y. Mitsui, Y. Yazaki, K. Goto and T. Masaki (1988c). A novel potent vasoconstrictor peptide produced by vascular endothelial cells [see comments]. *Nature* 332(6163): 411-415.

Yick, L. W., W. Wu, K. F. So, H. K. Yip and D. K. Shum (2000). Chondroitinase ABC promotes axonal regeneration of Clarke's neurons after spinal cord injury. *Neuroreport* 11(5): 1063-1067.

Yoshimoto, S., Y. Ishizaki, H. Kurihara, T. Sasaki, M. Yoshizumi, M. Yanagisawa, Y. Yazaki, T. Masaki, K. Takakura and S. Murota (1990). Cerebral microvessel endothelium is producing endothelin. *Brain Research* 508(2): 283-285.

Yoshizawa, T., O. Shinmi, A. Giaid, M. Yanagisawa, S. J. Gibson, S. Kimura, Y. Uchiyama, J. M. Polak, T. Masaki and I. Kanazawa (1990). Endothelin: a novel peptide in the posterior pituitary system. *Science* 247(4941): 462-464.

Young, W., I. Koreh, V. Yen and A. Lindsay (1982). Effect of sympathectomy on extracellular potassium ionic activity and blood flow in experimental spinal cord contusion. *Brain Research* 253(1-2): 115-124.

Yu, A. C., H. K. Wong, H. W. Yung and L. T. Lau (2001). Ischemia-induced apoptosis in primary cultures of astrocytes. *Glia* 35(2): 121-130.

Yu, C. G., O. Jimenez, A. E. Marcillo, B. Weider, K. Bangerter, W. D. Dietrich, S. Castro and R. P. Yezierski (2000). Beneficial effects of modest systemic hypothermia on locomotor function and histopathological damage following contusion-induced spinal cord injury in rats. *Journal of Neurosurgery* 93(1 Suppl): 85-93.

Zeman, W. and J. R. M. Innes (1963). *Craigie's Neuroanatomy of the Rat*. London, Academic Press.

Zhai, Q., J. Wang, A. Kim, Q. Liu, R. Watts, E. Hoopfer, T. Mitchison, L. Luo and Z. He (2003). Involvement of the ubiquitin-proteasome system in the early stages of wallerian degeneration. *Neuron* 39(2): 217-225.

Zidovetzki, R., P. Chen, M. Chen and F. M. Hoffman (1999). Endothelin-1-induced Interleukin-8 production in human brain-derived endothelial cells is mediated by the protein kinase C and protein tyrosine kinase pathways. *Blood* 94(4): 1291-1299.

Zoli, M., A. Jansson, E. Sykova, L. F. Agnati and K. Fuxe (1999). Volume transmission in the CNS and its relevance for neuropsychopharmacology. *Trends in Pharmacological Sciences* 20(4): 142-150.

Zuo, J., D. Neubauer, K. Dyess, T. A. Ferguson and D. Muir (1998). Degradation of chondroitin sulfate proteoglycan enhances the neurite-promoting potential of spinal cord tissue. *Experimental Neurology* 154(2): 654-662.